

**Titre:** Determination of generic seat contour shapes for wheelchair users  
Title: based on the development of a body-seat interface shape measurement instrument

**Auteur:** Yue Li  
Author:

**Date:** 2003

**Type:** Mémoire ou thèse / Dissertation or Thesis

**Référence:** Li, Y. (2003). Determination of generic seat contour shapes for wheelchair users based on the development of a body-seat interface shape measurement instrument [Thèse de doctorat, École Polytechnique de Montréal]. PolyPublie.  
Citation: <https://publications.polymtl.ca/7088/>

 **Document en libre accès dans PolyPublie**  
Open Access document in PolyPublie

**URL de PolyPublie:** <https://publications.polymtl.ca/7088/>  
PolyPublie URL:

**Directeurs de recherche:**  
Advisors:

**Programme:** Non spécifié  
Program:

**UNIVERSITÉ DE MONTRÉAL**

**DETERMINATION OF GENERIC SEAT CONTOUR SHAPES FOR  
WHEELCHAIR USERS BASED ON THE DEVELOPMENT OF A BODY-SEAT  
INTERFACE SHAPE MEASUREMENT INSTRUMENT**

**YUE LI**

**INSTITUT DE GÉNIE BIOMÉDICAL  
ÉCOLE POLYTECHNIQUE DE MONTRÉAL**

**THÈSE PRÉSENTÉE EN VUE DE L'OBTENTION  
DU DIPLÔME DE PHILOSOPHIAE DOCTOR (Ph.D.)  
(GÉNIE BIOMÉDICAL)**

**MAI 2003**

National Library  
of Canada

Bibliothèque nationale  
du Canada

Acquisitions and  
Bibliographic Services

Acquisitions et  
services bibliographiques

395 Wellington Street  
Ottawa ON K1A 0N4  
Canada

395, rue Wellington  
Ottawa ON K1A 0N4  
Canada

*Your file    Votre référence*

*ISBN: 0-612-80811-4*

*Our file    Notre référence*

*ISBN: 0-612-80811-4*

The author has granted a non-exclusive licence allowing the National Library of Canada to reproduce, loan, distribute or sell copies of this thesis in microform, paper or electronic formats.

L'auteur a accordé une licence non exclusive permettant à la Bibliothèque nationale du Canada de reproduire, prêter, distribuer ou vendre des copies de cette thèse sous la forme de microfiche/film, de reproduction sur papier ou sur format électronique.

The author retains ownership of the copyright in this thesis. Neither the thesis nor substantial extracts from it may be printed or otherwise reproduced without the author's permission.

L'auteur conserve la propriété du droit d'auteur qui protège cette thèse. Ni la thèse ni des extraits substantiels de celle-ci ne doivent être imprimés ou autrement reproduits sans son autorisation.

**Canada**

**UNIVERSITÉ DE MONTRÉAL**

**ÉCOLE POLYTECHNIQUE DE MONTRÉAL**

**Cette thèse intitulée:**

**DETERMINATION OF GENERIC SEAT CONTOUR SHAPES FOR  
WHEELCHAIR USERS BASED ON THE DEVELOPMENT OF A BODY-SEAT  
INTERFACE SHAPE MEASUREMENT INSTRUMENT**

présentée par : LI Yue

en vue de l'obtention du diplôme de : Philosophiae Doctor

a été dûment acceptée par le jury d'examen constitué de :

M. SAVARD Pierre, Ph.D., président

M. DANSEREAU Jean, Ph.D., membre et directeur de recherche

M. AISSAOUI Rachid, Ph.D., membre et codirecteur de recherche

M. CLEMENT Bernard, Ph.D., membre

Mme SMEESTERS Cécile, Ph.D., membre



## ACKNOWLEDGEMENTS

I would like to express my sincere gratitude to my thesis supervisors, Dr. Jean Dansereau and Dr. Rachid Aissaoui, for their initiation of the project and their constant guidance and dedication throughout the thesis work. Their valuable advice and contributions have helped in the completion of this thesis.

I am very grateful for my years at the Ecole Polytechnique de Montreal, especially the first four years in the Chaire ATP, made possible by the NSERC post graduate scholarship, Fonds FCAR scholarship, and the steadfast support of my family.

This research was also possible due to the support of Professor Francois Prince, director of the Movement Laboratory in the Centre de réadaptation Marie Enfant de l'Hôpital St-Justine, Professor Carl-Éric Aubin from the LIS3D in the Centre de recherche de l'Hôpital St-Justine, Ms. Hélène Bergeron from the Centre de réadaptation Lucie-Bruneau, and Professor Mohamed Cheriet from the LIVIA in École de technologie supérieure. I am especially grateful to the Seating Biomechanics Laboratory, University of Pittsburgh, for allowing me to use some of the experimental data on CASS interface shapes. I give special thanks to Dr. David M. Brienza for contributing his time and effort toward this project.

Many thanks to Michèle Lacoste who provided energetic support during the experimental stage and steady encouragement during the write-up stage. The warm support of all my friends in the Chair ATP, LIS3D, Movement Laboratory and LIVIA, especially Frédéric Parent, Éric Phan, Éric Wagnac and Nadine-Michèle Lalonde, who enabled me to complete this thesis and have a wonderful time along the way.

Many thanks to Marguerite Lacroix and Moira Rehmer whose editing suggestions and precise sense of language contributed to the final copy.

I have learned a tremendous amount about wheelchairs and seating by working with people with disabilities. I thank them for challenging me to continue to learn and try to understand.

I am forever grateful to my fiancé, Walter-John Hardy, for encouraging me throughout the entire process of writing this thesis. I also thank my sister, Nan Li 李楠, for her faithful and loving support.

This thesis is dedicated to my grandparents, Zhonghe Li 李衷和, Junhan Yu 于均汉, Yingfu Wang 王膺福, Yiqing Jin 晋益清, and my parents, Congxin Li 李从心 and Jing Wang 王经, for their unconditional support at each turn of the road. I thank them for enriching every aspect of my life with their goodness and rare gifts.

## RÉSUMÉ

La fonction première des coussins pour fauteuil roulant consiste à fournir une plateforme efficace qui permet à l'utilisateur d'exécuter un large éventail de tâches. Pour de nombreux usagers, le coussin joue un rôle primordial car il permet de réduire le niveau de pression que subissent les tissus mous, ce qui contribue par le fait même à prévenir la formation de plaies de pression. Les données théoriques et expérimentales démontrent qu'un coussin moulé de façon adéquate améliore la distribution des points de pression et réduit la distorsion tissulaire. La conception des coussins moulés suit deux principales approches sur le plan technique, à savoir le coussin générique prémoulé et le coussin moulé sur mesure. Il est facile de se procurer des coussins prémoulés sur le marché, mais ceux-ci ne conviennent pas dans les cas où l'on cherche à obtenir un soutien postural hautement personnalisé. Les coussins moulés sur mesure peuvent procurer ce soutien spécifique; leur fabrication exige toutefois beaucoup de travail et des compétences techniques considérables. Il apparaît donc souhaitable de mettre au point une nouvelle méthode qui permettrait de concevoir des coussins moulés pouvant non seulement être vendus sur le marché mais procurant également le soutien personnalisé qui fait défaut aux coussins génériques.

L'étude préliminaire effectuée dans un premier temps sur un ensemble de formes d'interfaces de surfaces d'appui avait permis de conclure qu'il était possible de définir des formes génériques d'interface séant-siège au moyen d'une analyse par classification hiérarchique. Quatre formes génériques ont été déterminées chez un groupe de personnes âgées en analysant la dissimilarité relative aux paramètres de forme géométrique. Les résultats appuient l'hypothèse de l'existence de formes génériques multiples et de la possibilité de classer ces formes pour obtenir des renseignements utiles relativement aux paramètres de forme géométrique. Par ailleurs, ces formes génériques

pourraient servir à la conception de coussins moulés de forme générique (GSC\*) dans la perspective d'offrir une solution de rechange aux coussins moulés sur mesure et aux coussins prémoulés. Toutefois, avant d'usiner des formes génériques dans de la mousse de polyuréthane pour fabriquer un coussin GSC, il importe de préciser que lors de notre étude préliminaire, nous avons utilisé les données provenant du Seating Biomechanics Laboratory de l'Université de Pittsburgh, obtenues au moyen d'un appareil de mesure rigide (*Electronic Shape Sensor* - ESS). Toutefois, les formes génériques découlant des formes d'interface n'illustraient pas l'interface séant-siège dans des conditions de charge réelle, étant donné que les propriétés mécaniques de la surface d'appui constituent l'un des facteurs majeurs qui donnent à l'interface sa forme. Jusqu'à maintenant, on ne rapporte pas avoir eu recours à une méthode clinique pratique de mesure de l'interface séant-siège dans le cas des matériaux de coussin typique (p. ex. la mousse). Le seul appareil portable pouvant être placé entre le sujet et le coussin est décrit dans un article de Yamazaki publié en 1992, mais il n'est pas commercialisé. Par conséquent, pour poursuivre notre recherche sur les formes génériques moulées, il était essentiel de mettre au point un dispositif efficace et facile à utiliser qui permettrait de capter rapidement la forme de l'interface séant-coussin.

L'hypothèse fondée sur la base de cette analyse préliminaire, est la suivante : il est possible de mettre au point un instrument de mesure de la forme de l'interface séant-siège et d'utiliser les données de base recueillies grâce à cet instrument pour concevoir une surface d'appui moulée générique qui répondrait mieux aux besoins des différents usagers de fauteuil roulant, réduirait les pressions d'interface et améliorerait le confort.

Dans un deuxième temps, un nouveau système de mesure de la forme d'interface, appelé le *Shape Sensing Array* (SSA) a été conçu, à partir d'un réseau de capteurs de forme en fibre optique. Les résultats des tests effectués sur le nouvel appareil indiquent que le

---

\* D'après le terme anglais *generic shape contoured cushion*

système SSA est capable d'effectuer des mesures reproductibles et relativement précises de la forme de l'interface séant-siège. Ce système fournit donc un outil permettant d'analyser et de quantifier les relations complexes entre les propriétés du siège, notamment la forme de la surface, la déformation du coussin et la déformation tissulaire sous différentes conditions de charge et de rigidité. Cette capacité devrait s'avérer d'une grande importance pour la recherche adaptée aux besoins cliniques. Une fois qu'il aura été perfectionné, le SSA est susceptible de devenir un instrument clinique et de recherche des plus utiles pour la conception de surfaces d'appui et la prescription de coussins.

Dans un troisième temps, une base de données a été constituée de formes d'interface au moyen du système SSA. Nous avons eu recours à une analyse par classification hiérarchique fondée sur le paramétrage géométrique pour produire un ensemble de formes génériques. Trois coussins moulés de forme générique (GSC) ont été fabriqués par transfert des formes de surface d'appui résultantes sur des coussins de mousse souple, pour ensuite être évalués. La pression moyenne et le pic de pression relevés étaient tous deux inférieurs sur le coussin GSC choisi au moyen de l'indice de similitude que sur les coussins GSC qui avaient été rejetés. L'évaluation subjective a également révélé que sur le plan de l'évaluation du confort, le premier coussin obtenait une marque sensiblement plus élevée que les autres. Les données obtenues indiquent que par rapport aux coussins plats en mousse, la distribution des pressions sur les coussins GSC retenus était plus uniforme et leurs valeurs moins élevées. Ces résultats permettent de croire que le coussin moulé de forme générique pourrait servir à résoudre les problèmes relatifs à l'assise éprouvés par les utilisateurs de fauteuil roulant.

Puisque la forme moulée des sièges dépend d'un ensemble de facteurs, les formes génériques obtenues peuvent varier grandement lorsque l'un de ces facteurs change. D'abord, les propriétés biomécaniques des structures tissulaires et musculaires varient d'une population d'utilisateurs à l'autre. Ensuite, le poids corporel et le tonus musculaire

d'un même individu peuvent varier dans le temps. Les sujets choisis pour réaliser ce projet appartenaient à une même catégorie, définie de la manière suivante : leurs besoins en matière d'appui postural allaient de légers à modérés et ils ne présentaient aucune difformité pelvienne importante. La rigidité et l'épaisseur des tissus mous différaient d'un sujet à l'autre, selon la nature du diagnostic : sclérose en plaques, amputation des deux jambes, paralysie cérébrale ou traumatisme cérébral. Si l'on élargissait la base de données sur les formes d'interface pour chacune de ces populations, par conséquent, on pourrait s'attendre à mieux saisir les relations complexes entre les facteurs propres à l'assise comme la déformation des tissus, la forme de la surface et la pression d'interface. De plus, la forme du siège dépend également des caractéristiques du coussin. Les caractéristiques du sujet étant généralement fixes, le seul moyen d'adapter les paramètres physiques est de modifier les caractéristiques des coussins. Comme notre projet de recherche le démontre, les coussins moulés de forme générique ne représentent pas une solution optimale pour tous les sujets. Changer la rigidité de la mousse pourrait être une autre voie de solution, puisque celle-ci a un effet sur le transfert des charges et, en dernière instance, sur la forme du coussin. Ces réflexions suggèrent qu'il faudra, dans le futur, approfondir l'analyse sur l'effet de la rigidité et de l'épaisseur en relation avec l'efficacité du coussin GSC. Enfin, la distribution du poids est un autre facteur une incidence très importante sur la forme du coussin. Grâce à la mise au point du système SSA, l'analyse des formes permet d'obtenir des données cliniques très utiles sur la répartition des surfaces de charge du coussin. Par conséquent, les mesures relatives aux formes complémentent les autres mesures comme la pression d'interface et l'analyse de la posture, pour fournir en définitive un portrait global de l'interface séant-coussin.

L'évaluation clinique et fiable des coussins est une entreprise difficile. Pour démontrer qu'un nouveau modèle de coussin améliore la distribution de la pression et le confort, il est nécessaire d'étudier un grand nombre de patients. La pression d'interface et les autres paramètres fournissent des données utiles lorsqu'il s'agit de comparer le rendement relatif de différents coussins pour un seul individu ou une population bien

définie. Toutefois, la relation entre ces mesures et l'incidence des plaies de pression ou de l'inconfort reste mal définie; elle donne lieu à de nombreux débats entre chercheurs.

## ABSTRACT

The primary role of a wheelchair seat cushion is to provide an effective platform from which the user may perform a wide range of tasks. For many users, the cushion performs a crucial function by reducing the concentration of pressure in soft tissues, thereby helping to prevent the formation of pressure ulcers. Theoretical and experimental data has shown that a properly fitted contoured cushion would improve the pressure distribution and reduce tissue distortion. The two basic technological approaches that have been used to design a contoured seat are the standard precontoured cushion technique and the custom-contoured cushion technique. The standard precontoured cushions are available off the shelf but they are inappropriate when intimately fitting body support is needed. The custom contoured cushions can provide intimate seating support, but they are usually labor-intensive and require considerable technical skill. Therefore, it is desirable to develop a new approach for designing contoured cushions which not only are available off the shelf but also provide a more intimate fit to the body than standard precontoured cushions.

Our preliminary study on a group of seat support interface shapes suggested that body-seat interface shape patterns could be identified using cluster analysis. Four distinct generic shapes were identified for a group of elderly subjects by analyzing the dissimilarity in geometrical shape parameters. The results support the notion that multiple generic shapes exist and that classifying interface shapes provides meaningful information with respect to the geometrical shape parameters. Furthermore, the generic shapes can potentially be used to design generic shape contoured (GSC) cushions, which could provide an alternative to the custom contoured seat cushions and precontoured seat cushions. GSC cushions would be fabricated by carving generic shapes into high resiliency polyurethane foam. However, the interface shape data used in the preliminary study was obtained from the Electronic Shape Sensor (ESS) when the subject's body was supported by an array of probes. Since the mechanical properties of the support



surface is one of the major factors that results in interface shape, the generic shapes derived from those interface shapes did not characterize the body-cushion interface. To date, a practical clinical method of measuring body-cushion interface shape has not been reported for typical cushion materials (e.g., foam). The only device that is portable and can be placed between the subject and the cushion was described in Yamazaki's 1992 paper. Unfortunately, such a device is not commercially available. Therefore, in order to investigate generic shape contoured approaches, the development of an efficient and easy-to-use device for rapidly capturing the body-cushion interface shapes is essential.

Based on the finding of the preliminary study, the hypothesis of this project could be formulated as follows: it is possible to develop an instrument to measure body-cushion interface shapes and the basic information gathered through the use of this instrument will lead to the successful design of generic contoured support surfaces, which will better accommodate different wheelchair users and are able to reduce interface pressure as well as improve sitting comfort.

A new interface shape-measuring system – Shape Sensing Array (SSA) has been developed by using an array of optical fiber shape sensors (Measurand Inc., Fredericton, New Brunswick, Canada). Results on the new device clearly indicate that the SSA system is capable of making repeatable and fairly accurate measurements of buttock-cushion interface shapes. The system RMS error in the Z direction was 2.19 mm and 4.72 mm when the measurements were not and were affected by pressure, respectively. The errors in the X and Y directions were lower than 1 mm. For the needs of the actual study, the accuracy of the SSA is acceptable. The SSA system is a new tool that could be used for the investigation and quantification of the complex relationships between seat properties such as surface shape, cushion deformation and tissue deformation under different load and stiffness conditions. This ability will be of great significance for clinical study and application. With further improvement the SSA itself is likely to be

developed into a useful research and clinical tool for support surface design and cushion prescription.

Benefiting from the development of the SSA system, a body-cushion interface shape database was generated for a group of wheelchair users who require mild to moderate body support and present no severe pelvic deformities. The cluster analysis method was chosen in this study to classify a group of interface shapes into different clusters on the basis of similarities. Seventeen geometric parameters are defined to quantitatively analyze the shape and to calculate the similarity measures for interface shapes. Cluster analysis was then performed on these 17 feature parameter variables to detect natural grouping in the input interface shape database.

The results of the cluster analysis suggested that three clusters could be identified, and the mean shape of each cluster was considered as a generic shape. Then the generic shapes were transferred to a cushion cutting machine where the generic shapes were carved into polyurethane foam cushions. By comparing a subject's own shape with generic shapes, the best matching GSC cushion was selected for this subject. A similarity index was calculated based on the 17 geometric parameters to quantify the difference between a subject's interface shapes and generic shapes. The GSC cushion that has the highest similarity index was chosen as the appropriate GSC cushion for this user.

The selected GSC cushions were compared with the rejected GSC cushions. Four aspects were evaluated, namely the pressure distribution, the posture, the comfort, and dynamic stability. The selected GSC cushions were also compared with two standard precontoured cushions. The evaluation results on interface pressure distribution revealed that the mean pressure on the selected GSC cushion was lower than those on the GSC cushions that were not selected by the similarity index method. Therefore, the similarity

index method gave useful information on how to select a GSC cushion that could provide optimized pressure distribution.

The results indicate that interface pressure on the compliant foam cushions contoured to the generic shapes were more uniform and had lower peak values than on flat foam cushions and one of the commercially available precontoured cushions. The subjects gave a positive evaluation to the GSC cushions. Seven out of ten subjects chose one of the GSC cushions as their favorite cushion. The comfort and stability of the selected GSC cushion were always judged “better than” or the “same as” the users’ regular cushions. The results also suggest that the ability to design a set of generic shapes by measuring and classifying a group of body-cushion interface shapes is quite valuable when serving clients with a variety of seating and positioning needs.

The approach used and the results derived do appear quite valid on the surface, and may provide a basis from which to provide more off-the-shelf devices that more accurately fit the individual patient's needs. However, the results of this study should be viewed as preliminary and further investigation is necessary to establish a reliable database for different wheelchair user populations and to choose appropriate foam materials.

## CONDENSÉ

La mesure de la forme de l'interface séant-siège est un moyen utilisé avec succès en recherche pour analyser les charges auxquelles sont soumis les tissus mous et fabriquer des coussins moulés génériques. Même si l'efficacité de la forme et de la déformation tissulaires pour caractériser l'interface séant-siège n'a pas été démontrée en clinique affirment Levine et al. (1990), ces deux paramètres fournissent, si on les compare à la mesure des pressions, une mesure directe de l'effet net de la charge externe, des propriétés mécaniques et des conditions aux limites (effets du coussin). Dans une expérience visant à évaluer le confort chez les conducteurs automobiles, Yamazaki (1992) a eu recours à des capteurs souples et minces pour mesurer la forme du contact entre la personne assise et la surface du siège. La forme du contact et la pression sont comparées qualitativement. L'auteur conclut entre autres que les patrons de répartition des pressions fournissent des données utiles pour l'évaluation des sièges, tandis que la mesure des formes de contact fournit des données pouvant servir à leur conception. Sprigle and Schuch (1993) suggèrent que les mesures de la forme du siège complètent les autres mesures effectuées en clinique, notamment les pressions d'interface et les évaluations globales de la posture, pour offrir un portrait global de l'interface séant-siège.

L'utilité des mesures de la forme dans le domaine de l'évaluation clinique reste limitée, pour le moment, à cause des limites techniques, du manque d'expérience et de l'absence de normes, et des coûts élevés. Jusqu'ici, quelques systèmes servant au positionnement personnalisé en fauteuil roulant ont été mis au point pour mesurer la forme du siège. Le *PinDot Shape Sensor* (Invacare Corp., Elyria, Ohio) utilise un système mécanique, dans lequel des tiges traversent une mousse d'une épaisseur de 12.5 cm; le déplacement vertical des tiges est numérisé et constitue la base d'un coussin fabriqué sur mesure. Pour leur part, Kadaba et al. (1984) ont conçu une méthode pour mesurer la forme de la

surface de l'interface séant-siège qui fait appel à des techniques ultrasoniques. Au Rehabilitation Engineering Center de l'université de Virginie (UVA REC), un dispositif appelé *Electronic Shape Sensor* (ESS) a été mis au point pour mesurer les formes d'interface des sièges. Un autre instrument mis au point à l'université de Pittsburgh, le *Computer-Automated Seating System* (CASS), permet de contrôler la forme de la surface du siège tandis qu'on mesure les pressions exercées sur le séant à l'interface. Chang (1996) utilise quant à lui un instrument appelé *Direct Contact Probe Measurement System* pour créer par ordinateur des images en trois dimensions servant à l'évaluation visuelle. Enfin, Yamazaki (1992) a recours à des réseaux de jauges de contraintes (ce sont en fait des rubans plats en métal) pour recréer la forme du siège.

Parmi les systèmes mentionnés ci-dessus, seul le *PinDot Sensor* est actuellement commercialisé; les cinq autres font encore l'objet de recherches et ne sont pas aisément utilisables en milieu clinique. Le *PinDot Sensor*, au demeurant, est passablement onéreux et lourd (structure: 23 kg; module de capteurs pour dossier: 31 kg; module de capteurs pour siège: 21 kg); il ne se transporte pas facilement. En outre, il ne permet pas de mesurer la forme de l'interface quand les usagers s'assoient sur de vrais coussins. Conséquemment, la **première question** de cette thèse de doctorat visait la faisabilité de mettre au point un appareil efficace, de faible coût et facile à utiliser qui permettrait de capter rapidement la forme de l'interface séant-siège en milieu clinique. Ce dispositif de capteur de formes devait être constitué de rubans souples et très minces pouvant être insérés entre le séant et le siège sans perturber la sensation normalement éprouvée par le sujet. Nous avons donc mis au point un appareil de mesure des formes permettant de recueillir des données de base qui devraient s'avérer, croyons-nous, d'une utilité fondamentale pour la conception de surfaces d'appui de forme générique. En outre, nous nous attendons à ce que ce nouvel instrument devienne un outil efficace et rapide pour l'évaluation des coussins et l'élaboration de normes cliniques en matière de prescription.

En offrant une plus grande surface et en réduisant les pics de pression dans la région des tubérosités ischiatiques, du sacrum et du coccyx, les coussins moulés réduisent le risque de plaies de pression et améliorent la tolérance de l'utilisateur en position assise. De manière générale, il est possible de cerner deux grandes approches sur le plan technique dans la conception des coussins moulés destinés à accroître la surface de contact entre le corps et le siège : le coussin générique prémoulé et le coussin moulé sur mesure. Les coussins prémoulés ont une forme concave et symétrique, une approche qui ne convient dans les cas où l'on cherche à obtenir un soutien postural hautement personnalisé. Les coussins moulés sur mesure exigent quant à eux beaucoup de travail et des compétences techniques considérables pour obtenir le soutien recherché. Il paraissait souhaitable, à la lumière de ces constatations, de mettre au point une méthode de conception de coussins préfabriqués de forme générique, offrant un soutien postural mieux ajusté que celui des coussins génériques prémoulés. Par conséquent, la **deuxième question** que nous avons soulevée est la suivante : les formes moulées génériques peuvent-elles mieux répondre aux besoins des différents usagers et permettre une meilleure répartition des pressions ?

L'objet principal de notre projet de recherche porte sur la conception et l'évaluation des coussins pour fauteuils roulants. Nous avons avancé deux hypothèses en relation avec les interrogations soulevées précédemment, l'une d'ordre technique et l'autre, d'ordre clinique :

- Hypothèse d'ordre technique : Il est possible de mettre au point un instrument efficace, de faible coût et facile à utiliser pour mesurer la forme de n'importe quel coussin, que celui-ci supporte la charge d'un usager ou non.
- Hypothèse d'ordre clinique : Il est proposé que les données de base qui seront recueillies grâce au nouvel instrument s'avéreront d'une utilité fondamentale pour la conception de surfaces d'appui de forme générique, capables de répondre aux besoins des différents usagers et d'améliorer la distribution des pressions.

Pour analyser les hypothèses présentées ci-dessus, nous avons proposé quatre objectifs globaux :

1. Mettre au point un nouvel instrument pour mesurer les formes d'interface séant-coussin;
2. Définir des formes génériques qui serviront à fabriquer des coussins moulés de forme générique (GSC);
3. Élaborer une méthode permettant de choisir des coussins GSC appropriés pour les usagers de fauteuil roulant;
4. Effectuer une évaluation clinique des coussins GSC.

Après avoir effectué des recherches sur les dispositifs offerts sur le marché qui auraient pu convenir à la mesure de la forme de l'interface séant-coussin, nous avons procédé à la mise au point d'un appareil efficace et facile à utiliser, que nous avons appelé le *Shape Sensing Array* (SSA), lequel est capable de remplir efficacement cette fonction en milieu clinique.

Le *Shape Sensing Array* (SSA) est un système conçu pour être utilisé en milieu clinique dans le but d'évaluer les formes d'interface séant-siège. Essentiellement, il est constitué d'un ensemble de rubans appelés ShapeTape™ (Measurand Inc., Fredericton, Nouveau-Brunswick, Canada). Le ShapeTape™ est un réseau plat de capteurs à fibre optique insérés dans un ruban souple. Chaque ruban, d'une épaisseur de 1,3 mm et d'une largeur de 12,5 mm, comporte 12 capteurs répartis sur une zone sensible d'une longueur de 480 mm à l'extrémité de cordons de fibres optiques de 1,5 m. Les fibres sont connectées en permanence à une boîte d'interface qui convertit les modulations de l'intensité lumineuse en signaux numériques. Les signaux électriques recueillis par l'ordinateur représentent les torsions et les courbures du ruban à des points géométriques particuliers de chaque fibre optique. On reconstruit ensuite les systèmes de coordonnées

géométriques représentant six degrés de liberté du ruban. De cette manière, la forme du ruban sera représentée par rapport au premier capteur à fibre optique.

La précision des mesures obtenues par le SSA a été évaluée en comparant les résultats aux mesures de référence acquises par le système de numérisation tridimensionnelle MicroScribe3D (Immersion Corp., San Jose, Californie). La précision du MicroScribe3D est de 0,38 mm. On a également effectué des essais pour évaluer la stabilité et la fidélité de notre instrument. Ces essais ont été menés à l'aide d'un appareil appelé Material Testing System (858 Bionix, MTS Systems Corporation, Eden Prairie, Minnesota) pour contrôler la déformation de la matrice SSA. On a suspendu un modèle géométrique rigide représentant la structure des muscles fessiers sur le dispositif hydraulique de l'appareil, lequel est capable de fournir une charge et un déplacement constants. Le modèle d'essai a été fabriqué en Duraform par un procédé de matriçage au laser avec préforme au moyen d'un appareil SLS 2500 (DTM Product Inc., Valencia, Californie).

L'erreur quadratique moyenne relevée pour le système était de 3,79 mm quand les mesures n'étaient pas influencées par la pression, et de 4,72 mm quand elles l'étaient. Les résultats révèlent que la pression uniforme avait une incidence significative sur les mesures du SSA; plus la pression était élevée, et plus les erreurs étaient importantes. La présence de la matrice SSA aura un certain effet sur les conditions au niveau de l'interface, de telle sorte que la forme d'interface mesurée pourrait différer de la forme véritable. Globalement, les mesures du SSA étaient plus précises lorsque aucune pression n'était exercée que dans le cas contraire. De plus, le système SSA est constant dans sa capacité à mesurer les déformations. Il faut donc reconnaître l'influence de la pression sur les mesures de formes d'interface, même s'il n'y a actuellement aucune façon pratique d'évaluer ce facteur.



Selon les résultats obtenus lors des essais, la fidélité de l'instrument SSA est bonne lorsque les conditions sont contrôlées (mesure de la forme de l'interface modèle-coussin). Dans des conditions de laboratoire, la fidélité du capteur même ne dépendait pas de l'étendue de mesure. L'écart moyen quadratique était inférieur à 0,8 mm quel que soit l'endroit où on avait placé le capteur. La fidélité du système était inférieure à 0,38 mm lorsque les conditions de charge étaient contrôlées. Toutefois, dans le cas des mesures des formes d'interface séant-siège, ces lectures se sont révélées moins fidèles, ce qui pourrait être attribuable au repositionnement du sujet.

Le nouveau système SSA permet de mesurer la forme de l'interface séant-siège en temps réel. Les essais de mise en charge indiquent clairement que le système est capable d'effectuer des mesures fidèles et raisonnablement précises de la déformation de l'interface, pouvant être utiles dans un contexte de recherche. Le système SSA permet également de mesurer la forme de l'interface séant-siège quel que soit le type de coussin ou de posture assise. Il fournit un outil permettant d'analyser et de quantifier les relations complexes entre certaines propriétés du siège comme la forme de la surface, la déformation du coussin et la déformation tissulaire sous différentes conditions de charge et de rigidité. Cette capacité devrait s'avérer d'une grande importance pour la recherche clinique. Le SSA permet de recueillir des données de base qui seront, croyons-nous, d'une importance fondamentale pour la conception de surfaces d'appui de forme générique; cela laisse présager que l'instrument pourra devenir un outil clinique des plus utiles.

Il existe peu de méthodes permettant de caractériser et de classer les formes d'interface séant-siège suivant les mesures anthropométriques des sujets. Celles qui ont été mises au point ne proposent qu'une forme unique d'assise par groupe d'utilisateurs de fauteuil roulant. Et même si certains de ces procédés ont servi à prescrire des formes de différentes tailles, les caractéristiques géométriques de celles-ci étaient toutes les mêmes. Un des objectifs de notre projet de recherche était de mettre au point une méthode pour

déterminer s'il était possible, en décelant la variabilité dans les paramètres géométriques des formes d'interface séant-siège, de cerner une ou plusieurs formes génériques d'assise chez un groupe d'utilisateurs ayant des besoins semblables en matière de soutien postural.

Les techniques statistiques de groupement hiérarchique ont servi à résoudre un large éventail de problèmes de recherche. Contrairement aux autres procédés statistiques, les méthodes d'analyse par classification hiérarchique sont utilisées dans les cas où il n'y a pas d'hypothèse a priori, alors que les travaux de recherche en sont encore à une phase exploratoire. En un sens, l'analyse hiérarchique permet d'établir quelle est la « la solution la plus probable ». Dans notre projet de recherche, nous ne savions pas au préalable combien de formes génériques il faudrait concevoir pour une population d'utilisateurs spécifique. C'est pourquoi il a été nécessaire d'avoir recours à l'analyse par classification hiérarchique pour classer un groupe de formes d'interface en différentes grappes, en fonction des similitudes et des distances entre elles (dissimilitudes). Pour calculer les mesures de similitude des formes d'interface, on a défini des paramètres géométriques permettant d'effectuer une analyse quantitative de la forme.

Pour chacune des formes, cinq contours horizontaux, trois courbes longitudinales dans la direction A-P (antéro-postérieure) et deux courbes transversales dans la direction M-L (médio-latérale) ont été identifiées. À l'aide de ces courbes et contours, il est possible de retenir la plus grande part des données sur la forme et d'en révéler les caractéristiques géométriques. Pour chacune des formes, la position des courbes et contours sont établis selon un pourcentage spécifique de la longueur, de la largeur et de la hauteur (par exemple, la position de la Courbe I correspond à 30 % de la largeur de la forme). Dans le but de fournir une description globale de la forme d'interface séant-siège, on a mesuré neuf (9) paramètres géométriques sur les courbes longitudinales A-P, quatre (4) paramètres sur les courbes transversales M-L, deux (2) paramètres sur les contours horizontaux et deux (2) paramètres sur la forme 3-D entière. Une liste de 17 paramètres

a ainsi été obtenue pour chacune des formes d'interface, sur lesquels on a effectué une analyse par classification hiérarchique a été effectuée pour déceler les regroupements naturels entre elles.

On a eu recours à la méthode de classification hiérarchique de Ward (STATISTICA 5.1, StatSoft Inc. Oklahoma) pour constituer un arbre hiérarchique (un dendogramme). À la base de cet arbre, chaque observation (la forme 3-D dans notre cas) représente sa propre grappe. Ensuite, de plus en plus d'observations sont regroupées, tandis que des grappes de plus en plus grandes contenant des éléments dissimilaires se constituent. À la dernière étape, toutes les observations sont regroupées. Par conséquent, à chaque nœud du dendogramme (là où une nouvelle grappe s'est formée), il est possible de vérifier le critère de mesure de la distance métrique selon lequel les éléments respectifs ont été regroupés en une nouvelle grappe. Lorsque les données comportent une « structure » définie par des groupes d'observations semblables, cette structure sera alors souvent représentée dans l'arbre hiérarchique sous forme de branche distincte.

L'analyse hiérarchique se fonde sur les distances entre les observations pour former des grappes. Le moyen le plus simple de quantifier les dissimilitudes entre les observations recueillies dans un espace multidimensionnel est de calculer les distances euclidiennes. Le nombre de dimensions dépend du nombre de variables (de mesures, dans ce cas-ci) comprises dans le calcul. Puisque les variables (les mesures) utilisées dans cette recherche ne sont pas exprimées par les mêmes unités (degrés, mm. etc.), il a été nécessaire d'avoir recours à une mesure d'une distance dérivée (produit-moment de Pearson) pour quantifier les dissimilitudes entre les formes.

Pour déterminer le nombre optimal de grappes correspondant aux différentes observations, on a mené une analyse des ratios R. Ce ratio mesure la réduction de la variance au sein d'une grappe. Le ratio R se définit ainsi:

$$R = \left[ \frac{e(N,K)}{e(N,K+1)} - 1 \right] (N - K + 1)$$

où  $e(N,K)$  est la somme quadratique des distances intra-grappes pour  $N$  observations et  $K$  grappes. Le nombre de grappes optimal est choisi lorsque le ratio  $R$  atteint une valeur maximale (souvent supérieure à 2). Une valeur de  $R$  maximale signifie une réduction importante dans la variance intra-grappe, et une homogénéité des grappes. Une fois que les grappes ont été définies, la forme moyenne correspondant à chaque grappe est générée et considérée en tant que forme générique.

L'hypothèse selon laquelle l'analyse des dissimilitudes entre les paramètres de forme géométrique permettrait de définir un ensemble de formes génériques a d'abord été vérifiée sur un groupe de formes d'interface recueillies chez un groupe de sujets âgés. Quatre formes distinctes ont été définies parmi un groupe de 30 sujets âgés. Étant donné que les données sur les formes d'interface ont été obtenues à l'université de Pittsburgh, il n'a pas été possible, pour des raisons d'ordre pratique, de tester ces formes génériques sur ces sujets. Toutefois, nos résultats ont confirmé qu'il existe des formes génériques d'interface séant-siège multiples, et que le classement de ces formes permettrait de fournir des renseignements utiles sur les paramètres géométriques des formes.

À la lumière de ces résultats, on a constitué une base de données sur les formes d'interface séant-siège à l'aide du système SSA précédemment mis au point. Puisque les usagers de fauteuil roulant répondront très différemment au même coussin d'une population à l'autre, et qu'il n'existe aucun coussin parfaitement adapté à une population spécifique, notre premier objectif était d'appliquer la technique des formes génériques à des usagers nécessitant un soutien postural de léger à modéré, et ne présentant aucune difformité pelvienne importante. Quatorze sujets (6 femmes et 8 hommes) ont été recrutés au Centre de réadaptation Lucie-Bruneau. On a consigné leurs caractéristiques anthropométriques et une description clinique de leur posture assise.

On a divisé les sujets en deux groupes : le premier a servi à la cueillette de données sur les formes d'interface et le second, à l'évaluation. Le premier groupe (G-I) comprenait neuf sujets; les formes d'interface qui leur correspondaient ont servi à établir une base de données à partir de laquelle on a défini un ensemble de formes génériques. Le deuxième groupe (G-II) comprenait cinq sujets à qui il a été demandé d'évaluer les coussins GSC. Cinq sujets du premier groupe ont également été rappelés pour se prononcer sur les coussins GSC; ils forment le sous-groupe G-I<sub>5</sub>.

Pour chacun des sujets du groupe G-I, on a mesuré la forme de l'interface séant-siège à l'aide du système SSA; le sujet était assis sur un coussin plat de 3" en mousse de polyuréthane que l'on avait placé sur un simulateur de positionnement. Cinq essais ont été répétés pour chacun des neuf sujets du groupe G-I. Les quarante-cinq formes d'interface ainsi obtenues (9 sujets x 5 essais) ont servi à définir des formes génériques. Les résultats de l'analyse par classification hiérarchique ont permis de cerner trois grappes; on a considéré la forme moyenne de chacune de ces grappes comme étant la forme générique recherchée. On a ensuite transféré ces formes génériques sur une machine automatique d'usinage des coussins, pour les sculpter dans une mousse de polyuréthane HR45 de 10 cm (4"), laquelle présente les mêmes caractéristiques que la mousse utilisée lors de la collecte de données. Tous les coussins GSC obtenus ont été recouverts d'une housse en néoprène imperméable.

Dix sujets ont participé à l'évaluation des coussins GSC. Cinq d'entre eux provenaient du groupe G-I et cinq du groupe G-II. Tous les coussins GSC ont été évalués par chacun des sujets dans le but de confirmer l'hypothèse à l'effet que le coussin GSC choisi à l'aide de l'indice de similitude offrirait une meilleure répartition des pressions que les autres coussins GSC. On a comparé les coussins GSC sélectionnés aux coussins GSC non retenus, dans le but d'évaluer quatre aspects : la répartition des pressions, la posture, le confort et la stabilité dynamique. La pression a été mesurée au moyen d'un système

de mesure des pressions (*Force Sensing Array*, FSA mat, Vista Medical Ltd., Winnipeg, Canada). Pour mesurer la posture, neuf repères anatomiques ont été numérisés à l'aide du Micro-Scribe 3D (Immersion Corp., San Jose, Californie). Le confort a été évalué à l'aide d'un questionnaire. On a en outre comparé les coussins GSC sélectionnés à deux coussins génériques prémoulés.

Les résultats de l'évaluation sur la répartition des pressions d'interface révèlent que la pression moyenne était inférieure sur le coussin GSC choisi au moyen de l'indice de similitude par rapport aux coussins non retenus. La méthode fondée sur l'indice de similitude a donc fourni des renseignements utiles pour choisir un coussin GSC offrant une répartition optimale des pressions.

Les données obtenues indiquent que si on les compare aux coussins plats en mousse et à l'un des coussins prémoulés vendus sur le marché, les coussins de mousse souple de forme générique offraient une répartition plus uniforme des pressions et des pics de pression moins élevés. Les sujets ont quant à eux donné une évaluation favorable aux coussins GSC. Sept sujets sur dix ont indiqué leur préférence pour l'un des coussins GSC. Les sujets ont jugé que le confort et la stabilité du coussin GSC choisi étaient « supérieurs » ou « équivalents » par rapport au coussin qu'ils utilisent régulièrement. Les résultats suggèrent aussi que la capacité de concevoir un ensemble de formes génériques à partir de l'analyse et de la classification d'un groupe de formes d'interface séant-siège est un atout pour qui cherche à satisfaire des clients aux besoins variés en matière de positionnement.

À première vue, l'approche que nous avons adoptée et les résultats qui en découlent semblent valides et pourraient constituer une base à partir de laquelle il serait possible d'offrir des coussins de série mieux adaptés aux besoins particuliers des patients. Il faut toutefois considérer que ce ne sont là que des résultats préliminaires; les recherches

futures permettront d'établir des bases de données fiables sur les différentes populations d'utilisateurs de fauteuil roulant et de choisir des mousses adéquates.

Puisque la forme moulée des sièges dépend d'un ensemble de facteurs, les formes génériques obtenues peuvent varier grandement quand l'un de ces derniers change. D'abord, les propriétés biomécaniques des structures tissulaires et musculaires varient d'une population d'usagers à l'autre. Ensuite, le poids corporel et le tonus musculaire d'un individu peuvent varier dans le temps. Les sujets choisis pour réaliser ce projet appartenaient à une même catégorie, définie de la manière suivante : ils nécessitaient un soutien postural de léger à modéré et ne présentaient aucune difformité pelvienne importante. La rigidité et l'épaisseur des tissus mous différaient d'un sujet à l'autre, selon la nature du diagnostic : sclérose en plaques, amputation des deux jambes, paralysie cérébrale ou traumatisme cérébral. Si l'on élargissait la base de données sur les formes d'interface pour chacune de ces populations, par conséquent, on pourrait s'attendre à mieux saisir les relations complexes entre les facteurs propres à l'assise comme la déformation des tissus, la forme de la surface et la pression d'interface. De plus, la forme du siège dépend aussi des caractéristiques du coussin. Les caractéristiques du sujet étant généralement fixes, le seul moyen d'adapter les paramètres physiques est de modifier les caractéristiques des coussins. Comme ce projet de recherche le démontre, les coussins moulés de forme générique ne représentent pas une solution optimale pour tous les sujets. Changer la rigidité de la mousse pourrait être une autre voie de solution, puisque celle-ci a un effet sur le transfert des charges et, en dernière instance, sur la forme du coussin. Ces réflexions suggèrent qu'il faudra, dans le futur, approfondir l'analyse sur l'effet de la rigidité et de l'épaisseur en relation avec l'efficacité du coussin GSC. Enfin, la distribution du poids est un autre facteur ayant incidence très importante sur la forme du coussin. Grâce à la mise au point du système SSA, l'analyse des formes permet d'obtenir des données cliniques très utiles sur la répartition des surfaces de charge du coussin. Par conséquent, les mesures relatives aux formes complémentent les

autres mesures comme la pression d'interface et l'analyse de la posture, pour fournir, en définitive, un portrait global de l'interface séant-coussin.



## TABLE OF CONTENTS

ACKNOWLEDGEMENTS.....	IV
RÉSUMÉ.....	VI
ABSTRACT.....	XI
CONDENSÉ .....	XV
TABLE OF CONTENTS.....	XXVIII
LIST OF TABLES .....	XXXIV
LIST OF FIGURES .....	XXXVII
LIST OF INITIALS AND ABBREVIATIONS.....	XLI
INTRODUCTION.....	1
CHAPTER 1 LITERATURE REVIEW .....	4
1.1    ANATOMICAL STRUCTURE.....	5
1.1.1    Anatomical structure of the pelvis .....	5
1.1.2    Anatomical structure of the spine .....	6
1.1.3    Muscles moving the pelvis.....	7
1.1.4    Anatomy of the buttocks .....	8
1.1.5    Bi-ischial distance .....	9
1.1.6    Biomechanics of seating .....	10
1.2    WHEELCHAIR USER POPULATIONS.....	12
1.3    SEATING PROBLEMS AND SOLUTIONS .....	14
1.3.1    Postural problems.....	15
1.3.2    Pressure ulcers.....	15
1.3.2.1    Cause of pressure ulcers.....	16

1.3.2.2	Prevention of pressure ulcers .....	18
1.3.3	Discomfort .....	20
1.3.4	Instability .....	20
1.4	SEATING SYSTEMS AND SEAT CUSHIONS.....	21
1.4.1	Classification of seating systems .....	22
1.4.2	Types of seat cushions .....	25
1.4.2.1	Fluid floatation cushions.....	26
1.4.2.2	Polyurethane foam cushions .....	28
1.4.2.3	Oscillating (dynamic) designs.....	31
1.4.2.4	Hybrid designs .....	32
1.4.3	Selection of seat cushions and seating systems.....	32
1.4.4	Seating system evaluation .....	33
1.4.4.1	Pressure measurement evaluation .....	34
1.4.4.2	Shear measurement evaluation.....	37
1.4.4.3	Shape measurement evaluation.....	38
1.4.4.4	Sitting stability evaluation .....	40
1.4.4.5	Comfort evaluation .....	41
1.5	SHAPE MEASUREMENTS IN SEATING .....	43
1.5.1	Body or seat surface shape measurements.....	43
1.5.2	Body-seat interface shape measurements .....	45
1.5.3	Summary .....	52
1.6	MULTIVARIATE ANALYSIS METHODS.....	55
1.6.1	Principal component analysis.....	55
1.6.1.1	Population principal components.....	56
1.6.1.2	Sample principal components .....	57
1.6.2	Discrimination and classification.....	58
1.6.2.1	Fisher's method for two populations .....	59
1.6.2.2	Classification methods .....	60
1.6.2.3	Discrimination methods .....	62

1.6.3	Cluster analysis .....	63
1.6.3.1	Similarity measures .....	63
1.6.3.2	Hierarchical clustering methods.....	66
1.6.3.3	Nonhierarchical clustering methods.....	69
1.6.3.4	Comparison of K-means method with hierarchical methods.....	70

## **CHAPTER 2 HYPOTHESIS, OBJECTIVES AND GENERAL APPROACH OF THE PROJECT.....72**

2.1	PROBLEM STATEMENT.....	72
2.2	HYPOTHESES .....	74
2.3	OBJECTIVES .....	75
2.3.1	General objectives .....	75
2.3.2	Specific objectives .....	75
2.4	GENERAL APPROACH OF THE PROJECT.....	76
2.4.1	Stage one: Using a similarity index to compare two seat support surface shapes 78	
2.4.2	Stage two: Determination of generic shapes from a group of shapes .....	78

## **CHAPTER 3 USING SIMILARITY INDEX TO COMPARE TWO SEAT SUPPORT SURFACE SHAPES.....81**

3.1	OBJECTIVES .....	81
3.2	METHODOLOGY .....	81
3.2.1	Shape measurements .....	81
3.2.2	Definition of curve parameters .....	83
3.2.3	Similarity Index.....	84
3.3	RESULTS & DISCUSSION .....	86
3.4	CONCLUSION.....	86

## **CHAPTER 4 ARTICLE 1: DETERMINATION OF GENERIC BODY-SEAT INTERFACE SHAPES BY CLUSTER ANALYSIS.....88**

4.1	ABSTRACT.....	89
4.2	INTRODUCTION.....	90
4.3	METHODS.....	93
4.3.1	Subject Group Description.....	93
4.3.2	Shape Measurements.....	93
4.3.3	Geometric Parameters Identification .....	94
4.3.4	Statistical Analysis .....	100
4.4	RESULTS .....	102
4.5	DISCUSSION .....	107
4.6	CONCLUSION.....	111
<b>CHAPTER 5 ARTICLE 2: DEVELOPMENT AND EVALUATION OF A NEW BODY-SEAT INTERFACE SHAPE MEASUREMENT SYSTEM.....</b>		<b>112</b>
5.1	ABSTRACT.....	113
5.2	INTRODUCTION.....	114
5.3	DESCRIPTION OF THE SSA SYSTEM.....	116
5.4	VALIDATION OF THE SYSTEM.....	119
5.4.1	Accuracy of SSA Measurements .....	119
5.4.1.1	Test 1: Assessing the accuracy without the influence of pressure .....	119
5.4.1.2	Test 2: Assessing the influence of uniform pressure .....	121
5.4.1.3	Test 3: Assessing the influence of cover materials .....	122
5.4.1.4	Test 4: Assessing the accuracy under the influence of non-uniform pressure	123
5.4.2	Stability and Repeatability of SSA Measurements .....	125
5.4.2.1	Test 5: Assessing the stability .....	126
5.4.2.2	Test 6: Assessing the repeatability.....	127
5.4.3	Data Analysis .....	127
5.5	RESULTS .....	128
5.5.1	Accuracy of SSA Measurements .....	128

5.5.1.1	Test 1: Assessing the accuracy without the influence of pressure .....	129
5.5.1.2	Test 2: Assessing the influence of uniform pressure .....	129
5.5.1.3	Test 3: Assessing the influence of cover materials .....	131
5.5.1.4	Test 4: Assessing the accuracy under the influence of non-uniform pressure	132
5.5.2	Repeatability and Stability of SSA Measurements .....	133
5.5.2.1	Test 5: Assessing the stability .....	133
5.5.2.2	Test 6: Assessing the repeatability .....	134
5.6	DISCUSSION .....	134
5.6.1	Accuracy of the System .....	134
5.6.2	Repeatability and stability of SSA measurements .....	136
5.7	CONCLUSION .....	137

## **CHAPTER 6 ARTICLE 3: DESIGN AND EVALUATION OF GENERIC SHAPE CONTOURED CUSHIONS BASED ON A NEW INTERFACE SHAPE**

### **MEASUREMENT SYSTEM .....138**

6.1	ABSTRACT .....	139
6.2	INTRODUCTION .....	140
6.3	METHODS .....	142
6.3.1	Subjects .....	142
6.3.2	Instrumentation .....	143
6.3.3	Protocol .....	145
6.4	RESULTS .....	151
6.5	DISCUSSION .....	158
6.6	CONCLUSION .....	162

## **CHAPTER 7 CLINICAL EVALUATION AND COMPARISON OF GENERIC SHAPE CONTOURED CUSHIONS WITH TWO STANDARD**

### **PRECONTOURED CUSHIONS.....163**

7.1	INTRODUCTION .....	163
-----	--------------------	-----

7.2	METHODS.....	164
7.3	RESULTS .....	167
7.4	DISCUSSION & CONCLUSION .....	169
<b>CHAPTER 8 GENERAL DISCUSSION.....</b>		<b>171</b>
8.1	BODY-CUSHION INTERFACE SHAPE MEASUREMENTS .....	171
8.2	DESIGN OF GENERIC SHAPE CONTOURED CUSHIONS .....	174
8.3	EVALUATION OF GENERIC SHAPE CONTOURED CUSHIONS.....	177
<b>CHAPTER 9 CONCLUSION .....</b>		<b>182</b>
<b>BIBLIOGRAPHY .....</b>		<b>185</b>
<b>APPENDIX .....</b>		<b>202</b>

## LIST OF TABLES

Table 1-1 Soft tissue coverage of pressure points (From Daniel and Faibisoff, 1982). ....	9
Table 1-2 Distance between midpoints of ischial tuberosities (From Akerblom, 1948). 10	
Table 1-3 Percent of wheelchair users by disability etiology (Cooper, 1998).....	13
Table 1-4 External factors in pressure ulcer formation (Summarized from Crenshaw and Vistnes, 1989, Barbenel, 1991, Webster, 1991, Patterson and Bennett, 1995, Van Marum et al., 2002).....	18
Table 1-5 Internal factors in pressure ulcer formation (Summarized from Zacharkow, 1984, Crenshaw and Vistnes, 1989, Barbenel, 1991, Webster, 1991, Patterson and Bennett, 1995).....	18
Table 1-6 Major characteristics of popular types of seat cushions (Wilson, 1992).....	25
Table 1-7 Comparisons of planar, precontoured and custom contoured cushions (Ward, 1994). ....	29
Table 1-8 Factors that affect the wheelchair cushion selection (Ferguson-Pell, 1990). ...	33
Table 1-9 Comparison of electropneumatic, pneumatic, hydraulic, and electronic pressure sensors (Summarized from Kosiak, 1959, Souther et al., 1974, Reger et al., 1988, Allen et al., 1993a & 1993b, Ferguson-Pell and Cardi, 1993, Gyi et al., 1998). .....	36
Table 1-10 Comparison of various types of electronic pressure sensors for internal and external measurements (Webster, 1991).....	37
Table 1-11 Mean pressures under the ischial tuberosities for the four cushion types (Webster, 1991). ....	37
Table 1-12 Comparison of the two shape sensors: S1280CS ShapeTape™ (Measurand Inc, Fredericton, NB, Canada) and Rachismetre (Biogest, Denain, France).....	55
Table 1-13 Counts of binary variables for two items (Everitt, 1993). ....	65
Table 1-14 Similarity coefficients for binary data (Johnson and Wichern, 1988).....	66

Table 1-15 Comparisons of single-linkage, complete-linkage and average linkage clustering methods (Summarize from Aldenderfer, 1984, Johnson and Wichern, 1988, Everitt, 1993).	69
Table 3-1 Digitized Interval.	82
Table 3-2 Similarity index	86
Table 4-1 Article 1: Significant Scheffé post hoc test results across the four clusters.	104
Table 4-2 Article 1: Coefficient of correlation between measurements P1 to P17 which contribute to distinguish the four clusters. Only significant values of $ r $ which are greater than 0.35 are presented.	105
Table 4-3 Article 1: Mean values of measurements P1 – P17 for the entire group and four clusters. $p$ values obtained from one-way ANOVA are listed in the last column.	106
Table 4-4 Article 1: Mean and standard deviation values for BMI, weight, height and age data for cluster C1 to C4 and entire group.	107
Table 5-1 Article 2: The accuracy of SSA measurements in the Z direction under different conditions	130
Table 5-2 Article 2: Error of SSA measurements in the Z direction under different uniform pressures. RMS: Root Mean Square. SD: standard deviation (N=3).	131
Table 5-3 Article 2: Repeatability of the sensors in the SSA system (standard deviation of 10 trials). All the values are in mm.	134
Table 6-1 Article 3: Characteristics of subjects.	144
Table 6-2 Article 3: Similarity indexes between the subjects' interface shapes and the generic shapes.	155
Table 6-3 Article 3: Comparison of static pressure variables between selected GSC cushion, rejected GSC cushions and flat cushion.	156
Table 6-4 Article 3: Comparison of posture variables between selected GSC cushion, rejected GSC cushions and flat cushion.	157



Table 6-5 Article 3: Comparison of stability variables between selected GSC cushion and rejected GSC cushions, as well as subjective evaluation of the comfort and stability.....	158
Table 7-1 Comparison of pressure distribution variables between the GSC, ISCUS and LB cushions on ten subjects. * indicates significant difference at $p < 0.05$ between the GSC cushion and the LB cushion. † indicates significant difference at $p < 0.05$ between the ISCUS cushion and the LB cushion. ....	168
Table 7-2 Comparison of posture variables between the GSC, ISCUS and LB cushions on ten subjects. * indicates significant difference at $p < 0.05$ between the GSC cushion and the LB cushion. † indicates significant difference at $p < 0.05$ between the GSC cushion and the ISCUS cushion. ....	168
Table 7-3 Comparison of dynamic stability variables between the GSC, ISCUS and LB cushions on ten subjects, as well as subjective evaluation on the comfort and stability. * indicates significant difference at $p < 0.05$ between the GSC cushion and the LB cushion. † indicates significant difference at $p < 0.05$ between the GSC cushion and the ISCUS cushion. ....	169
Table Appendix-1 Postura problem in the pelvis (Summarized from Zollars, 1993, Trefler et al., 1993, Ward, 1994, Mayall and Desharnais, 1995, Letts, 1991). ....	202
Table Appendix-2 Postural problem in the lower extremities (Zollars, 1993, Trefler et al., 1993, Ward, 1994, Mayall and Desharnais, 1995, Letts, 1991). ....	203
Table Appendix-3 Postural problem in the trunk (Zollars, 1993, Trefler et al., 1993, Ward, 1994, Mayall and Desharnais, 1995, Letts, 1991). ....	204
Table Appendix-4 Postural problem in the head and neck (Zollars, 1993, Trefler et al., 1993, Ward, 1994, Mayall and Desharnais, 1995, Letts, 1991). ....	204
Table Appendix-5 Postural problem in the upper extremities (Zollars, 1993, Trefler et al., 1993, Ward, 1994, Mayall and Desharnais, 1995, Letts, 1991). ....	205

## LIST OF FIGURES

Figure 1-1 The pelvis from the front (Hollinshead, 1974).....	6
Figure 1-2 The lateral view of the right hip bone (Hollinshead, 1974). ....	6
Figure 1-3 The vertebral column from the front and the side (Hollinshead, 1974). ....	7
Figure 1-4 The muscles moving the pelvis (Engström, 1993). ....	8
Figure 1-5 With the hip flexed in the sitting position, the gluteus maximums muscle slides superolaterally off the ischial tuberosity (Zacharkow, 1984). ....	9
Figure 1-6 Dimensions of the ischial tuberosities and perineum, pertaining to toilet seat design (McClelland and Ward, 1976). All measurements are in inches. ....	10
Figure 1-7 Shaped cushions help share the supporting forces $F_I$ and $F_T$ more equally between the ischial tuberosities ( $F_I$ ) and the trochanters ( $F_T$ ). On cushions with no shaping $F_I$ is considerably larger than $F_T$ and the ITs have to compress the cushion nearly 2 inches before the trochanters make contact (Ferguson-Pell, 1990). ....	12
Figure 1-8 Acceptable pressure/time interval guideline (Reswick and Rogers, 1976). ....	17
Figure 1-9 Generic classification of seating systems (Medhat and Hobson, 1992). ....	23
Figure 1-10 Examples of different seat cushions (Wilson, 1992). ....	24
Figure 1-11 The Roho cushion has individual air cells interconnected at the base (Roho Inc., IL). ....	27
Figure 1-12 Polymeric foams used for cushions (a) Closed cell. (b) Open cell. (c) Reticulated cell (Tang, 1991). ....	29
Figure 1-13 Viscoelastic foams can be modeled as a spring-dashpot-system (Tang, 1991). .....	31
Figure 1-14 (a) Cast measuring system using stainless steel rods (b) Ethafoam slabs stacked together to form the contoured cushion after being cut by a band saw (McGovern et al., 1988). ....	43
Figure 1-15 (a) Electronic Contour Measurement System (b) Display of the contour data. (Neth et al., 1989). ....	44
Figure 1-16 Digitization on the contour surface (Lemaire et al. 1996). ....	45

Figure 1-17 The ultrasound transducer emits a pulse that measures distance to the buttocks by time of flight (Kadaba et al., 1984). .....	46
Figure 1-18 Ultrasonic images of the buttocks from a single subject under three conditions: (a) suspended; (b) load/no EMS; (c) load/EMS (Levine et al., 1990). ..	47
Figure 1-19 Structure and arrangement of the developed tape sensor (size in mm) (Yamazaki, 1992).....	48
Figure 1-20 Computer-aided shape sensor (Sprigle and Schuch, 1993).....	49
Figure 1-21 Electronic Shape Sensor (ESS) used to measure the seated shape (Brienza et al., 1991). .....	50
Figure 1-22 Computer-Aided Seating System (CASS) (Brienza et al., 1996a).....	50
Figure 1-23 Direct contact probe system for subject-seatpan and seatback interface contour measurements (Chang et al., 1996). .....	51
Figure 1-24 PinDot Shape Sensor (Invacare Corporation, Elyria, OH).....	52
Figure 1-25 Illustration of shape sensor: SHAPE TAP (Measurand Inc, Fredericton, NB, Canada). .....	54
Figure 1-26 Illustration of shape sensor: Rachismetre (Biogest, Denain, France). .....	54
Figure 1-27 A pictorial representation of Fisher's procedure for two populations with $p=2$ (Johnson and Wichern, 1988).....	59
Figure 1-28 Inter-cluster distance (dissimilarity) for (a) single linkage, (b) complete linkage, and (c) average linkage (Johnson and Wichern, 1988).....	67
Figure 2-1 Schematic presentation of the different stages of the study.....	77
Figure 3-1 Local and global parameters defined on lateral curve.....	84
Figure 4-1 Article 1: (a) Location of five contours on a 3-D body-seat interface shape. (b) Location of five cross-sectional curves on the top view of the shape. ....	95
Figure 4-2 Article 1: (a) Location of Contour-1 and Contour-5 and sagittal plane which divides the shape into right and left parts; (b) Front view of the shape; (c) Contour-1; (d) Contour-5. ....	97
Figure 4-3 Article 1: (a) Curve-I; (b) Curve-II; (c) Curve-III; (d) Curve-IV; (e) Three-D interface shape; (f) Curve-V. ....	98

Figure 4-4 Article 1: Dendrogram of the cluster analysis for 30 shapes. Horizontal axis denotes the linkage distance (Pearson Product Moment correlation coefficient). At a distance level of 0.2, four clusters (C1 to C4) can be distinguished. The number listing on the vertical axis presents the identification number for the subject's interface shape. The order of the number is decided by the procedure of hierarchical method. ....	101
Figure 4-5 Article 1: Mean shapes of Clusters C1-C4.....	103
Figure 5-1 Article 2: Illustration of a SSA system. (1) ShapeTape™; (2) Interface boxes of ShapeTape™s; (3) Serial cable with a power inlet connector; (4) 4x1 serial-USB converter; (5) fixture-A; (6) fixture-B. The cove of the SSA is not shown in the figure.....	117
Figure 5-2 Article 2: Illustration of the experimental setup for assessing the accuracy without the influence of pressure. (a) Front view; (b) top view. ....	120
Figure 5-3 Article 2: Illustration of the SSA mat between different interface materials. (a) Between a rigid wood board and an inflator bag; (b) between a nylon cushion and an inflator bag; (c) between a neoprene cushion and an inflator bag; and (d) between two layers of neoprene cushions.....	122
Figure 5-4 Article 2: Illustration of the configuration for test 5 and 6 (top view).....	126
Figure 5-5 Article 2: Mean errors in the Z direction under 13.3 kPa (100 mmHg) pressure for different interfaces: (a) Between rigid wood board and inflator bag; (b) between nylon cushion and inflator bag; (c) between neoprene cushion and inflator bag; (d) between two layers of neoprene cushions. SD: standard deviation (N=3). ....	132
Figure 6-1 Article 3: Illustration of a Shape Sensing Array (SSA) system mounted on a seating simulator. ....	146
Figure 6-2 Article 3: Dendrogram of the cluster analysis for 45 shapes. The horizontal axis denotes the linkage distance (Pearson Product Moment correlation coefficient). At a distance level of 0.1, three clusters (C1 to C3) can be distinguished. The number listing on the vertical axis presents the identification number for the	

interface shapes. The order of the number is decided by the procedure of the hierarchical method.....	153
Figure 6-3 Article 3: Top view of the contour shapes of the generic shape contoured cushions. (a) cushion C1; (b) cushion C2; (c) cushion C3. The numbers are the depth of the contour in mm. The size of the cushion is 457x 457 mm (18"x18")..	154
Figure 7-1 Photographs of three generic shape contoured cushions. (a) cushion C1; (b) cushion C2; (c) cushion C3.....	165
Figure 7-2 Photograph of ISCUS cushion (Orthofab Inc., Quebec, Canada).....	166
Figure 7-3 Photograph of LB cushion (Lucie-Bruneau Rehabilitation Center, Montreal, Canada).....	166

## LIST OF INITIALS AND ABBREVIATIONS

2D	two dimensional
3D	three dimensional
AC	contact area
ANOVA	analysis of variance
A-P	anterior-posterior
ASIS	Anterior Superior Iliac Spine
BMI	body mass index
CASS	Computer-automated (aided) Seating System
Chaire ATP	Chaire industrielle CRSNG sur les aides à la posture
CMM	coordinate measuring machine
COP	center of pressure
CRSNG	Conseil de Recherches en Sciences Naturelles et en Génie du Canada
CT	computerized tomography
ECM	Expected Cost of Misclassification
EMS	electrical muscle stimulation
ESS	Electronic Shape Sensor
FES	Functional electrical stimulation
Fonds FCAR	Fonds pour la Formation de Chercheurs et l'Aide à la Recherche
FSA	Force Sensing Array
GSC	Generic Shape Contoured
HAA	Hip Abduction/Adduction
HFE	Hip Flexion/Extension
HR	High Resiliency
IFD	Indentation Force Deflection
IT	Ischial Tuberosity
LIS3D	Laboratoire informatique de Scoliose 3D

LIVIA	Laboratory for Imagery, Vision and Artificial Intelligence
MCD	maximum covered distance
MIA	maximum value of the index of asymmetry
M-L	medial-lateral
MP	mean pressure
MRI	magnetic resonance imaging
MS	Multiple Sclerosis
NSERC	Natural Sciences and Engineering Research Council of Canada
PG	peak pressure gradients
PO	Pelvic Obliquity
PP	peak pressure
PT	Pelvic Tilt
PTR	Pelvic Transverse Rotation
SCI	spinal cord injury
SD	standard deviation
SDP	standard deviation of pressure-distribution
SSA	Shape Sensing Array
T4G	mean of the top 4 gradients
T4P	mean of the top 4 pressures
TFE	Trunk Flexion/Extension
TSL	Thigh Sagittal Angle

## INTRODUCTION

Measuring the shape of the body-seat interface has been used successfully in research to study tissue loading and to fabricate custom contoured cushions. Levine et al. (1990) stated that the tissue shape and deformation as a characterization of the seating interface, provide a more direct measure of the net effect of external load, mechanical tissue properties, and boundary conditions (cushion effects) than pressure measurements. Yamazaki (1992) used flexible, thin tape sensors to measure contact shape between a seated person and the seat surface in an effort to evaluate sitting comfort. Contact shape and pressure were compared qualitatively. Among other things, the author concluded that pressure patterns provide data for seat evaluation, while contact shape data provide data for seat design. Sprigle and Schuch (1993) suggested that seat contour measurements complement other clinical measures, such as seat interface pressures and general postural assessments, to form a more complete picture of the buttock-cushion interface. However, the usefulness of shape measurements for clinical evaluation is restricted at the present time due to technical limitations, lack of experience and standards, and high costs.

The primary role of a wheelchair seat cushion is to provide an effective platform from which the user may perform a wide range of tasks. For many users, the cushion performs a crucial function by reducing the concentration of pressure in soft tissues, thereby helping to prevent the formation of pressure ulcers. Theoretical and experimental data has shown that a properly fitted contoured cushion would improve the pressure distribution and reduce tissue distortion. The two basic technological approaches that have been used to design a contoured seat are the standard precontoured cushion technique and the custom-contoured cushion technique. The standard precontoured cushions are available off the shelf but they are inappropriate when intimately fitting body support is needed. The custom contoured cushions can provide intimate seating



support but they are usually labor-intensive and require considerable technical skill. It is desirable to develop a new approach for designing contoured cushions which not only are available off the shelf but also provide more intimate fit to the body support than do standard precontoured cushions.

Therefore, the main motivation of this work was to provide a research tool to advance the state-of-the-art in body-seat interface shape measurement and seat support surface design. Therefore, the first objective of this study was to develop an efficient, low-cost and easy to use device for rapidly capturing the body-cushion interface shape in a clinical setting. The shape sensing device has to be flexible and very thin so that it could be placed between the subject and the seat without disturbing the subject's natural feeling. The second objective of this study was to develop an interface shape analyzing technique to design generic shape contoured (GSC) cushions and develop a method for selecting appropriate GSC cushions for wheelchair users based on the interface shape measurements obtained from the newly developed shape sensing device.

This thesis includes three articles that were published in or submitted to peer-reviewed journals. To introduce the articles, a literature review on seating and positioning technology, shape measurement techniques, and statistical analysis techniques for shape discrimination (Chapter 1), and the problem statement, hypothesis, and objectives of the overall thesis (Chapter 2) are presented. In the first stage of the study, a similarity index method was developed to compare two shapes (Chapter 3). However, as the similarity index could only be used to discriminate two shapes it is only used for shape selection. Determination of generic shapes from a group of interface shapes is solved by means of cluster analysis and is presented in article #1 (Chapter 4). A new shape measurement system based on optical fiber technology, which is described in article #2 (Chapter 5), has been developed to capture body-cushion interface shape in real-time. The design and evaluation of GSC cushions are presented in article #3 (Chapter 6) as well as comparison of GSC cushions with two standard precontoured cushions (Chapter 7). The

general results obtained in this study thus allowed us to make several conclusions and recommendations (Chapters 8 and 9). The initial finding of this study, along with further analysis on a larger sample and on different wheelchair populations, will give insight into this entirely new contoured cushion design technology that could substantially advance the field of body-seat interface shape measurement and seat support surface design.

## CHAPTER 1 LITERATURE REVIEW

In this chapter, concepts and problems related to postural support and seating are reviewed. Section 1.1 gives a brief anatomical description of the pelvis and the spine which are of particular concern to the seated posture. Section 1.2 describes the wheelchair users and Section 1.3 deals with commonly occurring problems among wheelchair users, such as pressure ulcer and discomfort. Seating system evaluation methods are summarized in Section 1.4.

In seating interface analysis, pressure measurements alone are inadequate for assessing loading effects and individual tolerance to mechanical suspension load may be better determined by considering deformation patterns. Thus, soft tissue deformation and body-seat interface shape measurements could be used to characterize seating interface, as well as fabricate seat cushions. Shape imaging techniques coupled with advanced numerically controlled machine tools or modeling techniques provide opportunities for quantification of tissue shape and deformation. However the usefulness of shape measurements for clinical evaluation is restricted at the present time due to technical limitations. In order to find potential techniques that could be used to measure seating interface, the shape measurement techniques involved in current seating interface research must first be summarized in Section 1.5.

One of the general objectives of this project is to determine generic shape patterns for wheelchair cushion design. The point data measured from the seat surfaces usually do not directly reveal the underlying discriminating processes. The data are mingled with major and minor trends so it is difficult to extract a direct interpretation of the discriminating processes from the raw data. Multivariate analysis aims to interpret or disclose the discriminating processes through data reduction and classifications. Three important multivariate analysis methodological tools that can be used for shape discrimination are discussed in Section 1.6.

## **1.1 Anatomical structure**

The vertical alignment between the pelvis, spine, and head are of particular concern to the sitter's safety and ability to function. Alignment of these skeletal segments affects the sitter's postural stability, soft tissue integrity, and muscular efficiency. These factors, in turn, influence his risk for soft tissue imbalance and secondary deformity.

### **1.1.1 Anatomical structure of the pelvis**

The pelvis is the central skeletal segment. As such, it biomechanically biases one's ability to sit. As the structural center, pelvic posture affects the posture and the movement of the segments that are above as well as those below the pelvis. Thus, pelvic posture is a key determinant of seated health and function.

The two hip bones articulate almost immovably with the sacrum and each other to form the bony pelvis (Figure 1-1). Each of the hip bones (Figure 1-2) consists of three separate bones, the ilium, the ischium, and the pubis (three bones are differently shaded in Figure 1-1).

Being the platform for the spine and the origin for many muscles, the pelvis carries and balances the trunk. When the pelvic position changes, the spinal alignment changes. The pelvis is connected to the trunk by the sacro-lumbar joint. The upper surface of the sacrum thus dictates the position of the fifth lumbar vertebra, and the alignment of the spine.

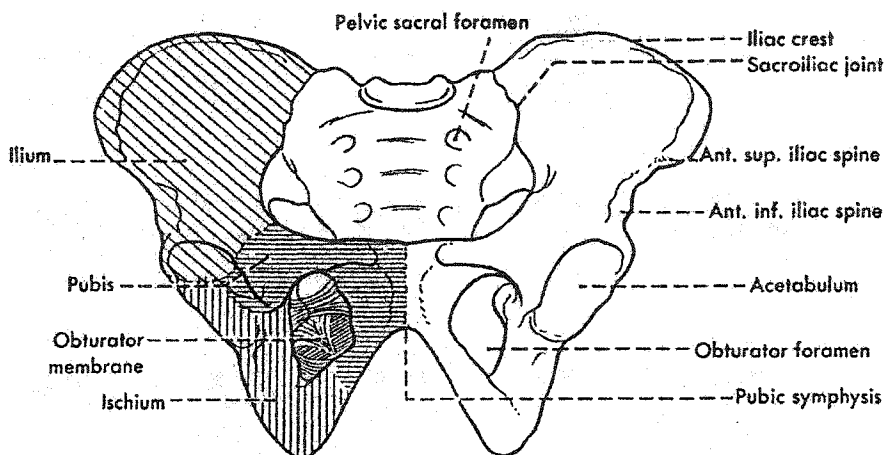


Figure 1-1 The pelvis from the front (Hollinshead, 1974).

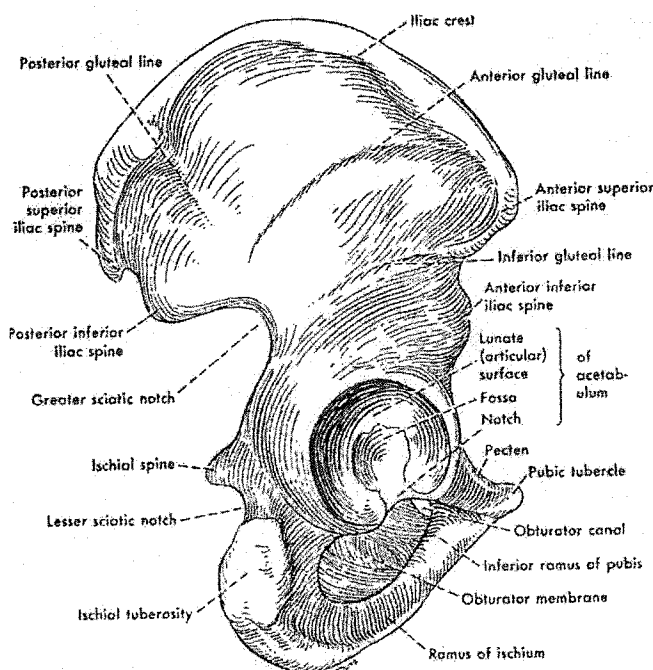


Figure 1-2 The lateral view of the right hip bone (Hollinshead, 1974).

### 1.1.2 Anatomical structure of the spine

The vertebral column, often called the spinal column, or simply "the spine" (Figure 1-3). The vertebral column in the adult typically consists of 7 cervical, 12 thoracic and 5

lumbar vertebrae. These are succeeded by the sacrum, formed usually by the fusion of 5 vertebrae and the coccyx. The coccyx is formed of rudimentary vertebrae, of which the first is commonly separate while the succeeding three are fused together. Thus, there are typically 33 vertebrae in the column.

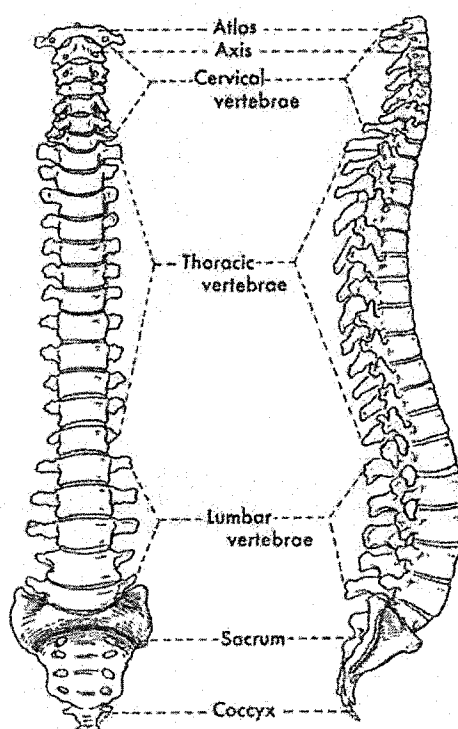


Figure 1-3 The vertebral column from the front and the side (Hollinshead, 1974).

### 1.1.3 Muscles moving the pelvis

Balanced and functional sitting is mainly based on the leg and trunk muscles (Figure 1-4). When these muscles contract they move the legs, the trunk and the pelvis.

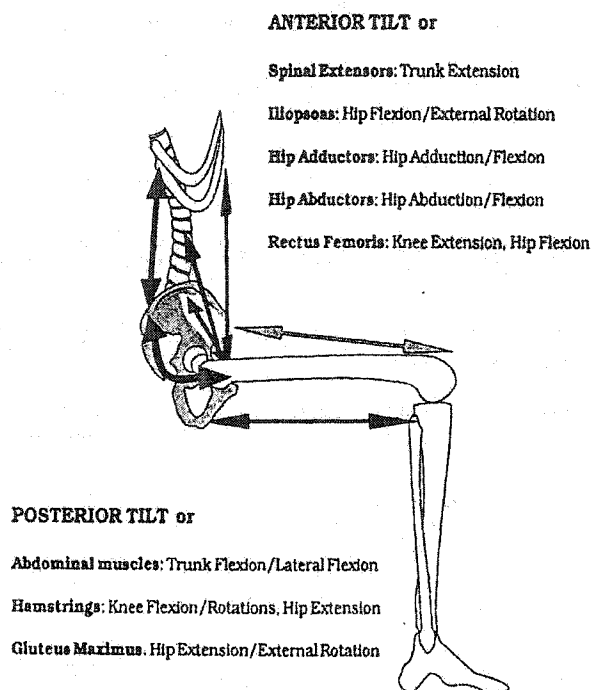
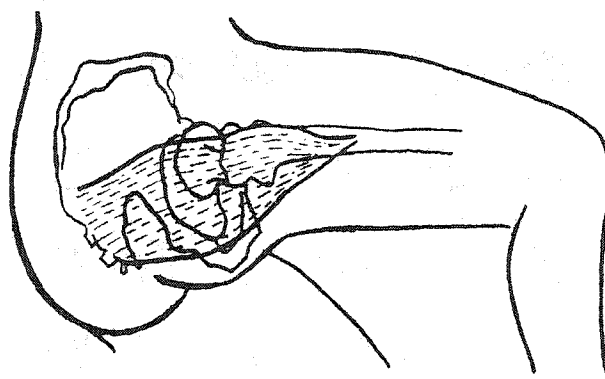


Figure 1-4 The muscles moving the pelvis (Engström, 1993).

#### 1.1.4 Anatomy of the buttocks

With the hip in an extended position the ischial tuberosity is covered by the gluteus maximus muscle. However, with the hip flexed in the sitting position, the gluteus maximus muscle slides superolaterally off the ischial tuberosity. The ischial tuberosity is therefore only covered by skin and subcutaneous fat when sitting (Figure 1-5). In a study involving the dissection of six cadavers, Daniel and Faibisoff (1982) described regarding the soft tissue coverage of the ischial tuberosities (Table 1-1).



**Figure 1-5** With the hip flexed in the sitting position, the gluteus maximus muscle slides superolaterally off the ischial tuberosity (Zacharkow, 1984).

**Table 1-1** Soft tissue coverage of pressure points (From Daniel and Faibisoff, 1982).

Tissue	Site		
	Sacrum (mm)	Trochanter (mm)	Ischium (mm)
Skin	1.0-3.5	0.5-1.5	0.5-2.0
Subcutaneous Tissue	5.0-30	5.0-60	5.0-60
Muscle	none	none	Extension: 5.0-45 Flexion: none

### **1.1.5 Bi-ischial distance**

An important measurement for proper seat design and pressure distribution is the distance between the midpoints of the supporting surfaces of the ischial tuberosities in the seated position (Figure 1-6). Akerblom (1948) measured the bi-ischial distance on 39 female and 51 male skeletons (Table 1-2) and calculated the average bi-ischial distance as approximately 12 cm in men and 13 cm in women.

Another critical dimension of the buttocks is the length of the perineum, measured from the buttocks cleavage to the front of the genital region (Figure 1-6). The length of the perineum in the seated position may range from 15.2 to 30.5 cm, with the mean length in the upright seated position being approximately 22.9 cm in males, and 17.8 cm in females (McClelland and Ward, 1976).



Table 1-2 Distance between midpoints of ischial tuberosities (From Akerblom, 1948).

Bi-ischial distance (cm)	% of 51 male skeletons	% of 39 female skeletons
9	5.9	0
10	5.9	0
11	19.6	7.7
12	51.0	23.1
13	13.7	41.0
14	3.9	20.5
15	0	7.7

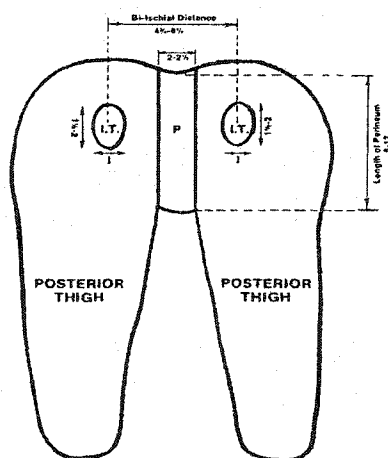


Figure 1-6 Dimensions of the ischial tuberosities and perineum, pertaining to toilet seat design (McClelland and Ward, 1976). All measurements are in inches.

### 1.1.6 Biomechanics of seating

The study of body position and movement, which is named biomechanics, is fundamental to the understanding of seating and positioning persons with disabilities. Force is a major element in biomechanics as well as seating for individuals with disabilities. There are three different types of force tension, compression and shearing forces. Each of these types produces a different effect on the body. Tension force acts in the same line but away from each other (pulling apart). Compression occurs when forces act toward each other (pushing together). Shearing occurs when forces are parallel to each other (sliding across the surfaces). Stress is the resulting molecular change inside of

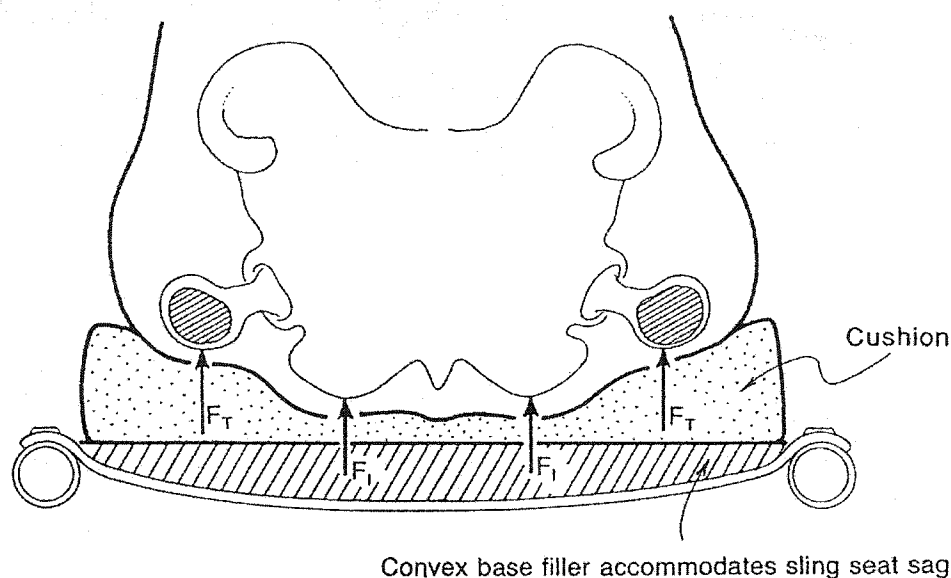
biological or nonbiological materials and is caused by the three types of forces. It can result in damage to the biological tissue or other material if prolonged. Pressure is defined as force per unit area. This means that a force applied over a very small area generates more pressure than the same force applied over a larger area. This basic concept of distributing pressure by increasing the area of application is applied extensively in seating and positioning.

When sitting, the body is positioned such that its weight is supported mainly by the ischial tuberosities of the pelvis and the surrounding soft tissues. Depending on the wheelchair and posture, some proportion of the total body weight will be transferred to the seat, backrest, legrests, and armrests of the wheelchair. When a person is in the sitting position in a wheelchair, the total force acting on the buttocks and thighs is the body weight minus the supporting forces of the footrest and backrest. The greatest proportion of body weight, when sitting, is therefore supported by the area over the ischial tuberosities (ITs). Stresses in the soft tissues are not usually evenly distributed, and are thought to be greatest in the muscle close to the ITs, the area in which pressure ulcers seem to start. Necrosis migrates outward to the skin as cell constituents are released and cause damage to nearby compromised tissue. Ferguson-Pell (1990) stated that if weight bearing can be shared equally by the ITs and the nearby lateral posterior aspect of the trochanters, the force at each IT is half of that when only the ITs are loaded. More soft tissues can thus share the burden. Weight distribution is, therefore, an important principle used for designing cushions that are shaped to encourage trochanteric and thigh support (Figure 1-7).

In summary, there are five major biomechanical factors that must be considered in the specification of interfacing shape (Ferguson-Pell, 1990, Levine et al., 1989, Sprigle et al., 1990a):

1. The distribution of the sitter's weight on the support (pressure mapping);
2. The undeformed shape of the sitter's weight-bearing segments (e.g., the buttocks);

3. The unloaded shape of the support surface;
4. The biomechanical properties and tissue structures of the weight-bearing tissue of the sitter's body (e.g., variances in tissue stiffness between the sitter's weight-bearing skin, fat, muscles, and bone);
5. The mechanical and structural properties of the support material.



**Figure 1-7 Shaped cushions help share the supporting forces  $F_I$  and  $F_T$  more equally between the ischial tuberosities ( $F_I$ ) and the trochanters ( $F_T$ ). On cushions with no shaping  $F_I$  is considerably larger than  $F_T$  and the ITs have to compress the cushion nearly 2 inches before the trochanters make contact (Ferguson-Pell, 1990).**

## 1.2 Wheelchair user populations

According to the Office des personnes handicapées du Québec (<http://www.ophq.gouv.qc.ca/>), 32,300 individuals in Quebec were using wheelchairs on a daily basis in 1994. According to the 1986 Canadian census, 13.2% of the population (over 3,300,000 Canadians) reports some level of disability. As a result, approximately 120,000 Canadian were requiring the use of wheelchairs and seating systems

(<http://www.hc-sc.gc.ca/>). According to the U.S. National Center for Health Statistics, 1,411,000 persons in the United States were using wheelchairs on a daily basis in 1992. This represents a 96.1% increase since 1980, whereas the total U.S. population grew by only 13% (Cutter, 1997). Finally, according to the U.S. National Health Interview Survey from 1994 and 1995, 1.5 million people in the United States were manual-wheelchair users and 155,000 were power-wheelchair users (Sprigle et al., 2001).

There are numerous reasons for a person to need wheelchair assistance. These causes fall into two major categories: traumatic injury and chronic degenerative disease. A survey conducted by the British Ministry of Health, which gave the diagnosis per hundred patients who obtained wheelchairs (Table 1-3) (Cooper, 1998).

**Table 1-3 Percent of wheelchair users by disability etiology (Cooper, 1998).**

Arthritis	28%
Organic nervous disease	14%
Cerebral vascular disease	13%
Other bone injuries and deformities	11%
Lower limb amputations	9%
Cerebral palsy	8%
Traumatic paraplegia	7%
Respiratory and cardiac disease	3%

It is estimated that 5% of people over 70 years of age are wheelchair users. This age-specific prevalence of disability is therefore higher for elderly persons and places them in a large subcategory of wheelchair users. For the elderly, the most common causes for wheelchair requirement are arthritis or rheumatism, hypertension, diabetes, cardiac, and respiratory disease. The prevailing reason given for requesting a wheelchair was arthritis and unsteadiness (18.2%), with strokes and frequent falls ranking second and third respectively. Most of these people (54.5%) use their wheelchairs all of the time (Cooper, 1998).

Wilson (1992) classified wheelchair users into three groups:

- Persons who have lost lower-limb function owing to: Spinal cord injury; Arthritis; Cerebral palsy; Poliomyelitis; Multiple sclerosis; Muscular dystrophy; Stroke and brain trauma; Bilateral amputation; Other diseases.
- Persons with insufficient postural stability owing to: Brain damage; Cerebral palsy; Cancer of the spine; and other diseases.
- Persons with general debilitation owing to: Aging; Alcoholism; Temporary illness.

Engström (1993) grouped wheelchair users by dysfunction and need: Thoracic kyphosis; Quadriplegia; Paraplegia; Hemiplegia; Head injuries; Cerebral palsy and related disorders; Hip contractures; Above knee leg amputations; and Elderly.

### ***1.3 Seating problems and solutions***

Seating can be approached biomechanically, ergonomically, neurologically, functionally, aesthetically and with respect to pressure. All the various factors must be taken into consideration when attempting to understand the reasons for a person's seating problems and when developing possible solutions for the problems (Zollars, 1993). There are many wheelchairs not appropriate for long-term sitting. It can be difficult to see the relationship between poor sitting and costs unless you realize that poor seating can cause problems like discomfort, pressure ulcers, joint contractures, decreased range of motion, spasticity, spinal curvatures, disturbed inner organ function, impaired mobility, and increased dependent (Zacharkow, 1988, Engström, 1993, Mayall and Desharnais, 1995). Many wheelchair users have abnormal body postures due to their physical impairment, their years of sitting improperly, or both (Cooper, 1995).

### **1.3.1 Postural problems**

The systematic approach to positioning is a result of the analysis of the seated posture, the key being the pelvis. The process of positioning in a wheelchair begins with the pelvis, followed by the lower extremities from proximal to distal, the trunk, the head and neck, and lastly, the upper extremities from proximal to distal (Mayall and Desharnais, 1995). The ultimate postural objectives are 1) pelvis: neutral or slightly anterior tilted; 2) lower extremities: 5-8 degrees of abduction, knees and ankles flexed at 90 degrees. 3) spine: erect and following the natural spinal curves; 4) head: upright and in the midline; 5) upper extremities: free to move, unless a person prefers arm strips to restrict uncontrolled arm movements (Zollars, 1993). The potential postural problems, their causes and possible solution for each area are listed in the Appendix.

### **1.3.2 Pressure ulcers**

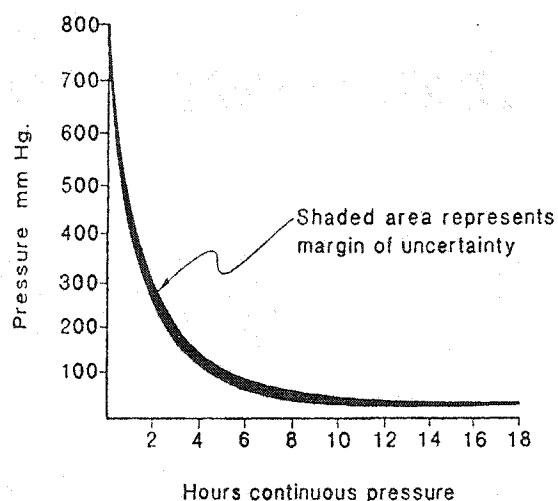
Pressure ulcers are a major problem for people who have areas of tissue that lack sensation or who have limited natural mobility. These deficits affect many who use wheelchairs and the prevention of pressure ulcers is a key consideration in the rehabilitation of patients who require a wheelchair and the provision of a suitable chair and cushion. Published studies from Canada, the U.S.A., Europe and South Africa reported that anywhere from 1.5% to 25.7% of hospitalized patients have pressure ulcers (Webster, 1991). Pressure ulcers can be painful, lead to infection, and are a marker for a greatly increased risk of death. Treatment of pressure ulcers is costly, both in terms of time and money, the cost of treating each pressure ulcer ranging from US\$2,000 to US\$25,000 (Conine et al., 1994). Thus, prevention of pressure ulcers continues to be a paramount objective for the wheelchair users (Maklebust et al., 1986, Foster et al., 1992, Patterson and Bennett, 1995).

### 1.3.2.1 Cause of pressure ulcers

A pressure ulcer is an ulceration caused by excessive pressure being applied to a tissue over an excessive duration. Pressure ulcers are also called decubitus ulcers, bed sores, or pressure sores. Pressure ulcers usually develop near regions of the body which have a bony prominence near the skin. The most common sites for pressure ulcers are the sacrum or coccyx (36%), the hips over the trochanter (17%), the buttocks over ischial tuberosities (15%), the heels (12%), the ankles (7%) and other sites (13%) (Smith, 1995).

The most commonly agreed upon primary cause of pressure-induced tissue necrosis is occlusion of capillary blood flow resulting in ischemic injury. The impairment of lymphatic drainage and/or interstitial fluid flow has also been proposed as a primary cause of pressure ulcers. Nonetheless, external pressure has long been the focus of etiological investigation on the mechanics of pressure ulcer formation (Krouskop et al., 1983). Brienza et al. (2001) investigated the relationship between pressure ulcer incidence and the buttock-wheelchair seat cushion interface pressure measurements and their results indicated that higher interface pressure measurements are associated with a higher incidence of sitting – acquired pressure ulcers for high-risk elderly people who use wheelchairs.

Reswick and Rogers (1976) described the maximum allowable interface pressure as a function of hours of continuous pressure: as the number of hours of continuous pressure increases, the allowable interface pressure decreases (Figure 1-8). Considering the differences in patient's skin and general health and the fact that relatively few controlled measurements were made, the authors themselves stated that the pressure-duration curve could only give general guidelines and should not be taken as absolute.



**Figure 1-8 Acceptable pressure/time interval guideline (Reswick and Rogers, 1976).**

Two studies have produced experimental evidence which support the theory that shear forces also play an important role in the formation of pressure ulcers. When applying pressure and shear to swines, Dinsdale (1974) found that the combination of pressure and shear caused ulceration with pressure as low as 45 mmHg. When applying pressure alone, 290 mmHg was required to produce ulcers. Bennett et al (1979) examined the effect of shear in reducing the pulsatile arteriolar blood flow. They showed that the magnitude of pressure necessary to produce occlusion can be nearly halved when accompanied by sufficient shear.

Levine et al (1989) classified risk factors into external factors which affect the skin through physical contact, and internal factors which depend on demographics and physiology. External factors (Table 1-4) are pressure, shear force, friction, moisture and skin temperature and internal factors (Table 1-5) are age, body type, infection, collagen formation, fibrinolytic activity, nutrition and smoking.



**Table 1-4 External factors in pressure ulcer formation (Summarized from Crenshaw and Vistnes, 1989, Barbenel, 1991, Webster, 1991, Patterson and Bennett, 1995, Van Marum et al., 2002).**

External factor	Relationship to pressure ulcer formation
<b>Pressure</b>	<ul style="list-style-type: none"> <li>Main causative factor in pressure ulcer formation;</li> <li>The damage caused will depend on the direction, magnitude, rate of application, and duration of the applied force;</li> <li>Low pressure sustained over a long period often causes more damage than high pressure over a short period.</li> </ul>
<b>Shear</b>	<ul style="list-style-type: none"> <li>Shear force is the second key factor in pressure ulcer formation;</li> <li>Shear constricts and distorts the microcirculation already compressed by pressure;</li> <li>When enough shear is present only half as much pressure is necessary to cause vascular occlusion.</li> </ul>
<b>Friction</b>	<ul style="list-style-type: none"> <li>Friction occurs when shear exceeds pressure, and the skin begins to move against its environment, an abrasion or blister will then form</li> </ul>
<b>Moisture</b>	<ul style="list-style-type: none"> <li>Moist tissue is weaker leading to both increased maceration and excoriation;</li> <li>Moisture can increase friction between two surfaces;</li> <li>Friction and moisture tend to produce their most damaging effects when coupled with excessive pressure.</li> </ul>
<b>Skin temperature</b>	<ul style="list-style-type: none"> <li>Increases in temperature by 1°C increases metabolic demands by 10%;</li> <li>Decreasing the temperature reduces the demand of the cells but also causes a vasoconstriction that can decrease the blood supply to the area.</li> </ul>

**Table 1-5 Internal factors in pressure ulcer formation (Summarized from Zacharkow, 1984, Crenshaw and Vistnes, 1989, Barbenel, 1991, Webster, 1991, Patterson and Bennett, 1995).**

Internal factor	Physiological consequence
<b>Age</b>	Increased stiffness and lower mechanical strength for the skin; Interstitial fluid is resisted less by tissue causing cells to rupture when subjected to pressure.
<b>Body type</b>	People with less fat and muscle have higher pressure at their bony prominences
<b>Infection</b>	Elevate body temperature, increased metabolism, and nutritional depletion.
<b>Collagen formation</b>	Factors such as stress, spinal cord injury, or old age tend to favor production of a water-soluble form of collagen at body temperature. This form is unstable decreasing the strength of the tissues.
<b>Fibrinolytic activity</b>	When fibrinolytic activity is reduced by factors such as ischemia or friction, fibrin accumulates in the region possibly occluding blood flow.
<b>Nutrition</b>	Malnutrition reduces fat and muscle tissue, causing higher pressure on bony prominences.
<b>Smoking</b>	Has the vascular effect of constricting blood flow to the skin thus increasing ischemia.

### 1.3.2.2 Prevention of pressure ulcers

Although there are many contributing factors in addition to the five external factors listed in Table 1-4, pressure ulcers are usually preventable with proper care and/or equipment that addresses these five factors. Bailey (1967) presented four methods to prevent pressure ulcers: 1) Produce weightlessness; 2) Reduce body mass; 3) Increase bearing area; and 4) Decrease time at risk. Method 1 is not practical and method 2 may increase pressure over bony prominences and is not favorable for thin and weak patients.

That is why methods 3 and 4 are used more often. In method 3, weight is distributed as widely as possible and pressure is distributed as evenly as possible. As an alternative to method 3, producing even pressure distribution by decreasing pressure at higher pressure area where patients frequently develop pressure ulcers and dispersing the forces to other lower pressure areas of the body. In method 4, the time at risk is reduced by relieving the pressure regularly.

The following are some methods used in pressure ulcer prevention (Krouskop et al., 1983, Fernandez, 1987, Webster, 1991, Yarkony, 1994, Patterson and Bennett, 1995, Edsberg et al., 2001, Clever et al., 2002).

1. Pressure/shear management by proper static seat cushion: Seat cushions are currently the most popular and highly researched method for pressure ulcer prevention for wheelchair users.
2. Pressure relief by dynamic systems: The dynamic systems could alter the pressures over the ischial tuberosities cyclically but the amount of pressure alternation depends on the relative position of the ischial tuberosities and their bellows (Rithalia and Gonsalkorale, 2000).
3. Pressure relief by performing regular push-ups (paraplegic patients) and forward or side leans (tetraplegic patients): Researchers have developed alarm systems that remind individuals sitting in their wheelchairs to shift their weight on a regular basis to prevent pressure ulcers.
4. Reducing pressure by seating posture arrangement. Wheelchair users tend to assume a seating posture that leads to forward sliding of the buttocks on the seat and the settling of the back low on the backrest. As a result, there is exposure of the ischial tuberosities to high values of pressure and shear. A postural support system that maintains the trunks as vertical as practical and that effectively resists kyphoscoliotic collapse has a profound effect on the management of both pressure and shear.

5. Functional electrical stimulation (FES): Levine et al. (1989) found the FES increased blood flow and lymph flow to the muscles, allowed higher oxygen delivery to trauma sites and allowed metabolite removal from trauma sites.

### **1.3.3 Discomfort**

Hockenberry (1977) suggested that discomfort in long term sitting is mainly due to improper pressure distribution resulting from a poor fit of the seat and backrest shape to the contours of the individual. He lists seven basic pressure factors, several referred to earlier by Hertzberg (1972), which must be considered in the seat design to reduce discomfort:

1. Pressures exerted on the ischial tuberosities must be reduced with a slight contouring of the seat in the buttocks region.
2. The backrest must be contoured to provide lumbar support.
3. Pressure under the posterior thighs must be kept to a minimum.
4. A 95 to 105 degree seat-back angle will result in an optimal pressure distribution over the seat and the back.
5. The seat and back cushion covers must be elastic enough to transmit local pressure loads directly to the cushion.
6. The sides of the seat should not exert pressure on the greater trochanters of the femurs.
7. The back and seat should both be contoured with a side to side radius that fits the 5<sup>th</sup> through 95<sup>th</sup> percentile of the adult population.

### **1.3.4 Instability**

The sitting position is basically unstable without additional external support. This is because the ischial tuberosities, with their rounded shape resembling the rockers of a rocking chair, provide only a linear base of support (Zacharkow, 1988). Certain seat

features are critical to help support the seated individual so that he can maintain a stable posture. The aim of proper support for all types of seat should be optimal stability with minimal restraint (Zacharkow, 1984). The important stabilizers include the backrest, armrests, and the type of seat cushion and upholstery cover. The proper seat dimensions are also critical in providing essential stabilization for the seated individual. These include proper seat inclination, seat height, seat depth, and seat to back angle (Janssen-Potten et al., 1999 & 2001, Seelen et al., 2001).

#### **1.4 Seating systems and seat cushions**

The primary goals of a seating system are to 1) provide comfort, 2) maximize function, 3) prevent secondary complications such as contractures, postural abnormalities, and pressure ulcers, 4) be practical for transport, and 5) be cosmetically acceptable (Letts, 1991, Ferrarin et al., 2000). Many types of seating systems are available. Cushions and backs can be prefabricated or custom-made. In addition to the many client factors to be considered when selecting a seating system, it is also important to consider the characteristics of the seating system itself, such as stability provided, frictional properties of the cushion and cover material, management of moisture, properties of heat insulation or dissipation, durability and maintenance profile, weight, cost, and flammability. An entire seating system includes cushion, and other accessories, such as back, lumbar support, lateral trunk support and headrest. Assembly of the parts allows the system to become individualized for the user and fit into the existing wheelchairs. The components are made from the same materials as the cushion. Therefore, the same factors that are considered when selecting the cushion must be weighted when selecting these accessories for an individualized seating system (Cutter, 1997).

### **1.4.1 Classification of seating systems**

The field of specialized seating systems is evolving along three distinct tracts, each of which has been guided largely by the needs of distinct user populations (Cooper, 1998, Karp, 1999). These tracts are: (a) seating for postural control and deformity management (cerebral palsy population); (b) seating for pressure and postural management (spinal cord injury population); and (c) seating for comfort and postural accommodation (multiple handicaps and the geriatric population) (Figure 1-9).

#### **a) Postural control and deformity management technologies**

This area of specialized seating has been guided largely by the needs of children and young adults with cerebral palsy. Within the cerebral palsy group, the seating needs vary significantly depending on the type and degree of damage to the immature brain. The associated technological approaches have taken two basic directions: those designed with planar (flat) surfaces in contrast to those that are contoured to provide more intimate support to the body. Both main categories can be further subdivided. Planar designs may be either custom fabricated or prefabricated. Contoured designs may be either precontoured or custom contoured.

#### **b) Pressure and postural management technologies**

Individuals with spinal cord injury are at risk of developing pressure ulcers in the tissues overlying the pelvic area. Many types of wheelchair cushions have been developed in an attempt to control pressure over the body prominences of the pelvis. Development of seating technologies designed for pressure and postural management has followed an evolutionary path somewhat different from the cerebral palsy group (postural control and deformity management). In general, cushion designs for the spinal cord injury population are first categorized by the media or mechanical technique used to obtain the pressure relief, rather than by whether the surface profile is planar or contoured. The basic media approaches are fluid flotation, polyurethane foam, and oscillating (dynamic)

devices. A fourth subcategory (hybrid) provides a means of classifying designs that use two or more of the first three approaches.

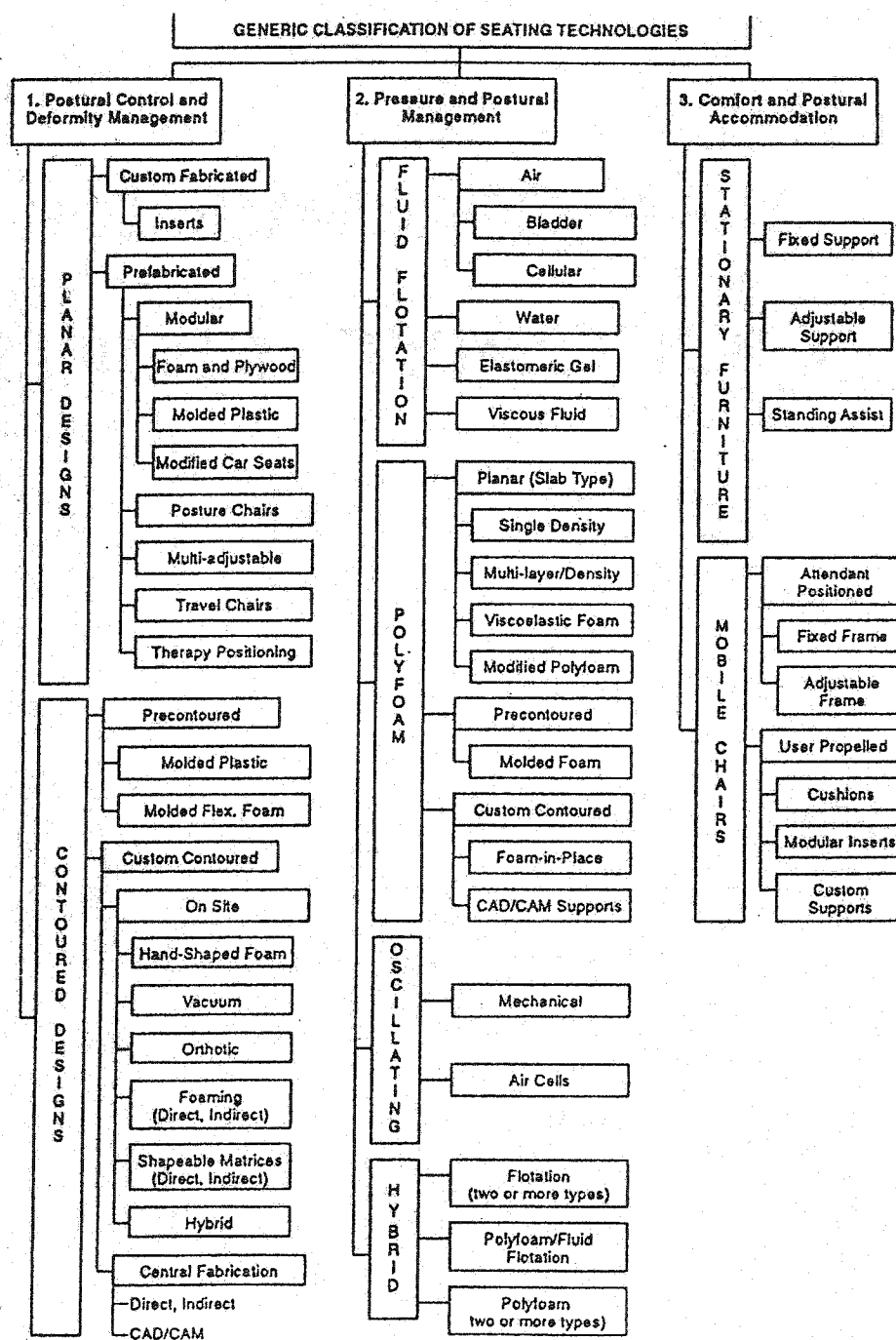


Figure 1-9 Generic classification of seating systems (Medhat and Hobson, 1992).

c) Comfort and postural accommodation technologies

Although by far the largest in numbers, seating technologies for the elderly population are still in their infancy. For example, relatively few commercial products have been developed to specifically enhance the care or independent functioning of people in nursing homes for the elderly. Even fewer attempts have been made to develop systems that facilitate the maintenance of these groups in the home and community. The existing designs and technologies employed can be classified into broad subgroup which are based largely on the manner in which the devices are intended to be used, i.e., whether they are intended to be stationary sitting furniture or whether they are to be mobile and propelled by an attendant or the user.

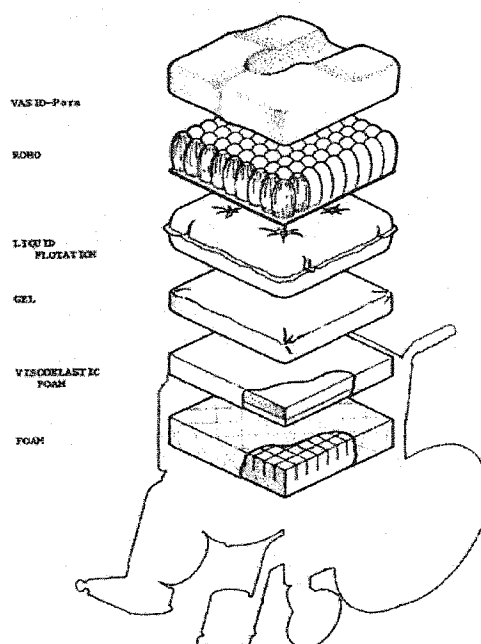


Figure 1-10 Examples of different seat cushions (Wilson, 1992).

### 1.4.2 Types of seat cushions

Many types of wheelchair cushions have been developed in an attempt to control pressure over the bony prominences of the pelvis (Figure 1-10). A wide range of materials, geometric configurations, and mechanical technologies have been tested and used in cushion designs (Table 1-6). Clinical experience clearly indicates that the requirements of individuals vary widely and that no single design meets every need. The cushions designed for pressure and postural management (Figure 1-9) are classified to four categories:

Table 1-6 Major characteristics of popular types of seat cushions (Wilson, 1992).

Characteristic	Foam (3" Thick)	Viscoelastic (3" Thick)	Gel (1" Thick)	Fluid-Filled (Liquid)	Air-Filled
Weight (16 <sup>2</sup> in lbs)	3-4	3.5-4.5	12-14	10-20	3-5
Heat transfer	Good insulator of heat	Good insulator of heat	Drains heat rapidly	Drains heat rapidly for up to 1 hour	Good insulator of heat
Resilience	Wide range available	Variable; varies with body heat and environmental temperature	Very firm	Tends to be firm	Soft
Patient stability (Security) Firmness	Good security	Moderately good initially; good when conformed to body	Firm, but may feel sloppy during propulsion	Usually feels unstable	Usually feels unstable
Durability (expected life)	6 mos, 10 hrs/day sitting	6 mos, 10 hr/day sitting if kept clean	2 years or more	Good, but vulnerable to puncture	Good; easily repaired if punctured
Resistance to water	Requires cover	Requires cover	Intrinsically resistant to water	Intrinsically resistant to water	Intrinsically resistant to water
Flammability	Usually treated with flame-retardant but essentially flammable	Can be treated with flame-retardant but essentially flammable	Flame resistant	Flame resistant	Depends upon containment material
Cost (\$)	Low: 10-20	Low: 10-20	High; 100-200	Moderate: 30-100	Variable; 50-200
Ease of cleaning	Depends on cover	Depends on cover	Easy	Easy	Varies

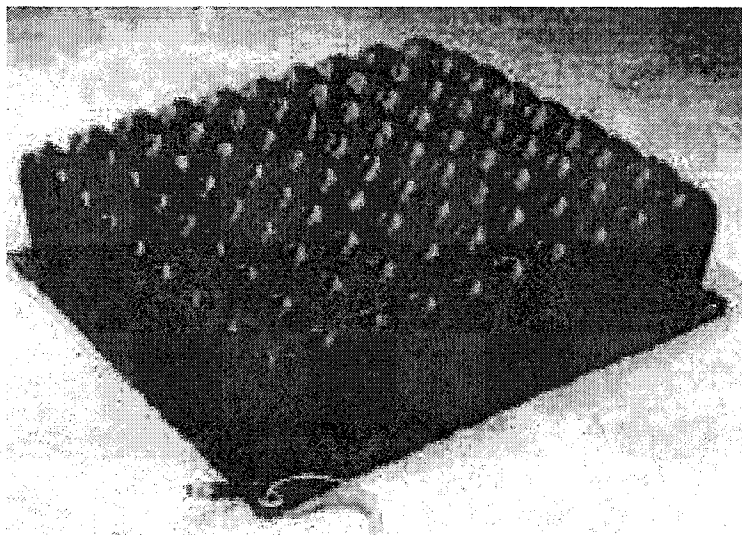


#### 1.4.2.1 Fluid floatation cushions

Four fluid mediums have been used in cushion design: air, water, elastomeric gels, and viscous fluids. Air-filled cushions generally have two configurations: (1) configured bladders or rubber membrane designs and (2) cellular designs. Over inflation or inadvertent loss of support pressure is possibly the most serious drawback to the air-filled cushions.

Air flotation cushions attempt to reduce pressure under the ischial tuberosities by evenly distributing the pressure across the whole body area at the cushion interface. The motivation for such a cushion comes from the application of Pascal's law which states that pressure exerted at any point upon a confined liquid is transmitted undiminished in all directions. Air flotation cushions are advantageous because of their lightweight and longevity. While air flotation cushions are not prone to environmental aging, they are susceptible to punctures and tears. Air flotation cushions also change their properties with changes in altitude. The most common instance is when flying on an airplane where the air pressure within the cushion can change considerably from take-off to cruising altitude. Some commonly used air cushions are the Roho, Bye Bye Decubiti, and Gaymar Sofeare.

The Roho has been the most researched air flotation cushion in recent years and has had mixed reviews; yet, it still remains the forerunner of all air flotation designs, and has become almost synonymous with the air flotation cushions class (Figure 1-11). The Roho now comes in various different schemes in an attempt to offer postural balance and customized specifications. The standard "High Profile" Roho has an array of 4-inch (100- mm) air bag cells that are interconnected at the base of the cushion. When the patient sits on the cushion, it deforms to the contours of the patient's buttocks. A pressure pump is supplied with instructions on how to properly inflate the cushion.



**Figure 1-11 The Roho cushion has individual air cells interconnected at the base (Roho Inc., IL).**

Water-filled cushions (e.g. Aqua Seat) are less common. Although they provide good dissipation of body heat, leaks, excessive weight, and hammocking effect created by the covering membrane are noted problem areas.

Gel cushions (e.g., Elasto Gel, Reston-3M) are produced from materials such as silicone elastomers, chosen to have a viscosity or consistency similar to body fat. Gel cushions also provide good heat dissipation, but are usually heavy and gel leakage has been a problem with some designs. Pressure distribution characteristics can be affected greatly by the design of the confining membrane and its outer covering material(s). More recently, high-viscosity fluids contained in oversized flexible membranes are being used (e.g., Jay-Bunjie pads). The high-viscosity fluid exhibits pressure equalization properties of a fluid, but is free to flow within the confines of the membrane from areas of higher loading to areas of lower loading. This in effect creates a custom contouring effect.

The viscous fluids floatation cushion operates in a manner that is very similarly to an air flotation cushion but it has more effective damping abilities. A gel cushion can be thought of as a fluid analogy to the viscoelastic foam cushion except that it doesn't have

nearly as much elasticity. The high viscosity of the gel prevents it from moving rapidly within its container. This property allows the gel cushion to provide a more stable seating surface than an air cushion. However, gel cushions tend to be much heavier than air flotation devices and also more expansive. Because of this, they are quite cumbersome and unstable during patient transfers. The Stryker flotation pad is one type of gel cushion. More common are cushions that have a smaller gel pouch on top of a contoured polyurethane foam base. Gel cushions are noted for their capacity to conduct heat away from the patient to avoid increased temperatures at the skin interface.

#### 1.4.2.2 Polyurethane foam cushions

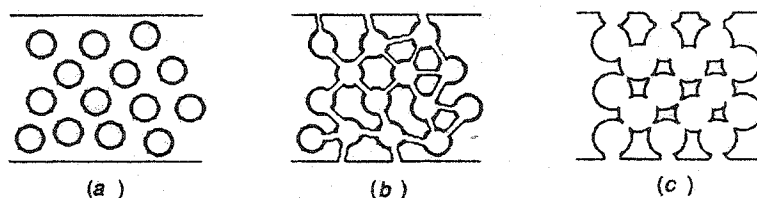
Polyurethane foams have been the mainstay of cushion technology over the years, particularly for those individuals at low to moderate pressure ulcer risk. The pressure distribution characteristics of foam cushions depend on the inherent mechanical properties of the foam and whether it is used in a single or multilayered "slab" configuration (planar) or is contoured to the pelvic area, either through precontoured molding or custom contouring to the precise shape of a person's pelvic area (Table 1-7).

Various densities and types of foam are commonly used in seating systems. The most common type cushion is made from medium density polymeric foam. Polymeric foams come in the different cell structures shown in Figure 1-12. There are three basic types of cell formation: closed, open, and reticulated. Closed cell foams consist of polyhedron structures enclosed by membranes of variable thickness. Closed cell foams are generally more rigid in compliance. Open cell foams have interconnected perforated membranes, allowing greater flexibility and better ventilation. Most types of foam have a mixture of open and closed cell structures and are characterized by the fraction of the open cells. Reticulated foams have a larger pore size and contain thinner membranes that have been chemically or heat-treated. Reticulated foams are less durable than open cell foam but

have a greater elastic performance. When manufacturing foam, the individual cell size and geometry can also be varied to provide different structural characteristics.

**Table 1-7 Comparisons of planar, precontoured and custom contoured cushions (Ward, 1994).**

<b>Planar cushion</b>	Interface shape is flat and parallel to the support's reference plane	
	<b>Advantages</b>	Provides an unbiased support surface that accommodates the greatest variety of postures
	<b>Disadvantages</b>	Increases the risk of peak pressure and shear in weight-bearing soft tissue, especially over bony prominences; Provides the least surface contact and the least postural support, which often increases the need for lateral and anterior supports
	<b>Applications</b>	For short-term sitting when significant postural variety is needed; May be used with manual or power tilt or recline mobility bases when the sitter needs to retain full freedom of postural variations
<b>Pre-contoured cushion</b>	Interface shape is pre-determined by anthropomorphic data	
	<b>Advantages</b>	Decreases the risk of peak pressures and shear on weight-bearing soft tissue, especially over bony prominences; Augments postural support and control, which often decrease the need for lateral and anterior supports
	<b>Disadvantages</b>	Shape may restrict prescriptive weight shifts and postural variety, especially if the anatomical contact is too thick; Sagittal or transverse plane shaping can cause shear or peak pressures when used with adjustable seat-to-back angle without linear adjustability of the back support
	<b>Applications</b>	For longer periods of sitting when postural support is desired; For use with power recliners that have superior-inferior adjustability of the back support
<b>Custom contoured cushion</b>	Interface shape is prescriptively designed for each client's needs	
	<b>Advantages</b>	Minimizes the risk of peak pressures and shear on weight-bearing soft tissue, especially over bony prominences; Individualizes the interfacing shape for best postural support and control, often decreases the need for lateral and anterior supports
	<b>Disadvantages</b>	Excessive thickness of anatomic contact can undesirably restrict necessary weight shifts and postural adjustments. It may also interfere with functional movement and decrease the air flow at the interfacing surface; Use of materials with high indentation factors may increase peak pressures and shear; Fixed shapes have limited ability to address changes in the sitter's size or shape or seasonal changes in the thickness of clothing
	<b>Applications</b>	For prolonged sitting, when postural support and peak pressure relief is needed; May be use with system tilt but is not recommended with reclining backs unless it has superior-inferior adjustability of the back, and even then is used only when the client needs maximal postural support and/or control



**Figure 1-12 Polymeric foams used for cushions (a) Closed cell. (b) Open cell. (c) Reticulated cell (Tang, 1991).**

The two most important terms used to specify the properties of polyurethane foam is indentation force deflection (IFD) and density (weight per unit volume). A high IFD is usually specified to help ensure that a sitter will not "bottom-out" on the cushion. A high density is usually specified since the high-density foam has an increased ability to retain its IFD values after repeated loading. However, as the density increases, the weight also increases which decrease the ease of handling. A commonly used polymer in foam cushions is medium density polyurethane (25% IFD is 30-70 lb and density is 1.5-4 lb/ft<sup>3</sup>). Polyurethane foams are noted for their lightweight and flexible properties. They are used to create resilient, easily transferable cushions. Ideally they exhibit very linear characteristics of stress  $\sigma$  versus strain  $\epsilon$ :  $\sigma = E \epsilon$ , where  $E$  is Young's modulus. However load-indentation curves exhibit nonlinear relationships.

These foams are less expensive than most other materials because they are readily available in bulk quantities. Higher density polyurethane foams can also be carved into specific contours that conform to the patient's buttocks. The main drawback to polyurethane foams is that they do not endure much environmental aging. Most foam last about six months before losing a significant amount of elasticity. Protective covers are also necessary to extend the lifetime of foam cushions.

Viscoelastic foams (also called "memory" foams) are very similar to regular polyurethane foams with the exception of having a higher damper factor. They can provide improved stability as they dampen loads rather than cause the patient to bounce. They also exhibit time dependent stress-strain characteristics:

$$\sigma = \eta \frac{d\epsilon}{dt}$$

This is important for paraplegics who require a firm "reaction point" for self-propulsion in a wheelchair. The mechanical properties of viscoelastic foams can be modeled by the spring-dashpot system (Figure 1-13). A viscoelastic material can also be characterized as

the combination of an ideal elastic solid and a perfectly viscous fluid. The resulting material is one with a nonlinear, time-dependent stress-strain relationship.



Figure 1-13 Viscoelastic foams can be modeled as a spring-dashpot-system (Tang, 1991).

#### 1.4.2.3 Oscillating (dynamic) designs

The fluid flotation and polymeric foam cushions are static devices which attempt to equalized or redistribute pressure over the contact surface of the pelvis. On the other hand, oscillating designs are dynamic and adhere to the principle that locally high pressures can be tolerated provided that the duration is kept within prescribed limits. Several approaches have been pursued; one is basically a mechanical design and the other includes undulating air cells on bellows. Houle and Minnesota (1969) were pioneers in dynamic systems testing. They concluded that the dynamic system could alternately shift the pressure from one area to another and would provide adequate protection against the development of ischemic ulcers. Kosiak (1976) described an experimental wheelchair seat that consisted of a series of rollers on a chain drive that moved under the sitter at a predetermined speed. Although the time-pressure profiles were within the tolerable limits described in his previous work (1959), the complexity, cost, and bulk of the device have precluded its commercialization and clinical use. Koo (1995) tested Talley active air bellows cushion (Talley Medical Ltd., England) and suggested that the active cushion could alter the pressures over the ischial tuberosities cyclically but the amount of pressure alternation depended on the relative position of the ischial tuberosities and their bellows. Clinical experiences with any of the oscillating

devices in North America are very limited (Hobson, 1990). The approach is technically intriguing and may offer significant advances in pressure management in the years ahead.

#### 1.4.2.4 Hybrid designs

The Hybrid designs employ two or more of the above approaches to address the specific needs of individuals. Several of the fluid floatation mediums have been combined into a single cushion design. Elatomeric gels and related high-viscosity fluids have been combined with polymeric foam structures (e.g., the Jay cushion uses a precontoured polymeric foam substructure with a top surface membrane filled with a high-viscosity fluid). Honeycomb materials are made to exploit the linear properties of some polymers and are combinations of air flotation and polymer structures. When these polymers are molded into a honeycomb, they behave like a collection of springs (i.e., similar to the linear behavior of foam). The properties of the honeycomb cushion materials can also be carefully controlled. There are indications that honeycomb materials may be more durable than foam, and honeycomb cushions can be contoured like foam. However, honeycomb cushions are typically contoured by the manufacturer for some standard shape. A drawback of honeycomb cushions is that they are considerably more expensive than foam, and do not come in the wide variety of stiffnesses that foam does.

### 1.4.3 Selection of seat cushions and seating systems

When users sit on a cushion, a number of interaction factors determine whether it is comfortable, functional, and clinically safe. Many of these factors are interrelated. Some factors are attributed to the properties of the cushion, and others are due to the characteristics and needs of the user. Ferguson-Pell (1990) highlights the factors that need to be considered when selecting wheelchair cushions (Table 1-8).

**Table 1-8 Factors that affect the wheelchair cushion selection (Ferguson-Pell, 1990).**

<b>Factors that affect comfort</b>	1). Poor distribution of stresses in soft tissues
	2). Moisture accumulation
	3). Heat accumulation and loss
	4). Compromised stability.
<b>Factors that determine functionality</b>	1). Stability provided
	2). Weight of the cushion
	3). Frictional properties of the cushion and cover
	4). Cushion thickness
	5). Appearance
	6). Cost
	7). Durability and the need for user maintenance.
<b>Factors that determine clinical safety</b>	1). Poor distribution of stresses in soft tissues
	2). Stability provided
	3). Frictional properties of the cushion and cover
	4). Moisture accumulation
	5). Heat accumulation and loss
	6). Durability and the need for user maintenance
	7). Flammability

The decision to use a prefabricated seating system, a custom seating system, or other seating systems must come from the identified goals for the seating system for that individual user. An appropriate prescription can then be formulated to support the individual user's personal and therapeutic goals (Staarink, 1995, Spinal outreach team, 2001).

#### **1.4.4 Seating system evaluation**

Within the past 15 years, prototype-seating simulators for both planar and custom seating have been developed and proven to be useful. Several models are now commercially available. The therapist can evaluate the client in the system, alter the angle of the seat to the back, try varying the positions in space, and determine component sizes and accessories that are required before making recommendations for a particular system.

In seating system evaluation, there are several clinical methods for comparing their efficacy. The three main purposes of wheelchair cushions are pressure management,



comfort and postural control. By stating the purpose for which the support surface is to be used, the evaluation method of seat cushions can be defined. Objective evaluation methods for evaluation include interface pressure measurement, interface shear measurements and interface shape measurements. The subjective evaluations include comfort, stability and handling, skin reaction, transfer ability, cost, maintenance and repair (Webster, 1991).

#### 1.4.4.1 Pressure measurement evaluation

Interface pressure evaluations allow the clinician to identify the support surface that provides the lowest peak pressure as well as the best pressure distribution over the supporting surface. Interface pressure provides "snapshot" data and can be used to compare the relative effectiveness of different products from the vast selection available today. A large percentage of pressure ulcers occur near the ischial tuberosities. It is common to principally evaluate cushion on how well they reduce pressure at that area (Webster, 1991).

Sitting pressure were first measured using mechanical valves and compressed air tanks (Kosiak, 1959, Houle and Minnesota, 1969). Optical techniques have been used, based on the prototype built in 1934 by Elftman (Treaster and Marras, 1987). Other techniques used include mechanical springs (Linden et al., 1965); thermographs (Trandel et al., 1975); capacitive sensors (Hills et al., 2001); and pressure-sensitive ink (Ferguson-Pell et al., 2000). The main problem with most of these techniques is the validity and the reliability of the measurements (Gross et al., 1994, Gyi et al., 1998).

The developments in electronics technology allow for more precise pressure measurements. Devices that have been used to measure interface pressure and its distribution over the support area ranged from a single transducer moved to new body locations for successive measurements, to entire arrays of transducers for simultaneous

observation of pressures from the entire support area. Single-sensor pressure evaluators such as the Skin Pressure Evaluator (Camp International Inc., Jackson, MI), Lotus Pressure Meter (Lotus, Naugatuck, CT), and Next Generation Interface Pressure Evaluator (Span America, Greenville, SC) are portable, affordable, and provide the clinician with objective pressure readings over single sites or small areas. New pressure mapping systems use seat-sized sensing pads and graphic displays that measure the full buttock-cushion interface, eliminating the need for multiple sensor placements over different sites. Examples of such systems are Force Sensing Array (FAS, Vista Medical, Manitoba, Canada), Xsensor (Crown Therapeutics, Inc., Belleville, IL), ClinSeat (Tekscan, Inc., South Boston, MA), Pliance (Novel Electronics, St. Paul, MN), TIRR Pressure Evaluator Pad (Tee Kay-Applied Technologies, Stafford, TX), Oxford Pressure Monitor (Camp International Inc., Jackson, MI), and QA Pad (Aandera Medical Instruments, Victoria, Canada).

Generally, the main types of sensors that have been reported in the literature to measure seat-body interface pressures are electronic, pneumatic, hydraulic and electropneumatic (Table 1-9). Because some pressure ulcers develop due to high internal pressure, it is desirable to know the pressure of the internal tissue. Three types of internal pressure measurement sensors and six types of external pressure measurement sensors have been compared (Table 1-10).

Several studies have provided data on the mean interface pressures of different cushions (Table 1-11). Although the studies are not altogether consistent, there are some general similarities. All studies indicated that the gel type cushion has the highest pressures. This could be associated with the hammock effect of the membrane holding the gel. Fluid flotation and foam cushions appear to produce consistently lower pressures. Air type cushions yield average-to-low pressures. Sprigle et al. (1990b) indicated that custom contouring a foam cushion lowers pressures even more: for a high-resiliency polyurethane cushion, contouring decreased pressures from 53 to 45 mm Hg.

**Table 1-9 Comparison of electropneumatic, pneumatic, hydraulic, and electronic pressure sensors**  
(Summarized from Kosiak, 1959, Souther et al., 1974, Reger et al., 1988, Allen et al., 1993a & 1993b, Ferguson-Pell and Cardi, 1993, Gyi et al., 1998).

Type	Sensor	Characteristics	Advantage	Disadvantage
Electropneumatic	Scimedics Inc.: <b>Single bladder sensor</b> Reger et al., 1988	1 cell surface area 64 cm <sup>2</sup> compressed thickness 0.4 mm Upper limit 120 mm Hg	Inexpensive Simple to operate	Large size Causes subject's weight to shift and imbalance
	Gaymar Inc.: <b>PSP-1 pressure transducers</b> Reger et al., 1988	1 cell surface area 21 cm <sup>2</sup> compressed thickness 0.6 mm	Simple good repeatability	Cushion effect
	Texas Institute of Rehabilitation Research: <b>Pressure Evaluating Pad (PEP)</b> Reger et al., 1988	144 cells, area of 1 cell 10 cm <sup>2</sup> surface area 2200 cm <sup>2</sup> compressed thickness 0.4 mm Upper limit 200 mm Hg	Covers large measuring surface	Cushion effect Reduces the applied pressure in adjacent high-pressure areas
	Next Generation Inc.: <b>Digital Interface Pressure Evaluator (DIPE)</b> Allen et al., 1993a & 1993b	100 mm diameter sensor system error 27% repeatability $\pm 0.12$ kPa	Simple good repeatability	not as accurate as Talley Pressure Evaluator SA500
	Talley Medical Equipment, Ltd.: <b>Talley Pressure Evaluator SA500</b> Allen et al., 1993a & 1993b	1 cell, 28 mm diameter sensor lower limit 20 mm Hg system error 12% repeatability $\pm 0.07$ kPa	Simple good repeatability	Cushion effect
Pneumatic	Oxford Orthopedic Engineering Center: <b>Oxford Pressure Monitor (OPM)</b> Reger et al. 1988, Hobson 1992	12 cells surface area 88 cm <sup>2</sup> compressed thickness 0.4 mm Upper limit 300 mm Hg	Reliable and durable device Provides reasonably accurate results within know limits	Weight shift effect The spatial resolution may not be fine enough Cushion effect
	Talley Medical Equipment, Ltd.: <b>Talley Pressure Monitor 3 (TPM3)</b> Ferguson-Pell and Cardi, 1993	48 sensors, 20 mm diameter surface area 48.5x48.5 cm range 0-246 mm Hg resolution 1 mm Hg precision $\pm 4$ mm Hg	More accurate, stable, and reproducible that Tekscan system and FSA	Limited in ease of use, speed, and data presentation
	<b>Rubber butterfly valve</b> Kosiak, 1959	12 cells, area of 1 cell 2 cm <sup>2</sup> surface area 220 cm <sup>2</sup> Upper limit 300 mm Hg	Simple good repeatability	Cushion effect
	<b>Henry surface pressure manometer</b> Souther et al., 1974	1 cell Upper limit 130 mm Hg	Simple good repeatability	Cushion effect
Hydraulic	<b>Water bladder system</b> Allen et al., 1993a & 1993b	19 mm diameter water bladder system 0.1 ml of water system error 17% repeatability $\pm 0.13$ kPa	Simple good repeatability	the volume of water within the bladder affected the accuracy markedly; not as accurate as Talley Pressure Evaluator SA500
Electronic	Vistamed Inc.: <b>Force Sensing Array (FSA)</b> Ferguson-Pell and Cardi, 1993	225 sensors, 25x25 mm surface area 51x51 cm range 0-255 mm Hg resolution 1 mm Hg	rated well in clinical application and data management	Shows some instability hysteresis $\pm 19\%$ and creep 4%
	Tekscan Inc.: <b>Tekscan System</b> Ferguson-Pell and Cardi, 1993	2064 sensors, 8x8 mm surface area 49x52.5 cm range 10-200 mm Hg resolution 1 mm Hg precision $\pm 10$ mm Hg	real-time display	hysteresis $\pm 22\%$ and creep 19%

**Table 1-10 Comparison of various types of electronic pressure sensors for internal and external measurements (Webster, 1991).**

Sensor		Cost	Size (mm) WxLxH	Repeatability	
External measurement sensor	Conductive polymer	\$1	10x15x0.2	Fair	
	Semiconductor strain gauge	\$10-1000	1x103x0.4	Excellent	
	Metal strain gauge	\$100-500	2.7x2.7x0.3	Excellent	
	Discrete capacitive	\$50-200	15x15x0.4	Good	
	Extrinsic optoelectronic	\$2-500	3x4x2	Good	
	Intrinsic optoelectronic	NA	20x11x0.2	Good	
Internal measurement sensor	Integrated circuit capacitive	\$50-1000	2x3x0.4	Excellent	
	Integrated circuit semiconductor	\$50-1000	1x1.3x0.4	Excellent	
	Wick catheter	\$10	1.0 OD	Good	
Sensor		Linearity	Hysteresis	Temp. Coeff.	Ease of use
External measurement sensor	Conductive polymer	Poor	Poor	Good	Excellent
	Semiconductor strain gauge	Good	Excellent	Fair	Good
	Metal strain gauge	Excellent	Excellent	Poor	Fair
	Discrete capacitive	Good	Good	Good	Poor
	Extrinsic optoelectronic	Good	Good	Good	Fair
	Intrinsic optoelectronic	Good	Good	Good	Poor
Internal measurement sensor	Integrated circuit capacitive	Good	Excellent	Excellent	Good
	Integrated circuit semiconductor	Good	Excellent	Fair	Good
	Wick catheter	Excellent	Excellent	Excellent	Fair

**Table 1-11 Mean pressures under the ischial tuberosities for the four cushion types (Webster, 1991).**

Cushion type	Pressures (mm Hg) (Cochran, 1981)	Pressures (mm Hg) (Souther, 1974)	Pressures (mm Hg) (Mooney, 1971)
Foam	67	58	68
Gel	93	67	80
Fluid flotation	71	41	70
Air	79	53	73

#### 1.4.4.2 Shear measurement evaluation

Shear stress is difficult to measure, and the mechanics of tissue destruction by shear are not easy to model. Because good research experiments and clinically relevant models are scarce, the shear measurement evaluation is limited by the lack of suitable transducers. Below, some methods of measuring shear forces are discussed:

- ◆ Lewis and Nourse (1978) measured shear using a pneumatic design. The basic operating principle of the device is the measurement of the relative motion between a small area of skin surface and the larger surrounding area of skin.
- ◆ Bennett et al. (1979) developed an instrument capable of measuring horizontal shear, pressure, and pulsatile arteriolar blood flow. Because the sensor is rigid and hard, it is not suited to measure interface shear forces between compliant surfaces.
- ◆ Fan et al. (1984) utilized a simple parallel plate capacitor where the top plate could slide horizontally under shear.
- ◆ Cooper (1986) used simple Hall-effect sensors to monitor shear forces. However, the sensors are quite large and not suitable to measure interface shear forces.
- ◆ Webster (1991) built a prototype silicon elastomer encased cantilever beam to measure shear forces under the sacrum in elevated hospital beds. The experimental results were quite linear.
- ◆ Goossen et al. (1997) introduced a capacitive shear sensor. The size of the sensor is 2.7x1.5x0.35 cm and the contact area is 4.05 cm<sup>2</sup>. Six sensors were glued onto a thin mat, thus the sensor mat can be used on soft surfaces. The results showed that the highest shear stress was in regions of highest pressure and local shear stress was highly affected by change in body postures.
- ◆ Aissaoui et al. (2001b) evaluated a newly developed shear sensor (VERG Inc., Winnipeg, Canada) on able-bodied subjects. The results of this study suggested that shear forces increased 10% -12% during seat tilting and backrest reclining. The shear force measurements could be used to better understand the body-seat interface. However, further study has to been done to validate the clinical application of this sensor on wheelchair users.

#### 1.4.4.3 Shape measurement evaluation

Their ease of use makes the pressure measurements practical within the clinical setting for seating assessment. There are, however, substantial limitations to the accuracy and

significance of pressure measurements. The interpretation of pressure measurements to identify adverse seating interface conditions is also seriously limited by the lack of knowledge of pressure ulcer etiology (Levine et al, 1990). Recently, seat contour measurements have been used to evaluate the buttock-cushion interface to further define the load bearing of the buttocks (Sprigle and Schuch, 1993).

The selection of seating support surface is influenced by many factors, such as unloaded cushion shape and tissue shape; the mechanical properties of seat materials or cushions; the location and shape of underlying skeletal structures; and tissue thickness, composition, and tone. The correct positioning of an individual in a seating system is crucial as it establishes a baseline for the location, size, and direction of the loads to be transmitted from the skeletal system through the tissues to the support surface. These loading characteristics, combined with mechanical tissue properties and underlying skeletal structures, determine the resultant tissue shape configuration (Levine et al, 1990).

Measurement of interface pressure distribution alone cannot predict tissue deformation because, in addition to the boundary conditions (seating surface or cushion), mechanical properties of skin, fat, muscle, and bone contribute to the resultant tissue configuration from a particular pressure distribution. Given that the combined mechanical properties of these tissues vary among locations on the seating surface, as well as among individuals, there is no guarantee that any particular pressure distribution (including an equalized one) will achieve an optimal seating configuration. It is therefore concluded that tissue shape and deformation (as compared to pressure) are more direct measures of the *net* effect of an external load on human tissue, especially for an individual seated on a wheelchair cushion. Using finite element analysis and in vivo soft tissue parameter measurements, Todd (1994) reached the conclusion that "buttock-cushion interface pressure does not provide adequate information as to the performance of a particular cushion in decubiti prevention". Bédard-Phan (1999) and Wagnac (2002) also developed

a biomechanical finite element model to simulate the interface between a seat cushion and the buttocks in seating conditions. The results from their studies showed that the deformation of a body-seat interface could be represented by a computer model.

Husain (1953) noted the importance of altered tissue shape as an evaluation parameter in pressure ulcer formation. Chow et al. (1976) studied tissue deformation produced from external forces (both normal and shear), using it as a direct measure of blood vessel occlusion. Graebe (1980) asserted that pressure measurements alone are inadequate for assessing loading effects and suggested that "individual tolerance to mechanical suspension loads may be better determined by considering deformation patterns." Reddy et al. (1981) stated that tissue deformation and the associated response of blood, lymph, and interstitial fluid elements needs to be included in an adequate model of pressure ulcer formation. Finally, a number of additional investigations have noted the importance of altered tissue shape as an evaluation parameter in pressure ulcer formation and used tissue deformation measurements in analyzing the seating interface.

The inherent problem with using tissue deformation measurements to characterize tissue mechanics is that presently there are no practical clinical methods for direct measurement of deformation. Imaging techniques such as ultrasound and magnetic resonance imaging are candidates but are undeveloped for this purpose.

#### 1.4.4.4 Sitting stability evaluation

Dynamic sitting refers to the continuous process of postural changes during sitting (Aissaoui et al., 2001a). Research related to the quantification of sitting stability has been oriented toward applications such as postural sway measurements (Reid and Sochaniwskyj, 1991), and functional reach (Curtis et al., 1995, Seelen et al., 2001), as well as wheelchair stability (Cooper et al., 1994, Kamper et al., 1999). However, ways of measuring sitting stability vary between investigators and applications. In wheelchair

seating, static stability has been measured by the angle at which the front or side wheel of the wheelchair loses contact with the ground on a tilting platform (Cooper et al., 1994). Recently, Kamper et al (1999) imposed a lateral tilting perturbation to individuals with spinal cord injury (SCI) and measured the displacement of the center of pressure (COP) at ground level. They found that the maximum COP displacement tolerated was highly related to dynamic stability.

The stability provided by seat cushions is considered to be the most important characteristic of sitting support after pressure distribution (Ferguson-Pell, 1990, Staarink, 1995). The effect that cushions have on stability can be critical especially for users with poor trunk control. Persons with spinal lesions often have an acute awareness of their trunk stability that is far more subtle and complex than position measurement systems are able to detect (Ferguson-Pell, 1990). In a clinical setting, compromises between cushion stability and pressure distribution capacity often have to be made. This is usually performed in practice by accepting a small increase in the accepted pressure over bony areas. Furthermore, it is suggested that maintaining postural stability requires control of both displacement and velocity of COP (Kamper et al., 1999). Aissaoui et al. (2001a) examined the effect of seat cushion on dynamic sitting stability during a controlled reaching task performed by individuals with paraplegia. The results of their study confirmed that sitting balance was influenced by the seat cushion, and that the seat cushion was considered stable when it allowed the COP to move rapidly and to cover a larger distance. Therefore, measuring the trajectory of the COP provides an objective method to assess the dynamic stability of wheelchair users when they perform a forward reaching task.

#### 1.4.4.5 Comfort evaluation

Comfort is the main design objective for the wheelchair users because of the many hours per day they spend sitting. They often use commercial wheelchair cushions in an attempt



to improve their sitting comfort. However, a review of the literature uncovered very few attempts to measure seat comfort in wheelchair users. Wheelchair seating comfort research is limited not only by a lack of awareness that the discomfort problem exists, but also by the fact that comfort assessment is challenging.

Comfort is an abstract noun for a personal feeling that is so complex that it does not appear to lend itself to an objective measure that is sufficiently relevant and all embracing. In situations of this kind it is fairly common to resort to the use of a judge as a measuring instrument. Under standardized testing conditions, a person's feeling of comfort can be assessed by a variety of subjective measurements: 1) general comfort rating, 2) body area comfort rating, 3) chair feature checklist, 4) method of adjustment, and 5) personal comments (Shackel et al., 1969, Christiansen, 1997, Fenety et al., 2000, Ebe and Griffin, 2000&2001, Kolich, 2003).

Harms (1990) used methods 2), 3) and 5) to evaluate conventional folding wheelchairs and found that the folding wheelchairs caused discomfort in both able-bodied and disabled subjects. Shaw (1991) used method 3) to evaluate folded cloth and water cushions and found that there was no relationship between peak sitting pressure and seat discomfort. Lee et al. (1993) used method 2) to measure car seat comfort and also concluded that the correlation between pressure data and subjective comfort were not high enough to be the basis for any design decision. Gyi et al. (1999) used methods 2) and 3) to evaluate different foam seats and found that there was no clear and simple relationship between interface pressure and driving discomfort. Gross et al. (1994) also used method 3) to evaluate seat comfort but he concluded that the pressure variables were closely related to comfort. The above four studies also showed that although anthropometry and seat geometry interact in complex ways to produce seat pressure, optimizing the comfort of prototype seats with respect to the magnitude and pattern of the pressure distribution can significantly reduce product development time.

## 1.5 Shape measurements in seating

### 1.5.1 Body or seat surface shape measurements

McGovern et al. (1988) completed a one-piece mold of the patient and then used a manual cast contour gauge system to measure discrete levels of the contour (Figure 1-14 a). The gage was made from 168 parallel 1/8" diameter  $\times$  12" long ( $4 \times 300$  mm) stainless steel rods that were held by two aluminum channels and could move independently from one another. Once the positional depths of the rods were set, the rods were removed from the cast and placed on a 1/2" or 1" (13 or 25 mm) thick blank Ethafoam slab. The contour was then cut out of the blank slab using a band saw. This process was repeated until the whole contour was represented by cross-sectional pieces of foam (Figure 1-14 b).

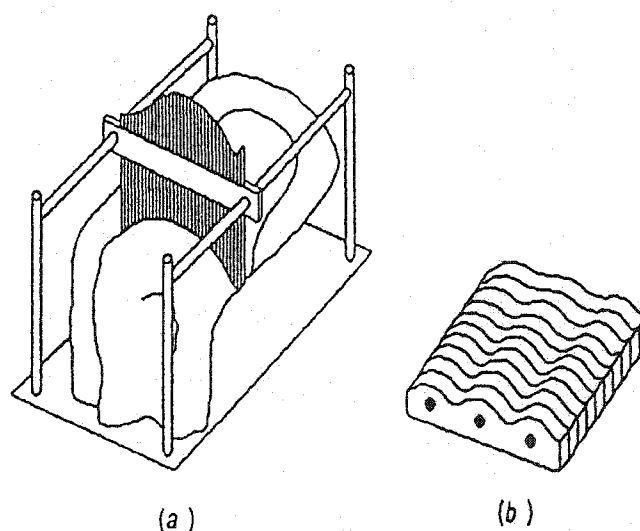


Figure 1-14 (a) Cast measuring system using stainless steel rods (b) Ethafoam slabs stacked together to form the contoured cushion after being cut by a band saw (McGovern et al., 1988).

Neth et al. (1989) enhanced the previous mechanical method of McGovern et al. (1988) by using thirty-two electronic linear potentiometers (Figure 1-15 a). The potentiometers were mounted onto aluminum shafts and recorded a voltage for each section of the contour. Voltage was sampled and sent to an analog-to-digital converter which was recorded by a computer. The linear potentiometers were placed side-by-side and spaced at  $\frac{1}{2}$ " (13 mm) intervals. The entire array of potentiometers could be moved longitudinally on guides supported by the molding frame. Figure 1-15 (b) depicted the display of the contour data.

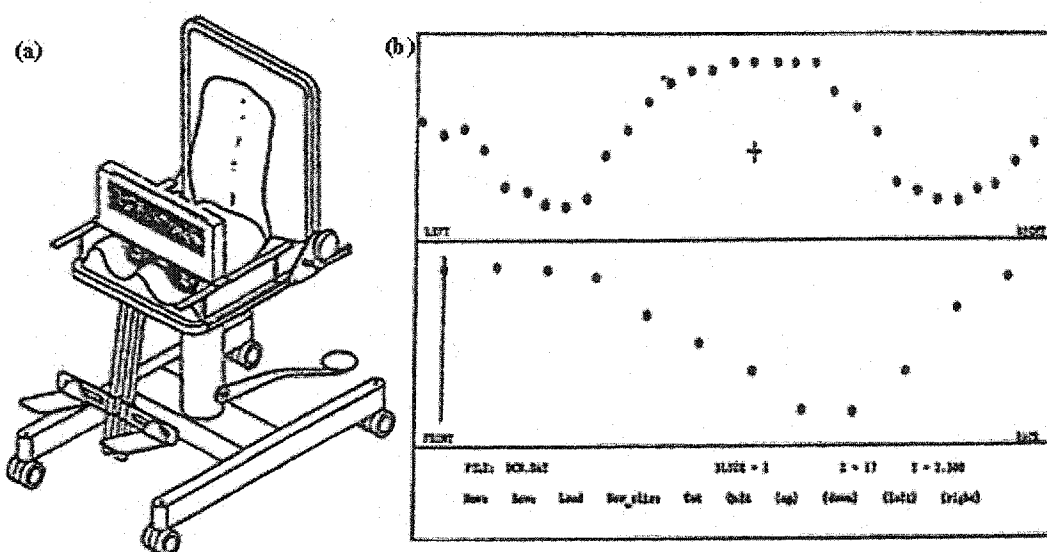


Figure 1-15 (a) Electronic Contour Measurement System (b) Display of the contour data. (Neth et al., 1989).

In the study of Toney et al. (1995), a Signature 2000 contour measurement system (Akron-Cleveland Home Medical Services, OH) was used to measure the contour of a cast. Thirty-two points per line were randomly chosen and printed out to represent the line chosen. Totally, eight lines were printed and labeled for each cast.

Lemaire et al. (1996) used a magnetic digitizer and micro-computer assembly to record surface contours manually. The digitizing unit located the three-dimensional position of

a hand-held stylus by creating a magnetic field around the surface, determining the strength of the field at the stylus location, and scaling the field strength to x, y, and z distances. The clinician digitized a series of medial-lateral parallel lines along the surface by positioning the stylus on the surface and pressing the mouse button on the computer (Figure 1-16). These data points were used to interpolate a mathematical representation of the surface's shape.

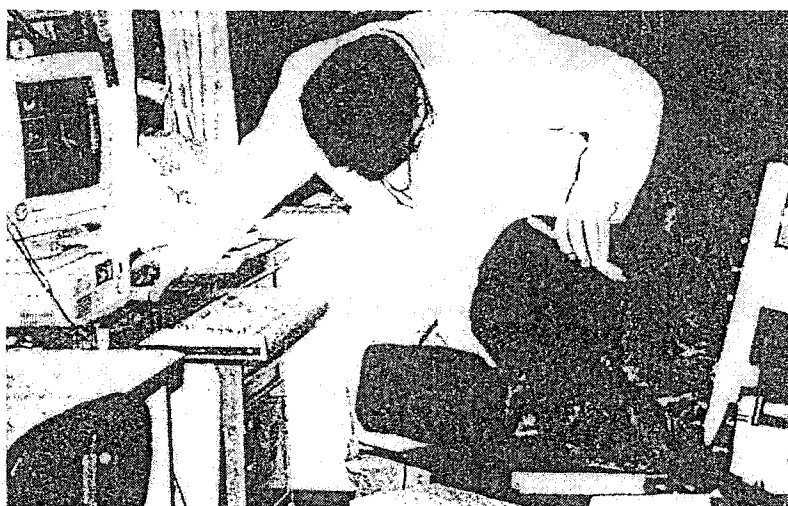
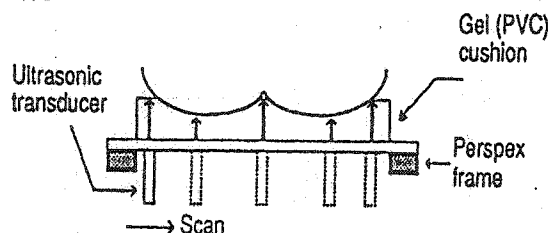


Figure 1-16 Digitization on the contour surface (Lemaire et al. 1996).

### 1.5.2 Body-seat interface shape measurements

Kadaba et al. (1984) introduced a prototype ultrasonic system to measure contours using the principle of refraction. A transducer sent an excitation pulse that traveled through the cushion medium (Figure 1-17) and the signal was reflected and refracted at each interface between two layers with dissimilar acoustic impedances. Thus, it was possible to accurately determine the thickness of the cushion based on the delay in the reflected echoes of the original pulse.



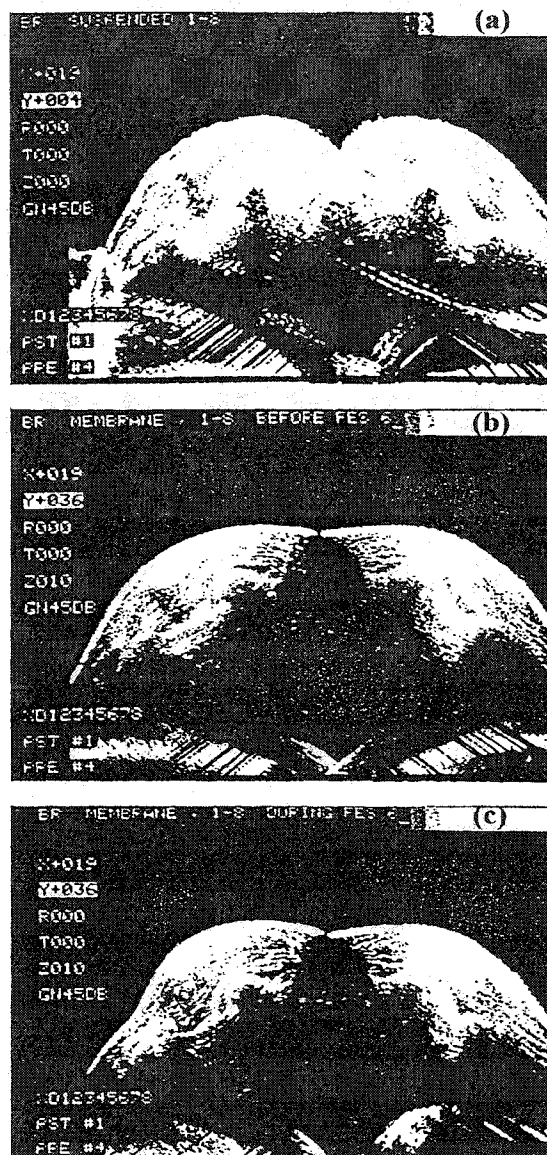
**Figure 1-17** The ultrasound transducer emits a pulse that measures distance to the buttocks by time of flight (Kadaba et al., 1984).

As the transducer was positioned across the frame at marked intervals, the delay time of the echo was digitized and stored on a PC. This technique was not only useful for measuring buttock-cushion contours, but it might help to describe the geometry of soft tissues deformed under a load.

Reger et al. (1985) developed an array of linear potentiometers to measure vertical displacement under a wheelchair cushion and produced a three-dimensional surface contour of the tissue shape. A six-order polynomial curve-fitting technique was used to characterize two-dimensional curves produced from each row of potentiometers. In 1986, Reger et al. also used magnetic resonance imaging (MRI) to illustrate the internal tissue changes in the buttocks that are associated with loading in the recumbent position. However, at present MRI does not permit measurements in the sitting position and cannot accommodate a wheelchair.

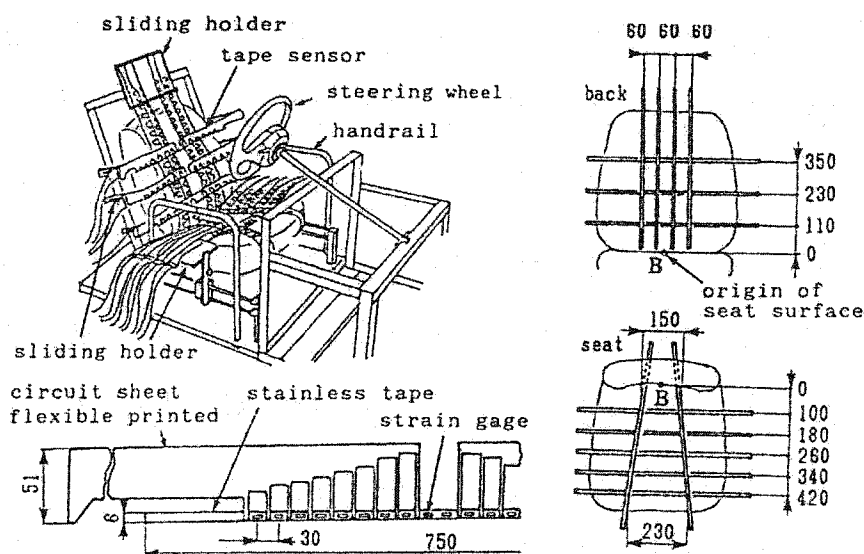
Levine et al. (1990) quantified the changes in buttocks shape at the seat interface using an eight transducer ultrasound imaging system to evaluate the effects of electrical muscle stimulation (EMS) for pressure ulcer prevention. High resolution echograms of a transverse section through the ischial tuberosities were generated for seated subjects under three conditions: buttocks suspended in water (no load); subject seated on a plastic membrane over water (loaded-no EMS); and subject seated with EMS applied (loaded-with EMS) (Figure 1-18). Mathematical quantification of surface contour differences

was performed by calculating the mean and maximum differences in the distances between curves. Quantitative measurements were performed only for surface contour differences, although information on shape and deformation of internal tissue was also contained in the high-resolution echograms.



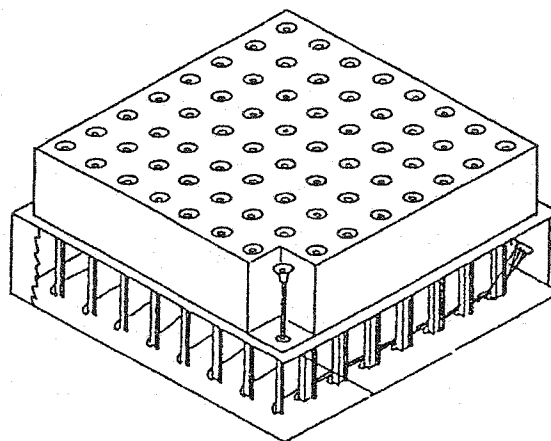
**Figure 1-18** Ultrasonic images of the buttocks from a single subject under three conditions: (a) suspended; (b) load/no EMS; (c) load/EMS (Levine et al., 1990).

Yamazaki (1992) used flexible, thin tape sensors to measure contact shape between a seated person and the seat surface to evaluate sitting comfort. Each tape has twenty strain gauges at 30 mm intervals, and the fourteen tape sensors were arranged on the seat and back (Figure 1-19). The tape is 0.15 mm thick and 6 mm wide. The author reported that the accuracy of the measurement was 3%. However, the accuracy decreased when there were some irregularities in the tack or seam line of the seat surface, and when there were large differences of cushion stiffness in the surface.



**Figure 1-19** Structure and arrangement of the developed tape sensor (size in mm) (Yamazaki, 1992).

In the study of Sprigle and Schuch (1993), contour of the buttocks-cushion interface was measured by a contour gauge, which formed the seat of a positioning system consisting of 64 probes arranged in a 16" by 16" area (Figure 1-20). Linear potentiometers, attached to each probe, were used to measure cushion deflection in the seating area. The probes passed through holes in a foam cushion, which had been predrilled to match the 8 by 8 array. Once the client was properly seated, the potentiometer deflections were collected using a computer and the data were interpolated to a 33×33 array.



**Figure 1-20 Computer-aided shape sensor (Sprigle and Schuch, 1993).**

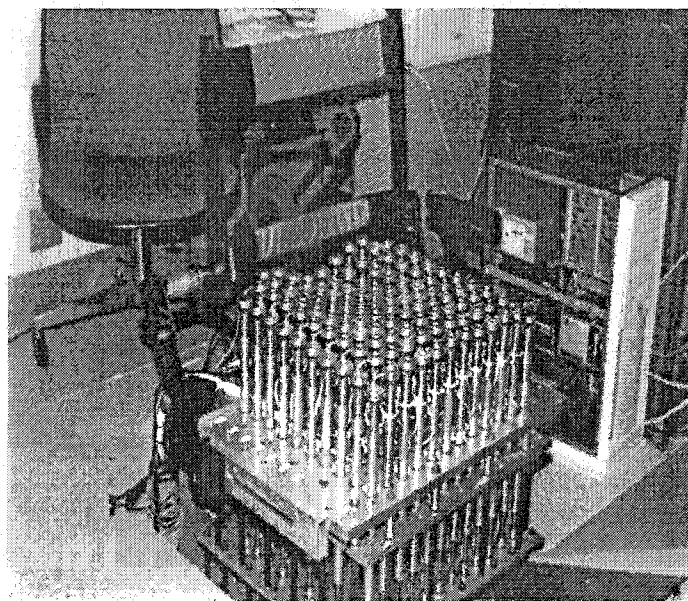
The foam contour gauge described above was one of the earliest versions of the Electronic Shape Sensing (ESS) system (Figure 1-21) which was developed at the University of Virginia's Rehabilitation Engineering Center (Brienza et al., 1991). The ESS support surface consisted of an  $11 \times 12$  rectangular array of support elements that are spring-loaded and deflect downward in response to loads applied to the spherical tops of the elements. With a person seated on the drive, the elements deflected downward until force equilibrium was reached. The deflection of each spring-loaded support element was measured using linear potentiometers coupled to each element. The support element resolution ranged from 5.08 to 3.81 cm.

Brienza et al. (1996a) also designed a second generation of the Computer-Aided Seating System (CASS) (Figure 1-22). As compared to the ESS, the CASS had the ability to adjust surface shape four times more rapidly, measure interface pressure directly at the support surface (as opposed to indirectly using force measurements), and used updated computing and interfacing equipment. The CASS is similar in its mechanical configuration to the ESS in that it consisted of an  $11 \times 12$  rectangular array of support elements.





**Figure 1-21 Electronic Shape Sensor (ESS) used to measure the seated shape (Brienza et al., 1991).**

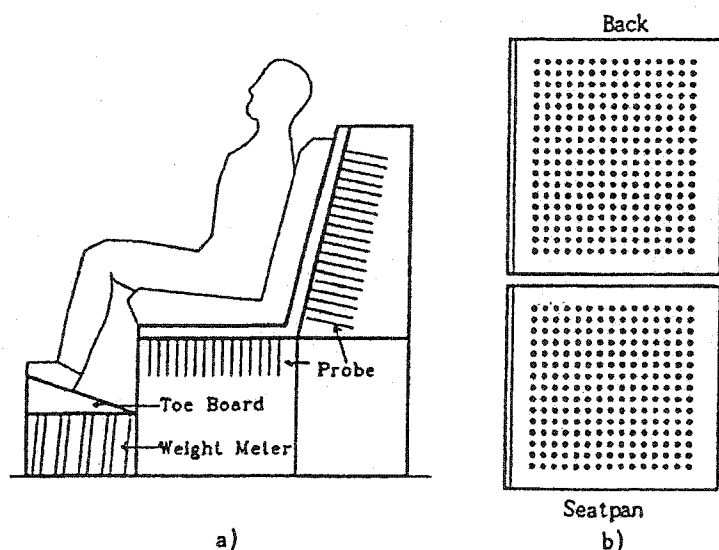


**Figure 1-22 Computer-Aided Seating System (CASS) (Brienza et al., 1996a).**

The distance between CASS support elements was 4.27 cm. Control of surface shape was mediated by selective linear translation of the support elements along their

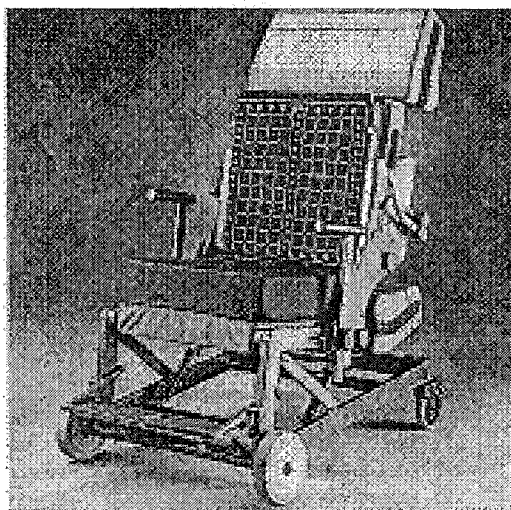
respective vertical axes. Closed-loop control of the system allowed for the dynamic formulation of a support surface on the basis of programmable criteria. The optimization algorithm was based on measurements of tissue stiffness and externally applied pressure. The goal of the algorithm was to minimize the gradient of the quantity "pressure multiplied by stiffness".

Chang et al. (1996) employed the "Direct contact probe measurement system" to measure the seatpan and seatback contours (Figure 1-23 a). These probes were arranged in a  $30 \times 30$  mm matrix (15 points longitudinally and 15 points laterally for the seatpan and 18 points longitudinally and 15 points laterally for the seatback, Figure 1-23 b). The probes (3 mm diameter) were placed throughout the seatpan and seatback in 5 mm diameter holes. The seat used in this study was the driver seat of a Korean car. The subject-seat interface contour shape was obtained visually from the positions of the probe ends.



**Figure 1-23 Direct contact probe system for subject-seatpan and seatback interface contour measurements (Chang et al., 1996).**

The PinDot Shape Sensor (Invacare Corporation, Elyria, OH) used a mechanical system in which wires pass through a 5" thick foam cushion, the translation of the wire end pieces can be digitized and form the basis of a custom cushion. The PinDot Shape Sensor (Figure 1-24) is a direct-measuring device that captures the shape of a client's body and prints that shape out onto a data form. The contoured cushions are carved from data taken on the Shape Sensor. The unit consists of a seat sensor module, a back sensor module, and a base frame.



**Figure 1-24 PinDot Shape Sensor (Invacare Corporation, Elyria, OH).**

### **1.5.3 Summary**

The measurement of body-seat interface shapes is becoming increasingly important to wheelchair cushion design and cushion evaluation. Among the techniques available for shape measurement, only a few can be considered to measure body-seat interface shape. Digitizing techniques such as coordinate measuring machines (CMM) and optical methods are ruled out because the interface cannot be exposed to those devices. Normal clinical radiographs or X-ray stereo photogrammetry give only indirect information

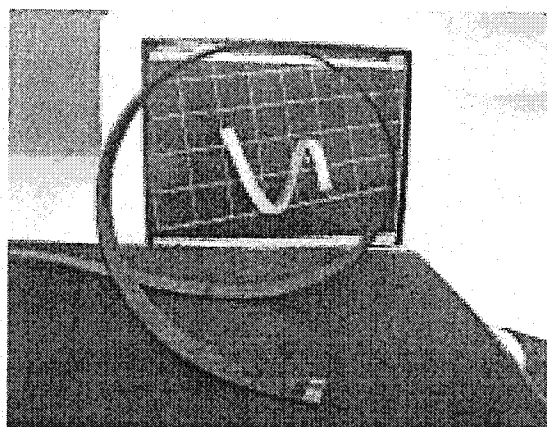
about the body-seat shape information. Moreover, full radiographic examinations lead to an undesirably high X-ray dose so that a non-invasive alternative for the assessment is highly desirable. Reger et al. (1986) used magnetic resonance imaging (MRI) to illustrate the internal tissue changes in the buttocks that are associated with loading in the recumbent position. But at present, computerized tomography (CT) scans and MRI does not permit measurements in the sitting position and cannot accommodate a wheelchair. Since the ultrasounds propagate poorly in the foam type cushions that are used by many patients, the ultrasonic contouring system developed by Kadaba et al. (1984) is limited. Therefore, medical imaging techniques such as radiographs, CT scans, MRI, and ultrasounds are also not suitable for body-seat interface measurement.

The body-seat interface measurement devices such as ESS (Brienza et al., 1991), CASS (Brienza et al., 1996a) and Direct contact probe system (Chang et al., 1996) provide useful contour and pressure information on seating support surface. However, the interface shapes measured by these devices are not body-cushion interface shapes. When the subjects sit on these devices, the probes support the body. Thus, these devices cannot be used clinically to select suitable cushions or configurations of cushion material for individual patients. Another disadvantage of these devices is that they are not portable. The PinDot Shape Sensor is now commercially available, whereas the other systems are still under investigation and are not readily applicable in the clinical setting. However, the PinDot Shape Sensor is expensive, heavy (frame 50 lbs., back sensor module 68 lbs., seat sensor module 46 lbs.) and cannot be carried easily. Furthermore, the PinDot Shape Sensor could not measure the interface shapes when users sit on the real cushions.

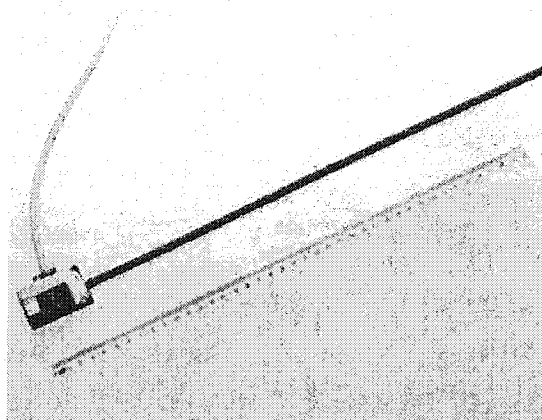
To date, practical clinical methods of measuring body-cushion interface shape have not been reported for typical cushioning materials (e.g., foam). The only device that is portable and could be placed between the subject and the cushion was described by Yamazaki (1992). However, it is not commercially available. Therefore, the first objective of this study was to develop an efficient, low-cost and easy to use device for

rapidly capturing the body-cushion interface shape in a clinical setting. The shape sensing device had to be flexible and very thin so that it could be placed between the subject and the seat without disturbing the subject's natural feeling.

Two commercially available flexible shape sensor tapes are the S1280CS ShapeTape™ (Measurand Inc, Fredericton, NB, Canada, Figure 1-25) and Rachismetre (Biogest, Denain, France, Figure 1-26). The Rachismetre can't be twisted which limits its application on a seating support surface (Table 1-12). On the other hand, the ShapeTape™ is an appropriate system for building an interface shape measurement system. In this study it has been used to measure body-cushion interface shapes.



**Figure 1-25 Illustration of shape sensor: SHAPE TAP (Measurand Inc, Fredericton, NB, Canada).**



**Figure 1-26 Illustration of shape sensor: Rachismetre (Biogest, Denain, France).**

**Table 1-12 Comparison of the two shape sensors: S1280CS ShapeTape™ (Measurand Inc, Fredericton, NB, Canada) and Rachismetre (Biogest, Denain, France).**

	<b>S1280CS ShapeTape™</b>	<b>Rachismetre</b>
<b>Type of sensor (number)</b>	Fiber optic curvature sensor (16)	strain gauge (4)
<b>Configuration</b>	sandwich of metal and elastomers	carbon fiber stem
<b>Dimensions of tape</b>	1.3 x 13 x 1800 mm	various lengths are available
<b>Sensitive zone</b>	480 mm	NA
<b>Output data</b>	x,y,z and orientation of 41 points along the sensitive zone	curves of the spine
<b>Range of each sensor</b>	± 40 mm radius bend; ±22.8 deg twist	100 mm radius
<b>Data acquisition speed</b>	120 Hz	NA
<b>Endpoint accuracy</b>	5 mm RMS	NA
<b>Resolution</b>	0.3 mm rms, x,y, or z; 0.5 deg, roll, pitch, or yaw	0.05 mm
<b>Operating temperature</b>	- 20 to + 50 deg c	NA
<b>Cost</b>	US\$2,100	US\$3,000
<b>Bendable</b>	Twist and bend	Bend only

## **1.6 Multivariate analysis methods**

The second objective of this study was to determine generic shape patterns for wheelchair cushion designs. The shape data measured from the seat surfaces does not directly reveal the underlying discriminating processes. The data are mingled with major and minor trends so it is difficult to extract a direct interpretation of the discriminating processes from the raw data. Multivariate analysis aims to interpret or disclose the discriminating processes through data reduction and classifications. Therefore, three important multivariate analysis methodological tools that can be used for shape discrimination are: principal component analysis, discrimination and classification, and cluster analysis.

### **1.6.1 Principal component analysis**

A principal component is concerned with explaining the variance-covariance structure through a few linear combinations of the original variables. Its general objectives are (1) data reduction, and (2) interpretation. Principal component analysis frequently serves as

an intermediate step in much larger investigations, such as multiple regression or cluster analysis.

#### 1.6.1.1 Population principal components

Algebraically, principal components are particular linear combinations of the  $p$  random variables  $X_1, X_2, \dots, X_p$ . Geometrically, these linear combinations represent the selection of a new coordinate system obtained by rotating the original system with  $X_1, X_2, \dots, X_p$  as the coordinate axes. The new axes represent the directions with maximum variability and provide a simpler and more parsimonious description of the covariance structure.

Principal components depend solely on the covariance matrix  $\Sigma$  (or the correlation matrix  $\rho$ ) of  $X_1, X_2, \dots, X_p$ . The  $i$ th principal component is given by

$$Y_i = e_i' X = e_{i1} X_1 + e_{i2} X_2 + \dots + e_{ip} X_p, \quad i = 1, 2, \dots, p$$

$$\text{with } \text{Var}(Y_i) = e_i' \Sigma e_i = \lambda_i \quad \text{Cov}(Y_i, Y_k) = e_i' \Sigma e_k = 0 \quad i \neq k$$
1.1

where  $(\lambda_1, e_1), (\lambda_2, e_2), \dots, (\lambda_p, e_p)$  are the eigenvalue-eigenvector pairs of  $\Sigma$  and  $\lambda_1 \geq \lambda_2 \geq \dots \geq \lambda_p \geq 0$ .

If some  $\lambda_i$  are equal, the choices of the corresponding coefficient vectors  $e_i$ , and hence  $Y_i$ , are not unique. From Eq. 1.1, the principal components are uncorrelated and have variances equal to the eigenvalues of  $\Sigma$ .

$$\text{Total population variance} = \sigma_{11} + \sigma_{22} + \dots + \sigma_{pp} = \lambda_1 + \lambda_2 + \dots + \lambda_p$$
1.2

and consequently, the proportion of total variance due to the  $k$ th principal component is

$$\left( \begin{array}{l} \text{proportion of total} \\ \text{population variance} \\ \text{due to } k\text{th principal} \\ \text{component} \end{array} \right) = \frac{\lambda_k}{\lambda_1 + \lambda_2 + \dots + \lambda_p}, \quad k=1, 2, \dots, p \quad 1.3$$

The correlation coefficients between the components  $Y_i$  and the variables  $X_k$  are

$$\rho_{Y_i, X_k} = \frac{e_{ki} \sqrt{\lambda_i}}{\sqrt{\sigma_{kk}}}, \quad i, k = 1, 2, \dots, p \quad 1.4$$

If most (for instance, 80 to 90%) of the total population variance, for large  $p$ , can be attributed to the first one, two, or three components, then these components can “replace” the original  $p$  variables without much loss of information.

#### 1.6.1.2 Sample principal components

The sample principal components are defined as those linear combinations which have the maximum sample variance. As with the population quantities, the following results are obtained:

- ♦ The  $i$ th sample principal component is given by

$$\begin{aligned} \hat{y}_i &= \hat{e}_i' x = \hat{e}_{1i} x_1 + \hat{e}_{2i} x_2 + \dots + \hat{e}_{pi} x_p, \quad i = 1, 2, \dots, p \\ \text{with } \text{simple\_variance}(\hat{y}_i) &= \hat{\lambda}_i \\ \text{simple\_covariance}(\hat{y}_i, \hat{y}_k) &= 0 \quad i \neq k \end{aligned} \quad 1.5$$

where  $(\hat{\lambda}_1, \hat{e}_1), (\hat{\lambda}_2, \hat{e}_2), \dots, (\hat{\lambda}_p, \hat{e}_p)$  are the eigenvalue-eigenvector pairs of the sample covariance matrix and  $\hat{\lambda}_1 \geq \hat{\lambda}_2 \geq \dots \geq \hat{\lambda}_p \geq 0$ .

- ♦ Total sample variance =  $\sum_{i=1}^p s_{ii} = \hat{\lambda}_1 + \hat{\lambda}_2 + \dots + \hat{\lambda}_p \quad 1.6$



$$\diamond \quad r_{\hat{y}_i, x_k} = \frac{\hat{e}_{ki} \sqrt{\hat{\lambda}_i}}{\sqrt{s_{kk}}}, \quad i, k = 1, 2, \dots, p \quad 1.7$$

When attempting to interpret of the principal components, the correlations  $r_{\hat{y}_i, x_k}$  may be more reliable guides than the component coefficients  $\hat{e}_{ki}$ . The correlations allow for differences in the variances of the original variables and avoid interpretive problems caused by different measurement scales.

### 1.6.2 Discrimination and classification

Discriminant analysis and classification are multivariate techniques concerned with separating distinct sets of objects (or observations) into groups and allocating new objects (observations) to the previously defined groups. Discriminant analysis is exploratory in nature. As a separatory procedure, it is often employed on a one-time basis in order to investigate observed differences when causal relationships are not well understood. Classification procedures are less exploratory in the sense that they lead to well-defined rules, which can be used to assign new objects. Classification ordinarily requires more problem structure than discrimination. Thus, the two immediate goals of discrimination and classification, respectively, are as follows:

- ◆ Goal 1: To describe either graphically (in three or fewer dimensions) or algebraically, the differential features of objects (observations) from several known collections (populations).
- ◆ Goal 2: To sort objects (observations) into two or more labeled classes, the emphasis being on deriving a rule that can be used to optimally assign a new object to the labeled classes.

A function that separates may sometimes serve as an allocator, and conversely, an allocatory rule may suggest a discriminatory procedure. In practice, Goals 1 and 2 frequently overlap and the distinction between separation and allocation becomes blurred.

### 1.6.2.1 Fisher's method for two populations

Fisher's idea was to transform the multivariate observations  $x$  to univariate observations  $y$  such that the  $y$ 's derived from populations  $\pi_1$  and  $\pi_2$  were separated as much as possible (Figure 1-27).

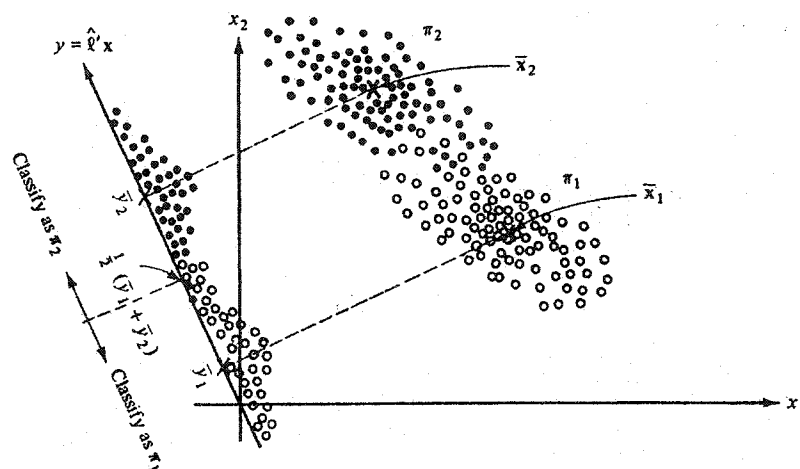


Figure 1-27 A pictorial representation of Fisher's procedure for two populations with  $p=2$  (Johnson and Wichern, 1988).

The Fisher's sample linear discriminant function is given by:

$$y = \hat{l}'x = (\bar{x}_1 - \bar{x}_2)'S_{\text{pooled}}^{-1}x$$

$$S_{\text{pooled}} = \frac{(n_1 - 1)S_1 + (n_2 - 1)S_2}{(n_1 + n_2 - 2)}$$

1.8

where  $S_1$  and  $S_2$  are sample covariance matrices.

The allocation rule based on Fisher's discriminant function is given by:

**Allocate  $x_0$  to  $\pi_1$  if**

$$y_0 = (\bar{x}_1 - \bar{x}_2)' S_{\text{pooled}}^{-1} x_0 \geq \hat{m} = \frac{1}{2} (\bar{x}_1 - \bar{x}_2)' S_{\text{pooled}}^{-1} (\bar{x}_1 + \bar{x}_2) \quad 1.9$$

**Allocate  $x_0$  to  $\pi_2$  if**

$$y_0 < \hat{m}$$

#### 1.6.2.2 Classification methods

Classification or allocation rules are usually developed from "learning" samples. A good classification procedure should result in few misclassifications. However, classification rules cannot usually provide an error-free method of assignment. This is because there may not be a clear distinction between the measured characteristics of the populations, that is, the groups may overlap. Suppose that classifying a  $\pi_1$  object as belonging to  $\pi_2$  represents a more serious error than classifying a  $\pi_2$  object as belonging to  $\pi_1$ . Then the classification should be cautious about making the former assignment.

A sensible classification rule could be determined by minimizing the Expected Cost of Misclassification (ECM). As ECM is given by

$$\text{ECM} = c(2|1)P(2|1)p_1 + c(1|2)P(1|2)p_2 \quad 1.10$$

where  $c(2|1)$  is the cost when an  $\pi_1$  object is incorrectly classified as  $\pi_2$ ,  $c(1|2)$  is the cost when an  $\pi_2$  object is incorrectly classified as  $\pi_1$ ,  $P(1|2)$  and  $P(2|1)$  are conditional probabilities, and  $p_1$  and  $p_2$  are the prior probability of  $\pi_1$  and  $\pi_2$ , respectively.

When two populations have a common covariance matrix, the allocation rule that minimizes the ECM is given by:

**Allocate  $x_0$  to  $\pi_1$  if**

$$(\mu_1 - \mu_2)' \Sigma^{-1} x_0 - \frac{1}{2} (\mu_1 - \mu_2)' \Sigma^{-1} (\mu_1 + \mu_2) \geq \ln \left[ \left( \frac{c(1|2)}{c(2|1)} \right) \left( \frac{p_2}{p_1} \right) \right] \quad 1.11$$

**Allocate  $x_0$  to  $\pi_2$  otherwise.**

In most practical situations, the population quantities  $\mu_1$ ,  $\mu_2$ , and  $\Sigma$  are unknown. Therefore, we substitute  $\bar{x}_1$  for  $\mu_1$ ,  $\bar{x}_2$  for  $\mu_2$ , and  $S_{pooled}$  for  $\Sigma$ , which gives the sample classification rule:

**Allocate  $x_0$  to  $\pi_1$  if**

$$(\bar{x}_1 - \bar{x}_2)' S_{pooled}^{-1} x_0 - \frac{1}{2} (\bar{x}_1 - \bar{x}_2)' S_{pooled}^{-1} (\bar{x}_1 + \bar{x}_2) \geq \ln \left[ \left( \frac{c(1|2)}{c(2|1)} \right) \left( \frac{p_2}{p_1} \right) \right] \quad 1.12$$

**Allocate  $x_0$  to  $\pi_2$  otherwise.**

Rule 1.12 is comparable to Rule 1.9 based on Fisher's linear discriminant function. Therefore, provided that the two normal populations have the same covariance matrix, Fisher's classification rule is equivalent to the minimum ECM rule with equal prior probabilities and equal costs of misclassification.

When the population covariance matrices are unequal, the allocation rule that minimizes the ECM is given by:

**Allocate  $x_0$  to  $\pi_1$  if**

$$-\frac{1}{2} x_0' (\Sigma_1^{-1} - \Sigma_2^{-1}) x_0 + (\mu_1' \Sigma_1^{-1} - \mu_2' \Sigma_2^{-1}) x_0 - k \geq \ln \left[ \left( \frac{c(1|2)}{c(2|1)} \right) \left( \frac{p_2}{p_1} \right) \right] \quad 1.13$$

$$k = \frac{1}{2} \ln \left( \frac{|\Sigma_1|}{|\Sigma_2|} \right) + \frac{1}{2} (\mu_1' \Sigma_1^{-1} \mu_1 - \mu_2' \Sigma_2^{-1} \mu_2)$$

**Allocate  $x_0$  to  $\pi_2$  otherwise.**

In practice, the classification rule is implemented by substituting the sample quantities  $\bar{x}_1$  for  $\mu_1$ ,  $\bar{x}_2$  for  $\mu_2$ ,  $S_1$  for  $\Sigma_1$ , and  $S_2$  for  $\Sigma_2$ :

$$-\frac{1}{2}x_0'(S_1^{-1} - S_2^{-1})x_0 + (\bar{x}_1'S_1^{-1} - \bar{x}_2'S_2^{-1})x_0 - k \geq \ln \left[ \left( \frac{c(1|2)}{c(2|1)} \right) \left( \frac{p_2}{p_1} \right) \right] \quad 1.14$$

One important way of judging the performance of any classification procedure is to calculate its “error rates”, or misclassification probabilities. The apparent error rate is defined as the fraction of observations in the training sample that are misclassified by the sample classification functions. This measure of performance does not depend on the form of the parent populations and can be calculated for any classification procedure.

$$APER = \frac{n_{1M} + n_{2M}}{n_1 + n_2} \quad 1.15$$

where  $n_{1M}$  = number of  $\pi_1$  items misclassified as  $\pi_2$  items

$n_{2M}$  = number of  $\pi_2$  items misclassified as  $\pi_1$  items

### 1.6.2.3 Discrimination methods

Fisher's discriminant analysis has several advantages in separating several populations for visual inspection or graphical descriptive purposes. It allows:

1. Convenient representations of the  $g$  populations that reduce the number of dimensions from a very large number of characteristics to relative few linear combinations.
2. Plotting of the means of the first two or three linear combinations (discriminants), which helps display the relationships between the populations and possible groupings of the populations.
3. Scatterplotting of the sample values of the first two discriminants, which can indicate outliers or other abnormalities in the data.

### **1.6.3 Cluster analysis**

Clustering, or grouping, can provide informal means for assessing dimensionality, identifying outliers, and suggesting interesting hypotheses concerning relationships. Clustering is distinct from classification methods. Classification pertains to a known number of groups, and the operational objective is to assign new observations to one of these groups. Cluster analysis is a more primitive technique in that no assumptions are made concerning the number of groups or the group structure. Grouping is done on the basis of similarities or distances (dissimilarities). The inputs required are similarity measures or data from which similarities can be computed.

#### **1.6.3.1 Similarity measures**

When items (units or cases) are clustered, proximity is usually indicated by some sort of distance. On the other hand, variables are usually grouped on the basis of correlation coefficients or like measures of association. There are four types of similarity measures: (1) correlation coefficients, (2) distance measures, (3) association coefficients, and (4) probabilistic similarity coefficients. Each of these has advantages and disadvantages that must be considered before a decision is made to use one or the other.

#### **Correlation coefficients**

The most popular correlation coefficient is the product-moment correlation coefficient suggested by Karl Pearson. Originally defined as a method to correlate variables, it has been used in quantitative classification to determine the correlation between cases. The correlation coefficient is defined as:

$$r_{jk} = \frac{\sum_{i=1}^p (x_{ij} - \bar{x}_j)(x_{ik} - \bar{x}_k)}{\sqrt{\sum_{i=1}^p (x_{ij} - \bar{x}_j)^2 (x_{ik} - \bar{x}_k)^2}} \quad 1.16$$

where  $x_{ij}$  is the value of variable  $i$  for case  $j$ ,  $\bar{x}_j$  is the mean of all values of the variables for case  $j$ , and  $p$  is the number of variables. The method is used with ratio or interval scale variables. In the case of binary data, correlation coefficient is transformed into the phi coefficient. The correlation coefficient is frequently described as a shape measurement, in that it is insensitive to differences in the magnitude of the variables used to compute the coefficient. Pearson's  $r$  is sensitive to shape because of its implicit standardization of each case across all variables. There are two drawbacks to the use of the correlation coefficient as a similarity measure: (1) Its sensitivity to shape is at the expense of the magnitude of differences between the variables. While similarity between profiles can be decomposed into three parts: shape, scatter (dispersion) and elevation (level or size), the product-moment correlation coefficient is sensitive only to shape, which means that two profiles can have a correlation of +1.0 and yet not be identical. Some information is lost and it is possible that misleading results can be obtained if the effects of scatter and the elevation on profiles of the data are not considered. (2) The use of the method to calculate the correlation of cases does not make statistical sense, because one must obtain the mean value across different variable types rather than across cases. Despite these drawbacks, the coefficient has been used successfully in a wide variety of research applications involving cluster analysis.

### Distances measures

Distance measures normally have no upper bounds and are scale dependent. The most commonly used distance measure is the Euclidean distance between  $p$ -dimensional observations:

$$d(x,y) = \left[ \sum_{i=1}^p |x_i - y_i|^2 \right]^{1/2} \quad 1.17$$

Another distance measure is the Minkowski metric:

$$d(x,y) = \left[ \sum_{i=1}^p |x_i - y_i|^m \right]^{1/m} \quad 1.18$$

For  $m=1$ ,  $d(x,y)$  measures the “city-block” distance between two points in  $p$  dimensions. For  $m=2$ ,  $d(x,y)$  becomes the Euclidean distance. In general, varying  $m$  changes the weight given to larger and smaller differences. The drawback of the use of the Euclidean and other distance metrics is that the estimation of the similarity between cases is strongly affected by elevation differences. Variables with both large size differences and standard deviations can essentially swamp the effects of other variables with smaller absolute sizes and standard deviations. Moreover, distance metrics are affected by transformations of the scale of measurement of the variables. In order to reduce the effect of the relative size of the variables, researchers routinely standardize the variables to unit variance and means of zero before the calculation of distance.

### Association coefficients

This type of measure is used to establish similarity between cases described by binary variables. Such data for two items  $i$  and  $j$  can be arranged in a  $2 \times 2$  table (Table 1-13). Many similarity coefficients have been proposed that combine the quantities  $a$ ,  $b$ ,  $c$ , and  $d$  (Table 1-14).

Table 1-13 Counts of binary variables for two items (Everitt, 1993).

		Item i		Total
		1	0	
Item j	1	a	b	a+b
	0	c	d	c+d
Total		a+c	b+d	p=a+b+c+d



Table 1-14 Similarity coefficients for binary data (Johnson and Wichern, 1988).

Coefficient	Rationale	Coefficient	Rationale
$\frac{a+d}{a+b+c+d}$	Equal weights for 1-1 matches and 0-0 matches.	$\frac{a}{a+b+c}$	No 0-0 matches in numerator or denominator. (The 0-0 matches are treated as irrelevant.)
$\frac{2(a+d)}{2(a+d)+b+c}$	Double weight for 1-1 matches and 0-0 matches.	$\frac{2a}{2a+b+c}$	No 0-0 matches in numerator or denominator. Double weight for 1-1 matches.
$\frac{a+d}{a+d+2(b+c)}$	Double weight for unmatched pairs.	$\frac{a}{a+2(b+c)}$	No 0-0 matches in numerator or denominator. Double weight for unmatched pairs.
$\frac{a}{a+b+c+d}$	No 0-0 matches in numerator.	$\frac{a}{b+c}$	Ratio of matches to mismatches with 0-0 matches excluded.

The two coefficients most commonly used in practice are the matching coefficient

$$\left(\frac{a+d}{a+b+c+d}\right) \text{ and Jaccard's coefficient } \left(\frac{a}{a+b+c}\right).$$

### Probabilistic similarity coefficients

Coefficients of this type are radically different from those described above in that, technically, the similarity between two cases is not actually calculated. Instead, this type of measure works directly upon the raw data. When forming clusters, the information gained by the combination of two cases is evaluated, and the combination of cases that provides the least information gain is fused. Probabilistic measures can be used only with binary data.

#### 1.6.3.2 Hierarchical clustering methods

Hierarchical clustering techniques proceed by either a series of successive mergers or a series of successive divisions. Agglomerative hierarchical methods start with the individual objects. Divisive hierarchical methods separate the individuals into finer groupings. Of the two types of hierarchical clustering schemes, the agglomerative

methods are far more widely used. Ward's method, average linkage and complete linkage methods are the most useful in practice.

### Linkage methods

Linkage methods are suitable for clustering items (cases), as well as variables. While at least 12 different linkage forms have been proposed, three have become widely popular: single linkage, complete linkage, and average linkage. The merging of clusters under the three criteria is illustrated schematically in Figure 1-28.

As shown in Figure 1-28, the single linkage results when groups are fused according to the distance between their nearest members. Complete linkage occurs when groups are fused according to the distance between their farthest members. Finally, average linkage occurs when groups are fused according to the average distance between the pairs of members in the respective sets.

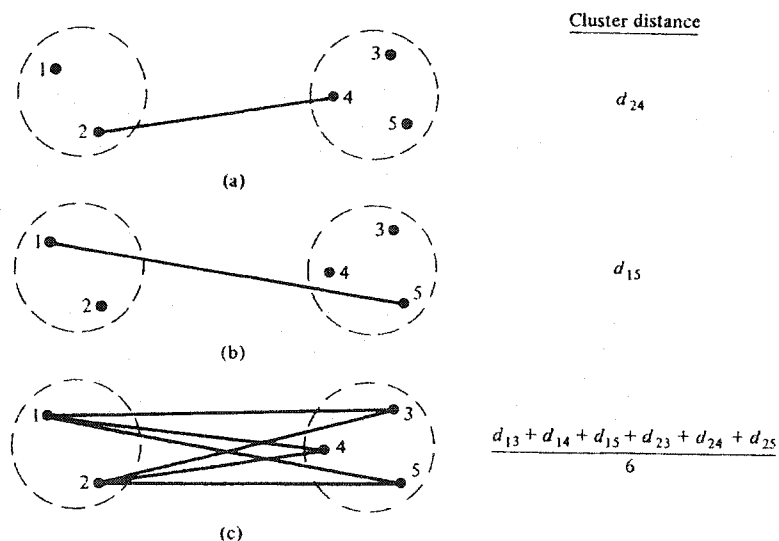


Figure 1-28 Inter-cluster distance (dissimilarity) for (a) single linkage, (b) complete linkage, and (c) average linkage (Johnson and Wichern, 1988).

The following are the steps in the agglomerative hierarchical clustering algorithm for grouping  $N$  objects (items or variables):

1. Start with  $N$  clusters, each containing a single entity and an  $N \times N$  symmetric matrix of distances  $D = \{d_{ik}\}$ .
2. Search the distance matrix for the nearest (most similar) pair of clusters. Let the distance between most similar clusters  $U$  and  $V$  be  $d_{UV}$ .
3. Merge clusters  $U$  and  $V$ . label the newly formed cluster ( $UV$ ). Update the entries in the distance matrix by (a) deleting the rows and columns corresponding to clusters  $U$  and  $V$  and (b) adding a row and column giving the distances between cluster  $UV$  and the remaining clusters ( $d_{(UV)W}$ ).
4. Repeat Steps 2 and 3 a total of  $N-1$  times. (All objects will be in a single cluster at the termination of the algorithm.) Record the identity of clusters that are merged and the levels (distances or similarities) at which the mergers take place.

Single-linkage, complete-linkage and average linkage clustering proceed in the same manner except that the calculations of distance ( $d_{(UV)W}$ ) are different. The comparisons of these three linkage methods are list in Table 1-15.

### Ward's method

This method is designed to optimize the minimum variance within clusters. This objective function is also known as the within-groups sum of squares or the error sum of squares. For univariate data, when  $n$  objects are clustered into  $g$  groups, the error sum of squares is given by:

$$\text{error sum of squares} = \sum_{k=1}^g \sum_{i=1}^{n_k} (x_{ik} - \bar{x}_k)^2 \quad 1.19$$

At the first step of the clustering process, there are  $n$  groups and each object is in its own cluster, the error sum of squares is 0. The method works by joining those groups or

objects that result in the minimum increase in the error sum of squares. The method tends to find clusters of relatively equal sizes and shapes as hyperspheres. In general, this method is regarded as very efficient; however, it tends to create clusters of small size.

**Table 1-15 Comparisons of single-linkage, complete-linkage and average linkage clustering methods (Summarize from Aldenderfer, 1984, Johnson and Wichern, 1988, Everitt, 1993).**

Method	$d_{(UV)W}$	Advantage	Disadvantage
<b>single-linkage</b>	$\text{Min}\{d_{UW}, d_{VW}\}$ $d_{UW}$ and $d_{VW}$ are the distances between the nearest neighbors of clusters U and W and clusters V and W.	It is invariant to monotonic transformations of the similarity matrix; It is unaffected by ties in the data.	Have a tendency to chain, or form long, elongated clusters.
<b>complete-linkage</b>	$\text{Max}\{d_{UW}, d_{VW}\}$ $d_{UW}$ and $d_{VW}$ are the distances between the most distant members of clusters U and W and clusters V and W.	Has a tendency to find relatively compact, hyperspherical clusters composed of highly similar items; Efficient when the objects form natural distinct clumps.	If the clusters tend to be somehow elongated or of a "chain" type nature, then this method is inappropriate..
<b>average linkage</b>	$\frac{\sum_i \sum_k d_{ik}}{N_{(UV)} N_W}$ $d_{ik}$ is the distance between object i in the cluster (UV) and object k in the cluster W, and $N_{UV}$ and $N_W$ are the number of items in clusters (UV) and W.	Efficient when the objects form natural distinct clumps; Performs equally well with elongated, "chain" type clusters.	Changes in the assignment of distances can affect the final configuration of clusters.

### 1.6.3.3 Nonhierarchical clustering methods

Nonhierarchical clustering techniques are designed to group items (cases), rather than variables, into a collection of K clusters. The number of clusters, K, may either be specified in advance or determined as part of the clustering procedure. Nonhierarchical methods start from either (1) an initial partition of items into groups or (2) an initial set of seed points, which will form the nuclei of clusters. Good choices for starting configurations should be free of overt biases. One way to start is to randomly select seed

points from among the items or to randomly partition the items into initial groups. One of the most popular nonhierarchical procedures is the K-means method.

### **K-means method**

The process of K-means method is composed of three steps:

1. Partition the items into K initial clusters.
2. Proceed through the list of items, assigning an item to the cluster whose centroid (mean) is the nearest. Distance is usually computed using the Euclidean distance with either standardized or unstandardized observations. Recalculate the centroid for the cluster receiving the new item and for the cluster losing the item.
3. Repeat Step 2 until no more reassignments take place.

Rather than starting with a partition of all items into K preliminary groups in Step 1, K initial centroids (seed points) could be specified and then proceed to Step 2. The final assignment of items to clusters will be, to some extent, dependent upon the initial partition or the initial selection of seed points. Experience suggests that most major changes in assignment occur within the first reallocation step. To check the stability of the clustering, it is desirable to rerun the algorithm with a new initial partition. In general, the choice of a particular K is not clear-cut and depends upon subject matter knowledge, as well as data-based appraisals. In cases where a single run of the algorithm requires the user to specify K, it is always a good idea to rerun the algorithm for several choices.

#### **1.6.3.4 Comparison of K-means method with hierarchical methods**

Unlike hierarchical agglomerative methods, which require the calculation and storage of an  $N \times N$  matrix of distance (similarities) between items (cases), the K-means method works directly upon the raw data. It therefore offers the opportunity of handling distinctly larger data sets than hierarchical methods. Moreover, the K-means method

makes more than one pass through the data and can compensate for a poor initial partition of the data, thereby avoiding one of the major drawbacks of hierarchical agglomerative methods. However, a major limitation of the K-means method is the problem of suboptimal solutions. Since this method can sample only a very small proportion of all possible partitions of a data set, there is the possibility that a suboptimal partition may be chosen. Unfortunately, there is really no objective way to determine if a solution obtained from the K-means method is globally optimal; one avenue to the solution of the problem, however, is to use the clustering method in conjunction with an appropriate validation procedure, such as a replication technique.

## **CHAPTER 2 HYPOTHESIS, OBJECTIVES AND GENERAL APPROACH OF THE PROJECT**

### ***2.1 Problem statement***

Measuring the shape of the body-seat interface has been used successfully in research to study tissue loading and as a means to fabricate custom contoured cushions. Levine et al. (1990) stated that measurements of body-seat interface shape and soft tissue deformation provide a more direct measure of the net effect of external load, mechanical tissue properties, and boundary conditions (cushion effects) than pressure measurements. Yamazaki (1992) used flexible, thin tape sensors to measure contact shape between a seated person and the seat surface in an effort to evaluate sitting comfort. Contact shape and pressure were compared qualitatively. Among other things, the author concluded that pressure patterns provide data for seat evaluation, while contact shape data provide data for seat design. Sprigle and Schuch (1993) suggested that seat contour measurements complement other clinical measures, such as seat interface pressures and general postural assessments, to form a more complete picture of the buttock-cushion interface.

The usefulness of shape measurements for clinical evaluation is restricted at the present time due to technical limitations, lack of experience and standards, and high costs. Currently, few systems have been developed to measure seat contours. The PinDot Shape Sensor (Invacare Corp., Elyria, OH) uses a mechanical system in which wires pass through a 5" thick foam cushion, the translation of the wire end pieces can be digitized and form the basis of a custom cushion. Kadaba et al. (1984) devised a method for measuring the contour of buttock-gel cushion interface using ultrasonic dimension gauging techniques. At the University of Virginia's Rehabilitation Engineering Center an Electronic Shape Sensor (ESS) was developed to measure seat interface contours.

The Computer-Automated Seating System (CASS) developed at the University of Pittsburgh has the ability to control the seating surface shape while measuring the pressure applied to the buttocks by the seating surface. Chang et al. (1996) used Direct Contact Probe Measurement System to provide a three-dimensional graphical output for visual evaluation. Yamazaki (1992) used arrays of strain gages (actually flat metal ribbons) to recreate seat shape.

The PinDot Shape Sensor is now commercially available, while the other five systems are still under investigation and are not readily applicable in the clinical setting. However, the PinDot Shape Sensor is expensive, heavy (frame 50 lbs., back sensor module 68 lbs., seat sensor module 46 lbs.) and cannot be carried easily. Furthermore, the PinDot Shape Sensor could not measure the interface shapes when users sit on the real cushions. Thus, the **first problem** to be addressed by this Ph.D. thesis was to develop an efficient, low-cost and easy to use system to rapidly capture the body-cushion interface shape in a clinical setting. The shape sensing device had to be flexible and very thin so that it could be placed between the subject and the seat without disturbing the interface itself. The basic information gathered using this shape measurement device may give fundamental input to successfully design generic contoured support surfaces. Furthermore, it is expected that this new device will provide a quick and effective tool for cushion evaluation and clinical guidelines for cushion prescription.

Contoured cushion lowers the risk of pressure ulcer development and improves sitting tolerance by providing more surface area and/or reducing peaking pressures near the ischial tuberosities, sacrum and coccyx regions of the sitting surface. Generally, two basic technological approaches have been used to design a contoured cushion that increases the area of contact between the body and the seating support namely precontoured and custom contoured cushioning. However, because the contours of precontoured cushions are standardized and symmetrical in shape, this approach



becomes inappropriate when an intimately fitting body support is needed. The custom contoured cushions are usually labor-intensive and require considerable technical skill to obtain an intimate fit. Therefore, it is desirable to develop a technique for designing generic contoured cushions which can be prefabricated and provide more intimate fit to body support than standard precontoured cushions. In a preliminary study, four generic contoured shapes have been derived from 30 body-seat interface shapes of elderly subjects using a cluster analysis method. The **second problem** to be addressed in this Ph.D. thesis was to determine whether the generic contoured support shapes are better at accommodating different wheelchair users and produce more uniform pressure distributions. In order to answer this question, a set of generic shapes for the selected wheelchair users group had to be determined using cluster analysis. Then a set of experimental generic-shape contoured (GSC) cushions had to be fabricated by carving the generic shapes into an appropriate material (high resiliency polyurethane foam). Finally, the pressure distribution effectiveness of the experimental GSC cushions had to be evaluated by recording the interface sitting pressure while the subjects sat on the GSC cushions.

## **2.2 Hypotheses**

The two main hypotheses related to the two problems discussed above were:

- Technical hypothesis: It is possible to develop an efficient, low-cost and easy-to-use instrument to measure the shapes of any cushion with and without users sitting on it.
- Clinical hypothesis: The basic information gathered through the use of this new instrument will give input to successfully design generic contoured support surfaces, which will better accommodate different wheelchair users and produce more uniform body-seat interface pressure distributions.

## **2.3 Objectives**

### **2.3.1 General objectives**

In order to study the above hypotheses, four general objectives were proposed:

1. Develop and evaluate a new instrument to measure the body-cushion interface shapes;
2. From a group of wheelchair users, determine the generic shapes which will be used to fabricate generic-shape contoured cushions;
3. Develop a method for selecting appropriate generic-shape contoured cushions for wheelchair users;
4. Clinically evaluate generic shape contoured cushions.

### **2.3.2 Specific objectives**

This doctoral thesis was then divided into the following specific objectives:

1. To develop a lightweight and flexible interface shape measuring pad using available optical bridge technology to obtain shape measurements;
2. To develop a software to visualize and modify the three-dimensional shape captured by the shape measuring pad;
3. To design tests to evaluate the performance and accuracy of the new shape measuring pad, on unloaded and loaded surfaces with known geometry;
4. To establish criteria for selecting a group of subjects from wheelchair users and to determine the number of subjects needed to determine generic shapes;
5. To determine a set of generic shapes for the selected wheelchair users group by means of cluster analysis;
6. To fabricate experimental generic-shape contoured (GSC) cushions by carving the generic shapes into high resiliency polyurethane foam;

7. To develop a similarity index method for initially selecting appropriate experimental GSC cushions for wheelchair users based on their buttock-cushion interface shape measurements;
8. To test the reliability of the similarity index method using seating pressure measurements;
9. To evaluate the pressure distribution effectiveness of the experimental GSC cushion by recording the interface seating pressure while the subjects sit on the GSC cushion. For comparison, the measurements will be repeated with the subjects sitting on three other cushions (flat foam cushion and commercially available precontoured cushions).

#### ***2.4 General approach of the project***

The primary motivation of this work was to provide a tool that could determine generic shapes for seat support surface design. To accomplish this objective, the first stage of the study was to develop a method to compare shapes (Figure 2-1). Two-dimensional and three-dimensional geometric parameters were defined to describe the intrinsic characteristics of curve shapes. Based on these parameters, a similarity index is computed to quantitatively show how similar two shapes are. However, the similarity index could only be used to distinguish between two shapes. Determination of generic shapes from a group of shapes was solved by means of cluster analysis in the second stage of the study. A shape analysis program written in MATLAB was developed to calculate a set of preliminary geometrical parameters that describe the intrinsic characteristics of the shape. Cluster analysis was used to identify different body-seat interface shape patterns by classifying the variability in the geometrical parameters calculated in a group of subjects. The mean shape of each cluster was considered as a generic shape. The generic shape contoured cushions were evaluated by their pressure distribution, stability and comfort characteristics.

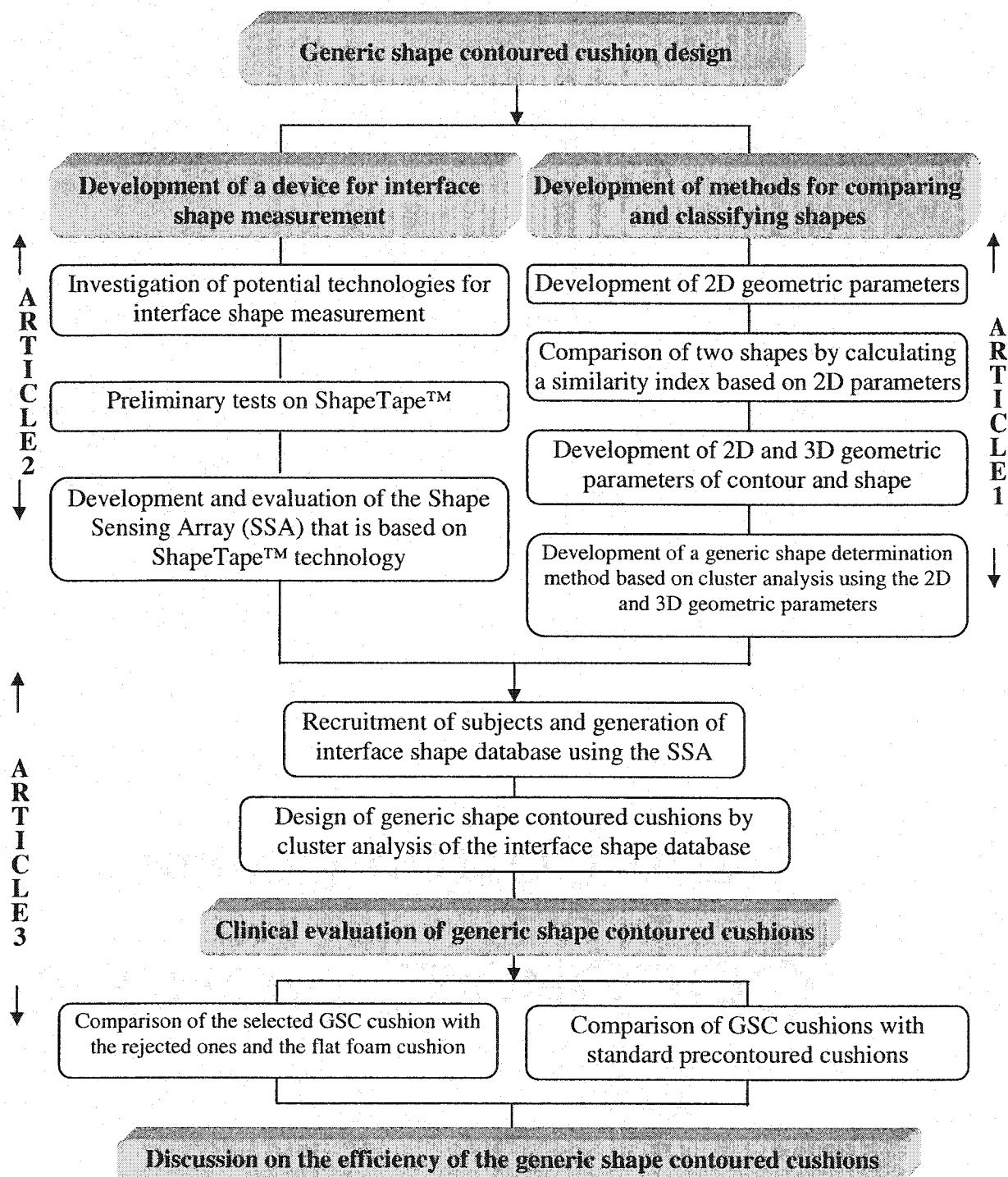


Figure 2-1 Schematic presentation of the different stages of the study.

#### **2.4.1 Stage one: Using a similarity index to compare two seat support surface shapes**

The primary role of a wheelchair cushions is to provide an effective platform from which the user may perform a wide range of tasks. Furthermore, for many users, the cushion performs a crucial function by reducing the concentration of pressure in soft tissues, thereby helping to prevent the formation of pressure ulcers.

Pressure measurements at the seating interface are routinely done in the selection and prescription of wheelchair cushions for users susceptible to develop pressure ulcers. There are, however, substantial limitations to the accuracy and significance of pressure measurements. Surface pressure distribution measurements are directly affected by the mechanical properties of underlying tissues. The high degree of variation in mechanical properties of gluteal tissues and structures makes it extremely difficult to determine what constitutes an optimal pressure distribution. (Levine et al., 1990). In that sense, contoured seating interface shapes become as important as interface pressure. In order to characterize the seating shape, it is important to establish a method for shape comparison. Therefore, a new mathematical method based on a similarity index calculated from curve shape parameters was developed to compare seating shapes (Chapter 3). It was shown that this method is able to distinguish shapes that are geometrically close and shapes that are dissimilar.

#### **2.4.2 Stage two: Determination of generic shapes from a group of shapes**

Since the similarity index method developed in stage one could only be used to compare two shapes, it was necessary to find a way to discriminate a group of shapes. The

objective of the second stage of the study was to develop a method to determine generic seat support surface shapes from a group of shapes.

In order to prove that cluster analysis of shape parameters was a promising method, thirty seat-body interface shapes from elderly subjects measured using the ESS were analyzed (Chapter 4) (Li et al., 2000a). Four distinct generic shapes were identified by means of the cluster analysis method. The results suggested that the generic shapes were mainly characterized by the lateral symmetry of the shapes. The allocation of individual's seat interface shapes into distinct clusters may lead to a more comprehensive understanding of the seat support interface and more effective seat cushion designs.

Although the above work confirmed that body-seat interface shape patterns could be identified using cluster analysis, an efficient and easy-to-use device that could rapidly capture body-cushion interface shapes in a clinical setting had to be developed (Chapter 5) (Li et al., 2003a). The ESS that provided the above interface shape data cannot be used for a body-cushion interface shape measurement in a wheelchair. Furthermore, no commercially available system currently permits measurement in the sitting position when a real cushion is used. Thus, we had to develop and evaluate a new body-cushion interface shape measurement system, the Shape Sensing Array (SSA) system. The SSA has the ability to make repeatable and accurate measurements of interface deformation.

In order to design a set of generic shape contoured cushions that could accommodate a significant percentage of the wheelchair user population, it was necessary to obtain a large sample of interface shapes (Chapter 6) (Li et al., 2003b). With the development of the SSA, this became possible. We thus collected a set of interface shapes from a group of wheelchair users, who required mild to moderate body support. Those shapes were compared and analyzed in order to classify them and a set of generic shapes was determined for this population. The generic shapes were then carved into high resiliency

foam cushions. The generic shape contoured (GSC) cushions were compared to two commercially available precontoured cushions by evaluating interface pressure distribution, dynamic stability during a reaching task, and overall comfort.

## **CHAPTER 3 USING SIMILARITY INDEX TO COMPARE TWO SEAT SUPPORT SURFACE SHAPES**

### **3.1 Objectives**

To develop a method for comparing seat support surface shapes.

### **3.2 Methodology**

#### **3.2.1 Shape measurements**

In this study two types of seating shapes are considered. The first type is precontoured shapes of contoured foam cushions, such as the ISCUS manufactured by Orthofab Inc (Quebec, Canada), which have different dimensions (15"x18", 17"x18", and 18"x18"), and were manually measured by a 3D digitizer (MicroScribe-3D, Immersion Corp, San Jose, CA). The second type is a seating interface contour obtained from an electronic shape sensor (ESS) (Brienza et al., 1996b).




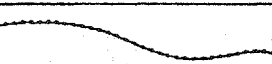
In the acquisition of precontoured cushion shapes, the digitized interval was determined to be the dominant factor affecting the fidelity of the reproduced shape. A technique to determine the optimal numbers of points (or the digitized interval) to be digitized along the cross-sectional curves of a precontoured cushion have been developed in order to keep all the intrinsic geometric characteristics of such curves. A limited number of digitized points along the curve (or a wide digitized interval) will result in a lost of



intrinsic shape definition and an attenuation of features. Three specific digitizing intervals used by other researchers were found in the literature: 1.2 inch (30 mm) (Chang et al., 1996, Yamazaki, 1992), 1.7 inch (42.7 mm) (Brienza et al., 1996a), 2 inches (50 mm) (Sprigle and Schuch, 1993).

In the present study, regularly spaced sample points along the cross-sectional curves of cushions are considered. To determine the optimum-digitizing interval, the following experiment was done. First, a precontoured 18"x18" cushion (ISCUS) was measured using a 33x33 rectangular array of marked points on its surface (involving a digitized interval of 14 mm). It was then possible to obtain 33 cross-sectional curves in the longitudinal direction of the cushion and another 33 cross-sectional curves in the lateral direction of the cushion. These curves could be classified into four typical shapes (Table 3-1). Based on the digitized points on each curve, cubic splines were used to interpolate 200 points in order to generate reference curves for analysis.

**Table 3-1 Digitized Interval.**

Typical curve	Description	optimum interval (mm)
curve I		45.0
curve II		32.1
curve III		37.5
curve IV		34.1

Typical curve I: lateral curve in the posterior seat region;

Typical curve II: lateral curve in the anterior seat region;

Typical curve III: longitudinal curve in the lateral parts of the cushion;

Typical curve IV: longitudinal curve located in the middle part of the cushion.

The next step was to sample each curve using different numbers of interpolated points (from 3 points to 30 points) and comparing the resulting curve to the reference curve.

Differences between reference curve and the resulting curve were calculated at 200 different locations and the mean value of the differences were computed.

Since seat cushions are formed of compliant materials, there can be possible errors in the digitizing process. There are also the intrinsic errors associated to the digitizer. As reported by the manufacturer, the accuracy of the MicroScribe-3D is 0.38 mm. To evaluate the digitizing process, the cushion was digitized four times on the same marked points and the resulting reproducibility was found to be close to 0.38 mm.

Since there was an optimum number of sample points (or optimum interval) for each cross-sectional curve, we were able to determine that the minimum interval for the four typical curves was between 32.1 mm and 45.0 mm (Table 3-1). Therefore, for digitization of contoured cushion shapes, the digitized interval was determined to be 40 mm. With the digitized interval now determined, the shapes of the three ISCUS cushions were manually measured using the MicroScribe-3D digitizer.

### **3.2.2 Definition of curve parameters**

The shapes of three ISCUS cushions (size 15"x18", 17"x18" and 18"x18") were represented by a 10x12 array, an 11x12 array, and a 12x12 array, respectively. The data was then interpolated to generate a 33 by 33 array for better comparison. Therefore, each shape was represented by 33 lateral cross-sectional curves. Six parameters were defined based on a study that was conducted by Yamazaki (1992). These parameters were chosen to describe the geometric characteristics of each cross-sectional curve (Figure 3-1). They were identified as local parameters (P1–P4) and global parameters (P5–P6):

P1: Absolute vertical height (h) divided by the absolute horizontal width (w) (Figure 3-1).

P2: Upper area divided by the lower area (Figure 3-1). The upper area is defined between the curve and the line passing through the highest point of the curve. The lower area is defined between the curve and the line passing through the lowest point.

P3: Length of the curve divided by the absolute horizontal width ( $w$ ) (Figure 3-1).

P4: Maximum slope of the whole curve (Figure 3-1).

P5: Height at location of the maximum slope ( $h_s$ ) divided by the absolute vertical height ( $h$ ) (Figure 3-1).

P6: Horizontal distance from the location of the maximum slope to the left end-point ( $w_s$ ) divided by the absolute horizontal width ( $w$ ) (Figure 3-1).

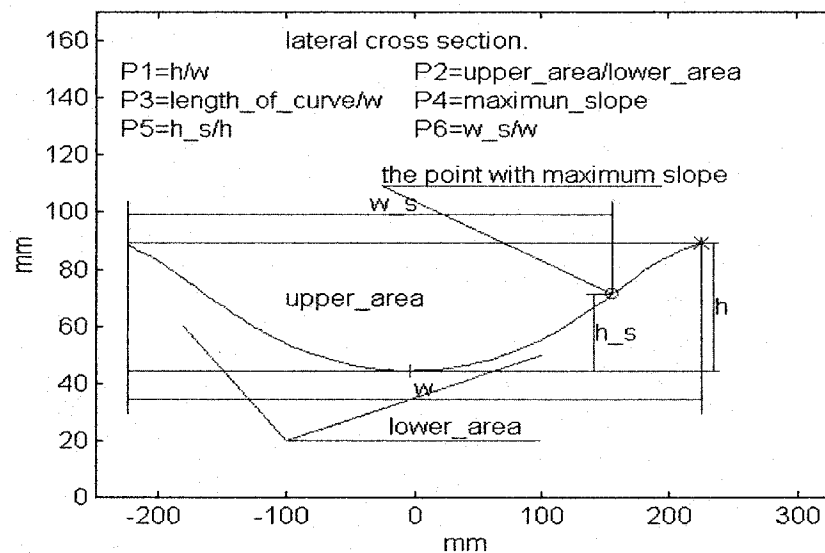


Figure 3-1 Local and global parameters defined on lateral curve

### 3.2.3 Similarity Index

A Similarity Index is a numerical value, which is intended to reflect the overall matching degree of two shapes. It ranges from 0 to 1, and the maximum value 1 indicates that two

shapes are identical. Similarity Index ( $SI_i$ ) was defined for each geometric parameter as follow:

$$SI_i = \frac{1}{n} \frac{\sum_{j=1}^n |\min(p_{i,j}^A, p_{i,j}^B)|}{\sum_{j=1}^n |\max(p_{i,j}^A, p_{i,j}^B)|} \quad 3-1$$

where  $n$  is the number of cross-sectional curves (33)

$i$  is the parameter number (from 1 to 6)

$j$  is the curve number (from 1 to 33)

A, B: the two types of seating shape (to compare 4 types of seating shapes in total)

$P_{i,j}^A$ : is parameter  $P_i$  of the  $j$ th curve for shape A.

$P_{i,j}^B$ : is parameter  $P_i$  of the  $j$ th curve for shape B.

A Global Similarity Index ( $GSI$ ) was also defined as following:

$$GSI = \frac{1}{6} \sum_{i=1}^6 SI_i \quad 3-2$$

The use of the formula 3-1 to calculate Similarity Index avoids producing indefinite value<sup>1</sup>. This formula (3-1) shows advantage in detecting small difference between shapes due to the fact that it utilizes maximum and minimum values instead of average values. Therefore, the formulae 3-1 and 3-2 were chosen to compare two seating shapes and were used in cushion selection as described in detail in the chapter 6.

---

<sup>1</sup> For example, if a  $SI_i$  is defined using the following formula:  $SI_i = \frac{1}{n} \sum_{j=1}^n \frac{|\min(p_{i,j}^A, p_{i,j}^B)|}{|\max(p_{i,j}^A, p_{i,j}^B)|}$ ,  $P_{i,j}^A$  and

$P_{i,j}^B$  on curve  $j$  might both be zero, that means one of the denominators is zero. Using the formula 3-1, the denominator is always greater than zero and that avoids indefinite value for  $SI_i$ .

### 3.3 Results & Discussion

Results of similarity indexes for comparison between shapes are presented in Table 3-2. The results showed that the pairs of shapes 1 and 2, 1 and 3, and 2 and 3 were quite similar with *GSI*s of 0.89, 0.85 and 0.94, respectively. These high values confirmed the fact that the precontoured shapes of the contoured ISCUS cushions were similar. This was not surprising as these precontoured cushions were manufactured in a similar way by Orthofab Inc (Quebec, Canada). The only difference between these cushions is the size that varies from 15"x18" to 18"x18". Comparison between these cushion shapes (shapes 1, 2 and 3) and the seating shape acquired from the ESS (shape 4) showed a great difference with *GSI*s of 0.69, 0.67, and 0.65, respectively. These differences came mainly from parameters P1 and P4 showing similarity indexes between 0.34 and 0.52. Therefore, it seems that this seating shape is different from the ISCUS cushion shapes.

Table 3-2 Similarity index

Similarity index	$\Lambda=1^*$ B=2	$\Lambda=1$ B=3	$\Lambda=2$ B=3	$\Lambda=1$ B=4	$\Lambda=2$ B=4	$\Lambda=3$ B=4
<b>GSI</b>	0.89	0.85	0.94	0.69	0.67	0.65
<b>SI<sub>1</sub></b>	0.90	0.78	0.87	0.43	0.39	0.34
<b>SI<sub>2</sub></b>	0.93	0.91	0.98	0.65	0.60	0.59
<b>SI<sub>3</sub></b>	0.99	0.95	0.95	0.89	0.89	0.84
<b>SI<sub>4</sub></b>	0.92	0.88	0.95	0.45	0.49	0.52
<b>SI<sub>5</sub></b>	0.96	0.96	0.92	0.86	0.90	0.83
<b>SI<sub>6</sub></b>	0.66	0.65	0.99	0.86	0.76	0.76

\*Shape 1: 15"x18" ISCUS; Shape 2: 17"x18" ISCUS;

Shape 3: 18"x18" ISCUS; Shape 4: seating shape from ESS

### 3.4 Conclusion

A new mathematical method based on a similarity index calculated from intrinsic curve shape parameters was developed to compare body-seat interface shape and precontoured

cushion shapes. It was shown that this method is able to distinguish shapes that are geometrically close and shapes that are dissimilar. Furthermore, it is possible to identify which parameters are mostly responsible for these dissimilarities. As geometry parameters can be used to compare two shapes by calculating similarity indexes, they can also be used to classify a group of interface shapes into different clusters on the basis of similarities or distances (dissimilarities). Therefore, cluster analysis was chosen to perform a multivariate analysis on geometry parameters in order to determine generic shape patterns in the following study (Chapter 4, Li et al., 2000a).

## CHAPTER 4 ARTICLE 1: DETERMINATION OF GENERIC BODY- SEAT INTERFACE SHAPES BY CLUSTER ANALYSIS

**Comments on the article:** In this article, cluster analysis was used to identify generic shapes for 30 elderly subjects based on the analysis of the dissimilarity in 17 geometrical shape parameters. As shown in Figure 4-5, four distinct generic shapes were determined and the depth of the shape was exaggerated for better revealing the differences between the generic shapes. The seventeen parameters were classified into three categories which described the symmetry, difference between the two lobes and flatness of the 3D shape, respectively. However, since the three categories were correlated, some of the parameters in the first category not only described how symmetry the 3D shape was, but also gave indications of the flatness, and vice versa. Overall, the results of this study support the hypotheses that multiple generic body-seat interface shapes exist and cluster analysis could be used to determine those generic shapes.

Yue Li<sup>1</sup>, Rachid Aissaoui<sup>1,2</sup>, David M. Brienza<sup>3</sup>, Jean Dansereau<sup>1,2</sup>

<sup>1</sup> Chaire Industrielle CRSNG sur les Aides Techniques à la Posture, Département de génie mécanique, École Polytechnique de Montréal, C.P. 6079, succ. Centre-ville, Montréal (Québec), Canada H3C 3A7;

<sup>2</sup> Institut Universitaire de Gériatrie de Montréal, 4565, Chemin Queen-Mary, Montréal (Québec), Canada H3W 1W5;

<sup>3</sup> Seating and Soft Tissue Biomechanics Laboratory, Department of Rehabilitation Science and Technology, University of Pittsburgh, PA 15260, U.S.A.

### **Acknowledgements**

This research was funded by the NSERC (Natural Sciences and Engineering Research Council of Canada), the Institut universitaire de gériatrie de Montréal, and Orthofab Inc.

**This paper was published in the journal IEEE Transactions on  
Rehabilitation Engineering, VOL. 8, NO. 4, DECEMBER 2000.**

### **4.1 Abstract**

The purpose of this study was to determine typical or generic shape patterns of the buttock-seat interface for elderly wheelchair users. The group of subjects was composed of 30 elderly people (aged 65 or older) and the shapes of the body-seat interface were measured by the electronic shape sensor (ESS). By analyzing the dissimilarity in geometrical shape descriptors or parameters, four distinct generic shapes were identified by means of the cluster analysis method. The results suggest that the generic shapes were mainly characterized by the lateral symmetry of the shapes. The determination of elderly people's seat interface shapes into distinct clusters may lead to a more comprehensive understanding of the seat support interface and more effective seat cushion designs.

Index terms-- Buttock-seat interface shape, geometric parameter, elderly wheelchair user, cluster analysis, generic shape.



## **4.2 Introduction**

The primary role of a wheelchair seat cushion is to provide an effective platform from which the user may perform a wide range of tasks. For many users, the cushion performs a crucial function by reducing the concentration of pressure in soft tissues, thereby helping to prevent the formation of pressure ulcers. Theoretical and experimental data has shown that a properly fitted contoured cushion would improve the pressure distribution and reduce tissue distortion (Chow and Odell, 1978, Sprigle et al., 1990b, Sprigle et al., 1990c, Brienza and Karg, 1998, Carlson et al., 1995).

Generally, two basic technological approaches have been used to design a contoured seat cushion that increases the area of contact between the body and the seating support. The first approach is termed as precontoured cushion, which can be manufactured using standard shapes. The second is termed as custom-contoured cushion, which obtains the contours by taking the shape directly from the client. The advantage of precontoured cushions is that they are available off the shelf and can be quickly assembled into a functional seating system. This approach is often adequate for those with mild to moderate physical involvement. However, because the contours are standardized and symmetrical in shape, this approach becomes inappropriate when intimately fitting body support is needed, such as in the case of deformity that necessitates custom-contoured seat and back modules. On the other hand, the advantage of the custom contoured cushions is that they can provide seating support at lower interface pressures, and improve posture and balance without impeding users' functional abilities (Sprigle et al., 1990c). This approach, however, is usually labor-intensive and requires considerable technical skill to obtain an intimate fit, especially when accommodation of gross deformities is necessary. Furthermore, the contour of a particular person may change over time. Any change in body weight or muscle tone may severely alter the buttock-cushion interface, and a reevaluation will be necessary. The ability to customize a

cushion by modifying contour shape or changing the material properties is quite valuable when serving clients with unique seating and positioning needs.

Given the benefits of custom contoured cushions and considering the difficulties involved in acquiring the measurements necessary for their design, it is desirable to develop a technique for designing generic contoured cushions which can be prefabricated and provide more intimate fit to body support than standard precontoured cushions. The generic shape cushion will fit a certain group of wheelchair users more accurately than the standard precontoured cushion, but not as intimately as the custom contoured cushion. In other words, the generic shape cushion will provide users allowance to change their body-seat interface a little bit at intervals. Thus, we expect that users could not only tolerate the generic shape cushion longer than they could on custom contoured cushions but also improve pressure distribution.

A review of literature suggests that few methods have been developed for the characterization and classification of body-seat interface shapes. Perakash et al. (1984) compared eight able-bodied persons' buttock molds by visualization and found that their shapes displayed little variance. He deduced that one seat design could accommodate a significant percentage of people because of the similarities between molds. However, Yamazaki (1992) found that there were large variations in contact shapes when different subjects were sitting on the same driver's seat. The author classified the contact shapes of 32 able-bodied subjects into two types: concave and flat. He concluded that the types of contact shapes were related to the body weight and body build. In order to describe the characteristics of the surface deformation and make quantitative shape comparisons, Yamazaki (1992) defined a set of geometrical parameters on the longitudinal and lateral seat contour curves, as well as on the longitudinal and horizontal back contour curves. However, the author (Yamazaki, 1992) did not find a generic shape for his group of subjects. Body-back interface shapes were studied by Nakaya et al. (1993) and 31 shapes of able-bodied subjects were divided into three sitting height groups, as well as three

cross-sectional width groups. It was suggested that the sitting height was related to the stature and the cross sectional width was related to the weight. But only one statistical human back contour model was developed from averaging longitudinal and horizontal back contour curves. Rosenthal et al. (1996) designed four wheelchair cushions to relieve pressure on bony prominences, but the shapes of these four cushions were the same, and the only difference between them was their sizes. In that study (Rosenthal et al., 1996), the selection of cushion sizes was based on the anthropometry measurement of subjects' inter-trochanter and inter-ischial tuberosity distances.

The above studies provided interesting suggestions for both classification and characterization of seating shapes based on anthropometric measurements of subjects. However, all of these methods proposed only one seating shape for one group of wheelchair users. Although some of these methods prescribed seating shapes with different sizes, the geometrical characteristics of seating shapes were the same. This study develops a method to determine whether one or more generic seating shapes could be found in a group of elderly people by discriminating the variability in geometric parameters of the buttocks-seat interface shapes. The purpose of this study is then twofold: 1) to develop a quantitative method in order to analyze the geometrical characteristic parameters of seating shapes; 2) and to use an advanced statistical method based on cluster analysis to classify seating shapes in a group of elderly people.

### **4.3 Methods**

#### **4.3.1 Subject Group Description**

This study is based on the data gathered at the Seating and Soft Tissue Biomechanics Laboratory at the University of Pittsburgh. Thirty elderly people (17 female; 13 male) participated in the data collection. Twenty-eight subjects were recruited from three nursing homes in the Pittsburgh area, two were independent recruits. The selection criteria were the following: the subject is a wheelchair user with an age of 65 years or greater and free of sitting induced pressure ulcers for the previous six months. The mean age of the selected subject group was  $81.6 \pm 8.4$  years (range 66-95 years). The subjects had a mean reported mass of  $64.6 \pm 15.7$  kg and a mean reported body mass index (BMI) of  $23.5 \pm 4.8$  kg/m<sup>2</sup>.

#### **4.3.2 Shape Measurements**

The instrumentation used in the data collection was the electronic shape sensor (ESS) (Brienza et al., 1996b). The ESS support surface consists of an 11 by 12 rectangular array of support elements that are spring-loaded and deflect downward in response to loads applied to the spherical tops of the elements. When a person sits on the device, the elements deflect downward until force equilibrium is reached. The deflection of each spring-loaded support element is measured using linear potentiometers coupled to each element. The deflection information is recorded and stored for processing by a host computer (Brienza et al., 1996b).

The subject was positioned by centering the pelvis on the seat surface, attempting to level the pelvis and tilt it anteriorly to an upright position. The thighs were parallel to the

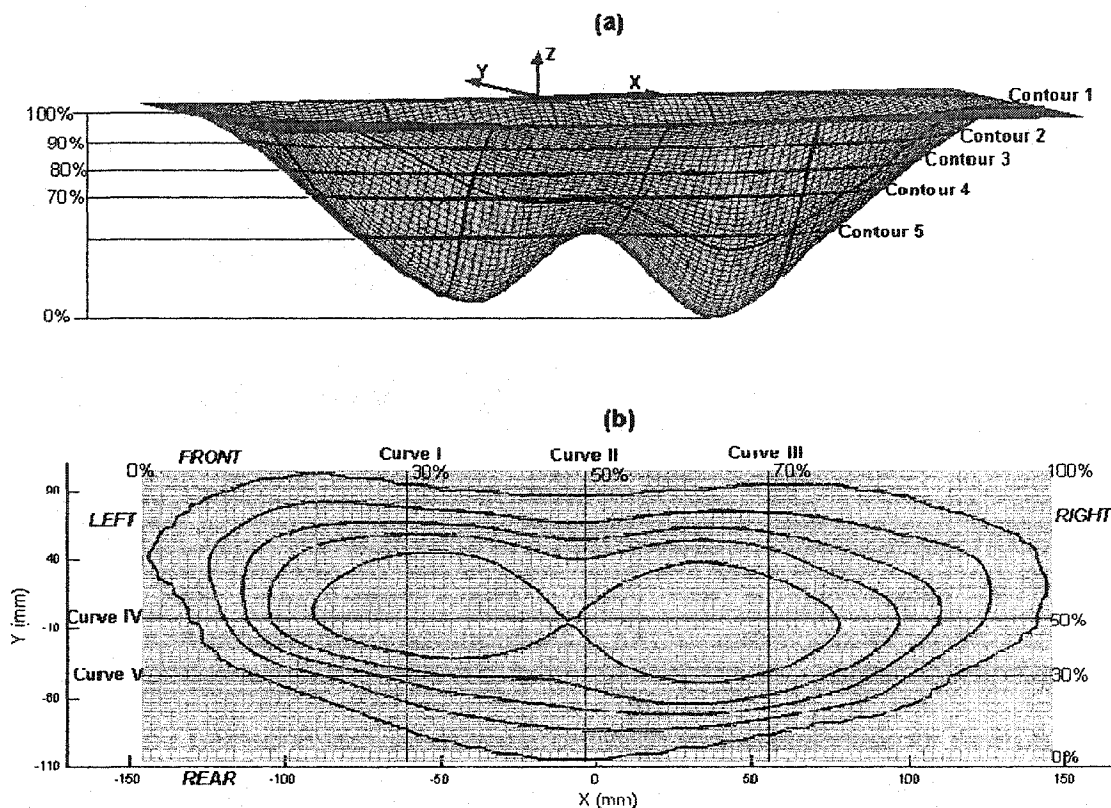
floor while the hands were placed on the lap and facing forward. Once the subject was positioned on the ESS, the resulting shape of the support surface, as measured by the deflections of the spring-loaded support elements, was recorded. Details concerning this process are presented in Brienza et al. (1996b).

#### **4.3.3 Geometric Parameters Identification**

Many parameters could be defined and calculated to quantitatively analyze the shape of the support surface. The resulting shape of the ESS support surface was represented by an  $11 \times 12$  array data. Then, the surface data was expanded to a 101 by 101 array for better resolution. Five horizontal contours and five cross-sectional curves (three anterior-posterior A-P, and two medial-lateral M-L) were identified on each shape (Figure 4-1). Using these curves and contours, it is possible to retain most of the information about the shape and reveal the dominant geometrical characteristics of the shape. For each shape, the positions of the cross-sectional curves and contours, as illustrated in Figure 4-1, are fixed to a specific percentage of length, width and height of the shape (for example, the position of Curve I is at 30% of the width of the shape). To represent all parameters in the same reference system, a global coordinate system referenced to the seat was defined (Figure 4-1). The positive direction of the X axis is the right side and represents the medial-lateral axis; the Y axis represents the forward direction, whereas the Z axis represents the gravitational axis.

Based on a set of preliminary parameters developed by Li et al. (1998), fourteen geometric parameters were measured on each A-P cross-sectional curve, twenty-three parameters on each M-L cross-sectional curve, four parameters on each horizontal contour, and six parameters on the whole 3-D shape to provide a global description of the seat-body interface shape. This yielded a list of 114 measurements for each buttocks-seat interface shape. Since the parameters were designed to reveal as many geometric

features as possible in order not to miss any potential dimension in the analysis, redundancy and repetition were inevitable. Reducing the number of variables (measurements) was called in order to make the clustering procedure feasible in practice.



**Figure 4-1 Article 1: (a) Location of five contours on a 3-D body-seat interface shape. (b) Location of five cross-sectional curves on the top view of the shape.**

The principal components analysis was performed to select primary measurements and consequently reduce the number of measurements. Since the loading of original measurements on the common factors might not be readily interpretable, the measurements which have high loading on the common factors were used as inputs for subsequent cluster analysis. The final measurement set includes 56 measurements, which not only reveal the dominant geometrical characteristics of the interface shape but also relate to anthropometric measurements such as the distance between ischial

tuberosities. All the measurements were defined as a ratio, i.e. their values ranging from 0 to 1. There are two main reasons for the choice of ratios. First, the units for measuring variables (measurements in our case) can arbitrarily affect the similarities among objects (shapes in our case). By converting raw data to ratios and recasting them in dimensionless units, the arbitrary effects were removed. Second, the ratios have the same range of values (from 0 to 1) that make variables contribute more equally to the similarities among objects.

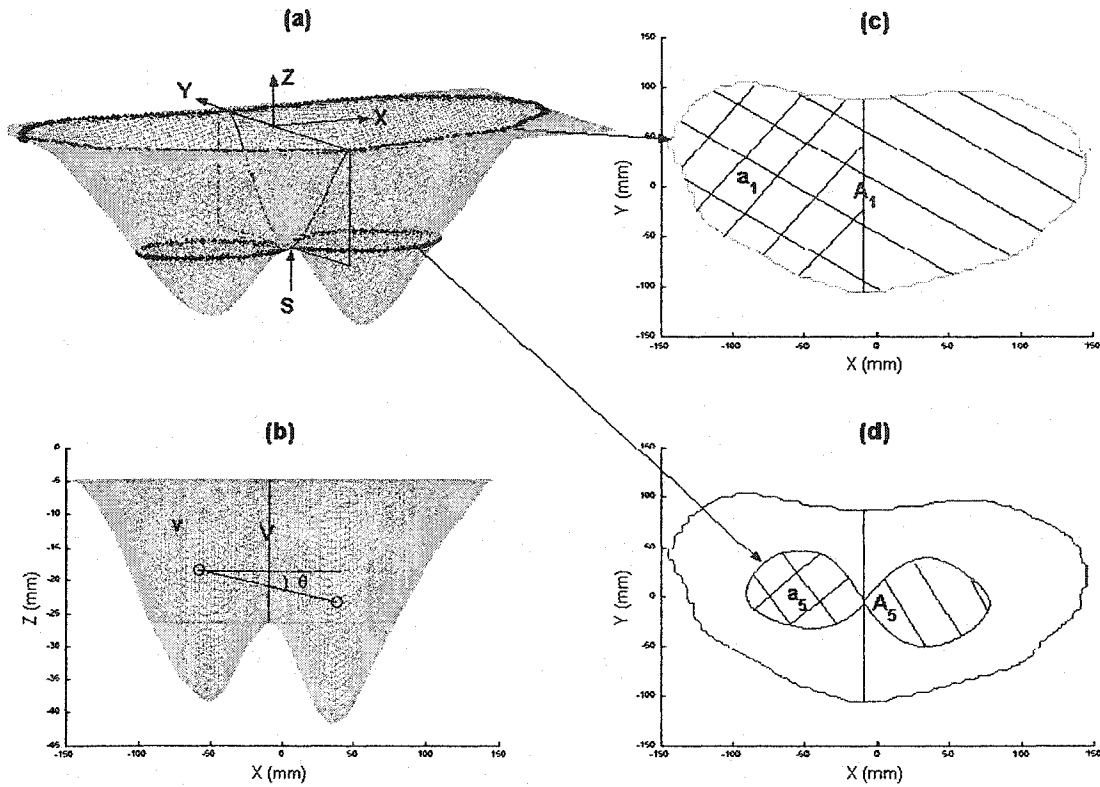
The statistical analysis (described in section D) indicated that 17 measurements out of these 56 measurements played an important role in distinguishing interface shapes. These 17 measurements (P1, P2, ..., P17) are listed below in the following three categories:

*1) Measurements Indicating Symmetry of the Shape:*

- $P1 = v / V$  (Figure 4-2.b): Defined as the volume of the left part<sup>2</sup> of the shape ( $v$ ) divided by the volume of the whole 3-D shape ( $V$ ). The more symmetrical the shape is, the closer  $P1$  is to 0.5.
- $P2 = (\theta + \pi/2) / \pi$ ,  $-\pi/2 < \theta < \pi/2$  (Figure 4-2.b):  $\theta$  defined as the angle between the medial-lateral axis  $X$  and the projected line in the frontal plane joining the centers of the left and right parts of the shape.
- $P3 = a_1 / A_1$  (Figure 4-2.c) : Defined as the area of the left part<sup>3</sup> of the contour-1 ( $a_1$ ) divided by the area of the whole contour ( $A_1$ ).  $P3$  describe the symmetry of the shape at the level of contour-1.

---

<sup>2</sup> If the shape has two lobes as shown in Figure 4-2, it is divided into two parts (right and left) by a sagittal plane (Y-Z plane) passing through saddle-point  $S$  (Figure 4-2.a). If the shape only has one lobe, then it is divided by a sagittal plane passing through the lowest point on the shape.



**Figure 4-2 Article 1: (a) Location of Contour-1 and Contour-5 and sagittal plane which divides the shape into right and left parts; (b) Front view of the shape; (c) Contour-1; (d) Contour-5.**

- $P4 = a_5 / A_5$  (Figure 4-2.d): Defined as the area of the left part of the contour-5 ( $a_5$ ) divided by the area of the whole contour ( $A_5$ ).  $P4$  describe the symmetry of the shape at the level of contour-5.
- $P5 = d_1 / D$  (Figure 4-3.a): Defined as the maximum depth of curve-I ( $d_1$ ) divided by the maximum depth of the shape ( $D^4$ ).

<sup>3</sup> As the shape is divided into right and left parts by the sagittal plane defined above, the contours shown in Figure 4-2.c & Figure 4-2.d are also divided into right and left parts by this sagittal plane.

<sup>4</sup> Symbol “D” used in this paper presents the maximum depth of the whole 3-D shape as shown in Figure 4-3.e.



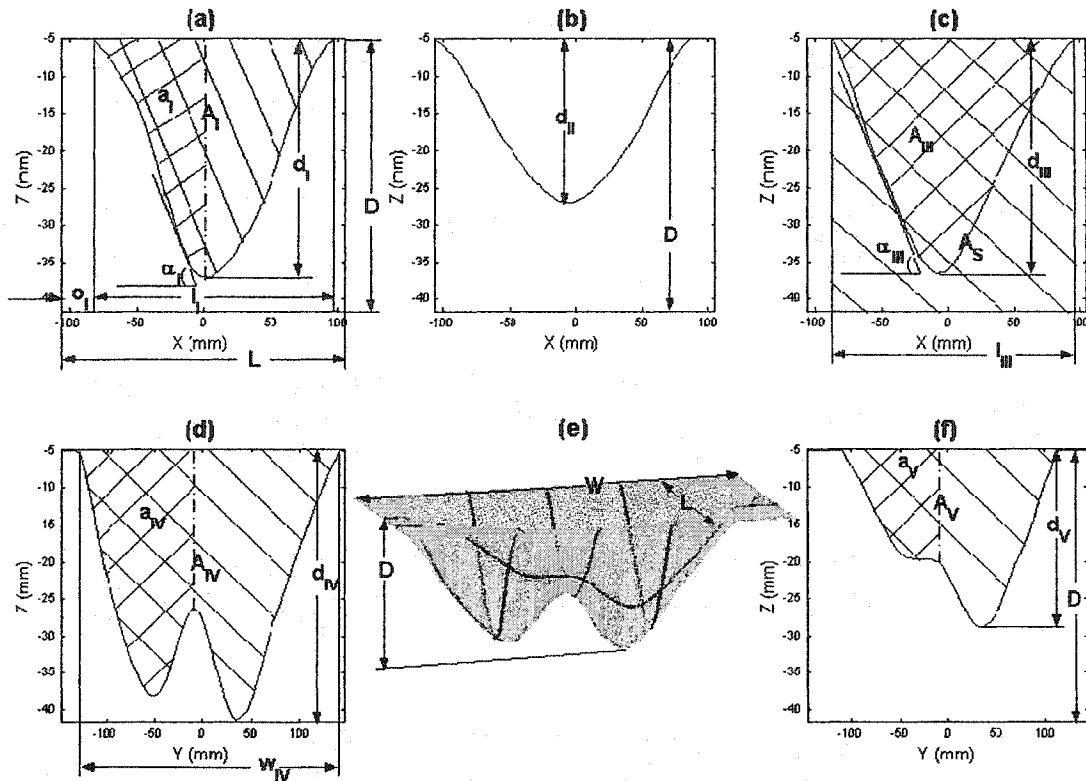


Figure 4-3 Article 1: (a) Curve-I; (b) Curve-II; (c) Curve-III; (d) Curve-IV; (e) Three-D interface shape; (f) Curve-V.

- $P6 = a_{IV} / A_{IV}$  (Figure 4-3.d): Defined as the area of the left part of the cross section passing through the curve-IV ( $a_{IV}$ ) divided by the area of the whole cross section ( $A_{IV}$ ). P6 describe the symmetry of the shape at the level of curve-IV.
  - $P7 = a_V / A_V$  (Figure 4-3.f): Defined as the area of the left part of the cross section ( $a_V$ ) passing through the curve-V divided by the area of the whole cross section ( $A_V$ ). P7 describe the symmetry of the shape at the level of curve-V.
- 2) *Measurements Indicating the Difference Between the Two Lobes of the Shape:*
- $P8 = d_{II} / D$  (Figure 4-3.b): Defined as the maximum depth of curve-II ( $d_{II}$ ) divided by the maximum depth of the shape ( $D$ ).
  - $P9 = A_{III} / A_S$  (Figure 4-3.c): Defined as the area of the cross section which passes through the curve-III ( $A_{III}$ ) divided by the area of the lateral cross section

which passes through the deepest point of the shape ( $A_S$ ). The flatter the curve-III is, the smaller  $P_9$  is.

- $P_{10} = d_V / D$  (Figure 4-3.f): Defined as the maximum depth of curve-V ( $d_V$ ) divided by the maximum depth of the shape ( $D$ ).

### 3) *Measurements Indicating Flatness of the Shape:*

- $P_{11} = o_I / L$  (Figure 4-3.a): Defined as the offset<sup>5</sup> of curve-I ( $o_I$ ) divided by the maximum length of the shape ( $L$ <sup>6</sup>).
- $P_{12} = d_I / l_I$  (Figure 4-3.a): Defined as the maximum depth of curve-I ( $d_I$ ) divided by the maximum length of curve-I ( $l_I$ ).
- $P_{13} = a_I / A_I$  (Figure 4-3.a): Defined as the area of the left part of the cross section passing through the curve-I ( $a_I$ ) divided by the area of the whole cross section ( $A_I$ ).
- $P_{14} = (\alpha_I + \pi/2) / \pi$ ,  $-\pi/2 < \alpha_I < \pi/2$  (Figure 4-3.a):  $\alpha_I$  defined as the maximum slope angle of the left part of the curve-I.
- $P_{15} = d_{III} / l_{III}$  (Figure 4-3.c): Defined as the maximum depth of curve-III ( $d_{III}$ ) divided by the maximum length of curve-III ( $l_{III}$ ).
- $P_{16} = (\alpha_{III} + \pi/2) / \pi$ ,  $-\pi/2 < \alpha_{III} < \pi/2$  (Figure 4-3.c):  $\alpha_{III}$  defined as the maximum slope angle of the left part of the curve III.
- $P_{17} = d_{IV} / w_{IV}$  (Figure 4-3.d): Defined as the maximum depth of curve-IV ( $d_{IV}$ ) divided by the maximum width of curve-IV ( $w_{IV}$ ).

---

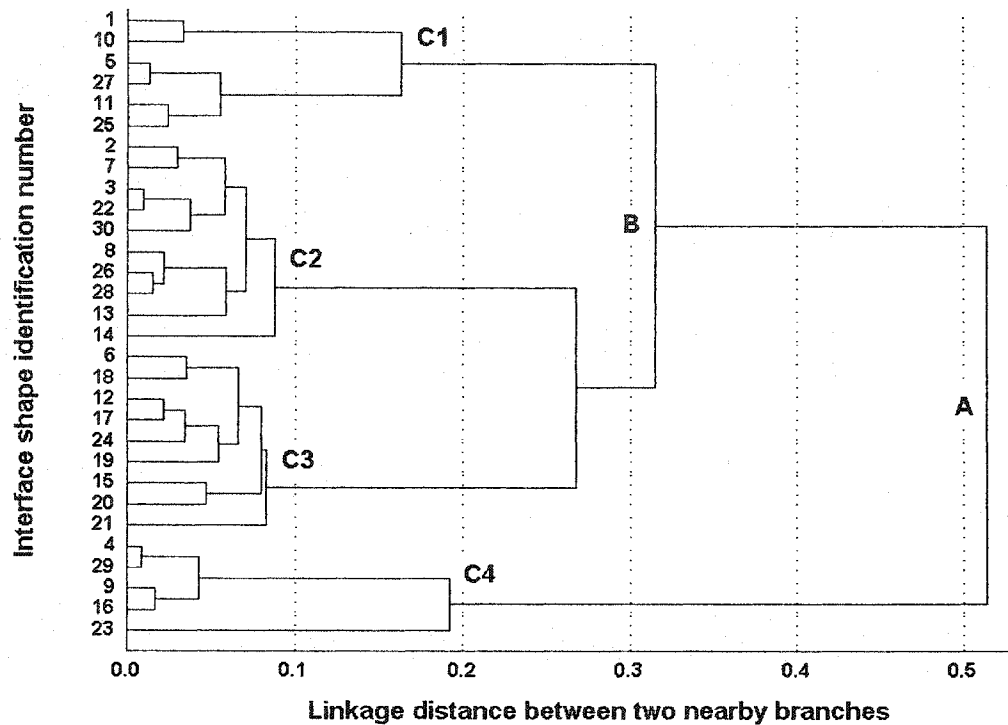
<sup>5</sup> The offset of an anterior-posterior curve is distance from the rear edge of the shape to the rear edge of the curve. The edge of a curve is defined as where the curvature of the curve changes from flat to concave.

<sup>6</sup> Symbol "L" used in this paper presents the distance from the rear edge to the front edge of the shape as shown in Figure 4-3.e.

#### **4.3.4 Statistical Analysis**

Cluster analysis was chosen as the multivariate procedure to detect natural groupings among the input shape data. The Ward's hierarchical method (Ward, 1963) was used for the cluster analysis procedure (STATISTICA 5.1, StatSoft Inc., Oklahoma, USA) to develop a hierarchical tree (dendrogram, see Figure 4-4). On the left of the dendrogram, each observation (3-D shape, in our case) represents its own cluster. Then, more and more observations are linked together and larger and larger clusters of increasingly dissimilar elements are aggregated. Finally, in the last step (on the right of the dendrogram), all observations are joined together. In Figure 4-4, the horizontal axis denotes the linkage distance. Thus, for each node in the dendrogram (where a new cluster is formed) it is possible to read off the criterion distance at which the respective elements were linked together into a new cluster. When the data contain a clear "structure" in terms of clusters of observations that are similar to each other, then this structure will often be reflected in the hierarchical tree as distinct branches.

The hierarchical method uses the dissimilarities or distances between observations when forming the clusters. The most straightforward way of quantifying dissimilarities between observations in a multi-dimensional space is to compute Euclidean distances. And the number of dimensions depends on how many variables (measurements, in our case) are included in the computation. Since the variables (measurements) used in this study are not in the same measurement units (degree, mm, etc.), a derived distance measure (Pearson Product Moment) which is more meaningful to our case was chosen to quantify the dissimilarities between shapes.



**Figure 4-4 Article 1: Dendrogram of the cluster analysis for 30 shapes. Horizontal axis denotes the linkage distance (Pearson Product Moment correlation coefficient). At a distance level of 0.2, four clusters (C1 to C4) can be distinguished. The number listing on the vertical axis presents the identification number for the subject's interface shape. The order of the number is decided by the procedure of hierarchical method.**

To determine the optimum number of clusters corresponding to the number of different observations, the R ratio analysis (Chen et al., 1990) was used. This ratio is a measure of the reduction of the intra-cluster variance by using  $K+1$  instead of  $K$  clusters. The R ratio is defined as:

$$R = \left[ \frac{e(N, K)}{e(N, K+1)} - 1 \right] (N - K + 1)$$

where  $e(N, K)$  is the summation of within cluster square distances for  $N$  observations (3-D shapes, in our case) and  $K$  clusters. Optimum number of clusters is decided when the R ratio is large, usually greater than 2. Large R ratio demonstrates a large reduction in the within cluster variability and shows that all clusters are quite homogeneous.

Once clusters had been identified, univariate ANOVA tests were performed on each of the dependent variables (56 measurements in our case), followed by Scheffe post hoc comparisons, to identify which measurements played an important role in distinguishing the clusters. The significant differences found were then used to describe the particular pattern of each shape cluster. Statistical significance was defined at the level of  $p < 0.05$ . Deletion of a number of variables from the analysis should not greatly alter the cluster found, if these clusters are real and not mere artifacts of the particular technique being used (Everitt, 1993). As soon as the significant measurements were identified by the Scheffe post hoc test, the cluster analysis was repeated using only these measurements and the results compared, in order to examine the stability of the clustering solution. A univariate ANOVA test followed by the Scheffe post hoc test was also performed at an alpha level of 0.05 to determine whether BMI, age and sex had an effect on the shape patterns.

#### **4.4 Results**

The purpose of this study was to identify different body-seat interface shape patterns by classifying the variability in the geometrical parameters calculated in a group of elderly subjects. The dendrogram obtained from the cluster analysis depicts large clusters characterizing loose associations of shape patterns, and smaller clusters that define more closely related patterns (Figure 4-4). At a small distance level, there are still many clusters with only a few subjects in each; at a larger distance level, the number of clusters decreases, but the number of subjects increases. The first dichotomy (A) divided the original 30 shapes into two clusters of 25 and 5 shapes. The larger cluster is hierarchically subdivided into two clusters of 6 and 19 shapes at the second dichotomy (B). At linkage distance 0.2, a four-cluster solution ( $k=4$ ) divided 30 interface shapes into four groups (C1, C2, C3 and C4). Then clusters C1 and C4 were subdivided into two more clusters at linkage distance 0.1, to form 6 clusters. Various cluster solutions

such as  $k=3, 4, 5$  and  $6$  were examined to find the optimal cluster number. R ratio was obtained as  $0.07$  for  $k=3$ ,  $2.73$  for  $k=4$ ,  $0.05$  for  $k=5$ , and  $0.48$  for  $k=6$ . Obviously, the R ratio peaked at the linkage distance  $0.2$  where four clusters were identified. The high R ratio value means that there is a jump in the sum of squared errors within clusters between  $k=3$  and  $4$ . As a consequence, based on the validity criteria mentioned above, a four-cluster solution was determined. The stability of a clustering solution could be examined by randomly dividing the data into two subsets and performing an analysis on each subset separately. Similar solutions should be obtained from both sets when the data is clearly structured (Everitt, 1993). Comparing the results obtained from the whole sample ( $30$  shapes) and two split samples, it was found that the clustering of the two split samples was similar to that of the whole sample when the four-cluster solution ( $k=4$ ) was chosen, indicating that the four-clustering solution may result in a stable replication. The mean shapes for clusters C1, C2, C3 and C4 are displayed in Figure 4-5.

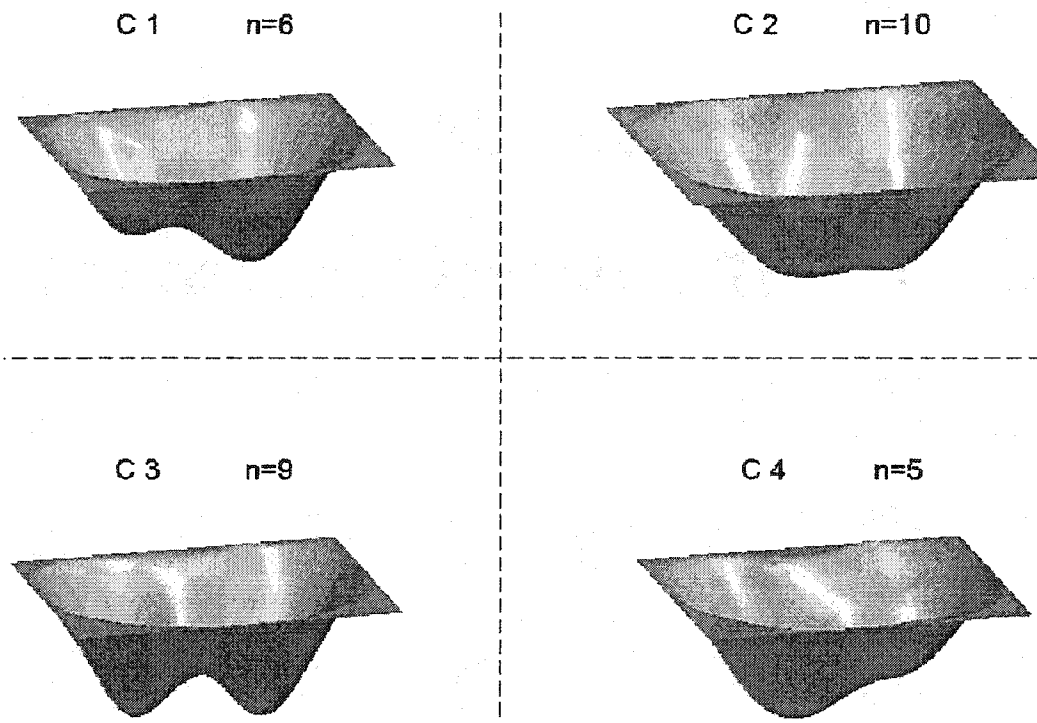


Figure 4-5 Article 1: Mean shapes of Clusters C1-C4

One-way ANOVA test was performed for each of the fifty-six measurements, followed by post hoc test to identify the significant descriptors (or measurements). The ANOVA analysis gave statistically significant results ( $p < 0.05$ ) for 21 measurements. Among these 21 measurements, the Scheffe post hoc tests indicated that 17 measurements (Table 4-1) played an important role in distinguishing the four clusters. These 17 measurements have already been described in section II. The cluster analysis was repeated using only 17 measurements in order to further examine the stability of the clustering solution. The analysis yielded four clusters that were similar (only two shapes changed clustering) to the clustering when 56 measurements were used. Thus, it is plausible to conclude that the four-cluster solution was stable.

**Table 4-1 Article 1: Significant Scheffé post hoc test results across the four clusters.**

Measurement	C1 vs. C2	C1 vs. C3	C1 vs. C4	C2 vs. C3	C2 vs. C4	C3 vs. C4
P1	*	*	*		*	*
P2	*	*	*		*	*
P3	*	*	*		*	*
P4	*	*	*		*	*
P5		*	*			
P6	*	*	*		*	*
P7			*			
P8				*		*
P9				*		
P10				*		
P11				*		
P12		*		*		
P13				*		
P14				*		
P15				*		
P16				*		
P17				*		

An asterisk (\*) in a cell indicates that the parameter listed in the left column identifies significant differences between the two clusters listed in the top line.

As shown in Table 4-2, the 17 measurements are divided into two groups (GI and GII). Seven measurements (P1 to P7) in the first group GI (which indicate the symmetry of the shape) contribute to distinguishing clusters C1 and C4 from clusters C2 and C3, as

well as distinguishing cluster C1 from cluster C4. Ten measurements (P8 to P17) in the second group GII (which indicate the discrimination between two lobes) contributes to distinguishing cluster C2 from cluster C3. The results of correlation analysis in Table 4-2 indicate that the measurements within the same group produce significant correlation ( $p < 0.05$ ), whereas weak correlation was found between different groups.

**Table 4-2 Article 1: Coefficient of correlation between measurements P1 to P17 which contribute to distinguish the four clusters. Only significant values of  $|r|$  which are greater than 0.35 are presented.**

	<i>Group GI</i>							<i>Group GII</i>									
	P1	P2	P3	P4	P5	P6	P7	P8	P9	P10	P11	P12	P13	P14	P15	P16	P17
P1		<u>0.92</u>	<u>0.94</u>	<u>0.98</u>	<u>0.63</u>	<u>0.82</u>	<u>0.63</u>										
P2			<u>0.83</u>	<u>0.85</u>	<u>0.75</u>	<u>0.67</u>	<u>0.5</u>										
P3				<u>0.94</u>	<u>0.49</u>	<u>0.81</u>	<u>0.53</u>										
P4					<u>0.49</u>	<u>0.82</u>	<u>0.64</u>										
P5						<u>0.48</u>	<u>0.39</u>				<u>0.57</u>			<u>0.49</u>			
P6							<u>0.66</u>										
P7																	
P8									<u>0.57</u>							<u>-0.45</u>	
P9									<u>0.55</u>	<u>-0.39</u>	<u>-0.53</u>		<u>-0.52</u>	<u>-0.58</u>	<u>-0.51</u>	<u>-0.49</u>	
P10										<u>-0.58</u>	<u>-0.52</u>	<u>-0.35</u>	<u>-0.58</u>	<u>-0.55</u>	<u>-0.56</u>	<u>-0.44</u>	
P11											<u>0.51</u>			<u>0.57</u>	<u>0.40</u>	<u>0.41</u>	
P12														<u>0.88</u>	<u>0.67</u>	<u>0.49</u>	<u>0.80</u>
P13														<u>0.51</u>			
P14															<u>0.60</u>	<u>0.43</u>	<u>0.67</u>
P15																<u>0.80</u>	<u>0.73</u>
P16																	<u>0.54</u>
P17																	

The mean values of measurements P1 to P17 are listed in Table 4-3. Shapes in cluster C1 ( $n = 6$ ), when compared to the other clusters, are found to have the smallest left lobe. This is indicated by the values of seven measurements P1 to P7 for cluster C1 which are significantly lower than those for clusters C2, C3 and C4 ( $p \leq 0.01$ ). Shapes in cluster C4 ( $n = 5$ ) are found to have the smallest right lobe. The mean values of measurements P1 to P7 for cluster C4 are significantly greater than the values of clusters C1, C2 and C3. Shapes in cluster C2 ( $n = 10$ ) and in cluster C3 ( $n = 9$ ) are more symmetrical than those in clusters C1 and C4. However, shapes in cluster C2 are observed to have



significantly highest values ( $p \leq 0.01$ ) on three measurements (P8, P9 and P10), which indicates that the two lobes of the shapes in cluster C2 cannot be identified as those in other clusters. Actually, six shapes in cluster C2 can be associated to oval shapes which have only one lobe. Furthermore, shapes in cluster C2 have significantly lower values ( $p \leq 0.04$ ) for seven measurements (P11 to P17), which indicates that the slopes of the rear part of the shapes in cluster C2 are significantly smaller than those in other clusters. Thus, shapes in cluster C2 exhibit a flatter, larger contour than those in other clusters.

**Table 4-3 Article 1: Mean values of measurements P1 – P17 for the entire group and four clusters.  $p$  values obtained from one-way ANOVA are listed in the last column.**

Measurement	Entire Group	Cluster 1	Cluster 2	Cluster 3	Cluster 4	$p$ value (ANOVA)
	N = 30	N = 6	N = 10	N = 9	N = 5	
P 1	0.463	0.265	0.472	0.457	0.694	<0.0001
P 2	0.499	0.493	0.499	0.499	0.507	<0.0001
P 3	0.461	0.131	0.468	0.451	0.861	<0.0001
P 4	0.477	0.335	0.489	0.467	0.640	<0.0001
P 5	0.817	0.638	0.820	0.876	0.922	0.0047
P 6	0.464	0.275	0.470	0.457	0.689	<0.0001
P 7	0.463	0.337	0.507	0.417	0.608	0.0086
P 8	0.738	0.753	0.849	0.561	0.816	0.0004
P 9	0.548	0.548	0.586	0.519	0.523	0.0093
P10	0.751	0.735	0.885	0.608	0.757	<0.0001
P11	0.053	0.043	0.028	0.082	0.062	0.0095
P12	0.114	0.097	0.093	0.145	0.121	0.0023
P13	0.464	0.483	0.414	0.497	0.479	0.0151
P14	0.601	0.593	0.577	0.625	0.616	0.0012
P15	0.121	0.133	0.099	0.146	0.106	0.0052
P16	0.609	0.615	0.589	0.634	0.594	0.0267
P17	0.100	0.098	0.087	0.114	0.103	0.0432

The mean values and standard deviations for the BMI, weight, height, and age for clusters C1 to C4 are presented in Table 4-4. The mean BMI and weight values for cluster C2 ( $27.82 \pm 3.84$  kg/m<sup>2</sup>,  $76.31 \pm 14.50$  kg) were significantly greater than the cluster C3 values ( $20.03 \pm 2.95$  kg/m<sup>2</sup>,  $53.98 \pm 9.26$  kg) ( $p = 0.005$  and  $0.02$ , respectively). However, no significant difference was detected for the BMI and weight values between

other cluster pairs. In addition, for mean height and age values, no significant difference was found between any of the cluster pairs.

**Table 4-4 Article 1: Mean and standard deviation values for BMI, weight, height and age data for cluster C1 to C4 and entire group.**

	<i>BMI</i> ( <i>kg/m<sup>2</sup></i> )	<i>WEIGHT</i> ( <i>kg</i> )	<i>HEIGHT</i> ( <i>m</i> )	<i>AGE</i> ( <i>year</i> )
<i>Cluster 1</i>	22.30 (3.52)	58.73 (14.67)	1.612 (0.112)	87.5 (5.3)
<i>Cluster 2</i>	27.82 (3.84)	76.31 (14.50)	1.669 (0.072)	78.1 (6.2)
<i>Cluster 3</i>	20.03 (2.95)*	53.98 (9.26)**	1.642 (0.095)	84.7 (9.1)
<i>Cluster 4</i>	23.33 (5.36)	66.48 (15.03)	1.689 (0.025)	76.2 (9.4)
<i>Entire Group</i>	23.50 (4.80)	64.55 (15.68)	1.652 (0.084)	81.6 (8.4)

\* Mean value of Cluster 3 is significantly different from value of Cluster 2,  $p = 0.005$ .

\*\*Mean value of Cluster 3 is significantly different from value of Cluster 2,  $p = 0.02$ .

#### 4.5 Discussion

The cluster analysis suggested to group body-seat interface shapes of 30 elderly subjects into four clusters. The mean shape of each cluster could be considered to be a generic shape (or shape pattern). It appeared that seventeen geometrical shape parameters mainly characterized the shape patterns. By calculating these measurements, it was possible to classify an interface shape to one of the four generic shapes as shown in Figure 4-5. The symmetry of the shape was denoted by seven measurements (P1 to P7). For a given interface shape, if these seven measurements were greater than 0.5 and close to 1.0, which indicated that the deepest point on the left part of the interface shape was lower than that on the right part, this shape should have a similar shape as the mean shape of cluster C4. On the contrary, if P1 to P4 and P5 to P7 were less than 0.5, the interface shape could be classified to cluster C1. However, it was difficult to distinguish symmetry shapes such as the mean shapes of clusters C2 and C3 by only comparing measurements P1 to P7. In this case, measurements P8 to P17 provided useful

information about the two lobes of the interface shape. As a final set of measurements, P1 to P17 characterized the key features of interface shapes and could be used to not only to determine generic shape, but also to prescribe generic shape.

Between-group analysis showed that there were significant differences among these four clusters. Although the fact that five shapes in cluster C4 all came from male subjects and that 5 out of 6 shapes in cluster C1 are from female subjects is an interesting finding, it is far fetched to conclude that male subjects tend to present left pelvic obliquity (as the mean shape of C4 shown in Figure 4-5) or that female subjects tend to present right pelvic obliquity. So far, no research has considered ethnicity of the subjects as a factor responsible for the variation of body-seat interface shapes. Consequently, the expected clustering was not due to ethnicity and sex of the subjects. But we expected that the variations between shapes could be due to some aspects related to wheelchair use, such as subjects leaning to one side or the other during the measurement procedure. The cluster differences were substantive, but it was unclear whether differences between shape patterns were associated with intrinsic characteristics of subjects such as altered body mass index (BMI), tissue tone and underlying skeletal structures, or with extrinsic factors such as subjects leaning to one side during the measurement procedure.

The effects of subjects' intrinsic characteristics on shape pattern have been studied by Yamazaki (1992). He relates deformation of the interface shape with body weight, and states that the contact shapes of obese subjects were flatter and smoother than those of thin subjects (Yamazaki, 1992). Yamazaki (1992) also states that the interface shape approximated the shape of parallel rugby balls in the slim type subject or the shape of a ball in the fat type subject. Unfortunately, no quantitative information about the interface shapes is given by the author. Thus, although it was not possible to establish a direct quantitative comparison between Yamazaki's data and ours, our results were visually similar to Yamazaki's. As shown in Figure 4-5, the mean shape of cluster C2 is flatter and smoother than the mean shape of cluster C3. The mean body mass index (BMI) and

weight values listed in Table 4-4 reveal that the difference between cluster C2 and C3 likely occurred as a result of different BMI or weight. The reason why the mean shape of cluster C3 has distinct lobes could be explained by the fact that this cluster contains more thin subjects than cluster C2. In a previous research (Garber and Krouskop, 1982), the authors stated that body build factors, such as height and weight, played an important role in pressure distribution in patients seated on wheelchair cushions. Furthermore, they suggested that the topography of the interface between the patient and the cushion might be an important consideration. It therefore seems reasonable to relate BMI with the generic shapes. Our study did reveal that thin subjects tend to have deeper contours and obese subjects tend to have flatter contours. Since BMI is a readily obtainable and understandable subject characteristic, the relationship between BMI and shape pattern found in this study could encourage considering BMI as a factor in the selection of seat cushion shape.

The differences between mean shapes of clusters C1 and C4 can likely be explained by altered seating postures or by bone structure deformities. The effect of posture on shape pattern could be reduced by controlling the position during measurement. In this study, care was taken to ensure that subjects were positioned in a neutral posture during the data collection process; and photographs were taken to record their postures. By reviewing these photographs, no obvious posture differences were detected among all 30 subjects. Thus, the effect of posture on shape pattern was ignored in this preliminary study. But in future research for this project, we plan to take landmark measurements or radiographs during the shape measurement process in order to quantify subject's seating position. Also, more emphasis should be put on the effect of bone structure deformity on shape pattern. A portion of the differences between mean shapes of cluster C1 and C4 could be caused by pelvic obliquity. Zacharkow (1988) and Buck (1996) state that geriatric population will usually adopt slumped, kyphotic postures and/or asymmetrical postures that might lead to pelvic obliquity and scoliosis. As well, such bone structure deformity could be considered as one of the intrinsic factors that might affect shape

patterns in the geriatric wheelchair population. These relationships will be investigated in a future study.

The discrimination of body-seat generic shapes may lead to a more comprehensive understanding of seat interface shapes. Furthermore generic shapes can potentially be used to develop generic-contoured seat cushions, which could be an alternative to the custom contoured seat cushions and precontoured seat cushions. As the curvature of the unloaded cushion changes from flat to concave, the peak contact pressures will decrease. The experiments done by Chow and Odell (1978) showed that matching a cushion to the shape of a penetrator would result in less indenter distortion and a lower interface pressure. The evaluation of Karg et al. (1996) indicated that the support shapes derived from the mechanical shape measurement system (ESS) carved into high resiliency foam cushions provide lower peak interface pressure than that of flat foam cushions. The contours resulting from the ESS are based on the seated contour only and are not modified. Since the generic shape can be associated to the mean shape of a subject group and since it reflects its common interface shape characteristics, it should provide a more intimate fit for this group than flat support shape or standard symmetrical shape. Thus, it is reasonable to assume that carving the generic shapes (C1 to C4) into foam cushions will also provide lower peak interface pressure than flat foam cushion or standard precontoured cushion. Further clinical evaluation is necessary to confirm this assumption.

On the whole, the four generic shapes (C1 to C4) identified in this paper are derived from 30 body-seat interface shapes of elderly subjects at a single point isolated in time. They cannot be viewed as fixed or optimal. If shape measurements are repeated on same subject, it is possible that shapes from same subject would be in different clusters; or if more subjects are included in the cluster analysis, different shape patterns or more or less generic shapes could be identified. Without establishing a proper generic shape database for certain populations and without clinical evaluation of these generic shapes,

it is difficult to judge whether these generic shapes are typical or if they represent all the possibilities for a certain population.

Our results should be viewed as preliminary and further investigation is necessary to determine shape patterns on a consistent number of subjects. Indeed, the small sample size of 30 elderly subjects may not represent all geriatric wheelchair users. It is expected that analysis on a larger sample could accommodate a significant percentage of the geriatric population. In addition, further data could be gained from other populations at high risk for pressure ulcers, such as persons with spinal cord injury. Analysis on these data should be done to discriminate shape patterns for these populations.

#### **4.6 Conclusion**

The present study suggested that body-seat interface shape patterns could be identified using cluster analysis. Four distinct generic shapes were identified for 30 elderly subjects by analyzing the dissimilarity in geometrical shape parameters. The discrimination of body-seat generic shapes might lead to a more comprehensive understanding of seat interface shapes. The results of this study support the notion that multiple generic body-seat interface shapes exist and that classifying interface shapes provides meaningful information with respect to the geometrical shape parameters. Furthermore the generic shapes can potentially be used to develop generic contoured seat cushions, which could provide an alternative to the custom contoured seat cushions and precontoured seat cushions. The approach used and the results derived do appear quite valid on the surface, and may provide a basis from which to provide more off-the-shelf devices that more accurately fit the individual patient's needs. This study's findings, along with further analysis on a larger sample and on different wheelchair populations, will give insight into the evaluation and design of new generic seat cushions.

## **CHAPTER 5 ARTICLE 2: DEVELOPMENT AND EVALUATION OF A NEW BODY-SEAT INTERFACE SHAPE MEASUREMENT SYSTEM**

Yue Li<sup>1,2</sup>, Rachid Aissaoui<sup>3</sup>, Michèle Lacoste<sup>2</sup>, Jean Dansereau<sup>1</sup>

<sup>1</sup>Institut de génie biomédical, École Polytechnique de Montréal, C.P. 6079, succ. Centre-ville, Montréal (Québec), Canada H3C 3A7;

<sup>2</sup>Laboratoire de mouvement, Centre de recherche du Centre de réadaptation Marie Enfant de l'Hôpital Ste-Justine, Montréal (Québec) Canada H1T 1C9

<sup>3</sup>Laboratoire de recherche en imagerie et orthopédie, Département de génie de la production automatisée, École de technologie supérieure, Montréal (Québec) H3C 1K3

### **Acknowledgements**

This research was funded by the NSERC (Natural Sciences and Engineering Research Council of Canada), Fonds FCAR (Le Fonds pour la Formation de Chercheurs et l'Aide à la Recherche), and Orthofab Inc.

**This paper was submitted to the journal *IEEE Transactions on Biomedical Engineering***

### **5.1 Abstract**

A system for capturing the body-cushion interface shape has been developed which has the ability to make repeatable and accurate measurements of interface deformation. The Shape Sensing Array (SSA) system uses optical fiber technology and is noninvasive. The system can cover an interface as large as 400 x 480 mm (16"x19") and the shape is measured over a 10x12 array of sensors laminated on ribbon substrates. Measurement errors were evaluated by comparing the shape with a reference shape obtained by a mechanical digitizer. The RMS error in the Z direction for the system was 3.79 mm. The repeatability of the system was less than 0.32 mm under controlled conditions. Different interface materials affected measurements remarkably. With the development of this interface shape measurement device, it can be expected that the basic information gathered through its use may prove to be fundamental in the successful design of generic-shape contoured support surfaces. Furthermore, we expect that the new shape measurement device will provide a quick and effective tool for cushion evaluation and clinical guidelines for cushion prescription.

***Index Terms:*** Body-seat interface shape, Shape Sensor Array, instrumentation, accuracy, generic shape, wheelchair cushion.



## 5.2 Introduction

Measuring the shape of the body-seat interface has been used successfully in research to study tissue loading and as a mean to fabricate custom contoured cushions. Levine et al. (1990) state that although the efficacy of tissue shape and deformation as characterizations of the seating interface has not been clinically proven, they provide a more direct measure of the net effect of external load, mechanical tissue properties, and boundary conditions (cushion effects) than pressure measurements. Yamazaki (1992) used flexible, thin tape sensors to measure contact shape between a seated person and the seat surface to evaluate sitting comfort. Contact shape and pressure were compared qualitatively. Among other things, Yamazaki concluded that pressure patterns provided data for seat evaluation, while contact shape data provided data for seat design. Sprigle and Schuch (1993) suggested that seat contour measurements complement other clinical measures such as seat interface pressures and general postural assessments, to form a more complete picture of the buttock-cushion interface.

The usefulness of shape measurements for clinical evaluation is restricted at the present time due to technical limitations, lack of experience and standards, as well as high costs. Currently, a few systems that measure seat contours have been developed for use in custom wheelchair seating. The PinDot Shape Sensor (Invacare Corp., Elyria, OH) uses a mechanical system in which wires pass through a 5" thick foam cushion; the translations of the wire end pieces can be digitized and form the basis of a custom cushion. Kadaba et al. (1984) devised a method for measuring the contour of buttock-gel cushion interface using ultrasonic dimension gauging techniques. At the University of Virginia's Rehabilitation Engineering Center (Brienza et al., 1991) an Electronic Shape Sensor (ESS) was developed to measure seat interface contours. The Computer-Automated Seating System (CASS) developed at the University of Pittsburgh (Brienza et al., 1996a) has the ability to control the seating surface shape while measuring the pressure applied to the buttocks by the seating surface. Chang et al. (1996) used the

pressure applied to the buttocks by the seating surface. Chang et al. (1996) used the Direct Contact Probe Measurement System to provide a three-dimensional graphical output for visual evaluation. Yamazaki (1992) used arrays of strain gauges (actually flat metal ribbons) to recreate seat shape.

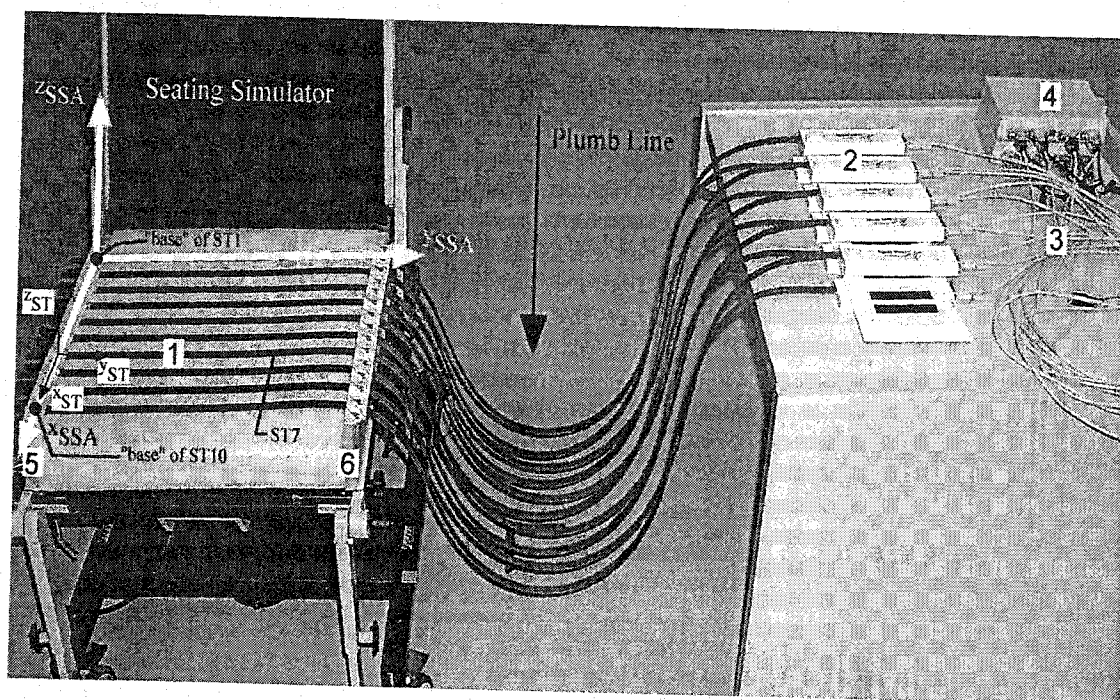
There are many methods and techniques that could be used to measure 3-D shapes, but few of them permit measurement in the sitting position and most of them cannot accommodate a wheelchair. The PinDot Shape Sensor is now commercially available, while the other five systems mentioned above are still being investigated and are not readily applicable in the clinical setting. However, none of the systems can measure interface shapes when users sit on foam cushions.

After having investigated the commercially available shape measurement devices which could be suitable for body-cushion interface shape measurement, we developed an efficient, low-cost and easy-to-use device – the Shape Sensing Array (SSA) system – to rapidly capture the body-cushion interface shape in a clinical setting. The SSA system uses optical fiber technology (Measurand Inc., Fredericton, New Brunswick, Canada) and is noninvasive. The SSA mat is flexible and very thin, and can be placed between the subject and seat without disturbing the subject's natural feeling. With the development of this interface shape measurement device, we expect that the basic information gathered through its use may prove fundamental to successfully design generic-shape contoured support surfaces. Furthermore, it is expected that this new shape measurement device will provide a quick and effective tool for cushion evaluation and clinical guidelines for cushion prescription. The objective of this project was to evaluate the performance of this new device.

### 5.3 Description of the SSA System

The Shape Sensing Array (SSA) is a system developed to be used as a clinical tool to evaluate interface shapes between the body and the support surface. The main component of SSA system is a set of ShapeTape™s. ShapeTape™ is a thin array of fiber optic curvature sensors laminated on a ribbon substrate (item (1) in Figure 5-1). Each tape has a cross section of 1.3 x 12.5 mm, and has 12 sensors along a 480 mm long sensing zone at the end of 1.5 m of fiber optic leads. The first sensor that indicates the start of the sensing zone is 30 mm from the tip of the tape, and the end of the sensing zone is 510 mm from the tip. From the end of the sensing zone to the interface box (item (2) in Figure 5-1) is the lead part of the tape that doesn't contain any sensor, but allows the fibers to pass through. The fibers are then attached permanently to the interface box that converts changes in light intensity to digital or analog signals (Danish et al., 1999). The signals are interpreted by software running on a personal computer (PC) to obtain calibrated bends and twists, and to calculate a set of six degree of freedom Cartesian data that is essentially continuous along the ribbon. By summing the bends and twists of the sensors along the tape, the shape of the tape relative to the start point or the end point of the sensing zone can be reconstructed.

A ShapeTape™ coordinate system ( $XYZ_{ST}$ ) was defined (see Figure 5-1). The origin of the  $XYZ_{ST}$  coordinate system was fixed on the first sensor which is the start point or "base" of the sensing zone. The end point of the sensing zone is called the "end". The  $y_{ST}$ -axis represents the direction along the ShapeTape™ and points from the "base" to the "end". The  $z_{ST}$ -axis is the normal to the tape surface and the  $x_{ST}$ -axis is defined as the cross product of the  $y_{ST}$  and  $z_{ST}$  vectors. The "end" is constrained in the X and Z directions. Therefore, the x and z coordinates of the "end" are always (0, 0). The errors propagate towards the middle of the ShapeTape™. Normally, the closer the sensor is to the middle of the ShapeTape™, the higher the error is. Details concerning the control and data acquisition of the ShapeTape™ are presented in Danish et al. (1999).



**Figure 5-1 Article 2: Illustration of a SSA system. (1) ShapeTape™; (2) Interface boxes of ShapeTape™s; (3) Serial cable with a power inlet connector; (4) 4x1 serial-USB converter; (5) fixture-A; (6) fixture-B. The cove of the SSA is not shown in the figure.**

The interface box is connected to a PC by a serial cable (item (3) in Figure 5-1) with a power inlet connector near one end. The power inlet accepts 9VDC from a wall-mounted AC Adapter. The serial cable may be extended with a conventional serial cable at either end. Analog sensor signals are digitized in the interface box and transmitted to the computer via the serial port, at a communication speed of 115.2 kb/s.

The SSA system consists of ten ShapeTape™s (from ST1 to ST10) that make up a sensing matrix which is called the SSA mat, a cover which protects the SSA mat, two fixtures (item (5) and (6) in Figure 5-1) to support the ShapeTape™s and keep them at equal intervals, two 4x1 serial-USB converters (item (4) in Figure 5-1) to connect the interface boxes to USB ports, and computer software that performs calibration, interpolation and transformation functions. The two fixtures were specially designed for certain seating simulators and might need to be modified to fit other simulators or

wheelchairs. The “bases” of the ShapeTape™s are fixed on fixture-A (item (5) in Figure 5-1). Channels in fixture-B (item (6) in Figure 5-1) allow the ShapeTape™s to slide in the lateral direction but keep the two ends at the same level.

The spatial interval between the shape sensors in each ShapeTape™, and the spatial interval between ShapeTape™s represent the maximal spatial resolution of the mat. Previous experiments (Li et al., 1998) determined that the optimal interval of measurement was 40 mm (1.575”). Therefore, the SSA system is designed so that the 10 ShapeTape™s each with 12 sensors cover a 400 x 480 mm area. These dimensions approximate those of a standard adult wheelchair cushion (16 inches of seat depth, 18 inches of seat width, and 4 inches of seat thickness) (Sprigle et al., 2001). The intervals between the sensors in both directions (along the ShapeTape™ and perpendicular to the ShapeTape™) are 40 mm.

Since the ten ShapeTape™s are connected to the computer individually, the measurements of the ShapeTape™s are independent from each other. And the 3D locations of the 12 sensors along each ShapeTape™ are measured with respect to their own local coordinate system ( $XYZ_{ST}$ ). A mechanically articulated arm (MicroScribe-3D, Immersion Corp., San Jose, CA) was used to digitize the locations of the “bases” and “ends” in order to calculate the position and the orientation of each  $XYZ_{ST}$  with respect to a global coordinate system  $XYZ_{SSA}$  (Figure 5-1). The origin of the  $XYZ_{SSA}$  was fixed on the “base” of ST1. The  $z_{SSA}$ -axis represented the gravitational line which was obtained by digitizing two landmarks on a metal rod aligned with a plumb line. The  $x_{SSA}$ -axis was defined by the line which connected the “bases” of ST1 to ST10. Finally, the  $y_{SSA}$ -axis was defined as the cross product of the  $x_{SSA}$  and  $z_{SSA}$  vectors. By digitizing the locations of the “bases” and “ends” during the SSA data acquisition, the position and the orientation of each  $XYZ_{ST}$  were calculated with respect to the  $XYZ_{SSA}$ . All the coordinates of the sensors were then transformed onto the  $XYZ_{SSA}$ .

## **5.4 Validation of the System**

Since the SSA has never been used for interface shape measurements, the following tests were designed to evaluate the accuracy, repeatability and stability of the SSA system.

### **5.4.1 Accuracy of SSA Measurements**

The accuracy of the SSA measurement was evaluated by comparing the results obtained by the SSA to a reference measurement acquired by the MicroScribe-3D digitizer. The accuracy of the MicroScribe-3D was 0.38 mm (as suggested by the manufacturer).

#### **5.4.1.1 Test 1: Assessing the accuracy without the influence of pressure**

The SSA actually measured how far away each sensor was moved from its original position. Before each measurement, the SSA should be flattened and the flat shape was recorded by the program. In this test, the accuracy of the SSA was evaluated by assessing the accuracy of ShapeTape™s one by one. The middle of one tape was moved downwards in order to match the shape of the precontoured foam cushion (Figure 5-2). The tape was then fixed on the cushion using double-sided tape. After the ShapeTape™ recorded its shape, the positions of the 12 sensors and the “base”, which were precisely marked on the tape (Figure 5-2), were digitized using the MicroScribe-3D. The same procedure was repeated on the other nine ShapeTape™s. The whole procedure was repeated twice.

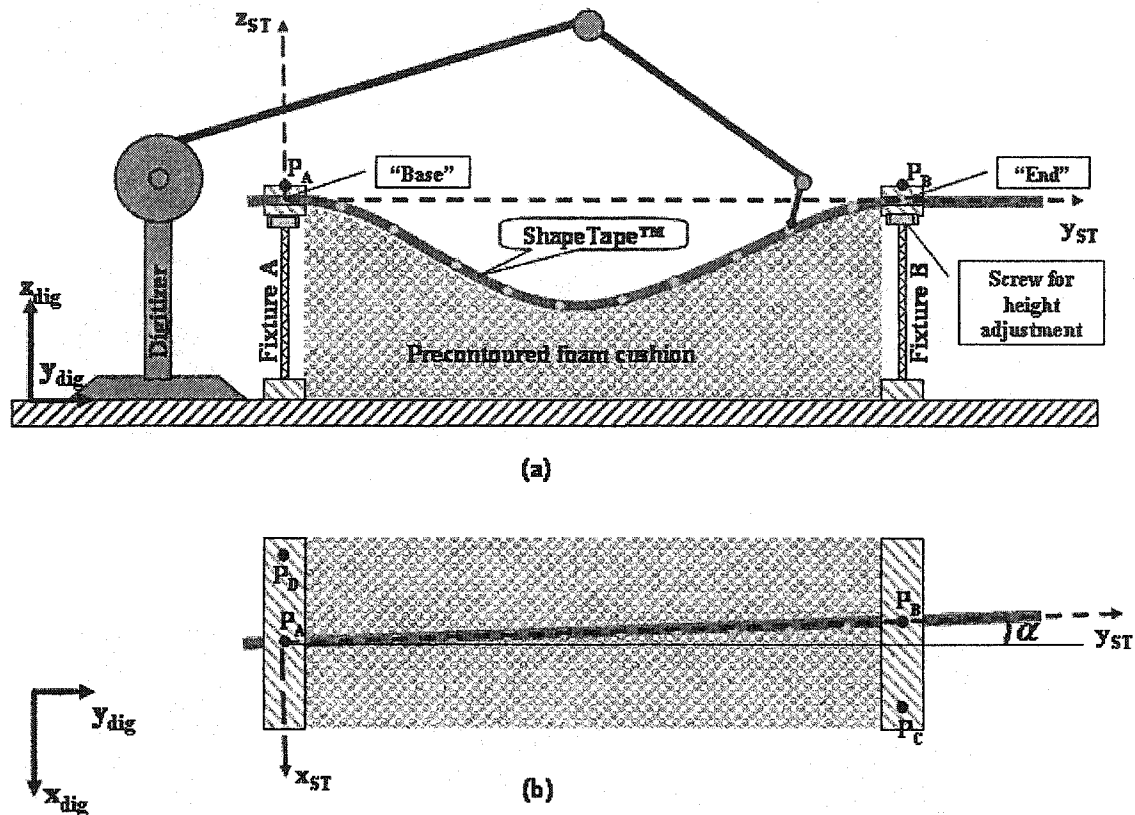


Figure 5-2 Article 2: Illustration of the experimental setup for assessing the accuracy without the influence of pressure. (a) Front view; (b) top view.

The coordinate data of the marks on the tape were recorded in two different coordinate systems (Figure 5-2). The coordinate system ( $XYZ_{dig}$ ) was defined with respect to the MicroScribe-3D digitizer while the coordinate system ( $XYZ_{ST}$ ) of the ShapeTape™ was defined with respect to its own "base" and "end". In order to simplify the coordinate transformations from  $XYZ_{ST}$  to  $XYZ_{dig}$ , the two systems were aligned so that the  $XY_{ST}$  plane was parallel to the  $XY_{dig}$  plane. To do so, the four points  $P_A$ ,  $P_B$ ,  $P_C$  and  $P_D$  (Figure 5-2) were digitized and the heights of the two fixtures were adjusted until all points were in the same plane. To transform the coordinates of the points  $P(x_{ST}, y_{ST}, z_{ST})$  obtained from the ShapeTape™ to the coordinate system ( $XYZ_{dig}$ ), a rotation  $\alpha$  was applied about the  $z_{dig}$ -axis through point  $P_A(x_0, y_0, z_0)$ :

$$(x'_{ST}, y'_{ST}, z'_{ST}) = (x_0, y_0, z_0) + \begin{pmatrix} \cos \alpha & \sin \alpha & 0 \\ -\sin \alpha & \cos \alpha & 0 \\ 0 & 0 & 1 \end{pmatrix} \begin{pmatrix} x_{ST} - x_0 \\ y_{ST} - y_0 \\ z_{ST} - z_0 \end{pmatrix}$$

where  $\alpha$  (Figure 5-2 (b)) was the angle between line  $P_{AB}$  and the  $y_{dig}$ -axis in the  $XY_{dig}$  plane.

After the transformation, the two sets of coordinates were aligned in the same coordinate system. The measurement error of each sensor was therefore defined as the differences between  $(x'_{ST}, y'_{ST}, z'_{ST})$  and  $(x_{dig}, y_{dig}, z_{dig})$ .

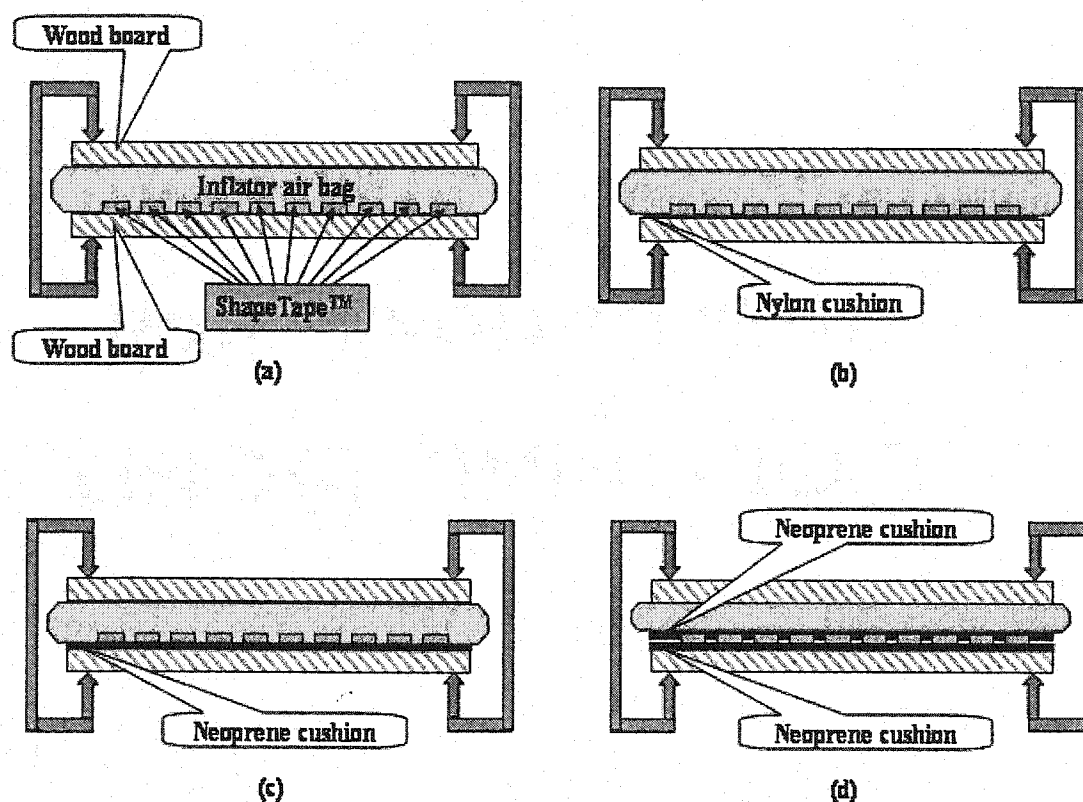
#### 5.4.1.2 Test 2: Assessing the influence of uniform pressure

Preliminary tests showed that pressure affected the measurements of the SSA (Li et al., 2002). Since the SSA will be used to measure body-seat interface shape, the pressure on the ShapeTape™s is unavoidable. Therefore, it is necessary to study the influence of the pressure under controlled conditions by applying known uniform pressure on the SSA mat. A pressure calibration apparatus (Vista Medical Ltd., Winnipeg, Canada), which can produce up to 26.7 kPa (200 mmHg) of uniform pressure, was used in this test. The SSA mat was placed on a flat rigid wood board with an inflator bag placed on top of it and another flat rigid wood board placed on top of the inflator bag (Figure 5-3 (a)), the top and bottom boards along with the SSA mat and the inflator bag were placed into the calibration jig. When the inflator bag was inflated, the two flat boards ensured that the SSA mat flat and that did not move. Therefore, the measurement error of each sensor was the shape measurement before inflating the inflator bag minus the shape measurement after inflating the inflator bag.

The SSA recorded the initial shape. Then the inflator bag was inflated and the pressure was increased in steps of 2.7 kPa (20 mmHg), up to 26.7 kPa (200 mmHg), and then



decreased to 0 kPa (0 mmHg). At each step, the SSA recorded the shape measurements 1 minute after the pressure was set or until the reading was stable. The whole procedure was repeated twice.



**Figure 5-3 Article 2: Illustration of the SSA mat between different interface materials. (a) Between a rigid wood board and an inflator bag; (b) between a nylon cushion and an inflator bag; (c) between a neoprene cushion and an inflator bag; and (d) between two layers of neoprene cushions.**

#### 5.4.1.3 Test 3: Assessing the influence of cover materials

Since the SSA mat needs to be covered by incontinent proof material, two types of interfaces materials were tested as cover materials. The first one is a 1 mm thick nylon cover that was provided by Measurand Inc (Fredericton, New Brunswick, Canada). The

second one is a 2 mm thick neoprene fabric that is commonly used in the clinical setting. The device described in Test 2 was used to assess the influence of different cover materials under the following conditions:

1. SSA mat placed on top of the rigid wood board (Figure 5-3 (a));
2. SSA mat placed on top of one layer of nylon cushion (thickness 1 mm) (Figure 5-3 (b));
3. SSA mat placed on top of one layer of neoprene cushion (thickness 2 mm) (Figure 5-3 (c));
4. SSA mat placed between two layers of neoprene cushions (thickness 2 mm) (Figure 5-3 (d)).

Under each condition, an inflator bag was then placed on top of the SSA mat or cushion and another flat rigid wood board was placed on top of the inflator bag. The top and bottom boards along with the SSA mat, the inflator bag and the cushions were slid into the calibration jig. The SSA recorded the initial shape. Then the inflator bag was inflated and the pressure was increased to 13.6 kPa (100 mmHg). The SSA recorded the shape measurements 1 minute after the pressure was set or until the reading was stable. The whole procedure was repeated twice.

As in Test 2, the measurement error was the shape measurement before inflating the inflator bag minus the shape measurement after inflating the inflator bag.

#### **5.4.1.4 Test 4: Assessing the accuracy under the influence of non-uniform pressure**

Since there was no commercially available device that could be used to measure the body-seat interface shape, the only possible way to evaluate the accuracy of the SSA interface shape measurements was to capture the interface shape by using a bead bag, and then compare the interface shape, which was recorded by the SSA, to the shape of

the bead bag digitized with the MicroScribe-3D digitizer. However, the SSA data was obtained while the subject sat on it, but the MicroScribe-3D data was obtained after the subject stood up. Therefore, the two sets of data were not recorded at exactly the same time and under exactly the same conditions.

One able-bodied subject participated in this test. A latex bag filled with plastic beads was placed on the seat of a seating simulator (Ringutte et al., 1998). The SSA mat was fixed on the bead bag by double-sided tape. Limited by the size of the bead bag, the SSA mat contained nine tapes instead of ten. The subject was asked to sit comfortably in the simulator with arms folded, feet on the footrests, and joints flexed at  $90^\circ$ . The pelvis was placed as far back in the seat as possible with the thighs in a level position. The seat surface was horizontal and the backrest was titled backwards by no more than  $10^\circ$  depending on the subject's comfort. This posture, which was controlled with an anatomical goniometer, was defined in accordance with the previous studies of Ferguson-Pell et al. (1993) and Hobson (1992). A vacuum pump was used to evacuate the air from the bag, which became firm and captured the body contour. Then the body-seat interface shape data acquisition was performed by the SSA after 1 min from the moment the interface shape was fixed. The acquisition lasted 20 seconds, during which time the subject was asked to keep his/her posture as still as possible. The locations of the "bases" and "ends" of the nine ShapeTape™s as well as the two landmarks on the metal rod aligned with the plumb line were also digitized during the SSA data acquisition. The subject got up and the marks that indicate the locations of the sensors along the tapes were digitized using the MicroScribe-3D digitizer. The shape of the bead bag was then again recorded by the SSA. The whole procedure was repeated twice.

In each trial, the coordinates of the location of the sensor measured by the SSA was presented as  $(x_{SSA}, y_{SSA}, z_{SSA})$  and the measurement obtained by the MicroScribe3D as  $(x_{dig}, y_{dig}, z_{dig})$ . Then  $(x_{SSA}, y_{SSA}, z_{SSA})$  was transformed from the  $XYZ_{SSA}$  coordinate system to  $XYZ_{dig}$  coordinate system and presented as  $(x'_{SSA}, y'_{SSA}, z'_{SSA})$ . The

measurement error of each sensor in the SSA mat was therefore defined as  $(x'_{SSA} - x_{dig}, y'_{SSA} - y_{dig}, z'_{SSA} - z_{dig})$ .

#### **5.4.2 Stability and Repeatability of SSA Measurements**

Tests were performed to evaluate the stability and repeatability of the SSA system. These tests were performed on a Material Testing System (858 Bionix, MTS Systems Corporation, Eden Prairie, Minnesota) to control the deformation of the SSA mat. A rigid test buttocks model was suspended on the hydraulic fixture of the MTS machine, which can provide a constant load/displacement. The test buttocks model was made of Duraform using a selective laser sintering process with an SLS 2500 machine (DTM Product Inc., Valencia, California). The dimensions of the test buttocks model were 312 x 240 x 51.2 mm (width x length x thickness). The shape and size of the test buttocks were taken from the mean interface shape of 30 elderly subjects (Li et al., 1999b).

A three-inch flat polyurethane foam cushion (density 2.5 lb/ft<sup>3</sup> and 35 IFD) was placed underneath the test buttocks model and the SSA mat was placed on the cushion. Limited by the size of the test buttocks model, the ten ShapeTape<sup>TM</sup>s in the SSA mat can't be tested at the same time. Therefore, a set of four ShapeTape<sup>TM</sup>s was tested first, and then another two sets of 3 ShapeTape<sup>TM</sup>s were tested. Finally, a FSA pressure mat (Force Sensing Array pressure mat, 430 x 430 mm (17"x17"), Vista Medical Ltd., Manitoba, Canada) was placed on top of the ShapeTape<sup>TM</sup>s (as shown in Figure 5-4). Since the test buttocks model is rigid and its surface is not smooth, a thin gel cushion (width = 405 mm, length = 230 mm, thickness = 6 mm, weight ≈ 0.454 kg) was placed on top of the FSA mat to protect the FSA and SSA mats.

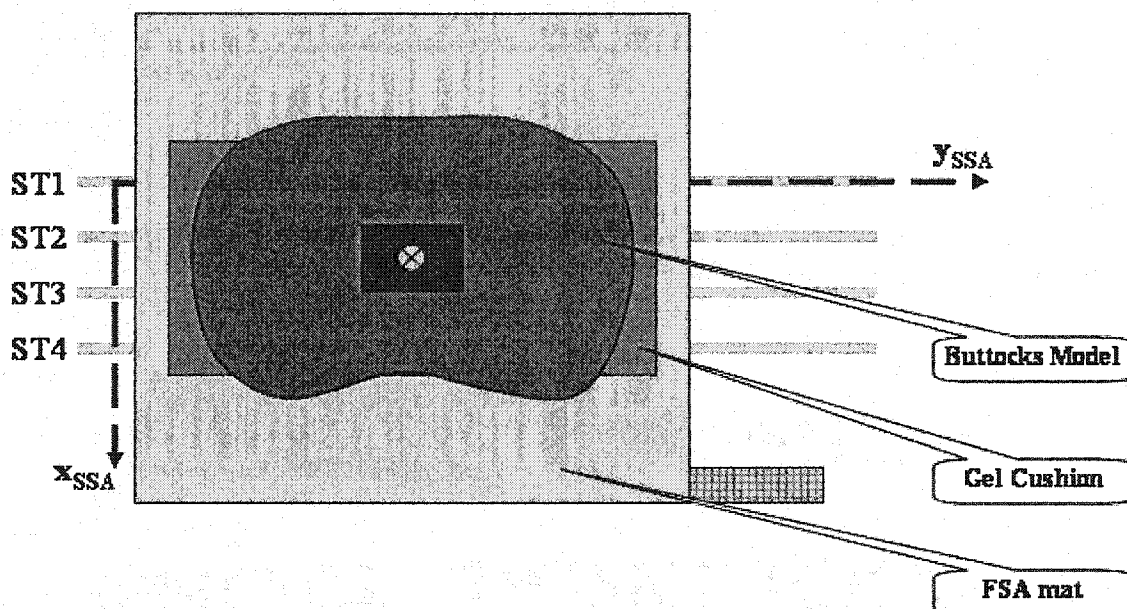


Figure 5-4 Article 2: Illustration of the configuration for test 5 and 6 (top view).

#### 5.4.2.1 Test 5: Assessing the stability

A force was gradually applied to the test buttocks to depress the foam cushion at an approximate rate of 1 mm/s until the displacement of the test buttocks model reached 39 mm. At that moment, the FSA mat indicated that the maximum interface pressure was around 13.3 kPa (100 mmHg). This load is based on 65% (weight of the legs excluded) of the seated weight of a 50<sup>th</sup> percentile elderly person (Stoudt, 1981). The interface pressure distribution on the cushion was measured then by the FSA mat and the interface shape was measured by SSA after 1, 2, 3, 5, 10, 15, 20, 25, and 30 minutes from the moment the test buttocks model reached the maximum displacement of 39 mm. Each acquisition contained 50 frames.

#### 5.4.2.2 Test 6: Assessing the repeatability

A force was gradually applied to the test buttocks model to depress the cushion at an approximate rate of 1 mm/s until the displacement of the test buttocks model reached 39 mm. The interface pressure distribution on the cushion was measured by FSA mat, and the interface shape was measured by the SSA after 1 minute from the moment the test buttocks model reached the maximum displacement of 39 mm or until the reading was stable. The acquisition contained 50 frames. The test buttocks model was then removed from the cushion and five minutes were allowed for the foam cushion to recover its initial shape. The test was repeated nine times.

#### 5.4.3 Data Analysis

The SSA measures the coordinates of the locations of the 120 sensors as well as the “ends” of ten ShapeTape™s. However, as the “bases” were constrained and remain unaltered, they were excluded from the error calculations. Therefore, the number of sensors involved was 110 ( $= 120 - 10$ ).

In tests 1 through 4, for each sensor, the mean error and the standard deviation (SD) of three trials were calculated. The error of the SSA was calculated based on the mean errors of the 110 sensors and presented as the maximum error and RMS error. The maximum error was defined as the highest error among the sensors while the RMS error was defined as the square root of the sum of the squared errors divided by the number of sensors.

For the first set of the ShapeTape™s in tests 5 (44 sensors were involved), calculating the mean of each set of 50 frames taken in one acquisition and subtracting the mean from each of the 50 readings produced a cumulative frequency distribution. The

cumulative frequency would have produced a linear relationship if the values had followed a Gaussian distribution. The Shapiro-Wilk's  $W$  test of normality was also performed. If the test indicated that the variances of the sensors reading were in most cases heterogeneous, the use of parametric statistical analysis would not be appropriate.

In Test 5, a Kruskal-Wallis nonparametric ANOVA was performed for each sensor for each acquisition, to test the hypothesis that the variability in readings after several minutes (while the test buttocks remained still) was no greater than the variability occurring after one minute.

In Test 6, measurements were centered around zero by subtracting the average reading of ten trials from the reading of each sensor. Variability of each sensor was obtained by calculating the standard deviation (SD) of 10 trials. The overall repeatability of the SSA was also found by calculating the standard deviation (SD) of all the centered data as a group of 1100 measurements (10 trials x 110 sensors). A Mann-Whitney  $U$  test was performed for each sensor, to test the hypothesis that the variability in readings produced by reseating the test buttocks was not greater than the variability occurring while the test buttocks remained still.

## **5.5 Results**

### **5.5.1 Accuracy of SSA Measurements**

As the errors in the  $X$  and  $Y$  directions were lower than 1 mm, and less sensitive to the pressure, the following discussions focused on the  $Z$  direction.

#### 5.5.1.1 Test 1: Assessing the accuracy without the influence of pressure

The accuracy of the sensors in the Z direction varied from sensor to sensor and thus from tape to tape. Since the errors propagate towards the middle of the ShapeTape™, the error was higher in the middle of the tape (Table 5-1). When there was no pressure on the SSA, the maximum error was 7.67 mm and occurred on sensor 7 (ST3). The RMS error of the 110 sensors was 3.79 mm which was close to the error of a single ShapeTape™ (5 mm RMS, provided by Measurand Inc.).

#### 5.5.1.2 Test 2: Assessing the influence of uniform pressure

In this test, uniform pressure was applied on the SSA mat while ensuring that the SSA mat remained flat. Therefore, if the pressure has no effect on the shape measurements, the Z coordinates of the sensors should be zeros. However, the measurements from SSA indicated that the Z coordinates of most sensors were not zeros. The differences from the zero were considered as the errors under uniform pressure. As shown in Table 5-1, when the pressure applied on the SSA mat was 13.3 kPa (100 mmHg), the RMS error of the 110 sensors in the Z direction was 6.33 mm while the maximum error was 12.63 mm and occurred on the sensor 3 (ST9). Although the pressures applied on the ShapeTape™s were the same, the reactions of the ShapeTape™s were different. Five of them (ST4, ST5, ST7, ST9 and ST10) were more sensitive to pressure than the rest. The results also revealed that the higher the pressure was, the bigger the errors were (Table 5-2). For example, when the pressure increased to 26.7 kPa (200 mmHg), the RMS error increased to 9.25 mm and the maximum error increased to 22.10 mm. Furthermore, when the pressure decreased to 0 mmHg, the RMS error of the SSA measurement was 0.28 mm. It was assumed that the weight of the wood board ensured that the SSA didn't move. Therefore, this phenomenon could be caused by the small hysteresis of the shape sensor.



**Table 5-1 Article 2: The accuracy of SSA measurements in the Z direction under different conditions**

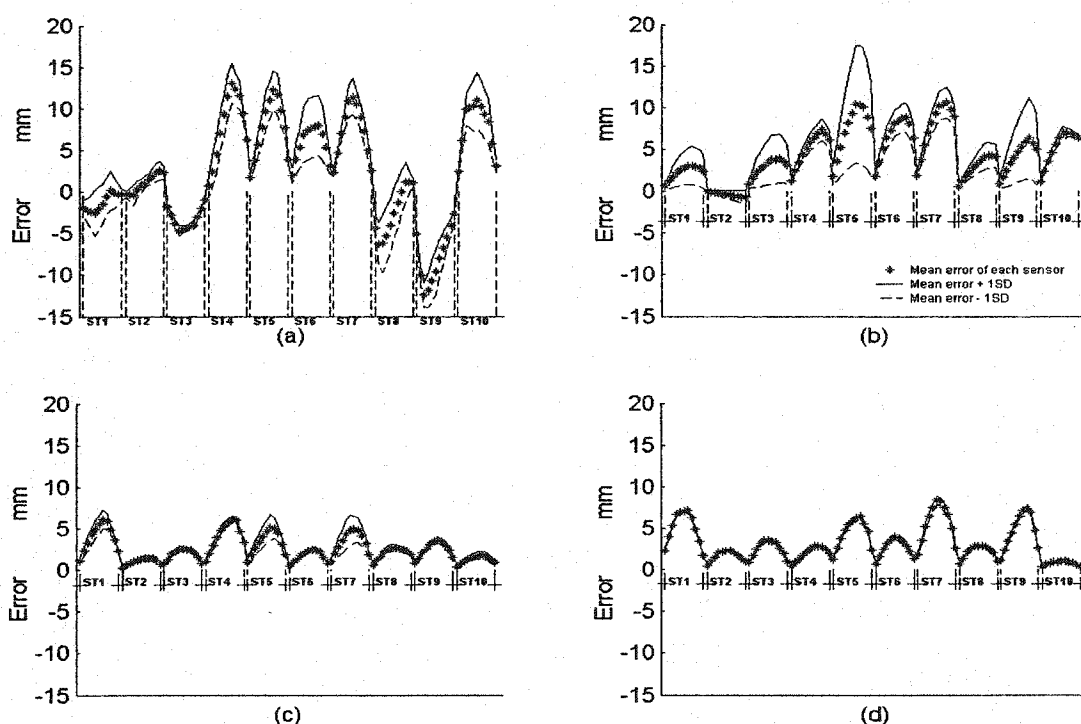
	Test 1 No pressure			Test 2 Under uniform pressure (100 mmHg)		
	RMS (mm)	Max Error		RMS (mm)	Max Error	
		Value (mm)	Location		Value (mm)	Location
ST1	3.68	5.03	s8	1.81	2.94	s4
ST2	4.14	5.31	s5	1.43	2.30	s10
ST3	5.49	7.67	s7	3.45	4.73	s4
ST4	1.82	2.40	s8	8.57	12.46	s7
ST5	3.82	5.84	s7	7.91	11.53	s7
ST6	3.09	4.28	s9	5.58	7.22	s8
ST7	5.39	7.23	s8	7.65	10.96	s6
ST8	2.94	3.81	s3	4.39	7.30	s3
ST9	5.50	7.60	s4	8.75	12.63	s3
ST10	0.81	1.52	s4	7.89	10.28	s6
SSA	3.79	7.67	ST3-s7	6.33	12.63	ST9-s3
	Test 4					
	Under non-uniform pressure			No pressure		
	RMS (mm)	Max Error		RMS (mm)	Max Error	
		Value (mm)	Location		Value (mm)	Location
ST1	7.61	9.38	s6	2.14	3.80	s6
ST2	1.11	1.84	s2	1.46	2.99	s5
ST3	1.88	3.15	s10	4.18	6.22	s5
ST4	6.61	8.51	s6	1.42	2.57	s5
ST5	3.65	5.85	s10	0.88	1.47	s11
ST6	2.25	4.16	s11	1.41	2.62	s5
ST7	8.41	10.97	s6	1.08	2.20	s4
ST8	2.18	4.05	s11	2.67	3.89	s4
ST9	0.66	1.35	s11	2.42	3.90	s4
ST10						
SSA	4.72	10.97	ST7-s6	2.19	6.22	ST3-s5

**Table 5-2 Article 2: Error of SSA measurements in the Z direction under different uniform pressures. RMS: Root Mean Square. SD: standard deviation (N=3).**

Pressure increased from 0 kPa (0 mmHg) to 26.7 kPa (200 mmHg) ⇒ ⇒											
Pressure (mmHg)		20	40	60	80	100	120	140	160	180	200
RMS error (mm)		3.12	4.53	5.35	5.90	6.33	6.77	7.24	7.81	8.47	9.25
Maximum error (mm)		9.40	11.65	11.84	11.97	12.63	14.81	16.52	18.32	20.17	22.10
SD (mm)		2.31	3.55	4.53	5.34	6.04	6.69	7.26	7.84	8.42	9.01
Pressure decreased from 26.7 kPa (200 mmHg) to 0 kPa (0 mmHg) ⇐ ⇐											
Pressure (mmHg)	0	20	40	60	80	100	120	140	160	180	
RMS error (mm)	0.28	3.35	4.66	5.52	6.26	6.98	7.60	8.13	8.56	8.98	
Maximum error (mm)	1.07	9.50	11.37	11.75	13.65	16.04	18.19	19.84	20.89	21.81	
SD (mm)	0.28	3.23	4.62	5.54	6.28	6.94	7.49	7.94	8.31	8.70	

### 5.5.1.3 Test 3: Assessing the influence of cover materials

The mean error of 110 sensors was shown in Figure 5-5 when the SSA mat was covered by different materials under the same pressure (13.3 kPa / 100 mmHg). The dots represent the mean error of sensors, as well as the solid lines present the mean values + 1 SD and the dashed lines present the mean values - 1 SD. Since SSA mat were pressed against a rigid board by an inflated air bag (with or without a thin cushion between the board and the SSA mat), there should be no deformation in the Z direction and all the dots would be located at  $z = 0$ . However, the previous test showed that the pressure did have influence on the measurements. The results of this test showed that the cover material also affected accuracy in the Z direction. Without a cushion of 2 mm between the board and the SSA mat (Figure 5-5-a), the errors in the Z direction were the highest with a maximum error of 12.63 mm and a RMS error of 6.33 mm (Test 2). When both sides of the interface were cushioned by a 2 mm neoprene layer (Figure 5-5-d), the errors were the lowest with a maximum error of 8.35 mm and a RMS error of 3.79 mm.



**Figure 5-5 Article 2: Mean errors in the Z direction under 13.3 kPa (100 mmHg) pressure for different interfaces: (a) Between rigid wood board and inflator bag; (b) between nylon cushion and inflator bag; (c) between neoprene cushion and inflator bag; (d) between two layers of neoprene cushions. SD: standard deviation (N=3).**

#### 5.5.1.4 Test 4: Assessing the accuracy under the influence of non-uniform pressure

The differences between the digitized data, which was obtained after the subject stood up, and the SSA data obtained when subject sat on the bead bag (SSA was under non-uniform pressure) were listed in Table 5-1. These differences were considered as errors associated to the sensors. The maximum error in the Z direction was 10.97 mm on sensor 6 (ST7) while the RMS error was 4.72 mm. For comparison, the maximum error

between the digitizing data and the SSA data obtained after the subject stood up (no pressure on the SSA) was 6.22 mm while the RMS error was 2.19 mm.

Pressure and other factors could cause the error. The influence of the pressure was evaluated in Test 3. Other factor could be that the SSA had a tendency to recover its original shape. After the subject stood up, there were tiny gaps between the SSA mat and the bead bag, even when the SSA mat was fixed on the bead bag surface by double-side tape. It is reasonable to assume that the SSA mat rose a little after the subject stood up.

### **5.5.2 Repeatability and Stability of SSA Measurements**

#### **5.5.2.1 Test 5: Assessing the stability**

The Shapiro-Wilk's W test indicated that the variances of the sensors reading were in most cases heterogeneous. This precluded the use of parametric statistical analysis on all subsequent results. The Kruskal-Wallis nonparametric ANOVA showed that the hypothesis was rejected at the 5 percent level. That is to say that the variability in the Z direction readings after several minutes (while the test buttocks remained still) was greater than the variability occurring after only one minute. However, longitudinal recordings from the sensors indicated that the maximum difference was 0.98 mm and the average difference was only 0.35 mm in a period of 30 minutes when the displacement was 39 mm.. Since the variations are lower than the errors that were detected in Test 4, the stability of the SSA measurements is considered as acceptable. The pattern of variation is that the longer the wait, the higher the variation is. For this reason, SSA data will be recorded after 1 minute. This time was chosen in order to minimize the influence of the instability of the sensor.

### 5.5.2.2 Test 6: Assessing the repeatability

The average repeatability for each sensor in the Z direction is shown in Table 5-3. The standard deviations in ten successive measurements that were carried out under the same conditions were very small. In fact, the overall repeatability of the SSA was 0.17 mm in the X direction, 0.09 mm in the Y direction, and 0.32 mm in the Z direction, respectively. The Mann-Whitney U test showed that the variability in readings produced by reseating the test buttocks was not greater than the variability occurring while the test buttocks remained still.

**Table 5-3 Article 2: Repeatability of the sensors in the SSA system (standard deviation of 10 trials). All the values are in mm.**

ShapeTape™ Sensor	ST1	ST2	ST3	ST4	ST5	ST6	ST7	ST8	ST9	ST10
s1	0.40	0.32	0.30	0.35	0.16	0.30	0.21	0.19	0.09	0.17
s2	0.43	0.55	0.47	0.37	0.21	0.40	0.34	0.26	0.12	0.28
s3	0.47	0.62	0.55	0.35	0.26	0.44	0.42	0.33	0.10	0.35
s4	0.56	0.59	0.68	0.37	0.35	0.45	0.49	0.45	0.12	0.45
s5	0.56	0.55	0.72	0.32	0.37	0.42	0.49	0.52	0.14	0.52
s6	0.52	0.53	0.67	0.30	0.32	0.38	0.46	0.53	0.13	0.55
s7	0.53	0.52	0.63	0.31	0.30	0.36	0.43	0.50	0.15	0.57
s8	0.57	0.48	0.55	0.30	0.30	0.39	0.38	0.44	0.15	0.63
s9	0.55	0.37	0.47	0.25	0.25	0.36	0.36	0.35	0.13	0.77
s10	0.39	0.24	0.35	0.24	0.15	0.23	0.29	0.23	0.14	0.68
s11	0.14	0.13	0.16	0.21	0.11	0.13	0.13	0.14	0.13	0.28

## 5.6 Discussion

### 5.6.1 Accuracy of the System

It is necessary to know the reliability of interface shape measurements before any further studies can be carried out. Dimensional accuracies vary across standards:  $\pm 1$  mm for 25

mm and  $\pm 2$  mm for 38 mm specimens in ASTM D-412-87 (ASTM, 1998a);  $\pm 3$  mm for thickness measures of specimen  $> 40$  mm,  $\pm 10$  mm for length and width measures from 150 mm to 300 mm and  $\pm 9$  mm accuracy allowed for specimens  $> 300$  mm in ASTM 1667 (ASTM, 1998b). As shown in Test 1 and 4, the accuracy of the SSA measurements was lower than these standards with RMS errors of 2.19 mm and 4.72 mm, respectively. Test 2 revealed that uniform pressure significantly affected SSA measurements and that higher pressure increased the errors.

However, the error-pressure relationship found in Test 2 could not be used to compensate for the influence of pressure in the body-cushion interface shape measurements, since a preliminary test found that the SSA measurements were also affected by interface pressure patterns. When the SSA was used in the body-seat interface shape measurements, the pressure on the SSA mat was not uniform and only the sensors that came into contact with the body were affected by the pressure. For example, the subject sat on a rigid surface with SSA and FSA mats under the ischial tuberosities (ITs), and the FSA showed that the maximum interface pressures under the ITs were over 26.7 kPa (200 mmHg) and the average interface pressure was only 5.33 kPa (40 mmHg). The maximum error of the SSA was 6.50 mm and the RMS error was 1.18 mm, which were much lower than the error in Test 2. As shown in Table 5-2, when the uniform pressure applied on the SSA mat was 5.33 kPa (40 mmHg), the maximum error of SSA was 11.65 mm and the RMS error was 4.53 mm.

Besides the influence of the pressure patterns, the measurements could also be affected by using different interface materials as illustrated in Test 3. This is most likely due to the different materials having different bulk moduli. In general, the more elastic and yielding an interface was, the less the pressure affected the SSA measurements. Furthermore, when one side of the interface was rigid, measurement errors were larger than if both were yielding. Tests 2 and 3 were performed on a yielding-rigid surface or a yielding-yielding surface. The tests showed that the errors due to pressure on a yielding-

yielding surface are lower than those on a yielding-rigid surface. This was to be expected, and has implications for using a rigid surface as a reference support for studying error-pressure relationship. Any interface shape measurement made between a subject and a rigid support surface will have falsely high errors due to the increased perturbation error, and so should be treated with caution.

Finally, the presence of the SSA mat it self will also affect conditions at the interface. Therefore, the measured interface shape may slightly differ from the true interface shape without the SSA mat in position. Furthermore, in the tests 5 and 6, the presence of the FSA mat could also interfere with the SSA measurements and the interference should be studied in the future. Overall, the SSA measurements were more accurate when no pressure was applied than when there was. The SSA system is also consistent in its ability to measure deformations. The influence of the pressure on the interface shape measurements should be acknowledged, while at present there is no convenient way of assessing these.

### **5.6.2 Repeatability and stability of SSA measurements**

The test results showed that the SSA system had good stability and repeatability under controlled laboratory conditions while measuring the test buttocks model-cushion interface shape. Furthermore, the repeatability of the sensor itself was not dependent on measurement range. No matter where the sensors were located, the standard deviations were all less than 0.8 mm. However, the readings were less repeatable in body-cushion interface shape measurements which may be due to repositioning of the subject.

## **5.7 Conclusion**

The new SSA system has the ability to measure the body-cushion interface shape in real-time. The tests clearly indicate that the system is capable of making repeatable, stable and accurate measurements of interface deformation in a research context. Pilot experiments have shown that the system could detect differences in interface shapes between subjects. However, further study must be performed on able-bodied subjects in order to study the repeatability of the system in a seating environment. The objective of the next stage of this study will be collecting a group of body-cushion interface shapes from wheelchair users by using SSA system, then compare and analyze those shapes in order to classify them and eventually find three to five generic shapes among them. The generic shapes then will be carved into high resiliency foam cushions, which are expected to provide lower peak interface pressures than flat-foam cushions. The new SSA system shows promise for cushion design and clinical guidelines for cushion prescription.



## **CHAPTER 6 ARTICLE 3: DESIGN AND EVALUATION OF GENERIC SHAPE CONTOURED CUSHIONS BASED ON A NEW INTERFACE SHAPE MEASUREMENT SYSTEM**

Yue Li<sup>1</sup>, Rachid Aissaoui<sup>2</sup>, David M. Brienza<sup>3</sup>, Michèle Lacoste<sup>4</sup>, Jean Dansereau<sup>1</sup>

<sup>1</sup>Institut de génie biomédical, École Polytechnique de Montréal, C.P. 6079, succ. Centre-ville, Montréal (Québec), Canada H3C 3A7

<sup>2</sup>Laboratoire de recherche en imagerie et orthopédie, Département de génie de la production automatisée, École de technologie supérieure, Montréal (Québec) H3C 1K3

<sup>3</sup> Seating and Soft Tissue Biomechanics Laboratory, Department of Rehabilitation Science and Technology, University of Pittsburgh, Pittsburgh, PA 15260, U.S.A.

<sup>4</sup>Laboratoire de mouvement, Centre de recherche du Centre de réadaptation Marie Enfant de l'Hôpital Ste-Justine, Montréal (Québec) Canada H1T 1C9

### **Acknowledgements**

This research was funded by the NSERC (Natural Sciences and Engineering Research Council of Canada). The authors also wish to acknowledge the collaboration of the Lucie-Bruneau Rehabilitation Center.

**This paper was submitted to the journal *Archives of Physical Medicine and Rehabilitation***

## **6.1 Abstract**

**Objective:** A method for designing generic shape contoured (GSC) cushions was evaluated. A cluster analysis approach based on geometric parameterization was adopted to derive a set of generic shapes from a group of body-seat interface shapes which were measured using a new shape sensing array.

**Design:** Repeated measures, randomized control trial.

**Setting:** Rehabilitation center.

**Participations:** Fourteen wheelchair users.

**Interventions:** One flat and three generic contoured foam cushions.

**Main Outcome Measures:** Interface shape measured using a shape sensing array system; interface pressure measured using a pressure sensing pad, comfort, dynamic stability.

**Results:** Three generic shape contoured (GSC) cushions were designed by transferring the resulting generic shapes to compliant foam cushions and evaluated during prescribed sitting in one specific population. The mean pressure and peak pressure gradient were lower on the GSC cushion that was selected by a similarity index method than on the rejected GSC cushions. Subjective evaluation also showed that the comfort rating on the selected GSC cushion was significantly higher than those on the rejected GSC cushions.

**Conclusions:** The results indicated that the pressure distribution on the selected GSC cushions was more uniform and had lower values than the distributions on flat foam cushions and the rejected GSC cushions. These findings suggest that generic shape contoured cushions could be used to manage wheelchair user's seating problems.

**Key Words:** Wheelchairs, Pressure; Rehabilitation; Buttocks; Cluster Analysis.

## **6.2 Introduction**

Ideal seat cushions are characterized by an even pressure distribution and low shear forces (Brienza et al., 1999). To achieve this condition, the support surface must envelop the buttock (Chow and Odell, 1978). The ability of contoured foam cushions to reduce pressures to levels that are well tolerated by the soft tissue of the buttocks is well documented (Perkash et al., 1984, Sprigle et al., 1990c, Rosenthal et al., 1996, Aissaoui et al., 1998, Brienza and Karg, 1998, Sy and Tam, 2000). Contoured cushion lowers the risk of pressure ulcer development and improves sitting tolerance by providing more surface area and/or reducing peak pressure near the ischial tuberosities, sacrum and coccyx regions of the sitting surface (Sprigle et al., 1990b).

Generally, two technological approaches have been used to design a contoured seat cushion that aim to increase the area of contact between the body and the seating support. The first approach is termed precontoured cushion, which can be manufactured using standard shapes. The second is termed custom-contoured cushion, which represents the user's shape. The advantage of precontoured cushions is that they are available off the shelf and can be quickly assembled into a functional seating system. This approach is often adequate for those with mild to moderate physical involvement. However, because the contours are standardized and symmetrical in shape, this approach becomes inappropriate when intimately fitting body support is needed, such as in cases where a deformity is present that necessitates custom-contoured seat and back modules. On the other hand, the advantage of the custom contoured cushions is that they can provide seating support at lower interface pressures, and improve posture and balance without impeding the users' functional abilities (Sprigle et al., 1990c). This approach, however, is usually labor-intensive and requires considerable technical skill to obtain an intimate fit, especially when accommodation of gross deformities is necessary. Furthermore, the contour of a particular person may change over time. Any change in body weight or

muscle tone may severely alter the buttock-cushion interface, and a reevaluation is then necessary.

Perkash et al. (1984) studied the possibility of producing universal contoured cushion and claimed that one contour shape could match the anatomical contours of a large percentage of the spinal cord injured population. Rosenthal et al. (1996) designed four wheelchair cushions to relieve pressure on bony prominences, but the shapes of these four cushions were the same, and the only difference between them was their sizes. Aissaoui et al. (1998) compared a commercially available precontoured cushion with flat foam cushions and suggested that precontoured cushions had a positive effect on reducing interface pressures. Although the above studies revealed that reduction of sitting pressure could be achieved using precontoured cushions, their results also showed that one shape could not satisfy all populations. On the other hand, many studies have focused on individually fitting contoured cushions using custom-contoured cushions. Vacuum consolidation and the foam-in-place technique are commonly used to provide custom cushion or body support surfaces for specialized seating. Recently, passive seating systems (Sprigle et al., 1990b) and active computer-aided systems (Brienza and Karg, 1998) have been developed to quantify contours resulting from the human buttocks and cushion interface. Furthermore, two new methods for custom-contoured cushion design using interface pressure measurements were developed by Brienza et al. (1999) and Sy and Tam (2000), respectively. Although their results indicated that custom contoured seat cushions can be generated using interface pressure measurements, the relationships between the interface pressure and shape still need to be investigated further in order to reduce reconstruction errors.

Despite these advances, there is still a gap between standard precontoured cushions and custom contoured cushions. Current techniques either provide one shape for all the wheelchair users or one shape for only one user. There is an urgent need for developing a technique to design generic shape contoured (GSC) cushions which can fit groups of

wheelchair users more accurately than the standard precontoured cushions, but not as intimately as the custom contoured cushions. In other words, the generic shape cushions will provide users allowances to change their body-seat interface a little bit a time. We expect that users could not only tolerate the generic shape cushions longer than they could custom contoured cushions but that the generic shape cushions could also improve pressure distribution.

Our previous study (Li et al., 2000a) suggested that body-seat interface shape patterns could be identified using cluster analysis. This method requires an interface shape database for each wheelchair user population that has similar body support needs. To do so, we have developed a new interface shape measuring device, the Shape Sensing Array (SSA) system (Li et al., 2003a). The SSA system has the ability to measure the body-cushion interface shape in real-time with accuracy. The goal of this project was twofold: 1) to determine a set of generic shapes from a group of wheelchair users; and 2) to show that the similarity index helps to select the generic shape that allows the lowest pressure during sitting in a group of wheelchair users.

### **6.3 Methods**

#### **6.3.1 Subjects**

Subjects were recruited from the Lucie-Bruneau Rehabilitation Center. All potential subjects were identified by the Center's physical therapy supervisor or occupational therapy supervisor. After obtaining the subject's consent, an initial screening was performed by using information from medical records. Screening criteria for inclusion comprised: (1) Be a wheelchair user of 18 years of age or older; (2) that is free of

pressure ulcers for the previous twelve months; (3) that requires mild to moderate body support and presents no severe pelvic deformities; (4) that has at least partially intact sensation over their buttocks and thighs and is able to rate their comfort; (5) and that the width of his or her cushion is no smaller than 16" and no greater than 18". Forty-one subjects met the eligibility criteria and were invited to participate in the study. Fourteen subjects (6 females; 8 males) entered and completed the study. The anthropometric characteristics of the subjects as well as clinical descriptions of their seated posture are presented in Table 6-1. All procedures were performed with the approval of the Lucie-Bruneau Rehabilitation Center's Ethics Committee.

The subjects were divided into two groups: interface shape data collection group and evaluation group. The first group (G-I) included nine subjects whose interface shapes were used to generate a database from which a set of generic shapes were derived. The second group (G-II) included five subjects who were asked to evaluate the GSC cushions. Five subjects from the first group were also called back to evaluate the GSC cushions and this subgroup was therefore named as G-I<sub>5</sub>.

### **6.3.2 Instrumentation**

The shape measurement instrument used in this study was the Shape Sensing Array (SSA) (Figure 6-1) which was developed by the authors (Li et al., 2003a). The SSA system consists of a set of ten ShapeTape™s and each of them is an array of twelve fiber optic curvature sensors laminated on a ribbon substrate. The mat is flexible and very thin (1.3 mm thickness), and can be placed between the subject and seat without disturbing the subject's natural feeling. With a person seated on the SSA mat, the ShapeTape™s deforms and follows the body-seat interface shape. The deflection of each ShapeTape™ is measured by summing the bends and twists of the sensors along the tape. The

deflection information is then recorded and a 3D shape of the interface can be reconstructed. The SSA system was used in this study to collect interface shapes when the wheelchair users sat on a flat foam cushion mad from high resiliency, polyurethane foam with a 25% IFD rating in the range of 178–222 N (40-50 lb) and a density of  $45 \pm 1.6 \text{ kg/m}^3$  ( $2.85 \pm 0.1 \text{ lb/ft}^3$ ).

**Table 6-1 Article 3: Characteristics of subjects.**

	Subject	Diagnosis	Gender	Age (year)	Weight (kg)	Height (cm)
G-I	s01	Bilateral leg amp below knee	Male	68	65.5	162.6
	s02	Bilateral leg amp above knee	Male	54	81.7	172.7
	s03	Traumatic brain injury	Male	53	98.1	177.8
	s04	Cerebral palsy	Female	40	63.0	152.4
	s05	Multiple Sclerosis	Female	33	60.3	180.3
	s06	Friedreich Ataxia	Female	30	52.2	160.0
	s07	Bilateral leg amp above knee	Male	59	66.3	165.1
	s08	Multiple Sclerosis	Female	63	84.0	170.2
	s09	Myelomeningocele	Male	33	74.0	160.0
G-II	s10	Bilateral leg amp above knee	Female	54	69.9	154.9
	s11	Bilateral leg amp above knee	Male	67	73.0	175.3
	s12	Polyneuropathy	Male	61	83.0	169.0
	s13	Multiple Sclerosis	Male	62	80.0	165.0
	s14	Multiple Sclerosis	Female	57	71.3	165.1

	Subject	Pelvic Width (cm)	Cushion Width (cm)	Cushion Depth (cm)	Participated in evaluation	Arm Length (cm)
G-I	s01	37.5	39.2	39.2	yes	66
	s02	41.5	41.7	41.7		73
	s03	40.5	44.1	46.6		76
	s04	35.5	41.7	36.8		65
	s05	35.5	41.7	46.6		75
	s06	34.5	39.2	39.2	no	
	s07	35.5	39.2	41.7		
	s08	38.3	41.7	39.2		
	s09	32.0	41.7	44.1		
G-II	s10	37.0	44.1	44.1	yes	61
	s11	38.0	44.1	41.7		74
	s12	37.0	44.1	39.2		72
	s13	36.0	41.7	39.2		76
	s14	39.0	44.1	41.7		71

Interface pressure distributions on flat foam cushions were measured using the commercially available Force Sensing Array (FSA mat, Vista Medical Ltd., Winnipeg,

Canada). The FSA mat consists of a 16 x 16 array of force sensing resistors contained in a flexible material base. The sensor mat was calibrated prior to the beginning of data collection for each subject according to the manufacturer's recommended procedure. The FSA pressure mapping device has been shown to be highly linear with a linear regression coefficient of 0.99 over a range from 0 to 160 mmHg, have maximum hysteresis errors of 18.7%, and 2.2% creep errors at 100 mmHg after 2 min (Ferguson-Pell and Cardi, 1993).

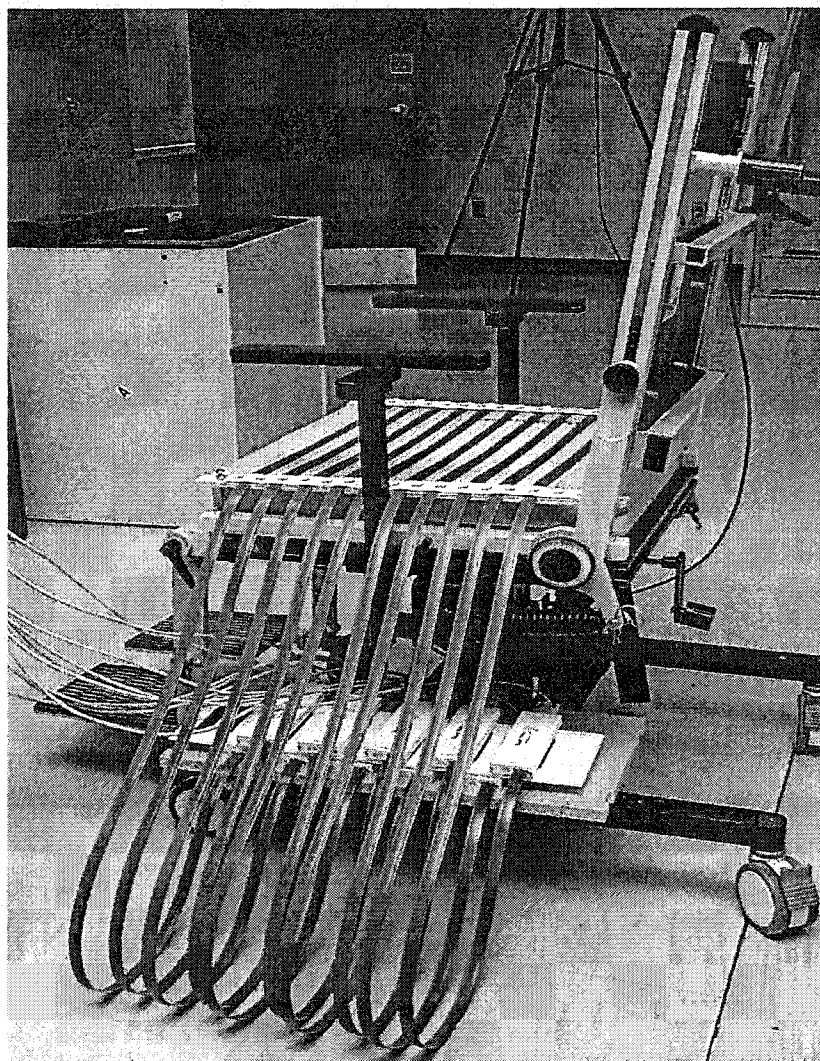
### **6.3.3 Protocol**

The 3-inch flat foam cushion was placed on a seating simulator (Ringutte et al., 1998) with the SSA mat on top of it and the FSA mat on top of the SSA mat (Figure 6-1). On top of all that was a waterproof neoprene cover. The cover was stretchable and did not interfere with cushion deflection. The subject sat on top of the cover and was positioned by an occupational therapist by centering the pelvis on the seat in the medial-lateral direction, placing the pelvis as far back in the seat as possible with the thighs in a level position, and placing the hands on the lap while facing forward. The occupational therapist ensured that there was no severe pelvic rotation or obliquity. The seat surface was horizontal and the backrest was titled backwards by no more than 10° depending on the subject's comfort.

In order to quantify the seating position, nine landmarks identified by the same clinician for each subject were marked on the subject with a pen and digitized using a Micro-Scribe-3D digitizer (Immersion Corp., San Jose, CA). The nine landmarks were: right acromion, left acromion, jugular notch, xiphoid process, right iliac crest, right Anterior Superior Iliac Spine (ASIS), left ASIS, right great trochanter, right lateral femoral epicondyle. The details to define these landmarks and calculate the associated geometric



parameters are fully described by Aissaoui et al. (2000). Seven geometric parameters were calculated to represent the joint rotation and segment orientation of the subject's posture: pelvic obliquity (PO), pelvic transverse rotation (PTR), pelvic tilt (PT), trunk flexion/extension (TFE), hip flexion/extension (HFE), hip abduction/adduction (HAA), and thigh sagittal angle (TSL). Four marks on the simulator and twenty marks on the SSA mat were also digitized in order to represent the orientation of the simulator as well as the location of the SSA mat with respect to the simulator (Li et al., 2003a).



**Figure 6-1 Article 3: Illustration of a Shape Sensing Array (SSA) system mounted on a seating simulator.**

Once the subject was positioned on the seating simulator, the resulting interface shape and pressure were measured by the SSA and FSA mats both before and after the landmarks were digitized. The subject was then transferred to his/her own wheelchair and repositioned in the same manner after 2 minutes rest. The whole process was repeated five times for each subject.

The forty-five interface shapes (9 subjects x 5 trials) from group G-I were used to derive the generic shapes. Each shape was represented by a raw matrix of 10x12 array of 3D coordinates data and the dimensions of the 45 interface shapes were all normalized to 18" by 18". The interface shape data was then interpolated to a 101 by 101 array for better comparison and each interface shape was globally described by a set of 17 normalized geometrical parameters (Li et al., 2000a).

Cluster analysis was performed on these 17 parameters to detect natural groupings in the 45 input shapes. The Ward's hierarchical method for the cluster analysis procedure (STATISTICA 5.1, StatSoft Inc., OK) was used. The hierarchical method uses the dissimilarities or distances between observations when forming clusters. The most straightforward way of quantifying dissimilarities between observations in a multi-dimensional space is to compute Euclidean distances. However, since the variables used in this study are not in the same measurement units (degree, mm, etc.), a derived distance measure, which was more meaningful to our case, was chosen to quantify the dissimilarities between shapes, i.e. the Pearson Product Moment (Li et al., 2000a).

After clusters had been identified, the mean shape of each cluster was generated and considered as a generic shape. Since the dimensions of the 45 interface shapes were normalized to 18" by 18", the dimensions of the mean shapes were also 18" by 18". The generic shapes were then transferred to a cushion cutting machine (Brienza et al., 1992). The shapes were carved into 4-inch-thick of the same HR45 polyurethane foam as the

foam used in the data collection. All the cushions were then covered with a waterproof neoprene cover.

Since the GSC cushions were going to be evaluated not only by some of the subjects from group G-I but also by subjects from group G-II, it was necessary to develop a method to select one of the GSC cushions for each subject. Rosenthal et al. (1996) used a fit factor based on anthropometry measurements to select cushion size. However, in our case the differences between GSC cushions are not only in size but also in shape. The selection of GSC cushions requires not only 2D information but also 3D information. Benefiting from the development of the SSA system, measurements of the subject's interface shape in real-time became possible. By comparing the subject's own shape with the generic shapes, the best matching GSC cushion could be selected for the subject based on a mathematical method developed by Li et al. (1998). Similarity indexes were calculated to quantify the differences between the interface shape and the generic shapes. If A and B are the two shapes characterized by the geometrical parameters  $P_i^A$  and  $P_i^B$ ,  $i = 1 \dots 17$ . The similarity index (*SI*) is then defined as (Li et al., 1998):

$$SI = \frac{1}{17} \frac{\sum_{i=1}^{17} |\min(P_i^A, P_i^B)|}{\sum_{i=1}^{17} |\max(P_i^A, P_i^B)|}$$

where  $\min(P_i^A, P_i^B)$  represents the lower value of the couple  $(P_i^A, P_i^B)$  and  $\max(P_i^A, P_i^B)$  represents the higher value of the couple  $(P_i^A, P_i^B)$ . Since five interface shapes were obtained from each subject, similarity indexes were calculated between the five interface shapes and generic shapes. Therefore, the similarity index between a subject's shape and a specific generic shape was the mean value of the five similarity indexes. Since the parameters are normalized, the value of the similarity index ranges between zero and

one. The closer the value is to 1, the more the two shapes are similar. Therefore, the GSC cushion that has the highest similarity index will be chosen as the most appropriate GSC cushion for that user.

Ten subjects participated in the evaluation of GSC cushions. Five of them were from the group G-I and five from the group G-II (as shown in Table 6-1). The average time between the first visit of the subject and the second one was 4 months. All the GSC cushions were evaluated in a random order on each subject to confirm the hypothesis that the GSC cushion selected by the similarity index method would provide a better pressure distribution than other GSC cushions. The test was blind to the subject. The selected GSC cushions were compared with the rejected GSC cushions. Four aspects were evaluated, namely pressure distribution, posture, comfort, and dynamic stability. Using the same method as before, the pressure was measured by the FSA and the posture was measured by digitizing the same nine anatomical landmarks.

Using a measuring tape, the arm length of the subject was measured in a seated position with the upper limb extended in horizontal plane and pointing in a forward direction. The distance was measured from the acromion process to the tip of the second finger. Once the subject was positioned on the seating simulator, the resulting interface pressure was recorded by the FSA mat and the landmarks were digitized. During the pressure recording and the landmark digitizing, the subject was asked to keep as still as possible. Therefore, this set of pressure measurements was called static pressure and was used to calculate seven static pressure variables.

Dynamic stability of the GSC cushions was assessed by a technique based on center of pressure (COP) trajectory during a reaching task (Aissaoui et al., 2001a). For this task, the subject was instructed to perform the reaching task. The subject, starting with his/her right hand resting on the armrest, was indicated to get prepared to reach and the FSA started to record the interface pressure. Then, the subject's right hand reached a button

that was located 45° ipsilaterally from the sagittal plane. Reaching distance was standardized to 130% of the arm length, and at a height of 100% of the glenohumeral joint height as measured from the floor in the seated posture. The subject's finger was maintained on the button for 3 seconds. The subject was then instructed to put his/her hand back on the armrest, which indicated the end of reaching task and interface pressure recording. This set of pressure measurements was called dynamic pressure and was used to calculate three stability variables. During reaching, the left hand was placed on top of the left thigh. After the subject performed the reaching task twice, the static interface pressure was recorded again with both his/her hands on the thighs.

Comfort and stability were evaluated by asking the subject a questionnaire. The clinician asked the subject to rate the overall comfort and stability of each cushion on a 1-5 scale (Shaw, 1991) referring to their regular cushion:

- 1: very uncomfortable / very unstable (much worse than regular cushion)
- 2: uncomfortable / unstable (worse than regular cushion)
- 3:  $\pm$  uncomfortable / unstable (same as regular cushion)
- 4: comfortable / stable (better than regular cushion)
- 5: very comfortable / very stable (much better than regular cushion)

The subject was then transferred to his/her own wheelchair. After 2 minutes rest, the subject returned to the simulator and repositioned in approximately the same position as previous trial. The whole process was repeated on all the GSC cushions for each subject. The order of the cushions being evaluated was randomly selected. After the subject finished evaluating all of the cushions, the clinician asked the subject to point out his/her favorite cushion.

For each cushion, seven static pressure variables, seven posture variables and three dynamic stability variables were calculated. The static pressure variables were: the mean pressure (MP), the standard deviation of the pressure-distribution (SDP), the contact area

(AC) where pressure was higher than 0.67 kPa (5 mmHg), the peak pressure (PP), the mean of the top 4 pressures (T4P), the peak pressure gradients (PG) and the mean of the top 4 gradients (T4G) (Brienza and Karg, 1998). The posture variables were: pelvic obliquity (PO), pelvic transverse rotation (PTR), pelvic tilt (PT), trunk flexion/extension (TFE), hip flexion/extension (HFE), hip abduction/adduction (HAA), and thigh sagittal angle (TSL). The dynamic stability variables were: the maximum covered distance (MCD) by the center of pressure, the maximum velocity (MV) of the center of pressure, and the maximum value of the index of asymmetry (MIA) (Aissaoui et al., 2001a). Each dependent variable was analyzed separately in a repeated measures ANOVA (2 factors: cushion x subject group), to determine if significant differences existed between the selected GSC cushion and rejected GSC cushion, as well as between the selected GSC cushion and flat foam cushion. If indicated, a least significant difference (LSD) test was performed to determine which pairs of means were significantly different ( $p < .05$ ).

#### **6.4 Results**

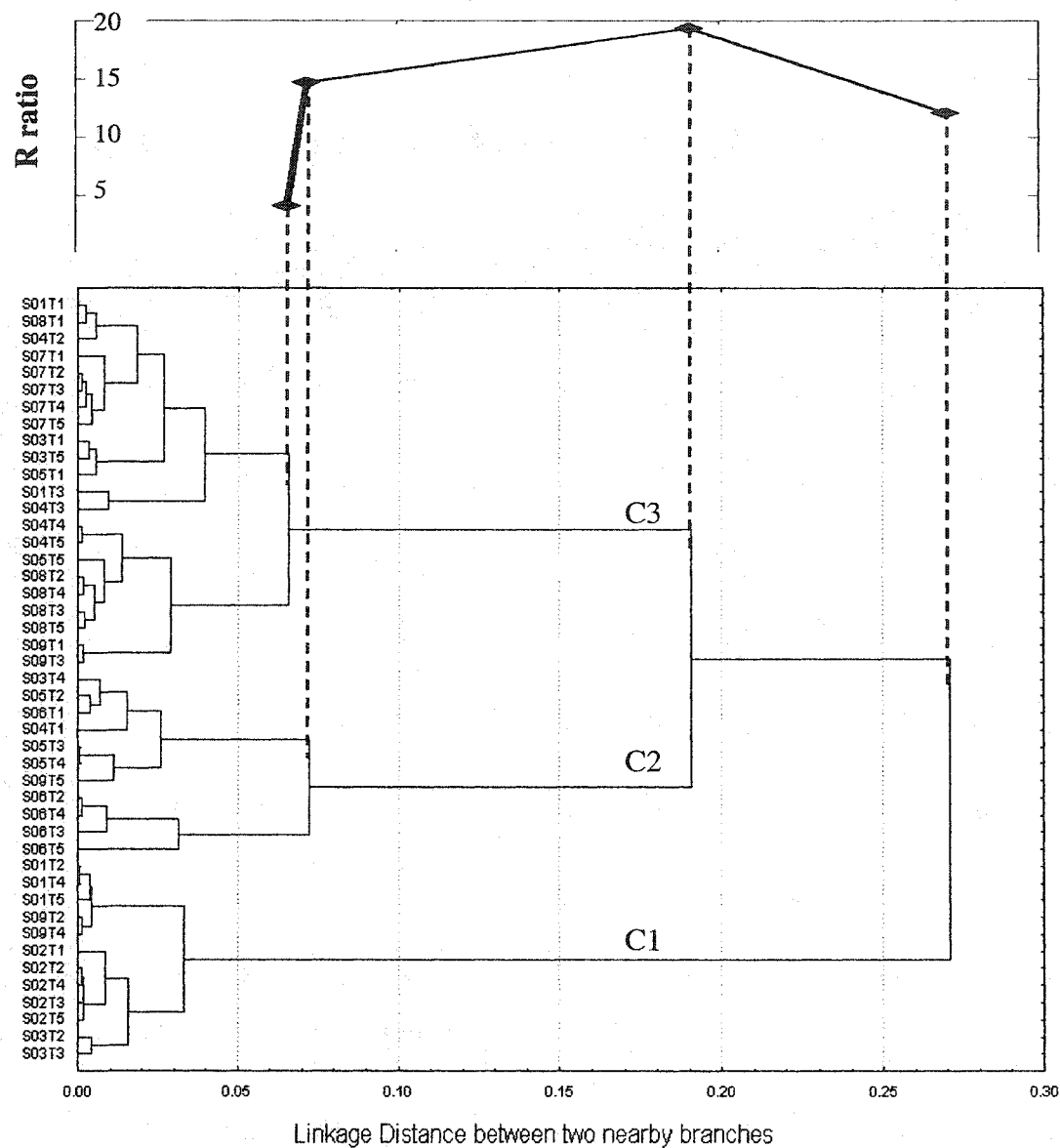
Three body-seat interface shape patterns were identified by classifying the variability in the geometrical parameters calculated in a group of subjects. The dendrogram obtained from the cluster analysis is shown in Figure 6-2. To determine the optimum number of clusters corresponding to the number of different observations, the R ratio analysis (Li et al., 2000a) was used. This ratio is a measure of the reduction of the intra-cluster variance by using  $K+1$  instead of  $K$  clusters. The R ratio peaked at value of 19.35 and a linkage distance of 0.19 where three clusters were identified Figure 6-2. Therefore, forty-five interface shapes were divided into three groups (C1, C2, and C3) at a linkage distance of 0.19. The mean shapes for clusters C1, C2, and C3 are considered as generic shapes. Three generic shape contoured cushions were then fabricated by carving these generic shapes into high resiliency foam. The three GSC cushions were named as C1, C2 and C3,

respectively. The differences between the three generic shapes are subtle. The maximum depths of the C1, C2 and C3 are 30.1 mm, 24.0 mm and 28.3 mm, respectively. The within-cluster variances of the maximum depths for C1, C2 and C3 are 1.7 mm, 4.2mm and 2.9 mm, respectively. The three contour shapes are displayed in Figure 6-3. Since the posture of the subject was controlled during the data collection and the ANOVA test revealed that there was no significant within-subject or between-cluster difference on the posture variables, it can be assumed that the differences between the generic shapes were not associated with the position.

The similarity indexes between the subjects' interface shapes and the generic shapes are listed in Table 6-2. For the subjects in group G-I<sub>5</sub>, the similarity indexes indicated that cushion C1 should be chosen for subject S02 and cushion C3 should be chosen for subjects S01, S03, S04 and S05. For the subjects in the group G-II, the similarity indexes indicated that cushion C1 should be chosen for subjects S10 and S13, cushion C2 for subjects S11 and S14 and cushion C3 should be chosen for subject S12.

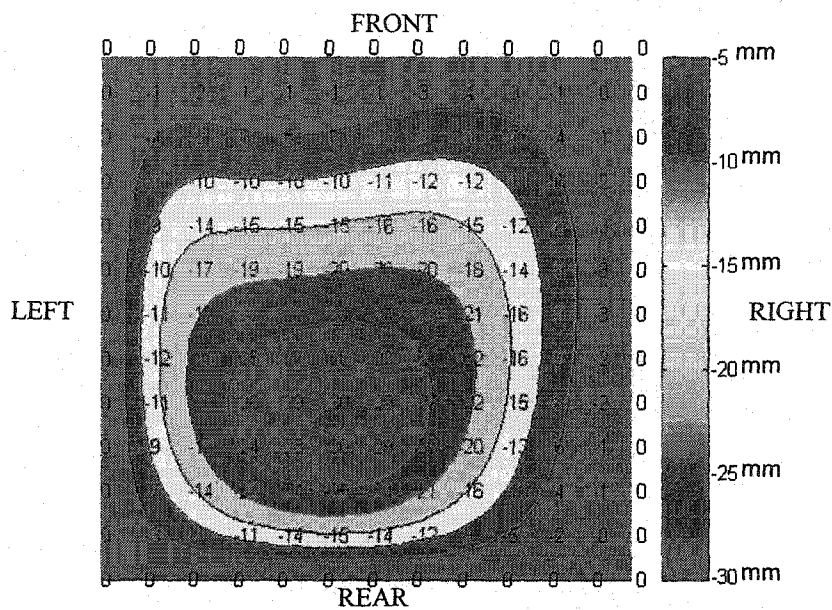
All the subjects were able to evaluate all the cushions. However, one subject was unable to reach the button on the right side while another one was unable to reach 130% of his arm length. Therefore, when comparing dynamic stability, only eight subjects were included in the statistical analysis. For comparison, the pressure distribution and posture data on flat foam cushions that were obtained in the data collecting stage were also analyzed and the results were listed in the Table 6-3 and Table 6-4.

The evaluation results on interface pressure distribution revealed that the mean pressure on the selected GSC cushion was lower than those on the GSC cushions that were not selected by the similarity index method. Other pressure variables such as SDP, PP and PG were all reduced on the selected GSC cushion (Table 6-3). Therefore, the similarity index method gave useful information on how to select a GSC cushion that could provide optimized pressure distribution.

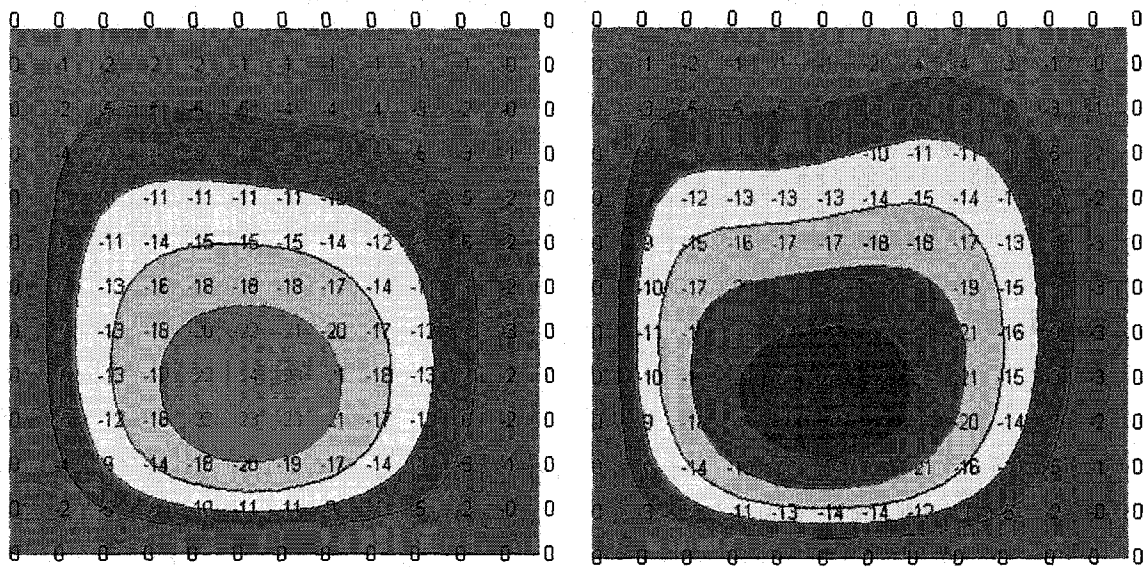


**Figure 6-2 Article 3: Dendrogram of the cluster analysis for 45 shapes. The horizontal axis denotes the linkage distance (Pearson Product Moment correlation coefficient). At a distance level of 0.1, three clusters (C1 to C3) can be distinguished. The number listing on the vertical axis presents the identification number for the interface shapes. The order of the number is decided by the procedure of the hierarchical method.**





(a)



(b)

(c)

**Figure 6-3 Article 3: Top view of the contour shapes of the generic shape contoured cushions. (a) cushion C1; (b) cushion C2; (c) cushion C3. The numbers are the depth of the contour in mm. The size of the cushion is 457x 457 mm (18"x18").**

**Table 6-2 Article 3: Similarity indexes between the subjects' interface shapes and the generic shapes.**

Group		Subject	C1	C2	C3
G-I	G-I <sub>5</sub>	s01	0.879	0.875	0.930
		s02	0.880	0.833	0.827
		s03	0.843	0.831	0.875
		s04	0.815	0.828	0.867
		s05	0.798	0.820	0.840
		s06	0.862	0.907	0.903
		s07	0.850	0.862	0.905
		s08	0.811	0.830	0.868
		s09	0.839	0.819	0.873
G-II		s10	0.854	0.851	0.845
		s11	0.818	0.843	0.821
		s12	0.828	0.833	0.869
		s13	0.843	0.823	0.836
		s14	0.832	0.842	0.838
		mean 1-14	0.840	0.843	0.864
		mean 1-9	0.842	0.845	0.877

The values of the static pressure variables estimated for selected GSC, rejected GSC cushions and flat cushion were shown in Table 6-3. For each type of cushion, the mean values of the variables for both subject groups are listed. ANOVA revealed that there wasn't a cushion effect on the static pressure variables. However, there was a subject group effect ( $p < 0.001$ ). Generally, the selected GSC cushions reduced the mean pressure and provided a larger support surface for the G-I<sub>5</sub> subjects. The mean pressures were  $28.8 \pm 4.0$  mmHg for group G-I<sub>5</sub> and  $32.7 \pm 5.9$  mmHg for group G-II on the selected GSC cushions. Overall, the selected GSC cushions provided a lower mean pressure ( $30.7 \pm 5.3$  mmHg) which is significantly lower ( $p < 0.05$ ) than that on the flat cushion ( $35.0 \pm 5.9$  mmHg). The selected GSC cushion also provided a larger contact area ( $1338.1 \pm 117.6$  cm<sup>2</sup>) comparing to those provided by the flat cushion ( $1322.3 \pm 110.7$  cm<sup>2</sup>). Finally, the standard deviations of the pressure across the seating surface (SDP), peak pressure and peak pressure gradients on the selected GSC cushion are all significantly lower than those on the flat cushion.

**Table 6-3 Article 3: Comparison of static pressure variables between selected GSC cushion, rejected GSC cushions and flat cushion.**

Cushions	Subject group	MP (mmHg)	SDP (mmHg)	CA (cm <sup>2</sup> )	PP (mmHg)	T4P (mmHg)	PG (mmHg/mm)	T4G (mmHg/mm)
Selected GSC	All	30.7 ± 5.3*	21.3 ± 4.6*	1338.1 ± 117.6	120.2 ± 35.1*	106.2 ± 24.0	2.04 ± 0.59*	1.81 ± 0.52
	G-I <sub>5</sub>	28.8 ± 4.0	21.2 ± 1.8	1353.6 ± 147.3	121.1 ± 36.2	104.9 ± 16.7	2.15 ± 0.73	1.91 ± 0.64
	G-II	32.7 ± 5.9	21.4 ± 6.4	1322.6 ± 83.5	119.4 ± 35.9	107.5 ± 30.6	1.93 ± 0.42	1.72 ± 0.38
Rejected GSC	All	33.3 ± 5.6	23.6 ± 5.7	1324.2 ± 110.4	132.3 ± 36.8	116.2 ± 29.1	2.19 ± 0.66	1.97 ± 0.57
	G-I <sub>5</sub>	31.9 ± 5.1	23.5 ± 4.5	1342.6 ± 132.1	126.6 ± 33.4	112.3 ± 24.9	2.18 ± 0.59	1.97 ± 0.51
	G-II	34.7 ± 5.9	23.7 ± 6.8	1305.8 ± 82.8	137.9 ± 39.9	120.1 ± 33.0	2.20 ± 0.73	1.97 ± 0.63
FLAT	All	35.0 ± 5.9*	24.7 ± 5.5*	1322.3 ± 110.7	142.2 ± 31.4*	121.9 ± 25.6	2.48 ± 0.67*	2.13 ± 0.56
	G-I <sub>5</sub>	33.8 ± 6.3	23.2 ± 4.5	1343.2 ± 144.5	131.8 ± 26.2	112.4 ± 20.6	2.25 ± 0.35	1.89 ± 0.36
	G-II	36.3 ± 5.4	26.3 ± 6.1	1301.3 ± 63.2	152.5 ± 34.0	131.4 ± 27.6	2.71 ± 0.84	2.36 ± 0.65
All Groups		33.1 ± 5.7	23.3 ± 5.5	1327.2 ± 111.0	131.8 ± 35.5	115.1 ± 27.4	2.22 ± 0.66	1.97 ± 0.56

\* indicates significant difference at  $p < 0.05$  between the selected GSC cushion and the flat cushion.

Table 6-4 shows the values of the posture variables estimated for selected GSC, rejected GSC cushions and flat cushion. For each type of cushion, the mean values of the variables for both subject groups are listed. ANOVA revealed that there was a cushion effect ( $p < 0.001$ ) and a subject group effect ( $p < 0.001$ ) on the posture variables. Generally, there was no significant difference between cushions for five of the variables (PT, PO, TFE, HFE and HAA). However, for pelvic transverse rotation, the mean values for the flat cushion were positive and significantly different from the selected GSC cushions ( $p < 0.05$ ). It seems that the flat cushion encourages left pelvic transverse rotation ( $\text{PTR} = 1.7^\circ \pm 3.7^\circ$ ) while the GSC cushions encourage right pelvic transverse rotation. Compared to the flat cushion, the selected GSC cushions were also more likely to provide thigh elevation ( $\text{TSL} = 1.8^\circ \pm 3.7^\circ$ ) which prevents the subjects from sliding forward. The differences of four variables (PT, PTR, TFE and HFE) between the two groups were not significant for all the cushions ( $p < 0.05$ ).

**Table 6-4 Article 3: Comparison of posture variables between selected GSC cushion, rejected GSC cushions and flat cushion.**

Cushions	Subject group	PT (°)	PO (°)	PTR (°)	
Selected GSC	All	84.1 ± 15.7	2.4 ± 4.8	-1.0 ± 3.5*	
	G-I <sub>5</sub>	91.3 ± 15.6	2.7 ± 6.3	-2.8 ± 3.9	
	G-II	76.9 ± 12.8	2.1 ± 2.9	0.9 ± 2.0	
Rejected GSC	All	86.4 ± 16.8	1.5 ± 3.9	-1.6 ± 3.3	
	G-I <sub>5</sub>	94.3 ± 15.2	1.6 ± 4.7	-2.8 ± 3.7	
	G-II	78.5 ± 14.7	1.4 ± 2.9	-0.5 ± 2.4	
FLAT	All	90.1 ± 16.7	0.8 ± 4.3	1.7 ± 3.7*	
	G-I <sub>5</sub>	101.2 ± 9.3	1.3 ± 5.9	2.1 ± 4.5	
	G-II	79.0 ± 15.2	0.3 ± 1.7	1.3 ± 2.9	
All Groups		86.8 ± 16.4	1.5 ± 4.2	-0.6 ± 3.7	
Cushions	Subject group	TFE (°)	TSL (°)	HFE (°)	HAA (°)
Selected GSC	All	3.6 ± 4.2	1.8 ± 3.7*	118.4 ± 10.9	91.1 ± 84.1
	G-I <sub>5</sub>	2.4 ± 3.8	1.9 ± 2.9	122.4 ± 13.3	89.2 ± 91.3
	G-II	4.7 ± 4.5	1.6 ± 4.5	114.4 ± 6.0	93.0 ± 76.9
Rejected GSC	All	3.8 ± 4.2	0.4 ± 3.6	122.7 ± 12.2	92.3 ± 86.4
	G-I <sub>5</sub>	2.6 ± 4.2	0.5 ± 3.9	126.6 ± 14.5	90.8 ± 94.3
	G-II	5.0 ± 3.9	0.3 ± 3.3	118.7 ± 7.9	93.8 ± 78.5
FLAT	All	6.2 ± 7.2	-0.7 ± 2.8*	122.4 ± 16.6	92.7 ± 90.1
	G-I <sub>5</sub>	4.5 ± 7.8	-1.7 ± 2.6	133.4 ± 6.0	93.7 ± 101.2
	G-II	7.9 ± 6.5	0.4 ± 2.8	111.3 ± 16.6	91.6 ± 79.0
All Groups		4.4 ± 5.2	0.5 ± 3.5	121.5 ± 13.1	92.1 ± 86.8

\* indicates significant difference at  $p < 0.05$  between the selected GSC cushion and the flat cushion.

Table 6-5 shows the values of the stability variables estimated from the evaluation of selected GSC and rejected GSC cushion as well as the subjective ratings on the comfort and stability. ANOVA revealed that there wasn't a cushion effect on the stability variables, but there was a subject group effect ( $p < 0.05$ ). The subjective evaluation on stability didn't show significant difference between cushions nor between groups. However, the subjective comfort ratings on the selected GSC cushion ( $3.9 \pm 0.9$ ) were

significantly higher than those on the rejected cushions ( $3.4 \pm 0.9$ ). Furthermore, as shown in Table 6-5, the rating of comfort on the selected GSC cushion from group G-I<sub>5</sub> ( $4.4 \pm 0.8$ ) was significantly higher than those from group G-II ( $3.4 \pm 0.5$ ) ( $p < 0.05$ ).

**Table 6-5 Article 3: Comparison of stability variables between selected GSC cushion and rejected GSC cushions, as well as subjective evaluation of the comfort and stability.**

Cushions	Subject group	MCD (mm)	MV (m/sec)	MIA
Selected GSC	All	$85.1 \pm 25.0$	$.139 \pm .045$	$.703 \pm .141$
	G-I <sub>5</sub>	$78.4 \pm 29.7$	$.138 \pm .053$	$.771 \pm .165$
	G-II	$91.7 \pm 18.5$	$.141 \pm .038$	$.635 \pm .067$
Rejected GSC	All	$87.2 \pm 17.9$	$.147 \pm .046$	$.702 \pm .210$
	G-I <sub>5</sub>	$84.4 \pm 22.6$	$.143 \pm .042$	$.693 \pm .213$
	G-II	$90.1 \pm 11.3$	$.152 \pm .050$	$.710 \pm .212$
All Groups		$86.5 \pm 20.4$	$.145 \pm .045$	$.702 \pm .189$
Cushions	Subject group	Subjective evaluation on comfort (1-5 scale)		Subjective evaluation on stability (1-5 scale)
Selected GSC	All	$3.9 \pm 0.9^*$		$3.4 \pm 1.0$
	G-I <sub>5</sub>	$4.4 \pm 0.8^\dagger$		$3.6 \pm 1.1$
	G-II	$3.4 \pm 0.5^\dagger$		$3.2 \pm 1.0$
Rejected GSC	All	$3.4 \pm 0.9^*$		$3.9 \pm 1.1$
	G-I <sub>5</sub>	$3.6 \pm 0.9$		$4.0 \pm 0.6$
	G-II	$3.2 \pm 0.8$		$3.8 \pm 1.4$
All Groups		$3.6 \pm 0.9$		$3.7 \pm 1.1$

\* indicates significant difference at  $p < 0.05$  between selected GSC cushion and rejected GSC cushion.

† indicates significant difference at  $p < 0.05$  between group G-I<sub>5</sub> and G-II

## 6.5 Discussion

This study suggests that contours for generic contoured seat cushions can be generated based on a group of interface shapes obtained from the SSA system. Three generic

shapes were successfully determined among forty-five interface shapes. However, the generic shapes found in this study are visually different to the generic shapes found in a previous study (Li et al., 2000a) where subjects were elderly people (mean age of  $81.6 \pm 8.4$  years,  $n = 30$ ). This observation is confirmed by calculating similarity indexes between these two sets of generic shapes. In our study, the subjects were wheelchair users who required mild to moderate body support and mean age of the first group subjects were  $48.1 \pm 14.3$  years ( $n = 9$ ). It thus seems that different wheelchair populations need different contour shapes for optimized pressure distribution efficiency. However, the difference between the two sets of generic shapes was also due to that the interface shape data was obtained from different devices. For the elderly subjects, an Electronic Shape Sensing (ESS) system (Brienza and Karg, 1998) was used to measure interface shape between the body and an array of spring-loaded support elements, which encourage maximum deformation where peak pressure occurs. In our study, the SSA system supports the whole buttocks and provides envelopment, which encourages a smoother interface shape. Furthermore, the FSA mat might interfere with the SSA mat and both mats might interfere with the deformation of the cushion. Further study is necessary to clarify these interferences.

The similarity index method was proved to be very efficient in initially selecting GSC cushions for subjects. Since the cluster analysis and similarity index were both based on the 17 geometrical parameters, the selection based on similarity indexes should be consistent with the results revealed by the cluster analysis. Therefore, if all or most of the interface shapes from one subject are classified into one cluster, the mean shape of this cluster should have a higher similarity index than the mean shapes of the other two clusters. This assumption was verified by most cases except for subjects S01, and S05 Figure 6-2. For example, three interface shapes from subject S05 were classified into cluster C2 while two interface shapes were classified into cluster C3, which suggested that cushion C2 should be chosen for subject S05. However, the similarity index indicated the choice of cushion C3. One of the possible explanations might be that the

subject's interface shapes from different trials are different. In fact, two shapes (S05T1 and S05T5) that were classified into cluster C3 were much more similar to generic shape C3 than the other three shapes (S05T2, S05T3 and S05T4) to C2. Therefore, the similarity index between S05T1 and generic shape C3 was much higher than that between S05T2 and generic shape C2. The pressure evaluation confirmed that mean pressures were lower on cushion C3 (22.3 mmHg) than on cushion C2 (25.5 mmHg) for subject S05. This result suggests that cluster analysis provide information for designing GSC cushion while similarity index provide information for selecting GSC cushion. However, the similarity index should only be used as a general guideline when prescribing a GSC cushion to a user. It should be used in addition to other preference factors (pressure distribution, heat dissipation, trunk stability, etc.) to select a cushion that is clinically satisfactory, comfortable and practical for the user.

Previous studies indicated that a properly fitted contoured cushion would improve the pressure distribution and reduce tissue distortion (Chow and Odell, 1978). The results of the pressure analysis suggest that the selected GSC cushion offered improved pressure distribution when compared to a flat foam cushion as the mean pressures (MP) and the standard deviations (SDP) of the pressure distribution were reduced for all cases (Table 6-3). The mean pressure has been found to be a very stable measure, and it affords a good representation of the pressures within the contact area. The standard deviation is an index of dispersion and provides insight into the relative variation with the pressure distribution. Less dispersion of pressure values signals a more uniform pressure profile and implies lower pressure gradients which contribute to shear forces on soft tissue. Lower seat interface pressure and a more uniform pressure distribution are characteristics of a safer sitting surface and are realized when sitting on the selected GSC cushion.

The clinical evaluation also proved useful in judging the usability of foam GSC cushions. Each subject was responsible for assigning a rating to overall comfort and stability as

well as choosing the favorite cushion. Judgment of these clinical variables was subjective and may have lacked reliability, which was a limitation of this study. Nevertheless, this evaluation measured the perception of cushion characteristics. This is important because a cushion which lends a poor image to its user will not be used regardless of its efficacy. Overall, the subjects gave a positive evaluation to the GSC cushions with comfort and stability of the selected GSC cushion always being judged "better than" or the "same as" the users' regular cushions.

Sprigle et al. (1990c) investigated the efficacy of custom contoured cushions and concluded that custom contoured foam cushions, when compared to flat foam, seem to provide a seat interface that is potentially less damaging to soft tissue. However, one of the limitations of the custom contoured cushions was that the user must sit in one location on the cushion. When the GSC cushions were designed, the repositioning effect was comprised by treating each trial as an individual data. Therefore, the GSC cushion not only reflects the common interface shape characteristics of different subjects but also takes into account the variation caused by repositioning. Thus, if the subject slides forward or leans side to side slightly, the shape of the GSC cushion will compromise the change.

Foam cushion will fatigue over time, and some estimate of the life span of a GSC cushion is needed. Sprigle et al. (1990c) conducted a material study to identify changes in the loading properties of the foam and found that seat pressure on a contoured foam cushion remained consistent for over 12 months. Therefore, since a GSC cushion does not deflect much after loading, sitting on a GSC cushion should be less fatiguing to the material than sitting on flat foam.

The contour of a particular person may change over time. Any change in body weight or muscle tone may severely alter the buttock-cushion interface, and a reevaluation will be necessary. An evaluation is suggested under these circumstances regardless of the



cushion. Furthermore, a softer material will be more tolerant of body contour changes, even though it will bottom out more quickly than stiffer foam. This tradeoff needs to be addressed during the fabrication of the GSC cushion. Further studies on choosing proper foam density for carving GSC cushions are necessary.

The GSC cushions provide increased pressure relief and comfort. However, the dynamic stability evaluation failed to show significant difference between the selected GSC cushions and the rejected ones. The reason may be that either too few subjects were involved in the evaluation or that the stability was dependent on other factors such as the stiffness of the foam used. Further studies on relationships between the stiffness of foam material and the generic shapes as well as a larger subject group are needed.

## **6.6 Conclusion**

This study has demonstrated the effectiveness of a method for designing seat support surfaces for a group of wheelchair users who require mild to moderate body support and presented no severe pelvic deformities. The results indicate that interface pressure on the selected GSC cushions were more uniform and had lower peak values than on flat foam cushion. The results suggest that the ability to design a set of generic shapes by measuring and classifying a group of body-cushion interface shapes is quite valuable when serving clients with a variety of seating and positioning needs. However, further investigation on foam materials and reliable databases for different wheelchair user populations are necessary.

## **CHAPTER 7 CLINICAL EVALUATION AND COMPARISON OF GENERIC SHAPE CONTOURED CUSHIONS WITH TWO STANDARD PRECONTOURED CUSHIONS**

### **7.1 Introduction**

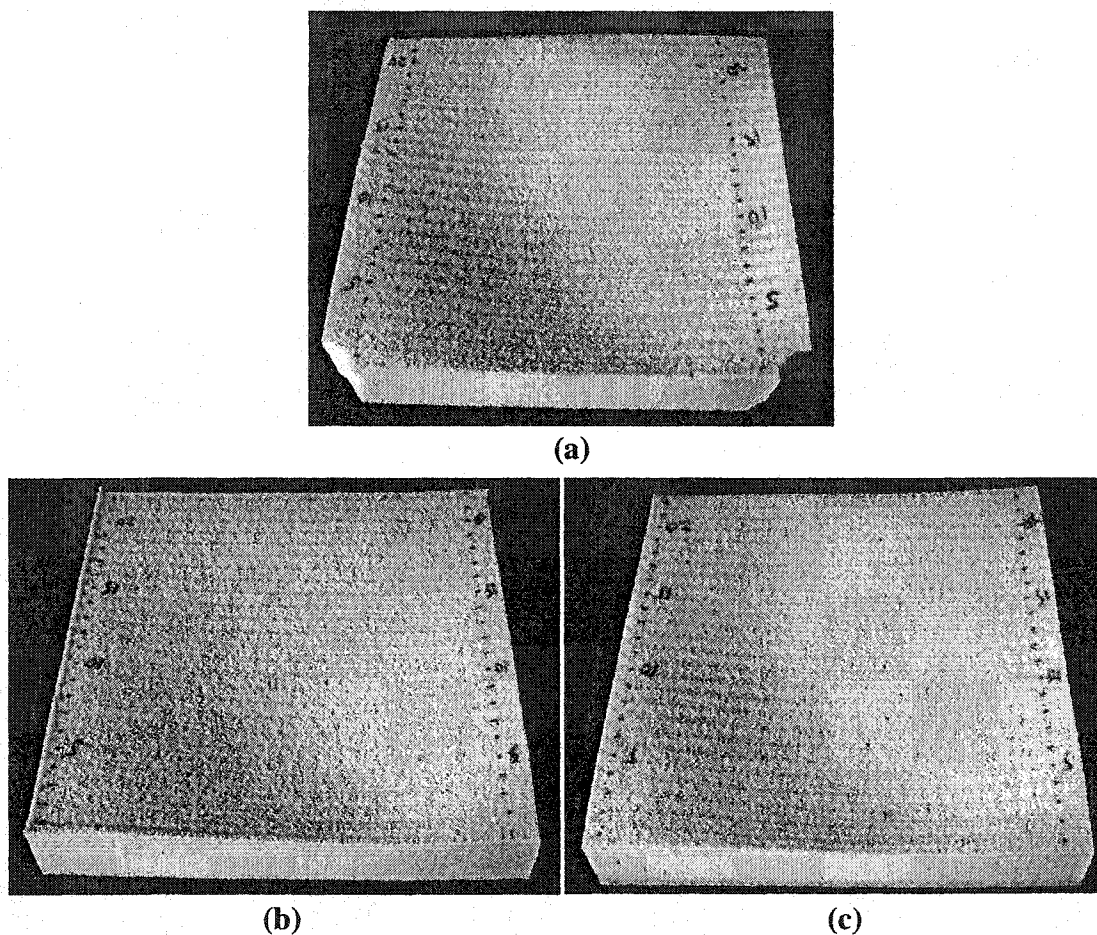
In recent years, many types of cushions have been developed in order to provide pressure relief at the ischial tuberosities and the sacrum. Air, gel and foam cushions are the three commonly used cushions (Sprigle et al., 2001). However, these cushions all have their pros and cons in terms of pressure relief characteristics, stability and cost. Air type cushion like the Roho (ROHO, Inc. Belleville, IL) behaves well in pressure relief but does not provide sufficient seating stability compared to gel and foam cushions (Letts, 1991, Koo et al., 1996, Aissaoui et al., 2001a). Both air and gel cushions are relatively expensive (around USD500). Foam cushion is the cheapest among the three, the cost ranging between 6 to US\$100 (ABLEDATA, 2003). Early studies conducted by Chung (1987), Sprigle (1989) and Sprigle et al. (1990c) have demonstrated that custom-contoured foam cushions are effective in both pressure relief and maintaining a good sitting posture. However, the production of such cushions are rather time consuming and costly. As a result, prescription of custom contoured cushions is often limited to those with severe skeletal deformity where the use of custom contoured cushion seems to be the only solution to provide sitting comfort and reduce the risk of pressure ulcers. This has limited the advantages offered by custom contoured cushion to other wheelchair users. For wheelchair users who are at moderate to low risk of formation of pressure ulcer, and whose needs are for an effective, reliable and moderately priced cushion that can be replaced with a minimum of effort, a new approach for designing contoured cushions has been developed. This approach attempts to design a set of generic shape

contoured (GSC) cushions which not only are available off the shelf but also provide more intimate fit to body support than do standard precontoured cushions (Li et. al., 2003b). This study is aimed at comparing GSC cushions with two standard precontoured cushions.

## **7.2 Methods**

Four aspects were evaluated, namely pressure distribution, posture, comfort, and dynamic stability. Pressure was measured by FSA mat and posture was measured by digitizing nine anatomical landmarks. The comfort was evaluated by asking subjects to rate the overall comfort of each cushion on a 1-5 scale. Finally, the effect of seat cushion on dynamic stability in sitting during a controlled reaching task was examined by analyzing the movements of the center of pressure. Full details for the definition and calculation of evaluation variables (pressure, posture, dynamic stability and comfort) as well as descriptions of the subjects are described in a previous study (Li et. al., 2003b). Ten subjects participated in the evaluation of the cushions. For each cushion, seven static pressure variables, seven posture variables and three dynamic stability variables were calculated. The static pressure variables were: the mean pressure (MP), the standard deviation of the pressure-distribution (SDP), the contact area (AC) where pressure was higher than 0.67 kPa (5 mmHg), the peak pressure (PP), the mean of the top 4 pressures (T4P), the peak pressure gradients (PG) and the mean of the top 4 gradients (T4G). The posture variables were: pelvic obliquity (PO), pelvic transverse rotation (PTR), pelvic tilt (PT), trunk flexion/extension (TFE), hip flexion/extension (HFE), hip abduction/adduction (HAA), and thigh sagittal angle (TSL). The dynamic stability variables were: the maximum covered distance (MCD) by the center of pressure, the maximum velocity (MV) of the center of pressure, as well as the maximum value of the index of asymmetry (MIA). Each dependent variable was analyzed using an repeated

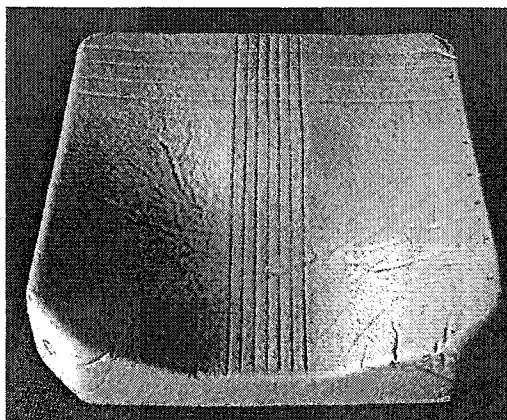
measure analysis of variance (ANOVA) to determine if significant differences existed between the cushions. If indicated, a Fisher least significant difference (LSD) test was performed to determine which pairs of means were significantly different ( $p < .05$ ).



**Figure 7-1** Photographs of three generic shape contoured cushions. (a) cushion C1; (b) cushion C2; (c) cushion C3.

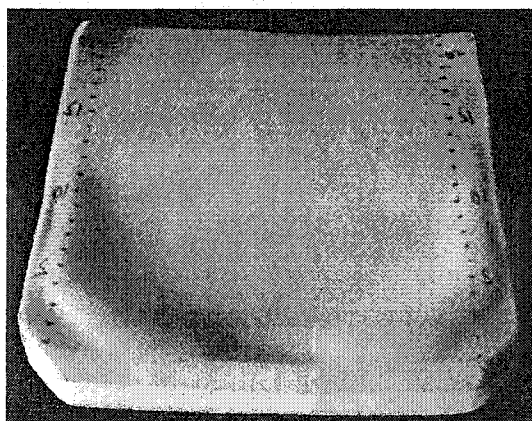
Three GSC cushions (Figure 7-1) were carved from 4-inch (10 cm) high resiliency polyurethane foam with a 25% IFD rating in the range of 178–222 N (40–50 lb) and a density of  $45 \pm 1.6 \text{ kg/m}^3$  ( $2.8 \pm 0.1 \text{ lb/ft}^3$ ). By comparing a subject's own shape with the generic shapes, the best matching GSC cushion was selected for this subject. And the selected GSC cushion was evaluated along with two precontoured cushions:

- The ISCUS cushion (Figure 7-2) is commercially available and fabricated by Orthofab Inc. (Quebec, Canada). It is a 3-inch polyurethane HR45 contoured foam cushion, with the ischial areas covered by a thin silicon gel pad.



**Figure 7-2 Photograph of ISCUS cushion (Orthofab Inc., Quebec, Canada).**

- The LB cushion (Figure 7-3) was designed by the Lucie-Bruneau Rehabilitation Center (Montreal, Canada). It is a 3-inch multilayer contoured foam cushion, which consists of four layers: from bottom to top there are a 1.5 inch contoured firm urethane foam base, a 1 inch HR45 polyurethane foam, a thin silicon gel pad and a 0.5 inch HR45 polyurethane foam.



**Figure 7-3 Photograph of LB cushion (Lucie-Bruneau Rehabilitation Center, Montreal, Canada).**

During the evaluation, all the cushions were covered by a waterproof neoprene cover. The top surface of the cover was stretchable so that it did not interfere with cushion deflection.

### 7.3 Results

The values of the pressure distribution variables estimated for the GSC, ISCUS and LB cushions were shown in Table 7-1. For each type of cushion, the mean values of the variables are listed. The ANOVA revealed that there was a cushion effect ( $F = 3.55$ ,  $p < 0.001$ ) on the pressure distribution variables. The GSC cushion provided the lowest mean pressure ( $30.7 \pm 5.3$  mmHg) that was significantly lower ( $p < 0.05$ ) than those on the LB cushion ( $35.0 \pm 6.9$  mmHg). Other pressure variables such as the standard deviation of pressure (SDP), the peak pressure (PP) and the peak pressure gradient (PG) were also significantly reduced on the GSC cushion when compared to the LB cushion. Furthermore, the GSC cushion provided a larger contact area ( $1338 \pm 118$  cm<sup>2</sup>) than the LB cushion ( $1247 \pm 108$  cm<sup>2</sup>). Except for contact area, the pressure distribution variables on the ISCUS cushion were all significantly different from those on the LB cushion. However, there was no significant difference between the GSC cushion and the ISCUS cushion for any of the pressure distribution variable.

The values of the posture variables estimated for the GSC, ISCUS and LB cushions were shown in Table 7-2. For each type of cushion, the mean values of the variables are listed. The ANOVA revealed that there was a cushion effect ( $F = 3.94$ ,  $p < 0.001$ ) on the posture variables. Compared to the ISCUS and LB cushions, the GSC cushion was more likely to provide thigh elevation ( $TSL = 1.8^\circ \pm 3.7^\circ$ ) which prevented the subjects from sliding forward. The hip flexion/extension (HFE) on the GSC cushion ( $118.4^\circ \pm 10.9^\circ$ ) was significantly smaller than the HFE on the ISCUS cushion ( $125.1^\circ \pm 13.1^\circ$ ). However,

there was no significant difference between cushions for the rest of the variables (PT, PO, PTR, TFE, and HAA).

**Table 7-1 Comparison of pressure distribution variables between the GSC, ISCUS and LB cushions on ten subjects. \* indicates significant difference at  $p < 0.05$  between the GSC cushion and the LB cushion. † indicates significant difference at  $p < 0.05$  between the ISCUS cushion and the LB cushion.**

Cushion	MP (mmHg)	SDP (mmHg)	CA (cm <sup>2</sup> )	PP (mmHg)	T4P (mmHg)	PG (mmHg /mm)	T4G (mmHg /mm)
GSC	30.7 ± 5.3	21.3 ± 4.6	1338 ± 118	120.2 ± 35.1	106.2 ± 24.0	2.04 ± 0.59	1.81 ± 0.52
ISCUS	31.9 ± 5.1†	22.4 ± 4.2†	1305 ± 123	117.1 ± 25.4†	104.1 ± 21.3†	2.09 ± 0.50†	1.84 ± 0.43†
LB	35.0 ± 6.9*	26.4 ± 7.4*	1247 ± 108*	143.0 ± 38.3*	123.9 ± 35.9*	2.70 ± 1.01*	2.35 ± 0.80*

**Table 7-2 Comparison of posture variables between the GSC, ISCUS and LB cushions on ten subjects. \* indicates significant difference at  $p < 0.05$  between the GSC cushion and the LB cushion. † indicates significant difference at  $p < 0.05$  between the GSC cushion and the ISCUS cushion.**

Cushion	PT (°)	PO (°)	PTR (°)	TFE (°)	TSL (°)	HFE (°)	HAA (°)
GSC	84.1 ± 15.7	2.4 ± 4.8	-1.0 ± 3.5	3.6 ± 4.2	1.8 ± 3.7	118.4 ± 10.9	91.1 ± 6.1
ISCUS	84.7 ± 17.5	0.4 ± 5.1	-1.6 ± 3.3	3.1 ± 4.8	-1.9 ± 4.6†	125.1 ± 13.1†	93.7 ± 6.6
LB	83.1 ± 16.6	0.9 ± 4.3	-0.5 ± 3.8	3.3 ± 4.4	-2.8 ± 4.0*	123.6 ± 11.8	93.3 ± 7.9

Table 7-3 shows the values of the dynamic stability variables estimated from the evaluation of GSC, ISCUS and LB cushions as well as the subjective ratings on the comfort and stability. The ANOVA revealed that there wasn't a cushion effect on the dynamic stability variables or of subjective rating on the stability. However, the subjective comfort rating on the GSC cushion ( $3.9 \pm 0.9$ ) was significantly higher than those on the ISCUS ( $2.9 \pm 0.7$ ) and LB cushions ( $3.0 \pm 1.3$ ) ( $p < 0.05$ ). Overall, seven subjects preferred the GSC cushions, two preferred the ISCUS cushion, and one preferred the LB cushion.

**Table 7-3 Comparison of dynamic stability variables between the GSC, ISCUS and LB cushions on ten subjects, as well as subjective evaluation on the comfort and stability. \* indicates significant difference at  $p < 0.05$  between the GSC cushion and the LB cushion. + indicates significant difference at  $p < 0.05$  between the GSC cushion and the ISCUS cushion.**

Cushion	MCD (mm)	MV (m/sec)	MIA	Subjective evaluation on comfort (1-5 scale)	Subjective evaluation on stability (1-5 scale)
GSC	85.1 $\pm$ 25.0	0.139 $\pm$ .045	0.70 $\pm$ 0.14	3.9 $\pm$ 0.9	3.4 $\pm$ 1.0
ISCUS	88.2 $\pm$ 20.6	0.156 $\pm$ .058	0.65 $\pm$ 0.16	2.9 $\pm$ 0.7+	3.8 $\pm$ 0.8
LB	93.7 $\pm$ 19.8	0.164 $\pm$ .056	0.75 $\pm$ 0.23	3.0 $\pm$ 1.3*	3.6 $\pm$ 1.0

#### **7.4 Discussion & conclusion**

The principal concern addressed in this study was the performance of contoured foam cushions. The statistical results indicated that sitting on the GSC or ISCUS cushions lowered pressure distribution more than sitting on the LB cushion. The subjective comfort ratings on the GSC cushion were also significantly higher than on the ISCUS or LB cushions. The study revealed that 70% of the subjects preferred the GSC cushion to the ISCUS or LB cushions. Therefore, this study demonstrates the effectiveness of the generic shape contoured method for designing seat support surfaces for a group of wheelchair users since the GSC cushion was able to provide pressure relief and improved sitting comfort.

Aissaoui et al. (2001a) found that the dynamic stability was improved when paraplegic subjects sat on an ISCUS cushion compared to a flat foam cushion or an air flotation cushion. Their results showed that when the shape of the support surface changed from flat to contoured, the dynamic stability of the cushion was enhanced. With this finding, it seemed reasonable to test the hypothesis that the better the support surface matches the subject's buttock shape, the more stable the seat is. Therefore, since the GSC cushion was designed based on the interface shapes from the subjects, we hypothesized that the



stability should be improved. However, although the similarity indexes of the ISCUS and LB cushions were less similar than the subject's shape, the stability during reaching on these two cushions were increased when compared to the stability on the GSC cushion. The difference was not significant. Due to the thin gel pad that was inserted in the ISCUS and LB cushions, these two cushions were stiffer than the GSC cushion. Therefore, it was possible that the higher stiffness of the ISCUS and LB cushions compromised their lack of envelopment of the buttocks. Further study is required to investigate the relationship between the foam stiffness and the stability characteristics to find foam materials that enhance sitting stability.

## CHAPTER 8 GENERAL DISCUSSION

The objectives of this Ph.D. thesis were to develop an efficient and easy-to-use instrument to measure the shape of any cushion with or without a user sitting on it, as well as to design generic contoured support surfaces based on the information gathered through the use of this new instrument. After having investigated the commercially available shape measurement devices which could be suitable for body-cushion interface shape measurements, the Shape Sensing Array (SSA) system was developed based on optical fiber technology and helped to create a body-cushion interface shape database. A cluster analysis approach based on geometric parameterization was then adopted to derive a set of generic shapes from this database. Three generic shape contoured cushions were fabricated by transferring the resulting support surface shapes to compliant foam cushions and evaluated on four aspects: interface pressure distribution, posture evaluation, dynamic stability and comfort. The results indicated that the pressure distributions on the GSC cushion were more uniform and had lower values than distributions on a flat foam cushion. Seventy percent of the subjects involved in the study reported that they preferred the GSC cushion to two commercially available precontoured cushions.

### ***8.1 Body-cushion interface shape measurements***

The usefulness of body-seat interface shape measurements for cushion design and clinical evaluation is restricted at the present time due to technical limitations, lack of experience and standards, as well as high costs. The SSA system developed in this study could be an alternative solution to this problem. To our knowledge, three types of techniques have been developed to measure body-seat interface shape. Early in 1984,

Kadaba et al. (1984) introduced a prototype ultrasonic system to measure contours using the principle of refraction. By using movable force sensing probes, four devices with similar mechanical configurations have been developed: the Electronic Shape Sensing (ESS) system (Brienza et al., 1991), the Computer-aided shape sensor (Sprigle and Schuch, 1993), the Computer-Aided Seating System (CASS) (Brienza et al., 1996a) and the direct contact probe system (Chang et al., 1996). Finally, Yamazaki (1992) used strain gauges to measure contact shape between a seated person and a driver's seat. Comparing the above devices to our newly developed SSA system, which is based on optical fiber technology, the major advantage of the SSA system is that it can be used to measure interface shape on any type of cushion and can be accommodated to a wheelchair. In regards to the other aspects, such as resolution, accuracy, repeatability, and portability, the SSA system also shows greater functionality (Li et al., 2003a).

Except for the device developed by Yamazaki (1992), the ultrasonic system or force sensing probe systems can only measure interface shapes on certain types of cushion or support surfaces. Since the ultrasounds propagate poorly in foam type cushions, which are used by the majority of wheelchair users, the ultrasonic contouring system developed by Kadaba (1984) can only be used to indicate buttock-gel cushion interfaces which limit its usefulness. The computer-aided shape sensor system developed by Sprigle and Schuch (1993) has probes that pass through holes in a foam cushion and therefore changes the supporting properties of the foam. Furthermore, it is not convenient or possible to drill holes in fluid floatation cushions. The ESS, CASS and the direct contact probe systems support the body by an array of probes, which form a noncompliant seat surface. Although the stiffness of the spring in the probe could be modeled to represent the stiffness of foam material, the supporting surface provided by the probes can not substitute for a real cushion. Therefore, the force sensing probe systems could provide data for seat design but not for cushion evaluation. On the other hand, the SSA system developed in our study consists of an array of optical fiber sensors that are laminated on ribbon substrates that are very thin and flexible and could be placed on any type of

cushion without changing its supporting properties. The device developed by Yamazaki (1992) also has this capability. Unfortunately, no further investigation on that device has been reported after his preliminary study. We expect that the development of our SSA system could provide useful information not only for designing contoured cushions, but also for cushion evaluation and clinical guidelines for cushion prescription.

The spatial resolution of the measurement from the SSA system is 40 mm and was determined by previous experiments (Li et al., 1998). Kadaba et al. (1984) measured the thickness of a PVC gel pad at 50 mm intervals across the cushion to provide the data to calculate a two-dimensional indentation curve. For the computer-aided shape sensor (Sprigle and Schuch, 1993) and the Computer-Aided Seating System (CASS) (Brienza et al., 1996b), the support element resolutions (the distance between probes) were 50.8 mm and 42.7 mm, respectively. The ESS has the same resolution as the CASS. The direct contact probe system developed by Chang et al. (1996) and the device developed by Yamazaki (1992) have a higher resolution (30 mm). As low resolution could cause attenuation of contour features, Brienza et al. (1993a) stated that a suitable resolution should be between 25 and 50 mm. However, the distance between probes in the CASS was limited by diameter of the stepper motor actuators and therefore 42.7 mm was the minimum achievable resolution. On the other hand, higher resolution for the SSA system could be easily achieved by simply adding more sensors in the ribbon substrates if necessary. The maximum allowable resolution for the SSA system is currently 20 mm.

The SSA system RMS error in the Z direction was 2.19 mm and 4.72 mm when the measurements were not and were affected by pressure, respectively. Pressure significantly affected the SSA measurements. The higher the pressure was, the larger the errors were. Since the CASS uses a computer to control the position of the support elements, a higher positioning accuracy of the system is guaranteed. Its positioning error was 1.3 % (0.127 mm) while the probe under test was loaded with 22 N (Brienza et al., 1996a). For the strain gauge developed by Yamazaki (1992), the average error of the

calculated radius was reported to be 3% (1.5 mm) when the sensor was attached to a circular plate. No accuracy information on the computer-aided shape sensor (Sprigle and Schuch, 1993) or the direct contact probe system (Chang et al., 1996) was provided. A direct comparison between the Shape Sensing Array (SSA) system and other seat-body interface shape measurement instruments was difficult as their technologies, principles and applications are so different. Furthermore, since there was no commercially available device that could be used to measure the body-cushion interface shape, the accuracy of the SSA measurements could not be "evaluated by comparison with reference techniques that are known to be accurate" (Latman and Lanier, 1998). Because of this, the accuracy of the SSA is considered to be acceptable.

The repeatability of the SSA system was less than 0.32 mm under controlled conditions. A good repeatability of the SSA is important for its potential usefulness in designing generic shape contoured cushions. As it is costly and non-portable, the CASS system has limited the potential for widespread use (Brienza et al., 1993b). The SSA system, on the other hand, is much easier to use and portable. With further studies and advanced evaluation methods, the SSA system is likely to be developed into a valuable research and clinical tool for support surface evaluation and design.

## ***8.2 Design of generic shape contoured cushions***

The present study suggested that body-seat interface shape patterns could be identified using cluster analysis. Four distinct generic shapes were identified among 30 elderly subjects by analyzing the dissimilarity in geometrical shape parameters (Li et al., 2000a). Furthermore, three generic shapes were identified among nine wheelchair users who required mild to moderate body support and presented no severe pelvic deformities (Li et al., 2003b). However, the latter generic shapes are different from the generic shapes

determined for the elderly subjects. This observation is confirmed by calculating similarity indexes between these two sets of generic shapes. The generic shapes for the elderly subjects often had two visible lobes (Figure 4-5) which were not observed in the three generic shapes found from the nine wheelchair users who had pathologies of the nervous system or amputation. One of the reasons could be that the interface shape data was obtained from different devices. For the elderly subjects, the Electronic Shape Sensing (ESS) system was used to measure interface shape between the body and an array of spring-loaded support elements, which encouraged the maximum deformation where peak pressures occur. For the second group of nine wheelchair users, the SSA system was used and the buttocks were evenly supported which encouraged a smoother interface shape. Moreover, the differences between intrinsic characteristics of populations could also affect the body-seat interface shapes. Ferrarin et al. (2000) investigated the pressure distribution on four cushions of different populations and showed that elderly subjects had higher mean pressures and lower contact surfaces than subjects with pathologies of the nervous system (mainly Multiple Sclerosis). Ferrarin et al. (2000) also found that there were more elderly people with peak pressures under the sacral area. Despite the fact that the cushions used in their study were gel-filled or air-filled cushions, their findings may help to explain the differences of the contour shapes between populations. Further studies to build a larger database using the SSA system and to determine generic shapes for different populations could help to clarify the assumption that different wheelchair populations need different generic contour shapes for optimized pressure distribution efficiency.

Cluster analysis was chosen in this study to identify a set of generic shapes. For the first group of subjects (Li et al., 2000a), the cluster analysis was performed on the 30 interface shapes that were obtained from 30 subjects. For the second group of subjects (Li et al., 2003b), the cluster analysis was performed on the 45 interface shapes that

were obtained from the nine subjects. Using all the interface shapes that obtained from the 5 trials for each subject instead of using the average one allowed us to obtain a large sample for cluster analysis. Since cluster analysis generally assumes a sample larger than 30 (Everitt, 1993), it was assumed that it was more desirable to pool all the shapes from the 9 subjects. This approach was used because of the small amount of subject recruited for the last study. It is obvious that using the average shapes of a larger group of subjects would have been preferable and would have produced a more representative result. It is recommended to increase the number of the subjects in the future studies.

The effect of body weight on shape pattern has been studied by Yamazaki (1992). He relates deformation of the interface shape with body weight, and states that the contact shapes of obese subjects were flatter and smoother than those of thin subjects. The effect of the body mass index (BMI) on pressure distribution has been studied by Garber and Krouskop (1982) and Kernozek et al. (2002). Their studies suggested that body build factors, such as height and weight, played an important role in pressure distribution in patients seated on wheelchair cushions. Furthermore, they suggested that the topography of the interface between the patient and the cushion might be an important consideration. It therefore seems reasonable to relate BMI with the generic shapes. Our two studies (Li et al., 2000a and 2003b) did reveal that the differences in BMI were significant between certain clusters. However, the two studies suggested that the relationships between BMI and contour depth were different for different populations. For elderly data (Li et al., 2000a), subjects with low BMI tended to have deeper contours than subjects with high BMI. For subjects with pathologies of the nervous system (mainly Multiple Sclerosis) or with amputation (Li et al., 2003b), the depth of the contour increased as BMI increased. Since BMI is a readily obtainable and understandable subject characteristic, the relationship between BMI and shape pattern found in this project could encourage considering BMI as a factor in the selection of seat cushion shape.

Polyurethane foams have been the mainstay of cushion technology over the years, particularly for those individuals at low to moderate pressure ulcer risk. The pressure distributing characteristics of foam cushions depend on the inherent mechanical properties of the foam, whether it is used in a single or multiple-layer planar configuration or contoured to the pelvic area. Sprigle et al. (1990a) investigated the influence of foam stiffness on pressure distribution and found out that sitting on a HR45 cushion resulted in a lower pressure distribution than sitting on a HR55 cushion. Staarink (1995) studied the influence of foam thickness on pressure using a test dummy and found that the pressure under the ischial tuberosities decreased from 319 mmHg to 126 mmHg as the thickness of the foam increased from 60 mm to 120 mm. In our study, only the HR45 foam (25% IFD = 45 lb) was used to carve the GSC cushion. Changing the stiffness of the foam might change the outcomes of this study. Sitting on a flat foam cushion with different stiffness will produce a different interface shape and will ultimately affect the resulting generic shapes. The pressure distributing characteristics of the GSC cushion will also change if foam with different stiffness is used to carve GSC cushion. Foam with different stiffness or different types of foam should be investigated in future studies to examine their effects on the contour of the generic shape as well as the pressure distribution characteristics of the GSC cushion.

### ***8.3 Evaluation of generic shape contoured cushions***

The evaluation results on interface pressure distribution revealed that the mean pressure for the selected GSC cushion was significantly lower than those for the GSC cushions that were not selected by the similarity index method ( $p < 0.05$ ). Other pressure variables such as standard deviation of pressure-distribution (SDP), peak pressure (PP), and peak pressure gradients (PG) were all reduced on the selected GSC cushion. Therefore, the



similarity index gave useful information on how to select a GSC cushion that could provide optimized pressure distribution. Rosenthal et al. (1996) used a fit factor based on anthropometry measurements to select cushion size. However, in our case the differences between GSC cushions are not only in size but also in shape. The selection of a GSC cushion requires not only 2D information but also 3D information. The similarity index was calculated based on the geometrical parameters that characterized the key features of the interface shapes. However, the similarity index should only be used as a general guideline when prescribing a GSC cushion to a user. It should be used in addition to other preference factors (pressure distribution, heat dissipation, trunk stability, etc.) to select a cushion that is clinically satisfactory, comfortable and practical for the user. Furthermore, all the subjects in this study were selected so that they could fit into an 18"x18" GSC cushion. But 16"x16" and 17"x17" GSC cushions should be fabricated in future studies and a better fit for certain subjects might be found by changing cushion size. For the subjects from the same population who have wider or narrower hips, a larger than 18" or smaller than 16" cushion is needed. Their interface shapes will have to be measured and a set of generic shapes could be determined for them. A better insight into the effects of hip width and bone structure on generic shape patterns might well contribute to the development of good support elements and to the optimization of sitting conditions.

The results of the pressure analysis suggest that a selected GSC cushion offers an improvement in pressure distribution when compared to flat foam cushions. The mean pressures were lowered for all subjects, and the standard deviations were reduced for all cases. The mean pressure has been found to be a very stable measure, and it affords a good representation of the pressures within the contact area. The standard deviation is an index of dispersion and provides insight into the relative variation with the pressure distribution. Less dispersion of pressure values signals a more uniform pressure profile and implies lower pressure gradients which contribute to shear forces on soft tissue. Lower seat interface pressure and a more uniform pressure distribution are

characteristics of a safer sitting surface and may be realized when sitting on a GSC cushion.

The clinical evaluation also proved useful in judging the usability of foam GSC cushions. Each subject was responsible for assigning a rating to overall comfort and stability as well as choosing a favorite cushion. In addition to the variables themselves, this evaluation also measured the perception of cushion characteristics. This is important because a cushion which lends a poor image to its user will not be used regardless of its efficacy. Overall, the subjects gave a positive evaluation to the GSC cushions. Seven out of ten subjects chose one of the GSC cushions as their favorite cushion. The comfort and stability of the selected GSC cushion were always judged "better than" or the "same as" the users' regular cushions.

Generic contoured shape cushions have been fabricated for wheelchair users exhibiting many types of disabilities such as multiple sclerosis, bilateral amputation, cerebral palsy, traumatic brain injury and polyneuropathy. The contouring system is capable of fabricating GSC cushions which provide increased pressure relief and comfort. However, the analysis of dynamic stability evaluation data did not reveal significant differences between GSC cushions and other types of cushions. The implication of this finding is that the GSC cushions were as successful as the others in stability improvement, and could be explained by the fact that too few subjects were involved in the evaluation or the stability was dependent on the stiffness of foam used. Further studies on the relationships between the stiffness of foam material and stability as well as on a larger subject group are indispensable.

Reliable clinical evaluation of cushions is difficult to accomplish fairly. To demonstrate improvement in pressure distribution and comfort using a new cushion design requires follow-up of a large number of patients. Measurement of interface pressure and other parameters is useful in comparing the relative performance of different cushions for an

individual or a well-defined population. However, the relationship between these measurements and pressure-ulcer incidence or comfort is still not very clear at present, in fact, it is the subject of much debate among researchers in the field. This study was undertaken to provide the user with a choice between cushions with different physical characteristics to relieve pressure that is comparable to many commercial cushions currently available.

Since seat contours are the result of a combination of factors, the resulting generic shapes may vary greatly if one of the factors changes. Firstly, biomechanical properties of buttocks and tissues structures vary from one wheelchair user population to another. Moreover, the body weight or muscle tones of a particular person may change over time. The subjects who were chosen for this study fell into the category defined as requiring mild to moderate body support and presenting no severe pelvic deformities. However, their soft tissue stiffness and thickness are all different due to different diagnoses such as multiple sclerosis, bilateral amputation, cerebral palsy, and traumatic brain injury. Therefore, it is expected that by extending the interface shape database for each specific population, the complex relationships among seating properties such as tissue deformation, surface shape and interface pressure will be better understood. Secondly, the seat contours are also affected by cushion characteristics. Since subject characteristics are generally fixed for an individual, changing cushion characteristics is the only way to accommodate the physical parameters. As shown in this study, the resulting generic shape contoured cushions are not optimal for every subject. Changing foam stiffness might be one of the solutions. Since foam stiffness will change the way load is transmitted to a cushion and therefore will affect the seat contour. For the future studies, it suggests that the influence of foam stiffness and thickness on effectiveness of the GSC cushion should be investigated. Finally, the weight distribution on the cushion is another very important factor that affects the seat contour. With the development of the SSA system, seat contours are able to provide useful clinical information on the weight-bearing surface of the cushion. Therefore, seat contour measurements

complement other clinical measures, such as seat interface pressure and posture assessments, to form a more complete picture of the buttock-cushion interface.

## CHAPTER 9 CONCLUSION

The new SSA system has the ability to measure the body-cushion interface shape in real-time. The performance of the system during the evaluations clearly indicates that the system is capable of making repeatable and accurate measurements of interface deformation and is a reliable research tool. The system's RMS error in the Z direction was 2.19 mm and 4.72 mm when the measurements were not and were affected by pressure, respectively. The errors in the X and Y directions were lower than 1 mm. For the needs of the actual study, the accuracy of the SSA is acceptable. However, as any other interface measurement device, the presence of the SSA mat itself might affect conditions at the interface to some degree, so that the measured interface shape may differ from the true interface shape without the SSA mat in position. Overall, the measurements of the SSA were more accurate when there was no pressure applied than when there was. Furthermore, the SSA system is consistent in its ability to measure deformations. The influence of the pressure on the interface shape measurements should be acknowledged, though at present there is no convenient way of assessing it.

With the development of the SSA system, body-cushion interface shapes can be measured on any type of seating material and seating posture. The SSA will provide a tool for investigation and quantification of the complex relationships among seat properties such as surface shape, cushion deformation and tissue deformation under different load and stiffness conditions. This ability will be of great significance for clinical studies and applications. Since the basic information gathered through its use leads to successful design of generic contoured support surfaces, the SSA itself will be likely to be developed into a valuable clinical tool for support surface design and evaluation.

The study on body-seat interface shape obtained from a group of elderly subjects suggested that body-seat interface shape patterns could be identified using cluster analysis. Four distinct generic shapes were identified for 30 elderly subjects by analyzing the dissimilarity in geometrical shape parameters. The discrimination of body-seat generic shapes might lead to a more comprehensive understanding of seat interface shapes. The results of this study support the notion that multiple generic body-seat interface shapes exist, and that classifying interface shapes provides meaningful information with respect to the geometrical shape parameters. Based on these preliminary results and benefiting from the development of the SSA system, a new approach – generic shape contouring technique - for cushion design has been developed and evaluated. The SSA system provides a reliable and easy to use tool to generate an interface shape database of the wheelchair user population and the cluster analysis provides a quantitative method to determine interface shapes patterns.

The efficiency of the generic shape contouring technique was confirmed when it was applied on a group of wheelchair users who required mild to moderate body support and presented no severe pelvic deformities. Three generic interface shape patterns were determined among a group of nine subjects and three generic shape contoured (GSC) cushions were fabricated by carving these generic shapes into high resiliency foam. Since the interface pressure distributions on the GSC cushion that was selected by the similarity index method were lower than those on the GSC cushions that were not selected. The similarity index method was proved to be very efficient in initially selecting a GSC cushion for the subjects.

This study represents the first phase in the development of a generic shape contoured seating system. The compliant foam cushions contoured to the generic shapes provides greater envelopment of the buttocks and a lower and more uniform pressure distribution than flat foam cushions. In addition, sitting on GSC cushions resulted in lower pressure than sitting on one of commercially available precontoured cushions. The subjects also

gave a positive assessment on the GSC cushions. Seven out of ten subjects chose one of the GSC cushions as their favorite cushion. Based on these conclusions, it is suggested that the generic shape contouring technique should be developed as a clinical tool for serving wheelchair users with a variety of seating and positioning needs.

The results of this study should be viewed as preliminary and further investigation is necessary to establish a reliable database for different wheelchair user populations, as well as to choose appropriate foam materials. Furthermore, the following studies are recommended: 1) design GSC cushions based on at least fifty subjects' interface shape, and evaluate the efficacy of the GSC cushions by clinical trials with a relatively large number of subjects over an extended period; 2) improve the accuracy of the SSA system by reducing the influence of pressure, such as using a metal substrate to support the sensors; 3) use the SSA to evaluate the cushion deformation with and without the FSA present in order to examine if the FSA mat interferes with the deformation of the cushion; 4) use the FSA to evaluate the interface pressure distribution with and without the SSA present in order to examine if the SSA mat interferes with the FSA measurements; 5) discover other principal geometrical parameters that could represent major features of an interface shape.

## BIBLIOGRAPHY

1. ABLEDATA. (2003). Seating Systems, Cushions, Therapeutic Seats. In site of the ABLEDATA. [Online]. [http://www.abledata.com/Site\\_2/seating.htm#Foam](http://www.abledata.com/Site_2/seating.htm#Foam) (cited on Jan 5, 2003)
2. AISSAOUI, R., BOUCHER, C., BOURBONNAIS, D., LACOSTE, M., DANSEREAU, J. (2001a). "Effect of seat cushion on dynamic stability in sitting during a reaching task in wheelchair users with paraplegia". Archives of Physical Medicine and Rehabilitation. 82:2. 274-281.
3. AISSAOUI, R., DANSEREAU, J., LACOSTE, M., GENDRON, M. (2001b). Evaluation and analysis of shear effect in wheelchair seating during repositioning using normal and shear pressure sensors. Montreal: Chair Industrielle CRSNG sur les aides techniques à la posture. 49p.
4. AISSAOUI, R., DANSEREAU, J., LALONDE, N., LACOSTE, M. (1998). "Repositioning the able-bodied: effect of the shape cushion on pressure distribution". 1998 RESNA Annual Conference. Arlington: RESNAPRESS. 110-112.
5. AISSAOUI, R., HEYDAR, S., DANSEREAU, J., LACOSTE, M. (2000). "Biomechanical analysis of legrest support of occupied wheelchairs: comparison between a conventional and a compensatory legrest". IEEE Transactions on Rehabilitation Engineering. 8:1. 140-148.
6. AKERBLUM, B. (1948). Standing and sitting posture. Stockholm, Nordiska Bokhandeln.
7. ALDENDERFER, M.S., BLASHFIELD, R.K. (1984). Cluster analysis. Beverly Hills: Sage Publications. 88p.
8. ALLEN, V., RYAN, D. W., LOMAX, N., MURRAY, A. (1993a). "Accuracy of interface pressure measurement systems". Journal of Biomedical Engineering. 15:4. 344-348.



9. ALLEN, V., RYAN, D. W., MURRAY, A. (1993b). "Repeatability of subject/bed interface pressure measurements". Journal of Biomedical Engineering. 15:4. 329-332.
10. AMERICAN SOCIETY FOR TESTING AND MATERIALS. (1998a). Standard test methods for Vulcanized Rubber and Thermoplastic Elastomers—Tension. Committee on Rubber, Subcommittee on Physical Testing. West Conshohocken, PA, American Society for Testing and materials, ASTM D412-98a.
11. AMERICAN SOCIETY FOR TESTING AND MATERIALS. (1998b). Standard specification for Flexible Cellular Materials--Vinyl Chloride Polymers and Copolymers. Committee on Plastics, Subcommittee on Cellular Materials--Plastics and Elastomers, Philadelphia, PA, American Society for Testing and Material, ASTM D 1667-97.
12. ANDREONI, G., SANTAMBROGIO, G.C., RABUFFETTI, M., PEDOTTI, A. (2002). "Method for the analysis of posture and interface pressure of car drivers". Applied Ergonomics. 33:6. 511-522.
13. APATSIDIS, D.P., SOLOMONIDIS, S.E., MICHAEL, S.M. (2002). "Pressure distribution at the seating interface of custom-molded wheelchair seats: Effect of various materials". Archives of Physical Medicine and Rehabilitation. 83:8. 1151-1156.
14. BAILEY, B.N. (1967). Bedsore. London: Edward Arnold. 130p.
15. BARBENEL, J.C. (1991). "Pressure management. [Review]." Prosthetics & Orthotics International. 15:3. 225-231.
16. BÉDARD-PHAN, E. (1999). Design de coussins de fauteuil roulant à l'aide d'un modèle biomécanique. 174p. Thèse (M.Sc.A.) en génie mécanique, École Polytechnique de Montréal.
17. BENNET, L., KAVNER, D., LEE, B.Y., TRAINOR, F.S. (1979). "Shear vs pressure as causative factors in skin blood flow occlusion". Archives of Physical Medicine and Rehabilitation. 60:7. 309-314.

18. BRIENZA, D.M., BRUBAKER, C.E., MCLAURIN, C.A., CHUNG, K.C. (1992). "A manufacturing system for contoured foam cushions". Journal of Rehabilitation Research & Development. 29:4. 32-40.
19. BRIENZA, D.M., CHUNG, K.C., BRUBAKER, C.E. (1991). "Computer design and fabrication of custom-contoured seating". Medical Design and Material. 1:1. 32-41.
20. BRIENZA, D.M., CHUNG, K.C., BRUBAKER, C.E., KWIATKOWSKI, R.J. (1993a). "Design of a computer-controlled seating surface for research applications". IEEE Transactions on Rehabilitation Engineering. 1:1. 63-66.
21. BRIENZA, D.M., CHUNG, K.C., BRUBAKER, C.E., WANG, J., KARG, T.E., LIN, C.T. (1996a). "A system for the analysis of seat support surface using surface shape control and simultaneous measurement of applied pressures". IEEE Transactions on Rehabilitation Engineering. 4:2. 103-112.
22. BRIENZA, D.M., INIGO, R.M., CHUNG, K.C., BRUBAKER, C.E. (1993b). "Seat support surface optimization using force feedback". IEEE Transactions on Biomedical Engineering. 40:1. 95-103.
23. BRIENZA, D.M., KARG, P.E. (1998). "Seat cushion optimization: A comparison of interface pressure and tissue stiffness characteristics for spinal cord injured and elderly patients". Archives of Physical Medicine and Rehabilitation. 79:4. 388-394.
24. BRIENZA, D.M., KARG, P.E., Geyer, M.J., Kelsey, S., Trefler, E. (2001). "The relationship between pressure ulcer incidence and buttock-seat cushion interface pressure in at-risk elderly wheelchair users". Archives of Physical Medicine and Rehabilitation. 82:4. 529-533.
25. BRIENZA, D.M., KARG, P.E., BRUBAKER, C.E. (1996b). "Seat cushion design for elderly wheelchair users based on minimization of soft tissue deformation using stiffness and pressure measurements". IEEE Transactions on Rehabilitation Engineering. 4:4. 320-327.
26. BRIENZA, D.M., LIN, C.T., KARG, P.E. (1999). "A method for custom-contoured cushion design using interface pressure measurements". IEEE Transactions on Rehabilitation Engineering. 7:1. 99-108.

27. BUCK, S. (1996) "Neglect ... or respect for our elders? Seating for the institutionalized elderly". 1996 International Seating Symposium. 211-214.
28. CANADIAN GENERAL STANDARDS BOARD. (1998). International vocabulary of basic and general terms in metrology. [Ottawa]: Minister of public works and government services Canada. 59p. Canadian General Standards Board CAN/CGSB-158.1.
29. CARLSON, J.M., PAYETTE, M.J., VERVENA, L.P. (1995) "Seating orthosis design for prevention of ducubitus ulcers", Journal of prosthetics and Orthotic. 7:2. 51-60.
30. CHANG, S.R., SON, K., CHOI, Y.S. (1996). "Measurement and three-dimensional graphic representations of Korean seatpan and seatback contours". International Journal of Industrial Ergonomics. 18:2-3. 147-152.
31. CHEN, J.J., SHIAVI, R. (1990). "Temporal feature extraction and clustering analysis of electromyographic linear envelopes in gait studies". IEEE Transactions on Biomedical Engineering. 37:3. 295-302.
32. CHOW, W.W. ODELL, E.I. (1978) "Deformations and stresses in soft body tissues of a sitting person". Journal of Biomechanical Engineering. 100. 79-87.
33. CHOW, W.W., JUVINALL, R.C., COCKRELLM J.L. (1976). "Effects and characteristics of cushion covering membranes". In: Bedsore biomechanics, eds Kened RH, Cowden JM, Scales JT, Baltimore: University Park Press, 95-102.
34. CHRISTIANSEN, K. (1997). "Subjective assessment of sitting comfort". Collegium Antropologicum. 21:2. 387-395.
35. CHUNG, K.C. (1987). Tissue contour and interface pressure on wheelchair cushions. 569p. Doctoral thesis on Biomedical Engineering, University of Virginia.
36. CLEVER, K., SMITH, G., BOWSER, C., MONROE, K. (2002). "Evaluating the efficacy of a uniquely delivered skin protectant and its effect on the formation of sacral/buttock pressure ulcers". Ostomy Wound Manage. 48:12: 60-67.
37. CONINE, T.A., HERSHLER, C., DAECHSEL, D., PEEL, C., PEARSON, A. (1994). "Pressure ulcer prophylaxis in elderly patients using polyurethane foam or Jay

- wheelchair cushions". International Journal of Rehabilitation Research. 17:2. 123-137.
38. COOPER, D., ROXBOROUGH, L. (1986). "Pressure monitoring chair". 1986 RESNA Annual Conference. Washington: RESNAPRESS. 390-393.
  39. COOPER, R.A. (1995). Rehabilitation Engineering Applied to Mobility and Manipulation. Bristol and Philadelphia: Institute of Physics Publishing. 516p.
  40. COOPER, R.A. (1998). Wheelchair Selection and Configuration. New York: Demos Medical Publishing Inc. 410p.
  41. COOPER, R.A., STEWART, K.J., VANSICKLE, D.P. (1994). "Evaluation of methods for determining rearward static stability of manual wheelchairs". Journal of Rehabilitation Research & Development. 31:2. 144-147.
  42. CRENSHAW, R.P., VISTNES, L.M. (1989). "A decade of pressure sore research: 1977-1987". Journal of Rehabilitation Research & Development. 26:1. 63-74.
  43. CURTIS, K.A., KINDLIN, C.M., REICH, K.M., WHITE, D.E. (1995). "Functional reach in wheelchair users: the effects of trunk and lower extremity stabilization". Archives of Physical Medicine and Rehabilitation. 76:4. 360-367.
  44. CUTTER, N.C. (1997). "Wheelchairs and seating systems: clinical applications". Physical Medicine and Rehabilitation. 11:1. 106-132.
  45. DANIEL, R.K., FAIBISOFF, B. (1982). "Muscle coverage of pressure points-the role of myocutaneous flaps". Annals of Plastic Surgery. 8:6. 446-452.
  46. DANISCH, L., ENGLEHART, K., TRIVETT, A. (1999). "Spatially continuous six degree of freedom position and orientation sensor". Sensor Review. 19:2. 106-112.
  47. DINSDALE, S.M. (1974). "Decubitus ulcers, role of pressure and friction in pressure sores". Archives of Physical Medicine and Rehabilitation. 55:4. 157-152.
  48. DYSON, M., SUCKLING, J. (1984). "Stimulation of tissue repair by ultrasound: a survey of the mechanisms involved". Physiotherapy. 64:4. 105-108.
  49. EBE, K., GRIFFIN, M.J. (2000). "Qualitative models of seat discomfort including static and dynamic factors". Ergonomics. 43:6. 771-790.

50. EBE, K., GRIFFIN, M.J. (2001). "Factors affecting static seat cushion comfort". Ergonomics. 44:10. 901-921.
51. EDSBERG, L.E., NATIELLA, J.R., BAIER, R.E., EARLE, J. (2001). "Microstructural characteristics of human skin subjected to static versus cyclic pressures". Journal of Rehabilitation Research and Development. 38:5. 477-486.
52. ENGSTRÖM, B. (1993). Ergonomics, wheelchairs and positioning: a book of principles based on experience from the field. Hässelby, Suède: Posturalis. 160p.
53. EVERITT, B.S. (1993). Cluster Analysis. 3rd ed. New York: Halsted Press. 170p.
54. FAN, L.S., WHITE, R.M., MULLER, R.S. (1984). "A mutual capacitive normal-and shear-sensitive tactile sensor". 1984 International Electron Devices Meeting (IEDM 1984). IEEE Institute of Electrical and Electronics Engineers Inc. 220-222.
55. FENETY, P.A., PUTNAM, C., WALKER, J.M. (2000). "In-chair movement: validity, reliability and implications for measuring sitting discomfort". Applied Ergonomics. 31:4. 383-393.
56. FERGUSON-PELL, M.W. (1990). "Seat Cushion Selection". Journal of Rehabilitation Research and Development Clinical Supplement 2. 49-73.
57. FERGUSON-PELL, M.W., CARDI, M.D. (1993). "Prototype development and comparative evaluation of wheelchair pressure mapping system". Assistive Technology. 5:2. 78-91.
58. FERGUSON-PELL, M.W., COCHRAN, V.B., PALMIERI, V., BRUNSKI, J.B. (1986). "Development of a modular wheelchair cushion for spinal cord injured persons". Journal of Rehabilitation Research and Development. 23:3. 63-76.
59. FERGUSON-PELL, M.W., HAGISAWA, S., BAIN, D. (2000). "Evaluation of a sensor for low interface pressure applications". Medical Engineering & Physics. 22:9. 657-663.
60. FERNANDEZ, S. (1987). "Prevention and treatment of pressure sores". Physiotherapy. 73:9. 450-454.

61. FERRARIN, M., ANDREONI, G., PEDOTTI, A. (2000). "Comparative biomechanical evaluation of different wheelchair seat cushions". Journal of Rehabilitation Research and Development. 37:3. 315-324.
62. FOSTER, C., FRISCH, S.R., DENIS, N., FORLER, Y., JAGO, M. (1992). "Prevalence of pressure ulcers in Canadian institutions". Canadian Association of Enterostomal Therapy Journal. 11:2. 23-31.
63. GARBER, S.L., KROUSKOP, T.A., (1982). "Body build and its relationship to pressure distribution in the seated wheelchair patient". Archives of Physical Medicine & Rehabilitation 63:1. 17-20.
64. GOOSSENS, R.H.M., SNIJDERS, C.J., HOLSCHER, T.G., HEERENS, W., HOLMAN, A.E. (1997). "Shear stress measured on beds and wheelchairs". Scandinavian Journal of Rehabilitation Medicine. 29:3. 131-136.
65. GRAEBE, R. (1980). "Static forces-cushion". 5<sup>th</sup> Meeting of the Wessex Tissue Viability Group. Salisbury, England: Odestock Hospital.
66. GROSS, C., GOONETILLEKE, R., MENON, K., BANAAG, J., NAIR, C. (1994). "Biomechanical assessment and prediction of seat comfort". In: Hard Facts About Soft Machines. Ed by: Lueder, R., Noro, K., Bristol, P.A: Taylor Francis. 231-253. 457p.
67. GYI, D.E., PORTER, J.M. (1999). "Interface pressure and the prediction of car seat discomfort". Applied Ergonomics. 30:2. 99-107.
68. GYI, D.E., PORTER, J.M., ROBERTSON, N.K. (1998). "Seat pressure measurement technologies: considerations for their evaluation". Applied Ergonomics. 29:2. 85-91.
69. HARMS, M. (1990). "Effect of wheelchair design on posture and comfort of users". Physiotherapy. 76:5. 266-271.
70. HEALTH CANADA. (2000). Publications of the National Forum on Health. In the website of Health Canada. [Online] [www.nfh.hc-sc.gc.ca/publicat/execsumm/lord.htm](http://www.nfh.hc-sc.gc.ca/publicat/execsumm/lord.htm). (cited on Jan 6, 2002)

71. HERTZBERG, H.T.E. (1972). The Human Buttocks in Sitting: Pressures, Patterns, and Palliatives. Society of Automotive Engineers. Publication no. 720005.
72. HILLS, A.P., HENNIG, E.M., MCDONALD, M., BAR-OR, O. (2001). "Plantar pressure differences between obese and non-obese adults: a biomechanical analysis". International Journal of Obesity. 25:11. 1674-1679.
73. HOBSON, D.A. (1990). Seating and mobility for the severely disabled, in Rehabilitation Engineering. Ed. by Smith, R.V., Leslie, J.H. Boca Raton: CRC Press. 548p.
74. HOBSON, D.A. (1992). "Comparative effects of posture on pressure and shear at the body-seat interface". Journal of Rehabilitation Research and Development. 29:4. 21-31.
75. HOCKENBERRY, J. (1977). "Seating Design for Worker efficiency". Furniture Design and Manufacturing. 49:12. 42-46.
76. HOLLINSHEAD, W.H. (1974). Textbook of Anatomy. Philadelphia: Harper & Row Publishers. 985p.
77. HOULE, R.J., MINNESOTA, S.P. (1969). "Evaluation of seat devices designed to prevent ischemic ulcers in paraplegic patients". Archives of Physical Medicine and Rehabilitation. 50:10. 587-594.
78. HUSAIN, T. (1953). "An experimental study of some pressure effects on tissue with reference to bed sore problem". Journal of pathology and bacteriology. 66. 347-358.
79. JANSSEN-POTTEN, Y.J., SEELEN, H.A., DRUKKER, J., HUSON, T., DROST, M.R. (2001). "The effect of seat tilting on pelvic position, balance control, and compensatory postural muscle use in paraplegic subjects". Archives of Physical Medicine and Rehabilitation. 82:10. 1393-1402.
80. JANSSEN-POTTEN, Y.J., SEELEN, H.A., DRUKKER, J., REULEN, J.P., DROST, M.R. (1999). "Postural muscle responses in the spinal cord injured persons during forward reaching". Ergonomics. 42:9, 1200-1215.
81. JOHNSON, R.A., WICHERN, D.W. (1988). Applied multivariate statistical analysis. 2nd ed. Englewood Cliffs: Prentice-Hall. 607p.

82. KADABA, M.P., FERGUSON-PELL, M.W., PALMIERI, V.R., COCHRAN, G.V.B. (1984). "Ultrasound mapping of the buttock-cushion interface contour". Archives of Physical Medicine and Rehabilitation. 65:8. 467-469.
83. KAMPER, D., BARIN, K., PARNIANPOUR, M., REGER, S., WEED, H. (1999). "Preliminary investigation of the lateral postural stability of spinal cord-injured individuals subjected to dynamic perturbations". Spinal Cord. 37:1. 40-46.
84. KARG, T.E., BRIENZA, D.M., CHUNG, K.C., BRUBAKER, C.E. (1996). "Evaluation of a surface shape optimization technique for custom contoured cushion design". 1996 RESNA Annual Conference. Arlington: RESNAPRESS. 229-231.
85. KARP, Gary. (1999). Choosing a Wheelchair: A Guide for Optimal Independence. First Edition. O'Reilly, UK: Patient-Centered Guides. 192p.
86. KERNOZEK, T.M., WILDER, P.A., AMUNDSON, A., HUMMER, J. (2002). "The effects of body mass index on peak seat-interface pressure of institutionalized elderly". Archives of Physical Medicine and Rehabilitation. 83:6. 868-871.
87. KOLICH, M. (2003). "Automobile seat comfort: occupant preferences vs. anthropometric accommodation". Applied Ergonomics. 34:2. 177-184.
88. KOO, T.K.K., MAK, A.F.T., LEE, Y.L. (1995). "Evaluation of an active seating system for pressure relief". Assistive Technology. 7:2. 119-128.
89. KOO, T.K.K., MAK, A.F.T., LEE, Y.L. (1996). "Posture effect on seating interface biomechanics: comparison between two seating cushions". Archives of Physical Medicine & Rehabilitation. 77:1. 40-47.
90. KOSIAK, M. (1959). "Etiology and pathology of ischemic ulcers". Archives of Physical Medicine and Rehabilitation. 40:2. 62-69.
91. KOSIAK, M. (1976). "A mechanical resting surface: its effect on pressure distribution". Archives of Physical Medicine and Rehabilitation. 57:10. 481-484.
92. KROUSKOP, T. A., NOBLE, P. C., GARBER, S. L., SPENCER, W. A. (1983). "The effectiveness of preventive management in reducing the occurrence of pressure sores". Journal of Rehabilitation Research and Development. 20:1. 74-83.



93. LATMAN, N.S., LANIER, R. (1998). "Expressions of accuracy in the evaluation of biomedical instrumentation". Biomedical Instrumentation and Technology. 32:3. 282-288.
94. LEE, J., FERRAIUOLO, P., TEMMING, J. (1993). "Measuring seat comfort". Automotive Engineering. 101:7. 25-30.
95. LEMAIRE, E.D., UPTON, D., PAIALUNGA, J., MARTEL, G., BOUCHER, J. (1996). "Clinical analysis of a CAD/CAM system for custom seating: A comparison with hand-sculpting methods". Journal of Rehabilitation Research and Development. 33:3. 311-320.
96. LETTS, R.M. (1991). Principles of seating the disabled. Boca Raton: CRC Press. 376p.
97. LEVINE, J.M., SIMPSON, M., MCDONALD, R. (1989). "Pressure sores: a plan for primary care prevention". Geriatrics. 44:4. 75-90.
98. LEVINE, S.P., KETT R.L., CEDERNA P.S., BOWERS, L.D., BROOKS, S.V. (1989). "Electrical muscle stimulation for pressure variation at the seating interface". Journal of Rehabilitation Research & Development. 26:4. 1-8.
99. LEVINE, S.P., KETT, R.L., FERGUSON-PELL, M. (1990). "Tissue shape and deformation versus pressure as a characterization of the seating interface". Assistive Technology. 2:3. 93-99.
100. LEWIS, D.W., NOURSE, W.B. (1978). "A device designed to approximate shear forces on human skin". Bulletin of Prosthetics Research. 30:10. 36-46.
101. Li, Y., AISSAOUI, R., BRIENZA, D.M., DANSEREAU, J. (1999a). "A method for obtaining body-seat interface shape pattern among elderly persons". International Society of Biomechanics XVII<sup>th</sup> Congress. 714.
102. Li, Y., AISSAOUI, R., BRIENZA, D.M., DANSEREAU, J. (1999b). "Determination of generic seat interface shapes by cluster analysis". 1999 RESNA Annual Conference. Arlington: RESNAPRESS. 254-256.

103. LI, Y., AISSAOUI, R., BRIENZA, D.M., DANSEREAU, J. (2000a). "Determination of generic body-seat interface shapes by cluster analysis". IEEE Transactions on Rehabilitation Engineering. 8:4. 481 –489.
104. Li, Y., AISSAOUI, R., BRIENZA, D.M., DANSEREAU, J. (2000b). "The effect of body mass index on seat interface shape patterns". XXV<sup>th</sup> Congress of the Société de Biomécanique & XI<sup>th</sup> Congress of the Canadian Society for Biomechanics. 75.
105. LI, Y., AISSAOUI, R., BRIENZA, D.M., LACOSTE, M., DANSEREAU, J. (2003b). "Design and Evaluation of Generic Shape Cushions based on a New Interface Shape Measurement System". Archives of Physical Medicine and Rehabilitation. (Submitted on March. 17, 2003)
106. Li, Y., AISSAOUI, R., DANSEREAU, J. (1998). "A mathematical method for comparison of contoured seating shapes". 1998 RESNA Annual Conference. Arlington: RESNAPRESS. 146-148.
107. Li, Y., AISSAOUI, R., LACOSTE, M., DANSEREAU, J. (2002). "Accuracy and Repeatability of a Revolutionary Interface Shape Measurement System". Archives of Physiology and Biochemistry. 110:Supplement September. 64.
108. LI, Y., AISSAOUI, R., LACOSTE, M., DANSEREAU, J. (2003a). "Development and Evaluation of a New Body-Seat Interface Shape Measurement System". IEEE Transactions on Biomedical Engineering. (Submitted on Feb. 12, 2003)
109. LINDEN, O., GRENWAY, M., PIAZZA, J.M. (1965). "Pressure distribution of the surface of the human body." Archives of Physical Medicine and Rehabilitation. 5. 378-385.
110. MAKLEBUST, J. A., MONDOUX, L., SIEGGREEN, M. (1986). "Pressure relief characteristics of various support surfaces used in prevention and treatment of pressure ulcers". Journal of Enterostomal Therapy. 13:3. 85-89.
111. MAYALL, J.K., DESHARNAIS, G. (1995). Positioning in a wheelchair: a guide for caregivers of the disabled adult, 2<sup>nd</sup> ed. Thorofare: SLACK Incorporated. 160p.

112. MCCLELLAND, I., WARD, J.S. (1976). "Ergonomics in relation to sanitary ware design". Ergonomics. 19:4. 465-478.
113. MCFADYEN, G.M., STONER, D.L. (1980). "Polyurethane foam wheelchair cushions: Retention of supportive properties". Archives of Physical Medicine and Rehabilitation. 61:5. 174-177.
114. MCGOVERN, T.F., REGER, S.T., SNYDER, E.N., SAUER, B.L. (1988). "A new technique for custom contoured body supports". International Conference of American Association Rehabilitation Therapy. 306-307.
115. MCLANE, K.M., KROUSKOP, T.A., MCCORD, S., FRALEY, J.K. (2002). "Comparison of interface pressures in the pediatric population among various support surfaces". Journal of Wound Ostomy Continence Nursing. 29:5. 242-251.
116. MEDHAT, M.A., HOBSON, D.A. (1992). Standardization of terminology and descriptive methods for specialized seating: A preference manual. RESNA, Washington D.C. 1-36.
117. NAKAYA, H., OKIYAMA, H. (1993) "A development of statistical human back contour model for backrest comfort evaluation". Seat System: Comfort & Safety". Society of Automotive Engineers, Warrendale, PA, Tech. Rep. 930114. 77-87.
118. NETH, D.C., MCGOVERN, T.F., REGER, S.I. (1989). "Computer aided measurement and fabrication of contoured body supports". 1989 RESNA Annual Conference. Washington, D.C.: RESNAPRESS. 234-235.
119. OFFICE DES PERSONNES HANDICAPÉES DU QUÉBEC. (2002). Information statistique. In the website of l'Office des personnes handicapées du Québec. [Online] [http://www.ophq.gouv.qc.ca/Recherche/Statistique/D\\_Population.htm](http://www.ophq.gouv.qc.ca/Recherche/Statistique/D_Population.htm). (cited on Jun 5, 2002)
120. PATTERSON, J., BENNETT, G. (1995). "Prevention and treatment of pressure sores". Journal of the American Geriatrics Society. 43:8. 919-927.
121. PERKASH, I., O'NEILL, H., POLITI-MEEKS, D., BEETS, C.L. (1984) "Development and evaluation of a universal contoured cushion". 1984 International Medical Society of Paraplegia. 358-365.

122. PHAN, E., AUBIN, C.-É., DIONNE, M.-J., LI, Y., DANSEREAU, J. (1999). "Computer model for the design of wheelchair cushions". 1999 RESNA Annual Conference. Arlington: RESNAPRESS. 260-262.
123. REDDY, N.P., PALMIERI, V., COCHRAN, G.V.B. (1981). "Subcutaneous interstitial fluid pressure during external loading". American Journal of Physiology. 240:5. R327-329.
124. REGER, S.I., CHUNG, K.C., MARTIN, G., MCLAURIN, C.A. (1985). "Shape and pressure distribution on wheelchair cushions". 8<sup>th</sup> Annual RESNA Conference. Washington, DC: RESNAPRESS. 341-343.
125. REGER, S.I., MANLEY, M.T., CHUNG K.C., BELHOBEC G.H. (1986). "Deformation and stiffness of soft tissues by magnetic resonance imaging". 8<sup>th</sup> Annual IEEE Engineering in Medical and Biology Society Conference. New York: IEEE/EMBS. 1842-1843.
126. REGER, S.I., MCGOVERN, T.F., CHUNG, K.-C., STEWART, T.P. (1988). "Correlation of transducer systems for monitoring tissue interface pressures". Journal of Clinical Engineering. 13:5. 365-370.
127. REID, D.T., SOCHANIWSKYJ, A. (1991). "Effects of anterior-tipped seating on respiratory function of normal children and children with cerebral palsy". International Journal of Rehabilitation Research. 14:3. 203-212.
128. RESWICK, J.B., ROGERS, J.E. (1976). "Experience at Rancho Los Amigos Hospital with devices and techniques to prevent pressure sores". in Bedsore Biomechanics, ed Kenedi, R.M., Cowden J.M., Scales, J.T. Baltimore: University Park Press. 357p.
129. RINGUTTE, J.P., DANSEREAU, J., TRUDEAU, F. (1997). "Adaptation of a clinical seating simulator into a research tool". 1997 RESNA Annual Conference. Arlington: RESNAPRESS. 222-224.
130. RITHALIA, S.V., GONSALKORALE, M. (2000). "Quantification of pressure relief using interface pressure and tissue perfusion in alternating pressure air mattresses". Archives of Physical Medicine and Rehabilitation. 81:10. 1364-1369.

131. ROSENTHAL, M.J., FELTON, R.M., HILEMAN, D.L., LEE, M., FRIEDMAN, M., NAVACH, J.H. (1996) "A wheelchair cushion designed to redistribute sites of sitting pressure". Archives of Physical Medicine and Rehabilitation. 77:3. 278-282.
132. SEELEN, H.A., POTTEN, Y.J., ADAM, J.J. (2001). "Motor preparation in postural control in seated spinal cord injured people". Ergonomics. 44:4. 457-472.
133. SHACKEL, B., CHIDSEY, K.D., SHIPLEY, P. (1969). "The assessment of chair comfort". Ergonomics. 12:2. 269-306.
134. SHAW, C.G. (1991). "Wheelchair seat comfort for the institutionalized elderly". Assistive Technology. 3:1. 11-23.
135. SMITH, D. M. (1995). "Pressure ulcers in the nursing home". Annals of Internal Medicine. 123:6. 433-442.
136. SOUTHER, S.G., CARR, S.D., VISTNES, L.M. (1974). "Wheelchair cushions to reduce pressure under bony prominences". Archives of Physical Medicine and Rehabilitation. 55:10. 460-464.
137. SPINAL OUTREACH TEAM. (2001). Cushion selection and prescription for clients with spinal cord injury. In site of Queensland Health. [Online] <http://www.health.qld.gov.au/spot/PDF/Cushion%20Selection.pdf>. (cited on Dec. 9, 2002)
138. SPRIGLE, S. (1989). Biomechanical analysis of contoured foam for use by spinal cord injured persons. 179p. Doctoral dissertation on Health Science, University of Virginia.
139. SPRIGLE, S., CHUNG, K.C., BRUBAKER, C.E. (1990a). "Factors affecting seat contour characteristics". Journal of Rehabilitation Research and Development. 27:2. 127-134.
140. SPRIGLE, S., CHUNG, K.C., BRUBAKER, C.E. (1990b). "Reduction of sitting pressures with custom contoured cushions". Journal of Rehabilitation Research and Development. 27:2. 135-140.

141. SPRIGLE, S., FAISANT, T.E., CHUNG, K.C. (1990c). "Clinical evaluation of custom-contoured cushions for the spinal cord injured". Archives of Physical Medicine & Rehabilitation. 71:9. 655-658.
142. SPRIGLE, S., PRESS, L., DAVIS, K. (2001). "Development of uniform terminology and procedures to describe wheelchair cushion characteristics". Journal of Rehabilitation Research and Development. 38:4. 448-461.
143. SPRIGLE, S., SCHUCH, J.Z. (1993). "Using seat contour measurements during seating evaluations of individuals with SCI". Assistive Technology. 5:1. 24-35.
144. STAARINK, H.A.M. (1995). Sitting posture, comfort and pressure; assessing the quality of wheelchair cushions. Delft: Delft University Press. 259p.
145. STOUDT, H.W. (1981). "The Anthropometry of the Elderly". Human Factors. 23:1. 29-37.
146. SY, C.P.L., TAM, E.W.C. (2000). "Fabrication of custom contour cushion using pressure mapping method: a preliminary study". 22<sup>nd</sup> Annual EMBS International Conference. 2256-2258.
147. TANG, S. (1991). "Seat cushions". in Prevention of pressure sore: engineering and clinical aspects, ed WEBSTER, J.G. Bristol, Philadelphia & New York: Adam Hilger. 56-74.
148. TODD, B.A., THACKER, J.G. (1994). "The three-dimensional model of the human buttocks, in vivo". Journal of Rehabilitation Research and Development. 31:2. 111-119.
149. TONEY, M.A., MCEWEN, I., THOMPSON, D., PARKER, D. (1995). "Reliability of contours of positive molds following seating simulation". 1995 RESNA Annual Conference. Arlington: RESNAPRESS. 300-302.
150. TRANDEL, R.S., LEWIS, D.W., VERHONICK, P.J. (1975). "Thermographical investigation of decubitus ulcers". Bulletin of prosthetics research. 10:24. 137-155.
151. TREASTER, D., MARRAS, W.S. (1987). "Measurement of Seat Pressure Distributions". Human Factors. 29:5. 563-575.

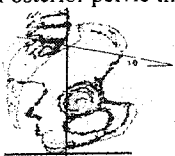
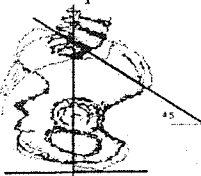
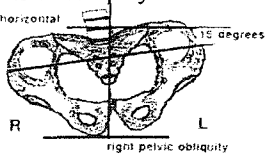
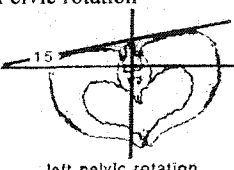
152. TREFLER, E., HOBSON, D.A., TAYLOR, S.J., MONAHAN, L.C., SHAW, C. (1993). Seating and Mobility: For Persons with Physical Disabilities. Tucson: Therapy Skill Builders. 293p.
153. US DEPT. OF VETERAN AFFAIRS. (1994). Wheelchair Seat Cushion Guide. Milwaukee: National Center for Cost Containment.
154. VAN MARUM, R.J., MEIJER, J.H., RIBBE, M.W. (2002). "The relationship between pressure ulcers and skin blood flow response after a local cold provocation". Archives of Physical Medicine and Rehabilitation. 83:1. 40-43.
155. WAGNAC, E. (2002). Modélisation biomécanique du complexe bassin-coussin en fauteuil roulant. 176p. Thèse (M.Sc.A.) en génie biomédical, École Polytechnique de Montréal.
156. WARD, D.E. (1994). Prescriptive seating for wheeled mobility: theory, application, and terminology. Kansas City: HealthWealth International. 213p.
157. WARD, J.H. (1963) "Hierarchical grouping to optimize an objective function". Journal American Statistical Association. 58. 234-244.
158. WEBSTER, J.G. (1991). Prevention of Pressure Sores: Engineering and Clinical Aspects. Bristol, Philadelphia & New York: Adam Hilger. 250p.
159. WILSON, A.B. Jr. (1992). Wheelchairs: a prescription guide. 2nd ed. New York: Demos Publications. 96p.
160. YAMAZAKI, N. (1992). "Analysis of sitting comfortability of driver's seat by contact shape". Ergonomics. 35:5-6. 677-692.
161. YARKONY, G. M. (1994). "Pressure ulcers: a review". Archives of Physical Medicine & Rehabilitation. 75:8. 908-917.
162. ZACHARKOW, D. (1984). Wheelchair posture and pressure sores. Springfield (IL): Charles C Thomas. 99p.
163. ZACHARKOW, D. (1988). Posture: sitting, standing, chair design, and exercise. Springfield (IL): Charles C Thomas. 433p.

164. ZOLLARS, J.A. (1993). Seating and moving through the decades: a literature review on seating and mobility through 1992. 2<sup>nd</sup> ed. Santa Cruz, CA: PAX Press. 110p.



## APPENDIX

**Table Appendix-1 Postura problem in the pelvis (Summarized from Zollars, 1993, Treffler et al., 1993, Ward, 1994, Mayall and Desharnais, 1995, Letts, 1991).**

Problem	Causes	Possible Solution
<b>Posterior pelvic tilt</b> 	<ul style="list-style-type: none"> <li>▪ Hamstring tightness</li> <li>▪ Discomfort</li> <li>▪ An attempt to find a balance point</li> <li>▪ Extensor thrust or spasticity</li> <li>▪ Weakness and sliding forward</li> <li>▪ Spinal deformity</li> <li>▪ Decreased hip flexion range of motion</li> </ul>	<ul style="list-style-type: none"> <li>▪ Firm back and set of correct length</li> <li>▪ Seat-to-back angle of <math>&lt;90^\circ</math> to inhibit hip extensor spasticity</li> <li>▪ Hip belt</li> <li>▪ Antithrust seat</li> <li>▪ Pelvic stabilizer</li> <li>▪ Pelvic bar</li> <li>▪ Sacral pad and knee block</li> </ul>
<b>Anterior pelvic tilt</b> 	<ul style="list-style-type: none"> <li>▪ Weakness</li> <li>▪ Low tone</li> <li>▪ Shortening of low back extensors</li> <li>▪ Surgical release of abdominals</li> </ul> <p>*often an anterior pelvic tilt is seen in persons with muscular dystrophy or meningomyelocele</p>	<ul style="list-style-type: none"> <li>▪ Inhibition of hip flexors tone through use of a flat seat</li> <li>▪ Accommodation of hip flexion contracture by wedging</li> <li>▪ Hip belt positioned over the anterior superior iliac spines to prevent anterior movement of the upper pelvis</li> </ul>
<b>Pelvic obliquity</b> 	<ul style="list-style-type: none"> <li>▪ Tonal asymmetry</li> <li>▪ Hip flexor, adductor or abductor contracture</li> <li>▪ Dislocated hip</li> <li>▪ Scoliosis</li> </ul>	<ul style="list-style-type: none"> <li>▪ Firm seat</li> <li>▪ Lateral pelvic supports</li> <li>▪ Bifurcate hip belt</li> <li>▪ Pelvic positioners</li> <li>▪ Pelvic bar</li> <li>▪ Accommodation through seat molding for fixed deformities</li> </ul>
<b>Pelvic rotation</b> 	<ul style="list-style-type: none"> <li>▪ Asymmetrical tone in hip adductor or abductors</li> <li>▪ Asymmetrical tone in trunk rotators</li> </ul>	<ul style="list-style-type: none"> <li>▪ Bifurcate hip belt in mild cases</li> <li>▪ Pelvic positioners placed below the anterior superior iliac spine on the side of the pelvis which is rotated forward</li> <li>▪ Appropriate accommodation of leg length discrepancy or hip abduction/adduction contracture</li> </ul>

**Table Appendix-2 Postural problem in the lower extremities (Zollars, 1993, Treffler et al., 1993, Ward, 1994, Mayall and Desharnais, 1995, Letts, 1991).**

<b>Problem</b>	<b>Causes</b>	<b>Possible Solution</b>
Hip extension	<ul style="list-style-type: none"> <li>▪ Spasticity of hip extensors</li> <li>▪ Difficulty silencing extensors following active contraction</li> <li>▪ Hamstring contracture</li> <li>▪ Sling seat</li> </ul>	<ul style="list-style-type: none"> <li>▪ Firm seat and back</li> <li>▪ Seat wedging to decrease extensor tone</li> <li>▪ Accommodation of hamstring contracture by allowing sufficient knee flexion</li> <li>▪ Pelvic support</li> </ul>
Hip flexion	<ul style="list-style-type: none"> <li>▪ Spasticity of hip flexors</li> <li>▪ Difficulty silencing flexors following active contraction</li> <li>▪ Hip flexion contracture</li> <li>▪ Footplates too high</li> </ul>	<ul style="list-style-type: none"> <li>▪ Inhibition of flexor using a flat or anteriorly tipped seat</li> <li>▪ Footplates at appropriate height</li> <li>▪ Accommodation through wedging if fixed contractures present</li> <li>▪ Good pelvic control required to prevent anterior pelvic tilt during flexor spasms</li> </ul>
Hip adduction	<ul style="list-style-type: none"> <li>▪ Adductor spasticity</li> <li>▪ Adductor contracture</li> <li>▪ Inability to silence adductors following active contraction</li> <li>▪ Abduction of the opposite hip, inducing pelvic rotation and passive adduction of the observed hip</li> <li>▪ Footplates too high</li> <li>▪ Sling seat</li> </ul>	<ul style="list-style-type: none"> <li>▪ Firm seat board with good thigh contact</li> <li>▪ Use of medial thigh support as part of the seat contour in mild cases, and a separate component in more severe cases</li> <li>▪ Control pelvic rotation</li> <li>▪ Accommodation of fixed contracture through construction of an asymmetrical seat and placement of the abductor off-center</li> </ul>
Hip abduction	<ul style="list-style-type: none"> <li>▪ Abductor spasticity</li> <li>▪ Abductor contracture</li> <li>▪ Inability to silence abductors following active contraction</li> <li>▪ Adduction of the opposite hip, inducing pelvic rotation and passive abduction of the observed hip</li> </ul>	<ul style="list-style-type: none"> <li>▪ Use of lateral thigh supports</li> <li>▪ Control pelvic rotation</li> <li>▪ Accommodation a fixed contracture through construction of an asymmetrical seat (if unilateral) or wide anterior seat surface (if bilateral)</li> </ul>
Windswept hips	<ul style="list-style-type: none"> <li>▪ Asymmetrical muscle tone above and/or below the hip</li> <li>▪ Different motor synergies present in each limb</li> <li>▪ Unilateral abductor or adductor spasticity or contracture including pelvic rotation and windswept positioning</li> </ul>	<ul style="list-style-type: none"> <li>▪ Good pelvic control of rotation with pelvic positioners or a pelvic bar</li> <li>▪ Correction of abduction/adduction posture of hips if range is available</li> <li>▪ Accommodation of fixed hip deformities using an asymmetrical seat</li> </ul>
Leg length discrepancy	<ul style="list-style-type: none"> <li>▪ Hip discrepancy</li> <li>▪ Surgical shortening (varus osteotomy)</li> <li>▪ Unequal skeletal development</li> </ul>	<ul style="list-style-type: none"> <li>▪ Accommodation is required in the case of a true leg length discrepancy through construction of a seat with a cutout at the anterior aspect for the shorter thigh</li> <li>▪ Correction of an apparent leg length discrepancy through control of pelvic rotation and hip position</li> </ul>

**Table Appendix-3 Postural problem in the trunk (Zollars, 1993, Treffler et al., 1993, Ward, 1994, Mayall and Desharnais, 1995, Letts, 1991).**

Problem	Causes	Possible Solution
Forward flexion (possibly leading to kyphosis)	<ul style="list-style-type: none"> <li>Compensation for posterior pelvic tilt</li> <li>Abdominal muscle hypertonicity</li> <li>Weight of the arm pulling the trunk into flexion</li> <li>Low trunk tone</li> <li>Weakness</li> <li>Shortened anterior muscle groups</li> </ul>	<ul style="list-style-type: none"> <li>Support the pelvis</li> <li>Firm backboard</li> <li>Use of arm support</li> <li>In severe cases, use of three-point sagittal plane control consisting of anterior pelvic control, firm backboard, and anterior trunk supports</li> <li>Use of a spinal orthosis if total contact required</li> <li>Accommodate through custom contouring if a fixed kyphosis present</li> <li>Alter the orientation in space to decrease the influence of gravity</li> </ul>
Trunk side flexion (possibly leading to scoliosis)	<ul style="list-style-type: none"> <li>Poor feedback</li> <li>Poor sustained control of trunk muscles</li> <li>Muscle tone imbalance in trunk side flexors</li> <li>Compensation for pelvic obliquity</li> </ul>	<ul style="list-style-type: none"> <li>Firm seat board with lateral pelvic support</li> <li>Use of standard precontoured lateral trunk molding to provide midline feedback for individuals who are able to self-correct, but lack position sense</li> <li>Lateral trunk supports</li> <li>Three-point frontal plane control in severe cases</li> <li>Use of thoraco-lumbar-sacral orthosis when total contact required</li> </ul>
Trunk rotation (possibly leading to rotational scoliosis)	<ul style="list-style-type: none"> <li>Asymmetrical muscle tone</li> <li>Asymmetrical trunk control</li> </ul>	<ul style="list-style-type: none"> <li>Use of curved trunk supports to provide anterior control on the side which is rotated forward (must be used in combination with a firm back)</li> <li>Chest straps and panels</li> <li>Anterior shoulder pads</li> </ul>

**Table Appendix-4 Postural problem in the head and neck (Zollars, 1993, Treffler et al., 1993, Ward, 1994, Mayall and Desharnais, 1995, Letts, 1991).**

Problem	Causes	Possible Solution
Flexion	<ul style="list-style-type: none"> <li>Spasticity of neck flexors</li> <li>Lack of stable origin for the neck extensors</li> <li>Inability to actively extend against gravity</li> </ul>	<ul style="list-style-type: none"> <li>Appropriate support of the pelvis, trunk, and shoulder girdle</li> <li>Good upper limb support on a tray</li> <li>Halo to prevent neck flexion beyond the point of active recovery</li> <li>Headband of elastic material to provide increasing resistance to flexion</li> <li>Alter the orientation of the seating system in space to decrease the influence of gravity</li> </ul>
Extension	<ul style="list-style-type: none"> <li>Spasticity of neck extensors</li> <li>Compensatory for forward trunk flexion</li> </ul>	<ul style="list-style-type: none"> <li>Appropriate control of the pelvis, trunk, and shoulder girdle</li> <li>Use of a neckrest (avoid occipital pressure)</li> </ul>
Cervical flexion with atlanto-occipital extension	<ul style="list-style-type: none"> <li>Compensatory for trunk flexion and scapular protraction</li> <li>Compensatory posture when head control is poor</li> </ul>	<ul style="list-style-type: none"> <li>Appropriate control of the pelvis, trunk, and shoulder girdle</li> <li>Neckrest contoured in two places (cup shaped)</li> </ul>

**Table Appendix-5 Postural problem in the upper extremities (Zollars, 1993, Trefler et al., 1993, Ward, 1994, Mayall and Desharnais, 1995, Letts, 1991).**

<b>Problem</b>	<b>Causes</b>	<b>Possible Solution</b>
Shoulder retraction	<ul style="list-style-type: none"> <li>▪ Spasticity in scapular retractors</li> <li>▪ Fixing of the shoulders to compensate for poor trunk control</li> </ul>	<ul style="list-style-type: none"> <li>▪ Provision of appropriate pelvic and trunk support</li> <li>▪ Provision of sternal pressure using a chest panel or anterior shoulder supports angled inward to facilitate active protraction</li> <li>▪ Use of a tray to support the upper limbs in forward flexion</li> <li>▪ Shoulder wedges (protractors)</li> </ul>
Shoulder protraction	<ul style="list-style-type: none"> <li>▪ Spasticity in scapular protractors</li> <li>▪ Weight of the arms when the trunk is forward flexed</li> </ul>	<ul style="list-style-type: none"> <li>▪ Good pelvic and trunk support</li> <li>▪ Armrests or a tray for arm support</li> <li>▪ Shoulder strips over the lateral aspect of the shoulders</li> <li>▪ Shoulder pads angled outward in more severe cases</li> </ul>
Shoulder elevation	<ul style="list-style-type: none"> <li>▪ Upward pull on the scapula by the upper fibers of trapezius and the levator scapulae when the neck is side flexed</li> <li>▪ Inability to stabilize scapulae during attempted, active head movements</li> </ul>	<ul style="list-style-type: none"> <li>▪ Shoulder straps with a slightly downward angle of pull over the shoulder</li> <li>▪ Rigid shoulder pads</li> </ul>